PB81-176539

An Evaluation Study for the Industrial Source Complex (ISC) Dispersion Model

H. E. Cramer Co., Inc.
Salt Lake City, UT

Prepared for

Environmental Protection Agency
Research Triangle Park, NC

Jan 81

U.S. Department of Commerce
National Technical Information Service
NTIS

United States
Environmental Protection
Agency

Office of Air Quality
Planning and Standards
Research Triangle Park NC 27711

EPA-450/4-81-002
January 1981

Air

PB81-176539

EPA

An Evaluation Study for the Industrial Source Complex (ISC) Dispersion Model

PRODUCT OF:
NATIONAL TECHNICAL
INFORMATION SERVICE
U.S. DEPARTMENT OF COMMERCE
SPRINGFIELD, VA. 22161

TECHNICAL REPORT DATA
(Please read Instructions on the reverse before completing)

1. REPORT NO. EPA-450/4-81-002	2.	3. RECIPIENT'S ACCESSION NO. PB81 176539
4. TITLE AND SUBTITLE An Evaluation Study for the Industrial Source Complex (ISC) Dispersion Model		5. REPORT DATE January 1981
		6. PERFORMING ORGANIZATION CODE
7. AUTHOR(S) J. F. Bowers and A. J. Anderson		8. PERFORMING ORGANIZATION REPORT NO.
9. PERFORMING ORGANIZATION NAME AND ADDRESS H. E. Cramer Company, Inc. University of Utah Research Park P. O. Box 8049 Salt Lake City, Utah 84108		10. PROGRAM ELEMENT NO.
		11. CONTRACT/GRANT NO. 68-02-3323
12. SPONSORING AGENCY NAME AND ADDRESS U. S. Environmental Protection Agency Office of Air Quality Planning and Standards Source Receptor Analysis Branch (MD-14) Research Triangle Park, NC 27711		13. TYPE OF REPORT AND PERIOD COVERED Final
		14. SPONSORING AGENCY CODE EPA-450

15. SUPPLEMENTARY NOTES

16. ABSTRACT

The Industrial Source Complex (ISC) Model contains several new features not contained in other guideline atmospheric dispersion models. The important features are the gravitational setting/dry deposition option and the building wake effects option. Performance of the ISC Model is compared with that of CRSTER for a single source and MPTER for multiple sources. Results indicate that these model options significantly improve model performance. Additional suggestions for model improvement are discussed.

17. KEY WORDS AND DOCUMENT ANALYSIS

a. DESCRIPTORS	b. IDENTIFIERS/OPEN ENDED TERMS	c. COSATI Field/Group
Air Pollution	Industrial Sources	
Atmospheric Models	Deposition	
Meteorology	Downwash	
Turbulent Diffusion	Dispersion	

18. DISTRIBUTION STATEMENT Release Unlimited	19. SECURITY CLASS *(This Report)* Unclassified	21. NO. OF PAGES 260
	20. SECURITY CLASS *(This page)* Unclassified	22. PRICE

EPA Form 2220-1 (9-73)

A

EPA-450/4-81-002

An Evaluation Study for the Industrial Source Complex (ISC) Dispersion Model

by

J.F. Bowers and A.J. Anderson

H.E. Cramer Company, Inc.
University of Utah Research Park
Post Office Box 8049
Salt Lake City, Utah 84108

Contract No. 68-02-3323

EPA Project Officer: Sharon R. Kraft

Work Assignment No. 5

Prepared for

U.S. ENVIRONMENTAL PROTECTION AGENCY
Office of Air Quality Planning and Standards
Source Receptor Analysis Branch
Research Triangle Park, North Carolina 27711

January 1981

This document is issued by the Environmental Protection Agency to report technical data of interest to a limited number of readers. Copies are available free of charge to Federal employees, current contractors and grantees, and nonprofit organizations - in limited quantities - from the Library Services Office (MD 35), U.S. Environmental Protection Agency, Research Triangle Park, NC 27711; or, for a fee, from the National Technical Information Service, 5285 Port Royal Road, Springfield, VA 22161.

This report was furnished to the Environmental Protection Agency by H.E. Cramer Company, Inc., University of Utah Research Park, P.O. Box 8049, Salt Lake City, Utah 84108, in fulfillment of Contract No. 68-02-3323. The contents of this report are reproduced herein as received from H.E. Cramer Company, Inc. The opinions, findings, and conclusions expressed are those of the author and not necessarily those of the Environmental Protection Agency.

Publication No. EPA-450/4-81-002

ACKNOWLEDGEMENTS

We are indebted to the staff of the Source Receptor Analysis Branch, U. S. Environmental Protection Agency, Research Triangle Park, North Carolina for their assistance and technical guidance in carrying out the evaluation study for the Industrial Source Complex (ISC) Dispersion Model described in this report. Mr. George Schewe served as the EPA Project Officer for Work Assignment No. 5 of EPA Contract No. 68-02-3323 until May 1980 when he accepted a position with private industry. Following Mr. Schewe's departure from government service, Mr. Joseph Tikvart acted as EPA Project Officer for Work Assignment No. 5. Mr. Alan Huber assisted us in obtaining and evaluating some of the data sets used to test the ISC Model. Mr. Schewe, Mr. Tikvart, Mr. Huber and Mr. James Dicke all provided helpful technical guidance and suggestions during the study. We also wish to thank Mrs. Sharon Kraft, the current Project Officer for EPA Contract No. 68-02-3323, for her assistance in coordinating the review and publication of this report. Additionally, we are indebted to Dr. Warren B. Johnson of SRI International for providing a copy of the SRI report on the tracer study at the Millstone Nuclear Power Station and to Dr. R. A. Gaska and Mr. J. M. Brown of the DOW Chemical USA Michigan Division for supplying data from the DOW plant in Midland, Michigan.

In addition to the authors, other staff members of the H. E. Cramer Company, Inc. made important contributions to the preparation of this report. We are especially indebted to Mr. Craig Cheney and Mr. William Hargraves for their assitance in performing the computer calculations. All technical illustrations in this report were prepared by Mr. Kay Memmott. The report was typed by Ms. Sarah Barlow, Ms. Cherin Christensen, Ms. Leri Siedenstrang and Ms. Bonnie Swanson.

EXECUTIVE SUMMARY

(See PB80-133036)

INTRODUCTION

This report summarizes the results of an evaluation study for the new Industrial Source Complex (ISC) Dispersion Model (EPA, 1979). The ISC Model, which is designed to assess the air quality impact of emissions from large industrial source complexes, contains several features which are not contained in any of the dispersion models recommended in the current Guideline on Air Quality Models (EPA, 1978). The most important of these new features are the gravitational settling/dry deposition option and the building wake effects option. (The ISC Model's distance-dependent plume rise option is considered in this report to be an integral part of the building wake effects option.) Because many of the basic components of the ISC Model have been previously tested by EPA and others, the focus of the ISC Model evaluation study was on testing the key features which distinguish the model from the other generally available dispersion models. Three sets of published deposition experiments, three sets of published diffusion experiments and the source, meteorological and air quality data for a large industrial source complex were used to evaluate the performance of these key ISC Model features. It is important to note that the available data sets were not sufficient in number or detail to validate the new features of the ISC Model in a strict statistical sense. However, it was possible to compare the performance of the ISC Model with that of current models. For example, the ISC Model short-term program ISCST in its default mode corresponds to the Single Source (CRSTER) Model for a single source and to the MPTER Model for multiple sources. The results of the ISC Model evaluation study are briefly summarized in the following paragraphs. All of the concentration or deposition calculations described in this report were made using the ISCST program.

RATIONALE FOR MODEL TESTING

Insofar as possible, consistent procedures were used throughout the ISC Model evaluation study. However, the model tests made using the various data sets may at times appear to be inconsistent because the data sets themselves are inconsistent in the information available. Additionally, some of the calculations that were performed were in part determined by the available source-specific information such as visual observations of plume behavior. Because the observed concentration or deposition values were reported in a variety of normalized, crosswind-integrated and/or non-dimensional forms, we selected the following parameters as the primary measures of model performance: (1) the mean ratio (MR) of concurrent calculated to observed concentration or deposition values, (2) the root mean square error (RMSE) as defined by Draxler (1980), and (3) the percentage error bands. The MR is defined as

$$MR = \frac{\sum_{i=1}^{N} \chi_{ci}}{\sum_{i=1}^{N} \chi_{oi}} \qquad \text{(I)}$$

where χ_{ci} is the calculated concentration or deposition for the i^{th} trial and χ_{oi} is the corresponding observed concentration or deposition. Because air quality observations usually span more than one order of magnitude, Draxler (1980) uses a geometric form of the RMSE:

$$RMSE = \exp\left[\sum_{i=1}^{N} (\ell n\ \chi_{ci} - \ell n\ \chi_{oi})^2/N\right]^{1/2} \qquad \text{(II)}$$

The percentage error bands, as used in this study, are simply the percent of the trials with calculated concentration or deposition values within a factor of 2 of the corresponding observed values.

In the absence of any systematic errors in a dispersion model, the model inputs, or the observed concentration or deposition values, the MR should tend toward unity for a large sample size. Although inspection of Equation (II) shows that the RMSE also equals unity for a perfect model, uncertainties on a trial-by-trial basis in the model inputs as well as in the concentration or deposition measurements may significantly affect the RMSE. That is, the RMSE for a given data set is in part determined by the accuracy of the model and is in part determined by the quality of the model inputs and the concentration or deposition measurements. The percentage error bands are also significantly affected by the quality of the model inputs and the concentration or deposition measurements. However, the RMSE and the percentage error bands are convenient indicators of relative model performance for a given data set.

THE GRAVITATIONAL SETTLING/DRY DEPOSITION OPTION

The three sets of deposition experiments used to test the gravitational settling/dry deposition option of the ISC Model were the continuous, elevated releases of glass microspheres with diameters of 50 to 200 micrometers described by Walker (1965) and Stewart (1968) and the line-source aerial spray releases with droplet diameters ranging from 15 to 180 micrometers described by Boyle, et al. (1975). The premise of these tests was that, if the ISC Model can match observed deposition patterns, mass continuity requires that the model also match ambient particulate concentrations with gravitational settling and dry deposition occurring. The results of the ISC Model calculations for the Walker and Stewart data sets provide an indication of the model's accuracy when used to calculate ambient particulate concentration or dry deposition patterns attributable to stack or fugitive emissions comprised of particulates with gravitational settling velocities ranging from about 0.1 to 1.5 meters per second. Similarly, the results of the ISC Model calculations for the Boyle, et al. data set provide an indication of the model's accuracy when applied to particulate emissions with gravitational settling velocities ranging from about 0.01 to 0.5 meters per second.

Additionally, the results of the ISC Model calculations for the Boyle, et al. trials test the model's representation of a line source by multiple volume sources.

Table I summarizes the comparisons of concurrent calculated and observed maximum deposition values for the Walker (1965), Stewart (1968) and Boyle, et al. (1975) data sets. For the Walker and Stewart data sets, calculated and observed crosswind-integrated deposition (CWID) values are compared in Table I in order to remove from the deposition values the effects of differences in the duration of emissions for the various trials. Because the maximum deposition for the Boyle, et al. trials occurred near the center of the line source where edge effects are unimportant, crosswind integration of the calculated and observed deposition values was not necessary. The maximum observed deposition for all of the Boyle, et al. trials and the maximum observed CWID values for some of the Walker trials occurred at downwind distances of less than 100 meters. The ISC Model does not make deposition calculations at distances less than 100 meters. Consequently, Table I compares calculated and observed deposition values at 100 meters for the Boyle, et al. trials and calculated and observed CWID values at 100 meters for the Walker trials in which the observed maximum CWID values occurred at distances of less than 100 meters. Stewart gives only the maximum CWID values, and Table I considers only the Stewart trials with maximum observed CWID values at or beyond 100 meters. As indicated by the MR values in Table I, the ISC Model, on the average, predicts the maximum deposition to within 30 percent for all three data sets. Also, the RMSE values are less than 2.0 for all three data sets. The concurrent calculated and observed maximum CWID values are within a factor of 2 for all of the Stewart trials and for all but two of the Walker trials. Similarly, the concurrent calculated and observed deposition values at 100 meters for four of the five Boyle, et al. trials are within a factor of 2.

The good performance of the ISC Model when used to calculate maximum deposition values for the Walker, Stewart and Boyle, et al. data

TABLE I

SUMMARY OF THE RESULTS OF THE ISC MODEL CALCULATIONS FOR THE WALKER (1965), STEWART (1968) AND BOYLE, *ET AL.* (1975) DEPOSITION EXPERIMENTS

Data Set	No. of Trials	MR of Maximum Deposition Values*	RMSE of Maximum Deposition Values*	% Within a Factor of 2
Walker (1965)	12	0.71	1.57	83
Stewart (1968)	6	1.12	1.51	100
Boyle, *et al.* (1975)	5	0.91	1.89	80

*Crosswind-integrated deposition (CWID) for the Walker (1965) and Stewart (1968) trials and maximum deposition at 100 meters for the Boyle, *et al.* (1975) trials.

sets is in part explained by the relatively large gravitational settling velocities of the glass microspheres used by Walker and Stewart and of the larger droplets used by Boyle, et al. That is, the effects of atmospheric turbulence on the mixing of the microspheres and larger droplets to the surface were small in comparison with the effects of gravitational settling. For example, Figure I compares the calculated and observed deposition profiles for Boyle, et al. Trial 1-5. There is a close correspondence between the calculated and observed deposition profiles within about the first 800 meters where deposition was principally determined by the gravitational settling of the larger droplets. At longer downwind distances, the only droplets available for deposition were the smaller droplets which were affected by both gravitational settling and atmospheric turbulence. The calculated and observed deposition profiles show a secondary maximum between about 4 and 8 kilometers that is explained by the downward reflection of the smaller droplets at the top of the surface mixing layer. Although the correspondence between the calculated and observed magnitudes and locations of the secondary maximum is not exact, the calculated deposition generally is within a factor of 2 of the observed deposition at all downwind distances. A similar correspondence between calculated and observed deposition profiles was obtained for the four other Boyle, et al. trials.

THE BUILDING WAKE EFFECTS OPTION

The three sets of diffusion experiments used to test the building wake effects option of the ISC Model were the tracer releases at Millstone Nuclear Power Station (Johnson, et al., 1975), the tracer releases at the Materials Test Reactor Engineering Test Reactor (MTR-ETR) Complex (Islitzer, 1965) and the tracer releases at the CANDU Nuclear Power Generating Station (Munn and Cole, 1967). Additionally, the DOW Midland, Michigan plant's source, meteorological and air quality data, which were provided to the U. S. Environmental Protection Agency (EPA) for use in this study by DOW Chemical USA, were used to test the building wake effects option. The calculations for each data set were

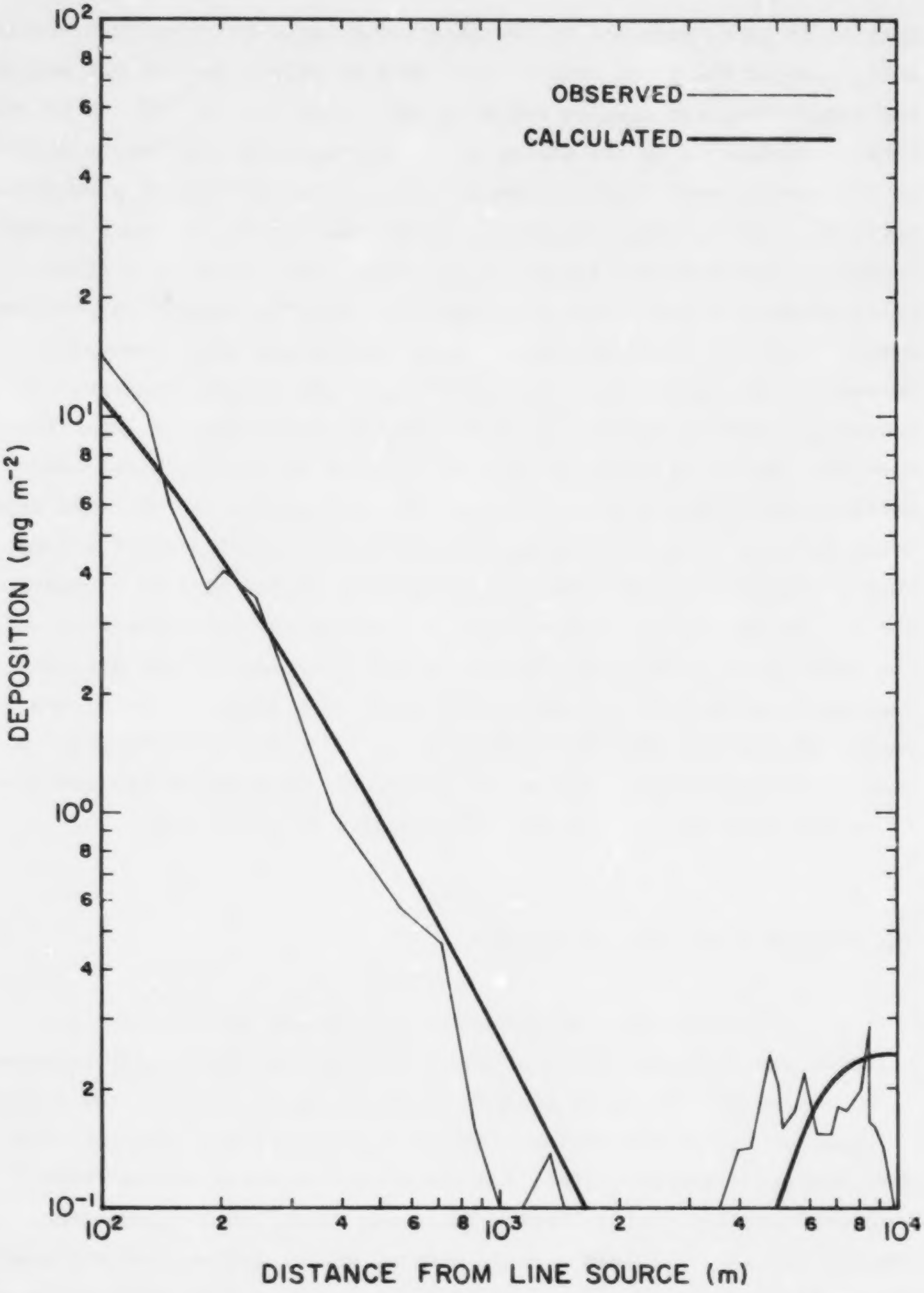

FIGURE I. Observed and calculated deposition profiles for Boyle, et al. (1975) Trial 1-5.

first performed without using the building wake effects or stack-tip downwash options to provide a reference for judging the effectiveness of these ISC Model features. The ISC Model calculations were then repeated using the building wake effects option. A third set of ISC Model calculations for the buoyant stack emissions combined the building wake effects and stack-tip downwash options.

The ISC Model building wake effects option enhances the initial rate of vertical dispersion if the plume height to building height ratio exceeds 1.2, but is less than 2.5, at a downwind distance of two building heights, where the plume rise used to determine the plume height is the rise due to momentum alone. If the plume height to building height ratio is less than or equal to 1.2, the ISC Model enhances both the initial rate of vertical dispersion and the initial rate of lateral dispersion. The dispersion coefficients calculated within the building wake region (three to ten building heights for a squat building and three to ten building widths for a tall building) are functions of the building dimensions and are independent of atmospheric stability. Thus, the ground-level concentrations calculated within the wake region are independent of stability. Table II summarizes the four data sets used to test the building wake effects option of the ISC Model. As shown by Table II, the results of the ISC Model calculations provide insight into the accuracy of the ISC Model when applied to either buoyant or non-buoyant industrial stack emissions subject to building wake effects and to non-buoyant low-level emissions subject to building wake effects.

The results of the tests of the building wake effects option of the ISC Model revealed that it is at times difficult to specify in advance the dimensions of buildings or groups of buildings affecting initial plume dispersion. The lateral dispersion coefficients (σ_y) measured in the building wake region for the Islitzer (1965) experiments were used to infer which buildings produced wakes affecting initial dispersion. The comparison of calculated and observed concentrations

TABLE II

SUMMARY OF THE DATA SETS USED TO TEST THE BUILDING WAKE EFFECTS OPTION OF THE ISC MODEL

Data Source	Type of Building*	Type of Release	Froude Number* $Fr = \frac{V_s^2}{g\left(\frac{T_s - T_a}{T_a}\right) d}$	Modified Dispersion Coefficients	
				Vertical	Lateral
Johnson, et al. (1975)	Squat ($1 \leq h_w/h_b \leq 5$) with $h/h_b \leq 1.2$	Elevated, Slightly Buoyant	>30	Yes	Yes
Islitzer (1965)	"Super-squat" ($h_w/h_b > 5$) with $h/h_b = 0$	Ground-level, Non-Buoyant	N/A	Yes	Yes
Munn and Cole (1967)	Squat ($1 \leq h_w/h_b \leq 5$) with $h/h_b \leq 1.2$	Elevated, Non-Buoyant	N/A	Yes	Yes
DOW Midland Plant	Squat ($1 \leq h_w/h_b \leq 5$) with $1.2 < h/h_b < 2.5$	Elevated, Buoyant	>3.0**	Yes	Yes

* The parameters used in the table are defined as follows: (1) h_w is the effective crosswind building width, (2) h_b is the building height, (3) h is the physical stack height above plant grade, (4) V_s is the stack exit velocity, (5) g is the acceleration due to gravity, (6) T_s is the stack exit temperature, (7) T_a is the ambient air temperature, and (8) d is the stack diameter.

** The full-load Froude numbers for all stacks exceed 3.0; however, because of the hour-to-hour variation in the stack exit velocities, Froude numbers as low as 0.1 occur with the DOW data set.

given below for Islitzer (1965) data set is based on the inferred building dimensions. With this exception, building dimensions were estimated following the general recommendations given in the ISC Model User's Guide.

Millstone Diffusion Experiments

Johnson, et al. (1975) summarize the results of tracer diffusion experiments conducted at Millstone Nuclear Power Station. The tracer SF_6 was released from the reactor building main vent and the tracer Freon-12B2 was simultaneously released from three vents on the adjacent turbine building. Sampling arcs were located at downwind distances of 350, 800, and 1500 meters. (The 350-meter sampling arc was within the building wake region.) The first set of ISC Model calculations that we performed assumed no building wake effects, which is equivalent to the Single Source (CRSTER) Model for the SF_6 trials and to the MPTER Model for the Freon trials. We then repeated the concentration calculations for the following combinations of ISC Model options:

- Case A - Distance-dependent plume rise and building wake effects options
- Case B - Distance-dependent plume rise, building wake effects and stack-tip downwash options

Additionally, concentrations were calculated under the assumption of surface-based emissions affected by building wakes (Case C) because of visual observations by Johnson, et al. that the plume often was intermittently entrained into the building's cavity zone and effectively acted as a ground-level source during these periods. The possible effects of intermittent entrainment into the cavity zone include enhanced vertical dispersion and reduced average plume heights.

Table III summarizes the comparisons of concurrent calculated and observed maximum centerline concentrations for the Millstone diffusion experiments. If the building wake effects option is not exercised (equivalent to current modeling techniques), the MR indicates that the model, on the average, underestimates the concentrations observed in the building wake region (i.e., at the 350-meter sampling arc) by an order of magnitude or more. The model's performance, as indicated by both the MR and the RMSE, is significantly improved if building wake effects are included in the model calculations for Cases A and B (the elevated releases). However, the MR indicates that the model has a systematic tendency to underestimate concentrations at all three sampling arcs for Cases A and B. The assumption of surface-based emissions affected by building wakes (Case C) yields the best overall model performance.

The systematic tendency of the ISC Model to underpredict concentrations near the source for the Millstone diffusion experiments could be a result of errors in the lateral dispersion coefficients, errors in the vertical dispersion coefficients, errors in the effective plume heights or a combination of these factors. A comparison of the lateral dispersion coefficients calculated with building wake effects included and the corresponding coefficients estimated from the concentration measurements by Johnson, et al. showed the calculated lateral dispersion coefficients to be less than or equal to the observed values. It follows that the ISC Model's underpredictions of concentrations near the source for the Millstone diffusion experiments are most likely caused by errors in the plume heights, vertical dispersion coefficients or both. Although no vertical concentration profiles are available for the Millstone experiments, the visual observations of plume behavior made by Johnson, et al during the experiments indicate that the hourly average effective emission height during most of the trials was intermediate between the release height and the ground surface. Also, the results of the model calculations for Case C suggest that the intermittent

TABLE III

SUMMARY OF THE RESULTS OF THE ISC MODEL CALCULATIONS FOR THE MILLSTONE DIFFUSION EXPERIMENTS (JOHNSON, ET AL., 1975)

Tracer	Sampling Distance (m)		
	350	800	1500
(a) Mean Ratio (MR) of Calculated to Observed Concentrations			
SF_6*			
No Buildings	0.00	0.18	0.62
Buildings: Case A	0.33	0.46	0.73
Buildings: Case B	0.33	0.46	0.74
Buildings: Case C	0.66	0.74	1.09
Freon-12B2**			
No Buildings	0.14	0.62	0.84
Buildings: Case A	0.47	0.55	0.68
Buildings: Case B	0.48	0.55	0.68
Buildings: Case C	0.74	0.72	0.83
(b) Root Mean Square Error (RMSE)			
SF_6*			
No Buildings	259.90	9.38	2.88
Buildings: Case A	3.17	2.31	1.79
Buildings: Case B	3.09	2.28	1.78
Buildings: Case C	2.06	1.83	1.88
Freon-12B2**			
No Buildings	19.76	5.07	1.94
Buildings: Case A	2.20	1.89	1.69
Buildings: Case B	2.12	1.88	1.68
Buildings: Case C	1.53	1.64	1.64
(c) Percent Within a Factor of 2			
SF_6*			
No Buildings	0	8	67
Buildings: Case A	31	42	83
Buildings: Case B	28	42	78
Buildings: Case C	56	86	83
Freon-12B2**			
No Buildings	0	77	81
Buildings: Case A	38	73	88
Buildings: Case B	38	73	88
Buildings: Case C	85	88	88

*The sample size is 36.
**The sample size is 26.

entrainment into the cavity zone, which currently is not fully accounted for by the ISC Model, may be the primary cause of the model's tendency to underestimate concentrations near the source for the Millstone diffusion experiments.

We point out that the majority of the Millstone diffusion experiments were conducted under very similar meteorological conditions (moderate or strong south-southwest winds in combination with the neutral Pasquill D stability category). Also, the upwind fetch was over water. Thus, the Millstone data set may represent a unique combination of source and meteorological factors. Additionally, the turbulent intensities, especially the vertical turbulent intensities, measured during the Millstone experiments generally were smaller than the median vertical turbulent intensities implicit in the Pasquill-Gifford dispersion coefficients used by the ISC Model. If these smaller vertical turbulent intensities apply, the vertical expansion is reduced and this may account for the model's tendency to underestimate centerline concentrations even when surface-based emissions are assumed (Case C).

MTR-ETR Complex Tracer Releases

Islitzer (1965) provides the results of ground-level non-buoyant tracer releases made downwind from the MTR-ETR Complex. Samplers were placed at downwind distances of 118, 350, 550 and 850 meters from the release point. The meteorological data available for the Islitzer tests are not sufficient to use the Turner (1964) stability classification scheme, the stability classification scheme routinely used with the ISC Model. Consequently, the Nuclear Regulatory Commission's vertical temperature difference (ΔT) and wind-direction standard deviation (σ_A) stability classification schemes were used to estimate the stability during each test. The Pasquill stability categories indicated for a given test by the two schemes differed by as many as six categories. However, with the exception of Test 7, one or both of the schemes indicated the very unstable Pasquill A stability category during all of the tests.

Table IV summarizes the comparisons of concurrent calculated and observed centerline concentrations for the Islitzer (1965) tests assuming that the Pasquill A stability category existed during all of the tests. The 118-meter sampling distance is within the wake region of the MTR-ETR Complex (i.e., between three and ten building heights downwind) where the calculated concentrations are entirely determined by building wake effects. As shown by the MR in Table IV, the inclusion of building wake effects in the model calculations improves the average correspondence between calculated and observed concentrations by almost a factor of 2. Also, the RMSE is decreased from 2.7 to 2.0, and the number of calculated concentrations within a factor of 2 of the corresponding observed concentrations is almost doubled. Under very unstable meteorological conditions (the Pasquill A stability category), the calculated effects of atmospheric turbulence on plume dispersion become far more important than the calculated effects of building wakes within a relatively short downwind distance. Thus, the concentrations calculated by the ISC Model at the 350-, 550- and 850-meter sampling distances are primarily determined by atmospheric turbulence and are not significantly affected by building wakes.

CANDU Nuclear Power Station Tracer Releases

Eleven tracer releases are described by Munn and Cole (1967), but only four of the tests were suitable for use in evaluating the ISC Model. The single sampling arc for six of the eleven elevated, non-buoyant tracer releases was within three building heights downwind (i.e., within the building's cavity zone) where the ISC Model does not calculate ground-level concentrations. Additionally, there is strong circumstantial evidence that the plume centerline missed the sampling arc during one of the five remaining trials in which the samplers were placed in the building wake region between three and ten building heights downwind.

TABLE IV

SUMMARY OF THE RESULTS OF THE ISC MODEL CALCULATIONS FOR THE ISLITZER (1965) TESTS ASSUMING A STABILITY FOR ALL TESTS

Downwind Distance (m)	No. of Valid Samples	MR of Centerline Concentrations		RMSE of Centerline Concentrations		% Within Factor of 2	
		No Bldgs	Bldgs	No Bldgs	Bldgs	No Bldgs	Bldgs
118	11	1.94	1.09	2.74	1.97	36	64
350	10	1.87	1.87	2.34	2.34	40	40
550	10	1.41	1.26	1.94	1.82	50	60
850	9	0.78	0.72	1.86	1.90	67	50

Table V summarizes the results of the comparisons of the calculated centerline concentrations and the corresponding maximum observed concentrations for the four Munn and Cole (1967) trials we determined were suitable for use for the reasons given above. (Because of the separation between samplers, the highest observed concentrations were not necessarily measured at the plume centerline.) The results presented in Table V illustrate the sensitivity of concentrations calculated in the wake region to different assumptions about the buildings with wakes affecting initial plume dispersion. However, whether or not the reactor building or all buildings are assumed to have affected initial plume dispersion, the overall model performance is significantly improved by the inclusion of building wake effects in the model calculations.

DOW Chemical Midland, Michigan Plant

The DOW Chemical USA Michigan Division plant in Midland, Michigan includes two power houses with large sulfur dioxide (SO_2) emissions. The DOW Midland plant currently uses a Supplementary Control System (SCS) to maintain the National Ambient Air Quality Standards (NAAQS) for SO_2. Because the plant's SCS curtails emissions whenever high ground-level SO_2 concentrations are anticipated or observed, the SO_2 emissions from the two power houses are highly variable. The air quality impact of the plant is measured by nine continuous SO_2 monitors. The DOW data set used to test the building wake effects option of the ISC Model consisted of the source, meteorological and air quality data for 90 hours which were selected for model testing because of the occurrence of high ground-level SO_2 concentrations in combination with meteorological conditions conducive to adverse building wake effects on plume dispersion. We point out that uncertainties in the source, meteorological and air quality data for the DOW data set tend to be larger than for the three sets of published diffusion experiments discussed above because the DOW data were compiled from routine records of plant

TABLE V

SUMMARY OF THE RESULTS OF THE ISC MODEL CALCULATIONS FOR THE MUNN AND COLE (1967) TRIALS*

Case	Mean Ratio of Calculated to Observed Concentrations (MR)	Root Mean Square Error (RMSE)	% of Centerline Concentrations within a Factor of 2 of Highest Observed Concentrations
No Buildings	0.01	176.84	0
Reactor Building	1.79	2.47	50
All Buildings	0.99	1.79	75

*Sample size is 4.

operations. Additionally, uncertainties about the locations of the plume centerlines arising from the uncertainties about the mean transport wind directions, which are not present in the data from the diffusion experiments because the locations of the plume centerlines were defined by the monitoring networks, cannot be removed from the DOW data set. Thus, the RMSE values for the DOW data set are expected to be much larger than for the diffusion experiments. Similarly, the percent of calculated concentrations within a factor of 2 of the corresponding observed concentrations is expected to be much smaller for the DOW data set than for the diffusion experiments.

Table VI summarizes the results of comparisons of concurrent calculated and observed 1-hour SO_2 concentrations for the 143 observed concentrations greater than or equal to 0.10 parts per million (ppm) during the 90 hours selected for model testing. As shown by the table, six combinations of ISC Model options were applied to the DOW data set. On the basis of a site survey of the DOW Midland plant, Urban Mode 2 was included in the model calculations (Combinations 4, 5 and 6 in Table VI) because the presence of numerous large roughness elements (buildings) at the plant indicated the possibility of enhanced turbulent intensities in the vicinity of the plant. Whether or not building wake effects are included in the ISC Model calculations, the correspondence between calculated and observed concentrations obtained in Urban Mode 2 is superior to that obtained in the Rural Mode. This result supports the hypothesis of enhanced turbulence at the DOW plant. Although the building wake effects and stack-tip downwash options improve the model's performance in both the Rural Mode and Urban Mode 2, the MR values suggest that there may be errors in the model inputs or a bias in the ISC Model towards underestimating concentrations for the DOW data set.

We are not certain that the MR, RMSE and percentage error bands are the most appropriate measures of model performance for the DOW data set because the density of the monitoring network is inadequate to deter-

TABLE VI

SUMMARY OF THE RESULTS OF THE ISC MODEL CALCULATIONS FOR THE DOW DATA SET FOR SIX COMBINATIONS OF ISC MODEL OPTIONS*

Model Option Combination Number	ISC Model Mode	Briggs (1973) Stack-Tip Downwash	Bldg. Wake Effects	Measures of Model Performance		
				MR	RMSE	% Within Factor of 2
1	Rural	No	No	0.15	12.37	10
2	Rural	No	Yes	0.31	8.79	29
3	Rural	Yes	Yes	0.37	8.34	34
4	Urban 2	No	No	0.48	4.55	46
5	Urban 2	No	Yes	0.54	4.43	48
6	Urban 2	Yes	Yes	0.58	4.19	49

*The sample size is 143.

mine the locations of the plume centerlines. The current Guideline on Air Quality Models (EPA, 1978) suggests that, as an alternative to direct comparisons of concurrent calculated and observed concentrations, short-term dispersion models may be evaluated by comparing the upper percentiles of the calculated and observed concentration frequency distributions. Additionally, Turner (1979) observes that a comparison of the maximum concentration observed at any point with the maximum concentration calculated at any point is of interest for regulatory purposes. We therefore used the results of the concentration calculation for model option Combinations 1 and 6 in Table VI to generate the cumulative frequency distributions of calculated and observed hourly SO_2 concentrations for the DOW data set shown in Figure II. We point out that the concentrations calculated by the ISCST program for model option Combination 1 are the same as calculated by conventional modeling techniques (for example, the MPTER Model). As shown by the figure, the upper end of the observed concentration frequency distribution is much more closely matched by ISCST for Combination 6 than by ISCST for Combination 1. It should be emphasized that the hourly concentrations used to form the observed concentration frequency distribution shown in Figure II were restricted to concentrations greater than or equal to 0.10 ppm. Thus, the observed concentration frequency distribution reflects the presence at the monitors of emissions from one or both of the DOW power houses during every hour. However, if the wind directions used as input to the model are assumed to be representative of the winds defining plume trajectories during every hour, the wind directions imply that emissions from one or both of the DOW power houses were not present at the monitors during every hour. Thus, it is not unexpected that the ISC Model underpredicts the lower end of the observed concentration frequency distribution in Figure II.

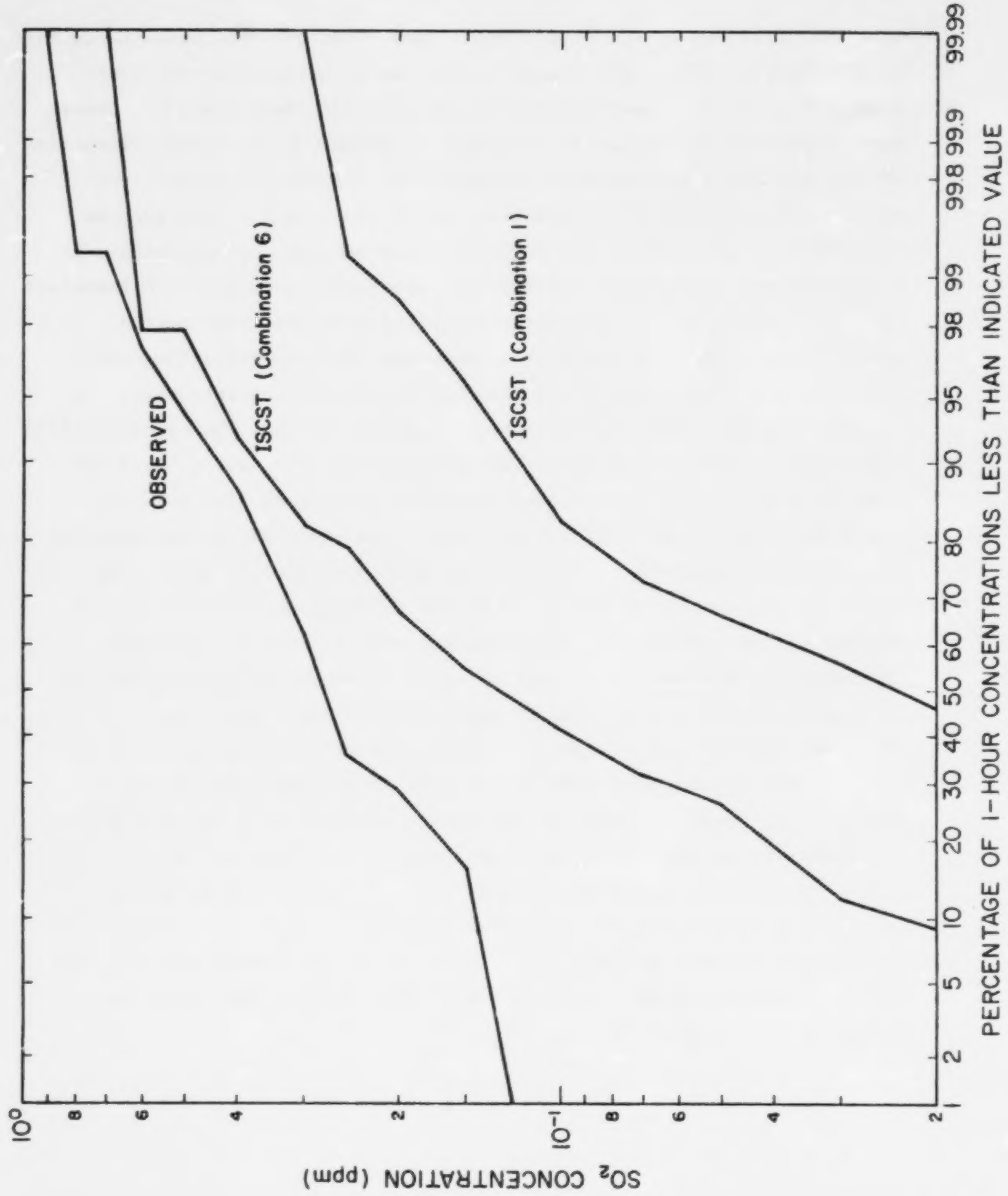

FIGURE 11. Comparison of calculated and observed cumulative 1-hour SO$_2$ concentration frequency distributions for the DOW data set.

CONCLUSIONS AND SUGGESTIONS FOR MODEL IMPROVEMENT

We conclude from the tests described in this report of the key features which distinguish the ISC Model from other generally available dispersion models that:

1. The gravitational settling/dry deposition option adds capabilities lacking in most current models, and the accuracy of this option for particulates with appreciable gravitationsl settling velocities appears to correspond to the approximate factor of 2 accuracy generally attributed to the results of short-term dispersion model calculations in the absence of complicating factors (AMS, 1978).

2. For plumes subject to building wake effects, the building wake effects option significantly improves the performance of the ISC Model over that of the corresponding models (CRSTER and MPTER) that do not consider building wake effects when used to calculate concentrations near the source.

However, the results of the model calculations for the Millstone data set indicate that it may be desirable to modify the model to consider a reduction in plume height due to initial entrainment into the cavity zone for stacks on or adjacent to squat buildings with stack height to building height ratios less than 1.2

The best overall model performance for the Millstone data set was obtained for Case C (see Table III), and essentially the same performance can be achieved by adding to the ISC Model the following definition of the effective emission height for the insignificantly buoyant plume from a stack on or adjacent to a squat building with a stack height to building ratio less than 1.2:

$$H\{x\} = \left\{ \begin{array}{ll} h + \Delta h\{x\} & ; \quad h + \Delta h_m\{2h_b\} \geq 1.2\ h_b \\ \\ 0 & ; \quad h + \Delta h_m\{2h_b\} < 1.2\ h_b \end{array} \right\} \qquad \text{(III)}$$

where

$H\{x\}$ = effective emission height at downwind distance x

h = physical stack height

$\Delta h\{x\}$ = plume rise due to momentum and/or buoyancy at downwind distance x, calculated by Equation (2-4) or Equation (2-7) in the ISC Model User's Guide

$\Delta h_m\{2h_b\}$ = plume rise due to momentum alone at a downwind distance of $2h_b$, where h_b is the building height

As explained above, we believe that the ISC Model's tendency to underestimate concentrations for Case C, as indicated by the MR, may be attributed to vertical turbulent intensities that are smaller than the median values associated with the Pasquill-Gifford vertical dispersion coefficients used by the model. It should be noted that the addition of Equation (III) to the ISC Model will have no effects on the model's performance for the DOW data set because the stack height to building height ratios exceed 1.2.

The results of the ISC Model calculations given in Table VI for the DOW data set indicate that the model's building wake effects option may have a systematic tendency to underestimate the concentrations produced near the source by buoyant stack emissions subject to building wake effects. As part of the ISC Model evaluation study, we added the Cramer, et al. (1975) stack-tip downwash correction and the Scire and

Schulman (1980) "downwash radius" correction to special versions of the ISCST program and repeated the concentration calculations for the DOW data set. Both corrections improved the model's performance as indicated by the MR, RMSE and percentage error bands. However, as noted above, the MR, RMSE and percentage error bands may not be the most appropriate measures of model performances for the DOW data set because the uncertainties about the locations of the plume centerlines arising from the uncertainties in the mean transport wind directions cannot be removed from the DOW data set, as was done in the diffusion experiments, because the density of the DOW monitoring network is inadequate for fixing the locations of the plume centerlines. It is not possible, from a comparison of the upper percentiles of calculated and observed concentration frequency distributions, to determine whether or not either of the two corrections significantly improves the model's performance for the DOW data set.

TABLE OF CONTENTS

Section Title Page

DISCLAIMER ii

ACKNOWLEDGEMENTS iii

EXECUTIVE SUMMARY iv

1 INTRODUCTION 1-1

1.1 Background and Purpose 1-1
1.2 Review, Evaluation and Selection of Candidate Data Sets 1-2
1.3 Rationale for Model Testing 1-3
1.4 Report Organization 1-6

2 TESTS OF THE GRAVITATIONAL SETTLING AND DRY DEPOSITION OPTION 2-1

2.1 Walker (1965) Depositon Experiments 2-1
2.2 Stewart (1968) Deposition Experiments 2-15
2.3 Boyle, et al. (1975) Aerial Spray Experiments 2-22

3 TESTS OF THE AERODYNAMIC WAKE EFFECTS OPTION 3-1

3.1 Millstone Nuclear Power Station Tracer Experiments (Johnson, et al., 1975) 3-2
3.2 Islitzer (1965) Tracer Releases 3-33
3.3 Munn and Cole (1967) Tracer Releases 3-50
3.4 Dow Midland, Michigan Plant Data 3-56

4 SUGGESTIONS FOR MODEL IMPROVEMENT 4-1

5 CONCLUSIONS 5-1

REFERENCES 6-1

Appendix

A CALCULATED AND OBSERVED DEPOSITION PROFILES FOR THE WALKER (1965) AND STEWART (1968) EXPERIMENTS A-1

SECTION 1
INTRODUCTION

1.1 BACKGROUND AND PURPOSE

The Industrial Source Complex (ISC) Dispersion Model (EPA, 1979) was developed by the H. E. Cramer Company, Inc. under Contracts 68-02-2547 and 68-02-3323 with the Source Receptor Analysis Branch (SRAB) of the U. S. Environmental Protection Agency (EPA). The ISC Model, which is designed to evaluate the air quality impact of emissions from large industrial source complexes, consists of two computer programs, one for short-term impact analyses and one for long-term impact analyses. The ISC Model short-term program ISCST, an advanced version of the Single Source (CRSTER) Model (EPA, 1977), is designed to use sequential hourly meteorological data to calculate ground-level concentration or dry deposition patterns for time periods ranging from 1 hour to 1 year. The ISC Model long-term program ISCLT, which combines and updates basic features of the Air Quality Display Model (EPA, 1969) and the Climatological Dispersion Model (Busse and Zimmerman, 1973), is designed to use statistical summaries of wind-speed and wind-direction categories, classified according to the Pasquill stability categories, to calculate seasonal and annual concentration or dry deposition values.

The ISC Model programs contain the following special features: (1) physical separation of multiple sources; (2) plume rise due to momentum and buoyancy as a function of downwind distance; (3) effects of aerodynamic building wakes on plume dispersion; (4) effects of stack-tip downwash on plume dispersion; (5) emissions from stack, area, volume and line sources; (6) effects of gravitational settling and dry deposition; (7) effects of variations in terrain height on ground-level concentrations ("full terrain adjustment") for receptors with elevations less than the stack top elevation; and (8) time-dependent exponential decay of pollutants.

Many of the basic components of the ISC Model have been previously tested by EPA (for example, Turner et al., 1972 and Lee, et al., 1975) and others. However, the ISC Model includes several dispersion model options (the building wake effects and gravitational settling/dry deposition options) that are not contained in any of the models currently recommended in the Guideline on Air Quality Models (EPA, 1978). Consequently, it is necessary to test these new features. The purpose of this report is to describe the results of an evaluation study in which these key ISC Model features were tested. *This report assumes that the reader is familiar with the detailed technical description of the ISC Model given in Section 2 of the Industrial Source Complex (ISC) Dispersion Model User's Guide (EPA, 1979).*

1.2 REVIEW, EVALUATION AND SELECTION OF CANDIDATE DATA SETS

A primary consideration in the review and evaluation of candidate data sets for use in the ISC Model evaluation study was to select data sets that would provide a test of one or more of the key features of the ISC Model. During the summer of 1978, an extensive review of published data sets was conducted to determine which data sets might be suitable for use in the ISC Model evaluation study. The selection criteria were as follows:

- Basic requirements -- simple terrain, absence of extraneous sources in the vicinity (unless their effects can be reliably quantified), reliable and sufficient air quality data (including background), reliable emissions data and representative meteorological data

- ISC Model requirements -- the source must exhibit one or more of the key ISC Model features listed in Section 1.1 above, adequate input data must exist for considering the feature (s) in the model calculations (for example, particulate size data, building dimensions, etc.) and air quality data must be sufficient to reflect the effect(s) of the complicating feature(s)

The review of the published data sets revealed that, in many cases, the published source, meteorological and concentration or deposition data lacked the detail required for model testing. Also, several excellent data sets collected at nuclear power plants (for example, Halitsky and Woodard, 1974 and Start, et al., 1977) reflected meteorological conditions that masked building wake effects so that the data were not suitable for testing the ISC Model building wake effects option. Table 1-1 lists the data sets that were found to be suitable for use in the ISC Model evaluation study. In addition to published data, Table 1-1 includes the data that were provided for use in this study by DOW Chemical USA for the Michigan Division plant in Midland, Michigan. As shown by Table 1-1, each unique ISC Model feature discussed in Section 1.1 is included in at least one of the selected data sets. Direct measurements of plume rise and stack-tip downwash are not available for any of the data sets. However, comparisons of calculated and observed concentrations for some of the data sets provide indirect tests of these ISC Model features.

It is important to note that the data sets listed in Table 1-1 are not sufficient in number or detail to validate the new features of the ISC Model in a strict statistical sense. However, the data sets provide a basis to evaluate the performance of these new features. Also, the data sets enable a comparison of the performance of the ISC Model with that of current models. For example, the ISC Model short-term program ISCST in its default mode corresponds to the Single Source (CRSTER) Model for a single source and to the MPTER Model (Pierce and Turner, 1980) for multiple sources.

1.3 RATIONALE FOR MODEL TESTING

Insofar as possible, consistent procedures were used throughout the ISC Model evaluation study. However, the model tests made using the various data sets may at times appear to be inconsistent because the data sets themselves are inconsistent in the information available. Additionally,

TABLE 1-1

DATA SETS SELECTED FOR USE IN THE ISC MODEL EVALUATION STUDY

Data Source	ISC Model Feature(s)
Walker, 1965	Gravitational settling and dry deposition
Stewart, 1968	Gravitational settling and dry deposition
Boyle, *et al.*, 1975	Gravitational settling and dry deposition; volume source representation of a line source
Islizter, 1965	Aerodynamic wake effects
Munn and Cole, 1967	Aerodynamic wake effects
Johnson, *et al.*, 1975	Aerodynamic wake effects; stack-tip downwash; plume rise as a function of downwind distance; and separation of multiple sources
DOW Chemical USA Michigan Division	Aerodynamic wake effects; stack-tip downwash; plume rise as a function of downwind distance; and separation of multiple sources

some of the calculations that were performed were in part determined by the available source-specific information such as visual observations of plume behavior. Because the observed concentration or deposition values were reported in a variety of normalized, crosswind-integrated and/or non-dimensional forms, we selected the following parameters as the primary measures of model performance: (1) the mean ratio (MR) of concurrent calculated to observed concentration or deposition values, (2) the root mean square error (RMSE) as defined by Draxler (1980), and (3) the percentage error bands. The MR is defined as

$$\mathrm{MR} = \frac{\sum_{i=1}^{N} \chi_{ci}}{\sum_{i=1}^{N} \chi_{oi}} \tag{1-1}$$

where χ_{ci} is the calculated concentration or deposition for the i^{th} trial and χ_{oi} is the corresponding observed concentration or deposition. Because air quality observations usually span more than one order of magnitude, Draxler (1980) uses a geometric form of the RMSE:

$$\mathrm{RMSE} = \exp\left[\sum_{i=1}^{N} (\ell n\ \chi_{ci} - \ell n\ \chi_{oi})^2/N\right]^{1/2} \tag{1-2}$$

The percentage error bands, as used in this study, are simply the percent of the trials with calculated concentration or deposition values within a factor of 2 of the corresponding observed values.

In the absence of any systematic errors in a dispersion model, the model inputs, or the observed concentration or deposition values, the MR should tend toward unity for a large sample size. Although inspection of Equation (1-2) shows that the RMSE also equals unity for a perfect model, uncertainties on a trial-by-trial basis in the model inputs as well as in the concentration or deposition measurements may significantly affect the RMSE. That is, the RMSE for a given data set is in part determined by the accuracy of the model and is in part determined by the quality of the model inputs and the concentration or deposition measurements. The percentage error bands are also significantly affected by the quality of the model inputs and the concentration or deposition measurements. However, the RMSE and the percentage error bands are convenient indicators of relative model performance for a given data set.

1.4 REPORT ORGANIZATION

The unique features of the ISC Model may be grouped into two general categories: (1) the gravitational settling/dry deposition option, and (2) the building wake effects option. The results of tests of the gravitational settling and dry deposition option, made using the Walker (1965), Stewart (1968) and Boyle, _et al_. (1975) data sets, are described in Section 2. The Boyle, _et al_. data also provide a test of the ISC Model representation of an elevated line source with initial source dimensions. The results of tests of the building wake effects option, made using the Johnson, _et al_. (1975), Islitzer (1965), Munn and Cole (1967) and DOW data sets, are discussed in Section 3. The Johnson, _et al_. and DOW data also include the effects of the physical separation of multiple sources and are used to illustrate the effects on calculated ground-level concentrations of the generalized plume rise equations and the stack-tip downwash option. Section 4 discusses possible improvements to the ISC Model. The study conclusions are given in Section 5. The deposition profiles for the Walker (1965) and Stewart (1968) experiments are presented in Appendix A.

SECTION 2

TESTS OF THE GRAVITATIONAL SETTLING AND DRY DEPOSITION OPTION

Three sets of deposition experiments (Walker, 1965; Stewart, 1968; and Boyle, et al., 1975) were used to test the gravitational settling and dry deposition option of the ISC Model. The premise of the tests was that, if the ISC Model can match observed deposition patterns, the ISC Model can also be expected to match ambient concentrations with gravitational settling and dry deposition occurring because of mass continuity. The tests made using the Walker and Stewart data sets, both of which involved continuous, elevated releases of glass microspheres, are discussed in Sections 2.1 and 2.2, respectively. Section 2.3 discusses the use of the deposition data from the aerial spray releases reported by Boyle, et al. to test both the ISC Model gravitational settling and dry deposition option and the ISC Model line source representation.

2.1 WALKER (1965) DEPOSITION EXPERIMENTS

Walker (1965) summarizes the results of twelve 30-minute to 60-minute continuous, elevated releases of solid glass spheres. The experiments were conducted at the Suffield Experimental Station in Ralston, Alberta, Canada. The emission heights were 15 and 7.42 meters, and the diameters of the glass spheres ranged from 56 to 107 micrometers. Samples were collected on sticky paper at radial distances of 27.4, 45.7, 73.2, 86.9, 100.6, 114.3, 128.0, 146.3, 201.2, 274.3, 402.3 and 804.6 meters. The angular separation between sampling locations was 3.6 degrees. (No illustration of the experimental layout is provided by Walker.) For each trial and downwind distance, Walker gives the standard deviation of the crosswind deposition pattern σ_y in radians and the crosswind-integrated deposition (CWID), divided by the total emissions Q_T. The source data for the Walker experiments are discussed in Section 2.1.1, the meteorological data are discussed in Section 2.1.2, and the ISC Model calculation procedures and results are given in Section 2.1.3.

2.1.1 Source Data

During the deposition experiments described by Walker (1965), solid glass spheres were emitted from a continuous elevated point source with no buoyancy and minimal momentum. Three sizes of glass spheres were used. For Trials A through F, the mass mean diameter of the glass spheres was 107 micrometers and the density was 2.4 grams per cubic centimeter. For Trials G, H, I and L, the mass mean diameter was 56 micrometers and the density was 2.2 grams per cubic centimeter. For Trials J and K, the mass mean diameter was 49 micrometers and the density was 2.0 grams per cubic centimeter. Walker gives terminal fall velocities V_{sn} of 0.58, 0.19 and 0.14 meters per second, respectively, for the 107-, 56- and 49-micrometer spheres. We computed terminal fall velocities for the three sphere sizes using the methods of McDonald (1960) and found very good agreement with the values given by Walker. We estimated the surface reflection coefficient γ_n for the three sphere sizes from Figure 2-8 of the ISC Model User's Guide. During Trials A through F, the glass spheres were emitted at a height of 15 meters above the ground. The height of emission from Trials G through L was 7.42 meters. The source parameters for all twelve trials are given in Table 2-1. For each trial, these parameters include the date, the start time, the duration of the trial, the total weight of the glass spheres emitted, the settling velocity and the surface reflection coefficient.

2.1.2 Meteorological Data

Walker (1965) gives the mean wind speed, mean wind direction and ambient air temperature for each of the twelve deposition experiments. Wind speeds were measured on a tower at heights of 0.5, 1.0, 2.0, 4.0 and

TABLE 2-1

METEOROLOGICAL PARAMETERS FOR THE WALKER (1965) EXPERIMENTS

Trial	Date	Start Time (MST)	Duration (min.)	Amount Emitted Q_τ (g)	Settling Velocity V_{sn} (m/sec)	Emission Height h (m)	Reflection Coefficient γ_n
A	26 Feb 59	1950	30	152.7	0.58	15.0	0
B	15 Mar 60	1851	60	221.8	0.58	15.0	0
C	9 Jan 59	1120	60	427.5	0.58	15.0	0
D	9 Jan 59	1530	44	497.0	0.58	15.0	0
E	1 Sep 59	1127	49	261.2	0.58	15.0	0
F	27 Nov 59	1225	60	138.5	0.58	15.0	0
G	27 Feb 64	1715	30	35.5	0.19	7.42	0.27
H	12 Nov 63	1519	56	32.8	0.19	7.42	0.27
I	13 Jan 64	1532	30	22.3	0.19	7.42	0.27
J	15 Oct 59	1407	60	51.6	0.14	7.42	0.40
K	20 Aug 59	1100	30	33.9	0.14	7.42	0.40
L	2 Oct 61	1130	45	52.9	0.19	7.42	0.27

8.0 meters during all trials and at 16.0 meters during Trials A through F. For each trial, Walker gives the mean wind speed at each tower level and for the layer between the emission height and the surface. We used a logarithmic least-squares regression technique with the tower wind speed measurements to calculate a wind-profile exponent p for each trial. The Pasquill stability category was estimated for each trial using the Turner (1964) criteria, which are based on wind speed and solar radiation (insolation). Insolation indices were estimated on the basis of the dates and times of the various trials. The 9-meter wind speeds were used in determining the stability category because this level is closest to both the airport wind measurement height used by the Turner (1964) stability classification scheme and the 10-meter measurement height used by the original Pasquill (1961) scheme. Because of the low emission heights and relatively short distances to the sampling arcs, the depth of the surface mixing layer did not significantly affect the results of any of the trials. Consequently, unrestricted vertical mixing was assumed for all of the Walker trials.

Table 2-2 lists, for each of the twelve trials, the meteorological input parameters required to apply the ISC Model short-term computer program ISCST to the Walker trials. The ambient air temperature and vertical potential temperature gradient are used by the ISC Model to calculate plume rise. Because the experiments described by Walker involved non-buoyant emissions with essentially no initial vertical momentum and no plume rise, estimates of the vertical potential temperature gradients and measurements of the ambient air temperatures for the Walker trials are not given in Table 2-2. All of the trials were conducted under neutral (D stability) conditions. As explained in Section 2.1.3, the ISC Model deposition calculations were performed in two ways. First, the mean wind speed at the measurement height nearest the emission height (shown as $\bar{u}(h)$ in Table 2-2) was used as the reference wind speed and was adjusted to the emission height using the observed wind-profile exponent.

TABLE 2-2

METEOROLOGICAL PARAMETERS FOR THE WALKER (1965) EXPERIMENTS

Trial	Average Flow Vector (Deg)*	Wind Speed		Wind Profile Exponent	Pasquill Stability Category
		$\bar{u}_L$**	$\bar{u}(h)$***		
A	070	5.53	7.65	0.34	D
B	125	6.19	7.64	0.22	D
C	010	6.06	7.39	0.23	D
D	010	5.52	6.96	0.26	D
E	130	8.20	9.14	0.16	D
F	005	4.87	5.65	0.20	D
G	078	2.43	2.56	0.32	D
H	289	4.96	6.29	0.21	D
I	025	2.78	4.09	0.32	D
J	155	5.98	7.13	0.20	D
K	065	5.58	6.54	0.18	D
L	060	7.37	8.89	0.18	D

*Direction toward which the wind is blowing.

**Mean wind speed for the layer from the surface to the emission height.

***Mean wind speed at the measurement height nearest the emission height.

Second, the mean layer wind speed (shown as $\bar{u}_L$ in Table 2-2) was used as the reference wind speed and the wind-profile exponent was set equal to zero.

2.1.3 Calculation Procedures and Results

The source data given in Section 2.1.1 and the meteorological data given in Section 2.1.2 were used with the ISC Model short-term computer program ISCST in the Rural Mode to calculate, for each trial, the total deposition along the plume centerline at the sampling distances and at several intermediate distances to aid in defining the distribution of the deposited glass spheres. For each trial, the calculated centerline deposition values were then multiplied by $\sqrt{2\pi}\,\sigma_y$, where σ_y is the lateral dispersion coefficient, and divided by the amount of material emitted Q_τ to obtain a profile of the calculated normalized crosswind-integrated deposition $CWID/Q_\tau$ for comparison with the observed values reported by Walker (1965). Model σ_y values for the appropriate Pasquill stability category were used in the normalized CWID calculations. (It is important to note that the crosswind integration removes from the observed deposition values the effects of differences in the duration of emissions for the various trials.)

The mean wind speed that is appropriate for use in dispersion model calculations for particulates with appreciable gravitational settling velocities is the average wind speed through the layer between the plume stabilization height and the ground surface. The ISC Model approximates this wind speed by the wind speed at the emission height, an approximation that is appropriate for buoyant stack emissions. However, the trials summarized by Walker involved non-buoyant emissions of glass spheres with relatively large gravitational settling velocities. Consequently, the ISC Model deposition calculations for the Walker trials were performed in two ways. First, the mean wind speed at the measurement height nearest the emission height was adjusted to the emission height using the wind-profile exponent calculated from the wind measurements. Second, the wind-profile exponent was set equal to zero (wind speed independent of height above the surface) and the average wind speed given by Walker for the layer between the emission height and the surface was used in the deposition calculations.

Figures A-1 through A-12 in Appendix A compare the calculated and observed normalized CWID profiles for the twelve trials. In each case, the normalized CWID profile calculated using the mean layer wind speed $\bar{u}_L$ is a better approximation to the observed normalized CWID profile than is the profile calculated using the mean wind speed at the emission height $\bar{u}\{h\}$. The shapes of the normalized CWID profiles calculated using the mean layer wind speed $\bar{u}_L$ are generally in good agreement with the shapes of the corresponding observed profiles. That is, the differences between the calculated and observed CWID values at various downwind distances for a given trial tend to be systematic. An uncertainty about the amount of material emitted during a trial or a systematic error in the estimates of the observed CWID could account for this result.

Table 2-3 compares the calculated and observed distances to the maximum normalized CWID values for the Walker (1965) trials. The distances to the maximum calculated and observed normalized CWID values were obtained by inspection of the plotted CWID profiles. As shown by Table 2-3, the maximum observed CWID values occurred at downwind distances of less than 100 meters during about half of the trials. Because the ISC Model cannot make deposition calculations at downwind distances less than 100 meters, direct comparisons of calculated and observed distances to maximum CWID values are not possible for about half of the trials. For the trials with calculated and observed distances to maximum CWID values greater than or equal to 100 meters, the overall performance of the ISC Model is about the same if the mean wind speed at the emission height $\bar{u}\{h\}$ or the mean wind speed for the layer between the emission height and the ground $\bar{u}_L$ is used in the calculations. Because $\bar{u}\{h\}$ always exceeds

TABLE 2-3

COMPARISON OF CALCULATED AND OBSERVED DISTANCES TO MAXIMUM NORMALIZED CWID VALUES FOR THE WALKER (1965) EXPERIMENTS

Trial	Distance to Maximum CWID/Q_T Value (m)			Ratio of Predicted to Observed	
	Observed	ISC ($\bar{u}(h)$)	ISC ($\bar{u}_L$)	$\bar{u}(h)$	$\bar{u}_L$
A	128	135	115	1.05	0.90
B	135	135	120	1.00	0.89
C	120	135	120	1.13	1.00
D	115	130	115	1.13	1.00
E	145	150	145	1.03	1.00
F	90	115	*	1.28	*
G	80	*	*	*	*
H	100	*	*	*	*
I	80	*	*	*	*
J	95	*	*	*	*
K	100	*	*	*	*
L	130	100	100	0.77	0.77
			Mean Ratio (MR)	1.04	0.92

*The ISC Model cannot make deposition calculations at distances less than 100 meters. Inspection of the calculated CWID profile indicates that CWID values higher than the value calculated at 100 meters may have occurred at distances less than 100 meters.

$\bar{u}_L$, the distance to the maximum CWID value is always greater if $u\{h\}$ is used in the calculations that if $\bar{u}_L$ is used in the calculations.

Table 2-4 compares the calculated and observed maximum normalized CWID values for the Walker trials, obtained by inspection of the plotted CWID profiles. As explained above, the ISC Model cannot make deposition calculations at downwind distances less than 100 meters. Consequently, for each trial with the maximum observed CWID located within 100 meters of the source (see Table 2-3), Table 2-4 compares the calculated and observed CWID values at 100 meters. The mean ratio (MR) of calculated to observed maximum CWID values is 0.56 if the mean wind speed at the emission height $\bar{u}\{h\}$ is used in the calculations and 0.71 if the mean wind speed between the emission height and the surface $\bar{u}_L$ is used in the calculations. There is more than a factor of 2 difference between calculated and observed maximum CWID values for four of the twelve trials if $\bar{u}\{h\}$ is used in the calculations and for two of the twelve trials if $\bar{u}_L$ is used in the calculations.

It is important to note that the values of the surface reflection coefficient γ_n suggested for use in the ISC Model User's Guide are principally based on experiments involving spray droplets (see Section 2.3) and may not be applicable to glass spheres. The maximum possible deposition is calculated if the reflection coefficient γ_n is set equal to zero. Because Trials G through L have non-zero reflection coefficients (see Table 2-1), we repeated the calculations for Trials G through L with the reflection coefficient γ_n set equal to zero. Figures A-13 through A-18 in Appendix A show the observed normalized CWID profiles for Trials G through L and the corresponding profiles calculated with the reflection coefficient set equal to zero. Also, Table 2-5 compares the calculated and observed maximum CWID values with the reflection coefficient set equal to zero for all trials. (If the maximum observed CWID is located within 100 meters of the source, Table 2-5 compares the calculated and observed CWID values at 100 meters.) The MR is 0.63 if the mean wind speed at the emission height $\bar{u}\{h\}$ is used in the calculations

TABLE 2-4

COMPARISON OF CALCULATED AND OBSERVED MAXIMUM NORMALIZED CWID VALUES FOR THE WALKER (1965) EXPERIMENTS*

Trial	Maximum CWID/Q_τ (mg/(g·m))			Ratio of Predicted to Observed	
	Observed	ISC ($\bar{u}\{h\}$)	ISC ($\bar{u}_L$)	$\bar{u}\{h\}$	$\bar{u}_L$
A	20.6	5.4	7.9	0.26	0.38
B	10.8	5.2	8.0	0.48	0.74
C	6.0	5.5	7.2	0.92	1.20
D	7.4	6.0	8.3	0.81	1.12
E	6.0	4.2	4.7	0.70	0.78
F	9.6	8.2	10.0	0.85	1.04
G	8.8	4.3	4.6	0.49	0.52
H	3.9	2.8	3.4	0.72	0.87
I	9.4	3.7	4.5	0.39	0.48
J	2.7	1.7	1.9	0.63	0.70
K	2.9	1.8	2.0	0.62	0.69
L	3.1	2.2	2.5	0.71	0.81
			Mean Ratio (MR)	0.56	0.71

*If the maximum observed CWID for a trial occurs at a distance of less than 100 meters, the calculated and observed CWID values in the table are the values at 100 meters because the ISC Model cannot make deposition calculations at distances less than 100 meters.

TABLE 2-5

COMPARISON OF CALCULATED AND OBSERVED MAXIMUM NORMALIZED CWID VALUES FOR THE WALKER (1965) EXPERIMENTS WITH ZERO REFLECTION COEFFICIENTS FOR ALL TRIALS*

Trial	Maximum CWID/Q_τ (mg/(g·m))			Ratio of Predicted to Observed	
	Observed	ISC ($\bar{u}\{h\}$)	ISC ($\bar{u}_L$)	$\bar{u}\{h\}$	$\bar{u}_L$
A	20.6	5.4	7.9	0.26	0.38
B	10.8	5.2	8.0	0.48	0.74
C	6.0	5.5	7.2	0.92	1.20
D	7.4	6.0	8.3	0.81	1.12
E	6.0	4.2	4.7	0.70	0.78
F	9.6	8.2	10.0	0.85	1.04
G	8.8	5.9	6.3	0.67	0.72
H	3.9	3.5	4.1	0.90	1.05
I	9.4	5.1	6.1	0.54	0.65
J	2.7	2.9	3.2	1.07	1.19
K	2.9	3.0	3.3	1.03	1.14
L	3.1	3.0	3.4	0.97	1.10
			Mean Ratio (MR)	0.63	0.79

*If the maximum observed CWID for a trial occurs at a distance of less than 100 meters, the calculated and observed CWID values in the table are the values at 100 meters because the ISC Model cannot make deposition calculations at distances less than 100 meters.

and 0.79 if the mean wind speed between the emission height and the surface $\bar{u}_L$ is used in the calculations. There is more than a factor of 2 difference between calculated and observed CWID values for two of the twelve trials if $\bar{u}\{h\}$ is used in the calculations and for one of the twelve trials if $\bar{u}_L$ is used in the calculations. Consequently, the discrepancies between calculated and observed maximum CWID values for Trials G through L may in part reflect uncertainties about the appropriate value of the reflection coefficient for glass spheres.

Table 2-6 summarizes the comparisons of concurrent calculated and observed maximum CWID values for the Walker data set. The best overall model performance is obtained if the mean layer wind speed $\bar{u}_L$ is used in the deposition calculations with the surface reflection coefficient set equal to zero for all trials. For this combination of model inputs, the MR indicates that the ISC Model, on the average, predicts the maximum CWID to within about 20 percent for the Walker trials. Also, the minimum root mean square error (RMSE) is obtained for this combination of inputs, and the concurrent calculated and observed maximum CWID values are within a factor of 2 for all but one of the trials.

Walker also gives, for each trial and sampling distance, the standard deviation of the crosswind deposition pattern σ_y in radians. We multiplied each σ_y value in radians by the appropriate downwind distance in meters to obtain the corresponding σ_y in meters. Table 2-7 gives the ratios of calculated (Pasquill-Gifford) to observed σ_y values. In general, the calculated to observed σ_y ratio is approximately the same at all sampling distances for an individual trial. The departures from unity of the calculated to observed σ_y ratios probably reflect the effects of using discrete stability categories in the ISC Model.

TABLE 2-6

SUMMARY OF THE RESULTS OF THE ISC MODEL CALCULATIONS FOR THE WALKER (1965) DEPOSITION EXPERIMENTS*

ISC Model Inputs		MR of Maximum CWID** Values	RMSE of Maximum CWID** Values	% Within a Factor of 2
Wind Speed	Reflection Coefficients			
$\bar{u}\{h\}$	From Table 2-1	0.56	1.86	67
$\bar{u}_L$	From Table 2-1	0.71	1.57	83
$\bar{u}\{h\}$	0 for all trials	0.63	1.66	83
$\bar{u}_L$	0 for all trials	0.79	1.42	92

*The sample size is 12.

**Crosswind-integrated deposition.

TABLE 2-7

RATIOS OF CALCULATED TO OBSERVED STANDARD DEVIATIONS OF THE CROSSWIND DEPOSITION PATTERN σ_y FOR THE WALKER (1965) EXPERIMENTS

Trial	Downwind Distance (m)									
	100.6	114.3	128.0	146.3	201.2	274.3	402.3	804.6	1097.3	Mean Ratio**
A	1.47	-	1.52	-	1.49*	-	-	-	-	1.49
B	0.95	0.95	0.97	0.83	1.15	0.99*	-	-	-	0.98
C	0.79	-	0.73	-	0.82	-	0.85*	0.95*	-	0.78
D	1.19	-	1.14	-	1.12	-	0.39*	0.33*	-	1.14
E	0.50	-	0.50	-	0.44	0.45	0.42*	0.58*	-	0.46
F	0.62	-	0.63	-	0.56	0.58*	0.61*	-	-	0.60
G	0.42	-	0.42	-	0.56	0.81*	2.43*	-	-	0.47
H	0.81	-	0.86	-	0.83	0.76	0.83*	1.59*	-	0.80
I	1.12	-	1.23	-	0.62	0.90*	0.97*	-	-	0.84
J	0.47	-	0.49	-	0.49	0.48	0.42	0.39*	0.55*	0.46
K	0.41	-	0.39	-	0.33	0.29	0.27	0.23*	0.26*	0.31
L	0.45	-	0.46	-	0.46	0.45	0.33	0.24*	-	0.46
Mean Ratio**	0.64	0.95	0.64	0.83	0.58	0.45	0.33	-	-	0.54

*Observed σ_y value reported as unreliable.

**Mean ratios exclude unreliable measurements.

2.2 STEWART (1968) DEPOSITION EXPERIMENTS

Stewart (1968) summarizes the results of seven continuous, elevated releases of glass spheres. Five of the experiments (the B series) were conducted at the Baie du Dore Research Station of the Great Lakes Institute, University of Toronto, Ontario, Canada. The release height for the B series was 18.6 meters, and the sphere diameters ranged from 100 to 200 micrometers. The two other experiments (the S series) were conducted at the Suffield Experimental Station, Ralston, Alberta, Canada. The release heights for the S series were 30.5 and 92.4 meters, and the sphere diameters ranged from 50 to 200 micrometers. For both series, sticky-tape samplers were placed at 1.3- or 2-degree intervals at radial distances of 2, 3, 5, 7, 9, 11 and 13 stack heights. (No illustration of the experimental layout at either site is given by Stewart.) The results of the experiments presented by Stewart for each trial are in non-dimensional form and are restricted to: (1) the maximum crosswind-integrated deposition (CWID), multiplied by the release height h and divided by the total amount of material emitted Q_T; and (2) the distance to the maximum CWID, divided by the release height h. Thus, the results given by Stewart are far less detailed than the results given by Walker (1965). The source data for the Stewart experiments are discussed in Section 2.2.1, the meteorological data are discussed in Section 2.2.2, and the ISC Model calculation procedures and results are given in Section 2.2.3.

2.2.1 Source Data

The deposition experiments described by Stewart (1968) consisted of the continuous, elevated release of solid glass spheres over a period of 10 to 43 minutes. The spheres were emitted with no buoyancy and minimal momentum. In all but one of the seven trials, two sizes of glass spheres were emitted and the deposition of each size of sphere was evaluated separately, resulting in the equivalent of 13 separate trials.

For Trials B1, B2, B3, B4 and S2, glass spheres with diameters of 100 and 200 micrometers were used. For Trial B5, only 100-micrometer spheres were used. Spheres with diameters of 50 and 100 micrometers were used in Trial S1. The gravitational settling velocities of the three sizes of glass spheres given by Stewart are in good agreement with the corresponding settling velocities that we computed using the methods of McDonald (1960). We determined the surface reflection coefficient γ_n for each trial from Figure 2-8 of the ISC Model User's Guide. The source parameters used in the ISC Model calculations for the Stewart trials are given in Table 2-8. For each trial, these parameters include the emission height, total amount of material emitted, gravitational settling velocity and surface reflection coefficient. Additionally, Table 2-8 gives the date, start time and duration of each trial.

2.2.2 Meteorological Data

The only meteorological inputs to the ISC Model short-term computer program ISCST that are given by Stewart (1968) are wind speed and wind direction. Wind measurements were made at heights of 2, 4, 8, 12 and 18 meters for Trials B1 through B5 and at heights of 2, 8, 16, 48, 64, 80 and 92 meters for Trials S1 and S2. However, Stewart gives only one wind speed and wind direction for each trial. We believe that the reported wind speeds and directions probably are for the layer between the emission height and the ground surface. As in the case of the Walker (1965) trials discussed in Section 2.1, the mean layer wind speed $\bar{u}_L$ is probably appropriate for use in ISC Model calculations for the type of experiments summarized by Stewart. We therefore used the wind speeds reported by Stewart with the wind-profile exponent set equal to zero (wind speed independent of height above the surface). Although Stewart does not give any mixing height data for the seven trials, it is extremely unlikely that the mixing height affected the maximum deposition for these trials because of the low emission height and the relatively large gravitational settling velocities of the glass spheres. Consequently,

TABLE 2-8

SOURCE PARAMETERS FOR THE STEWART (1968) EXPERIMENTS

Trial/Diameter (μm)	Date	Start Time (LST)	Duration (min.)	Amount Emitted Q_τ(g)	Settling Velocity V_{sn}(m/sec)	Emission Height h (m)	Reflection Coefficient γ_n
B1/100	17 Jul 64	1020	15.5	200	0.52	18.6	0
B1/200	17 Jul 64	1020	15.5	230	1.42	18.6	0
B2/100	28 Jul 64	1035	10.0	200	0.52	18.6	0
B2/200	28 Jul 64	1035	10.0	116	1.42	18.6	0
B3/100	28 Jul 64	1805	13.0	200	0.52	18.6	0
B3/200	28 Jul 64	1805	13.0	113	1.42	18.6	0
B4/100	10 Aug 64	1610	16.5	200	0.52	18.6	0
B5/100	27 Aug 64	1225	4.0	200	0.52	18.6	0
B5/200	27 Aug 64	1225	4.0	100	1.42	18.6	0
S1/50	14 Jul 65	1108	10.2	1361	0.17	30.5	0.325
S1/100	14 Jul 65	1108	10.2	1361	0.52	30.5	0
S2/100	14 Jul 65	1511	42.6	9072	0.52	92.4	0
S2/200	14 Jul 65	1511	42.6	1500	1.48	92.4	0

we assumed unrestricted vertical mixing in the ISC Model calculations for the Stewart trials.

Table 2-9 gives the meteorological inputs used in the ISC Model calculations for the deposition experiments reported by Stewart. For each trial, these inputs include the average flow vector, the mean wind speed and the Pasquill stability category as determined using the Turner (1964) criteria. All but two of the trials were conducted under slightly unstable (C stability) conditions. One trial was conducted under neutral (D stability) conditions and one of the trials was conducted under slightly stable (E stability) conditions. As explained above, the wind-profile exponent was set equal to zero for all trials. The ambient air temperature and vertical potential temperature gradient, which are used by the ISC Model to calculate plume rise, were not required as model inputs because the experiments described by Stewart involved non-buoyant emissions.

2.2.3 Calculation Procedures and Results

The source data discussed in Section 2.2.1 and the meteorological data discussed in Section 2.2.2 were used with the ISC Model short-term computer program ISCST in the Rural Mode to calculate, for each trial, the total deposition along the plume centerline at the sampling distances and at several other distances to aid in defining the downwind distribution of the deposited spheres. These centerline deposition values were then multiplied by $\sqrt{2\pi}\,\sigma_y\,h$, where h is the emission height, and divided by the total amount of material emitted Q_τ to obtain the calculated non-dimensional crosswind-integrated deposition (CWID) values for comparison with the observed maximum values given by Stewart (1968). (The crosswind integration removes from the observed deposition values the effects of differences in the duration of emissions for the various trials.)

TABLE 2-9

METEOROLOGICAL PARAMETERS FOR THE STEWART (1968) EXPERIMENTS

Experiment	Average Flow Vector* (deg)	Wind Speed (m/sec)	Pasquill Stability Category
B1	034	6.3	C
B2	046	5.6	C
B3	012	4.6	E
B4	032	2.5	D
B5	007	4.9	C
S1	040	5.4	C
S2	099	4.8	C

*Direction toward which the wind is blowing.

The observed maximum non-dimensional CWID and the calculated non-dimensional CWID profile for each combination of trial and sphere diameter (except Trial B3 for 200-micrometer spheres) are presented in Figures A-19 through A-28 in Appendix A. Trial B3/200 is omitted because the calculated nondimensional CWID at 100 meters is five orders of magnitude lower than the maximum observed value at 56 meters. The maximum observed CWID values were found at distances less than 100 meters from the source for five combinations of trial and sphere diameter. Although the ISC Model cannot be applied at distances less than 100 meters from a source, subjective extrapolations of the calculated CWID profiles for these cases show a good qualitative agreement between the observed and calculated values of maximum non-dimensional CWID (see Figures A-19, A-20, A-22 and A-24). It is important to note that the non-dimensional CWID values calculated by the ISC Model at 100 meters for these trials cannot be compared with the observed non-dimensional CWID values because Stewart gives only the maximum non-dimensional CWID values.

Table 2-10 compares the calculated and observed values of the magnitude and location of the maximum non-dimensional CWID for each of the Stewart trials. For the six trials with maximum observed CWID values located more than 100 meters from the source, the MR values indicate that, on the average, the ISC Model predicts the magnitude and location of the maximum CWID to within about 10 percent for the Stewart trials. All of the concurrent calculated and observed maximum CWID values for these trials are within a factor of 2, and the RMSE is only 1.51. Thus, the performance of the ISC Model for the Stewart deposition experiments is equivalent to the model's performance for the Walker (1965) deposition experiments discussed in Section 2.1.

TABLE 2-10

COMPARISON OF CALCULATED AND OBSERVED VALUES OF THE MAGNITUDES AND LOCATIONS OF THE MAXIMUM NON-DIMENSIONAL CWID FOR THE STEWART (1968) EXPERIMENTS

Trial/Diameter (μm)	Maximum Non-Dimensional CWID ($CWID \cdot h/Q_T$)			Distance to the Maximum (m)		
	Observed	ISC	Predicted/Observed	Observed	ISC	Predicted/Observed
B1/100	0.501	*	*	93.0	*	*
B2/200	0.448	*	*	55.8	*	*
B3/100	0.316	0.174	0.55	167.4	150	1.12
B3/200	1.800	*	*	55.8	*	*
B4/100	0.354	*	*	93.0	*	*
B5/100	0.121	0.104	0.86	167.4	115	1.46
B5/200	0.354	*	*	55.8	*	*
S1/50	0.017	0.023	1.35	305.0	275	1.11
S1/100	0.059	0.093	1.58	183.0	190	0.963
S2/100	0.074	0.112	1.51	462.0	590	0.783
S2/200	0.406	0.610	1.50	277.2	275	1.01
	Mean Ratio (MR)		1.12	Mean Ratio (MR)		1.02

* The ISC Model cannot make deposition calculations at downwind distancess less than 100 meters.

2.3 BOYLE, ET AL. (1975) AERIAL SPRAY EXPERIMENTS

Boyle, et al. (1975) present the results of five releases of oil spray from a low-flying DC-7B aircraft. The experiments were conducted at the U. S. Army Dugway Proving Ground in Utah for the Food and Agriculture Organization of the United Nations. The aircraft flew at heights of 27 to 88 meters above the surface. However, the effects of aircraft wake vortices in combination with atmospheric turbulence determined the effective emission height and initial dimensions of the source. Spray was released along a pre-marked flight path over distances ranging from 7.4 to 14.1 kilometers. For three of the five trials (Trials 1-5, 1-6 and 1-7), the aircraft released oil spray along a line nearly perpendicular to the mean wind direction. The sampling grid for these trials is shown in Figure 2-1. During the two remaining trials (Trials 2-2R and 2-3), the aircraft flew approximately into the mean wind. The sampling grid for the two alongwind releases is shown in Figure 2-2. The drop sizes for the oil spray ranged from about 15 to 180 micrometers. Deposition samples were collected on Printflex cards placed directly on the ground at the sampling locations shown in Figures 2-1 and 2-2. Boyle, et al. give the total deposition determined at each sampling location by drop-size category. The data are also summarized in graphical form. The source data for the Boyle, et al. experiments are discussed in Section 2.3.1, the meteorological data are discussed in Section 2.3.2, and the ISC Model calculation procedures and results are given in Section 2.3.3.

2.3.1 Source Data

The Boyle, et al. (1975) experiments consisted of five aerial releases from a DC-7B aircraft of an oil spray at a height of 27 to 88 meters above the surface. The aircraft flew along a straight line and released oil spray over distances ranging from 7.4 to 14.1 kilometers. The spray, which was released just above the wing of the aircraft, was

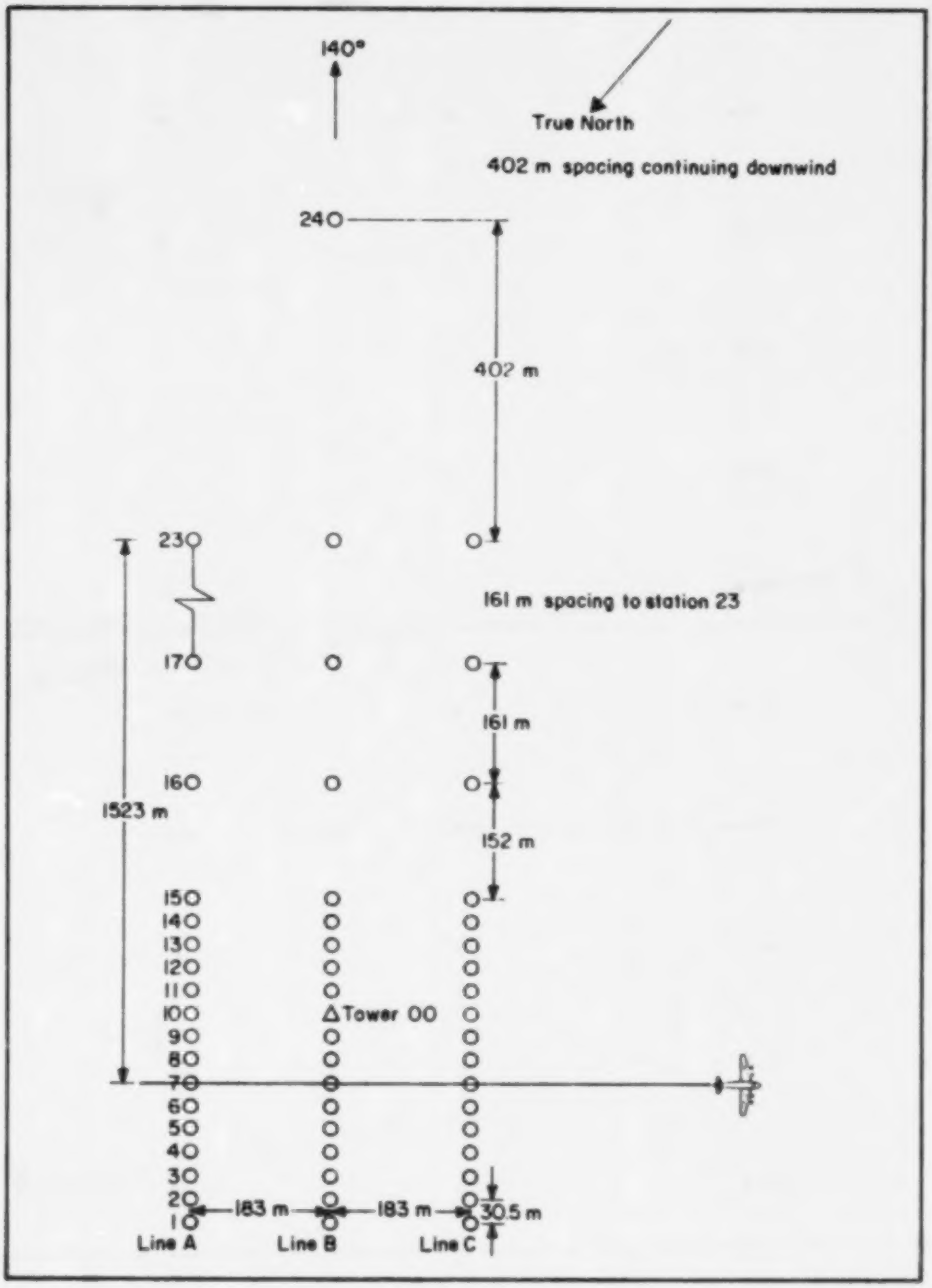
140°
True North
402 m spacing continuing downwind
240
402 m
23
161 m spacing to station 23
17
161 m
16
1523 m
152 m
15
14
13
12
11
10
Tower 00
9
8
7
6
5
4
3
2
1
183 m
183 m
30.5 m
Line A
Line B
Line C

FIGURE 2-1. Sampling locations for the crosswind spray releases reported by Boyle, *et al*. (1975).

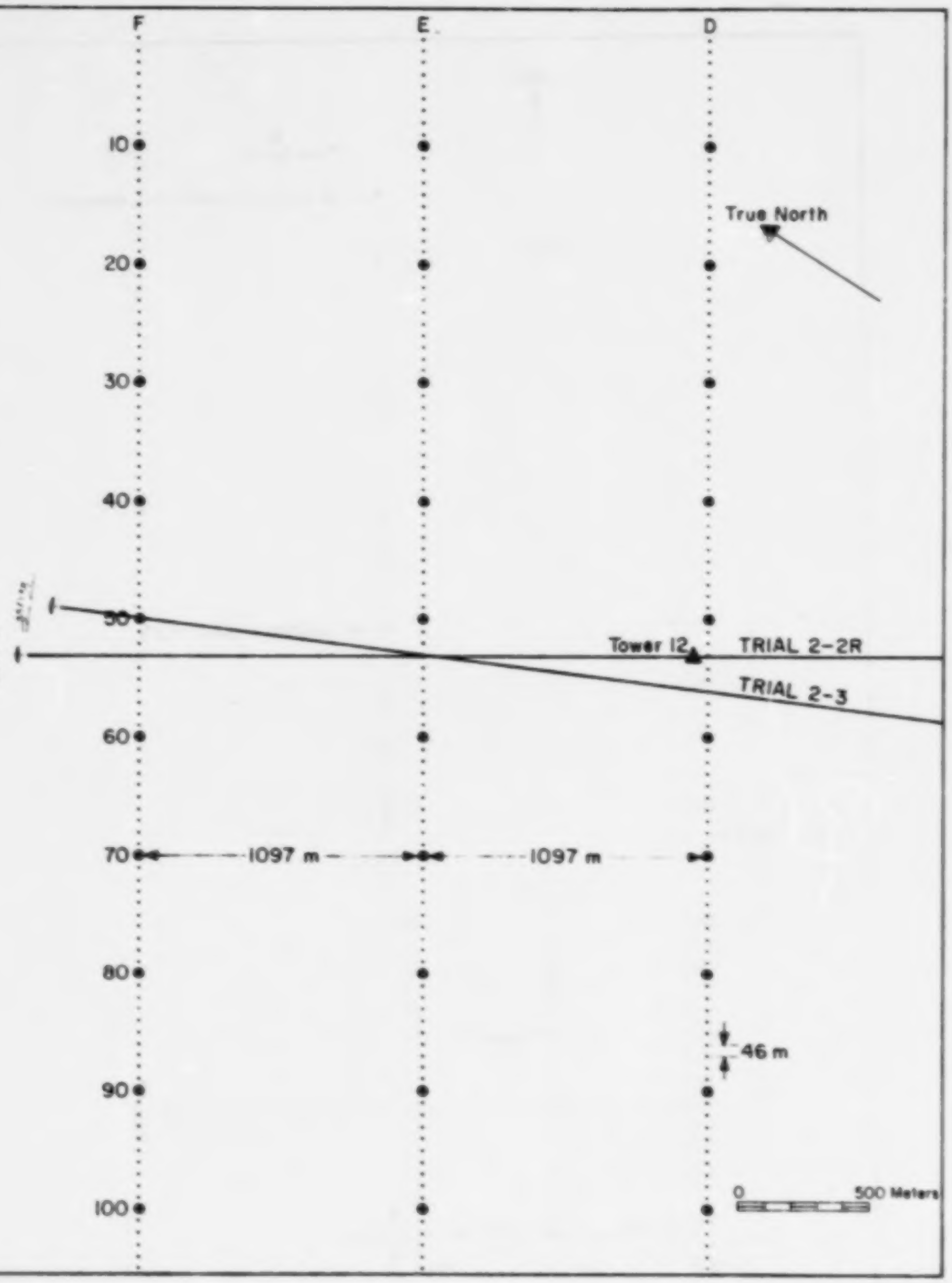
F
E
D
10
20
30
40
50
60
70
80
90
100
True North
Tower 12
TRIAL 2-2R
TRIAL 2-3
1097 m
1097 m
46 m
0
500 Meters

FIGURE 2-2. Sampling locations for the alongwind spray releases reported by Boyle, *et al.* (1975).

vigorously mixed with ambient air by the aircraft's wake vortices. The wake vortices sank toward the ground as they dissipated, resulting in long, narrow volume sources with effective emission heights less than or equal to the actual release heights.

The ISC Model represents a long, narrow volume source (i.e., a line source) by a series of adjacent volume sources. The individual volume sources have initial horizontal dimensions (σ_{yo}) equal to the width of the line source divided by 2.15. Boyle, et al. estimated the effective width of the spray plume to be equal to three wingspans, or 84 meters. Therefore, for all five trials, the initial lateral dispersion coefficient σ_{yo} for an individual volume source was set equal to 84 meters divided by 2.15, or 39 meters. The number of volume sources was determined for each trial by dividing the length of the spray release path by 84 meters. The effective emission heights of the volume sources and the initial vertical dispersion coefficients σ_{zo} were estimated by Boyle, et al. primarily on the basis of vertical measurements of spray dosage made on a tower downwind of the release line. The height of the peak dosage was defined as the effective emission height and the distance from the peak dosage to the top of the cloud was divided by 2.15 to obtain σ_{zo}. Table 2-11 lists, for each trial, the effective emission height, the effective source strength (amount disseminated multiplied by the dissemination efficiency and divided by the number of sub-sources), the length of the dissemination path, and the number of sub-sources used to simulate the spray releases.

The spray drops released in the trials described by Boyle, et al. varied in size from about 15 to 180 micrometers. The droplet size distributions and corresponding settling velocities were determined experimentally and are given in the report by Boyle, et al. These data, which were used directly as ISC Model inputs, are reproduced in Table 2-12. Also given in Table 2-12 are the surface reflection coefficients γ_n and the mass fractions ϕ_n that correspond to the various drop-size

TABLE 2-11

SOURCE PARAMETERS FOR THE SUB-SOURCES OF THE BOYLE, ET AL. (1975) EXPERIMENTS

Source Parameter	Trial				
	1-5	1-6	1-7	2-2R	2-3
Effective Emission Height (m)	15	15	15	46	27
Initial Vertical Dispersion Coefficient σ_{zo} (m)	22.3	35.8	35.8	15	15
Effective Source Strength* (g)	1205	2290	1033	1212	503
Length of Dissemination Path (m)	1.408×10^4	7.376×10^3	7.488×10^3	1.028×10^4	8.662×10^3
Number of Sub-Sources	168	88	89	122	103

*Total amount of spray, multiplied by the dissemination efficiency and divided by the number of sub-sources.

TABLE 2-12

DEPOSITION PARAMETERS FOR THE BOYLE, *ET AL.* (1975) EXPERIMENTS

Mean Drop Diameter (μm)	Settling Velocity (m/sec)	Mass Fraction ϕ_n	Reflection Coefficient γ_n
Trial 1-5			
17.0	$7.25\text{x}10^{-3}$	$8.00\text{x}10^{-3}$	0.80
29.7	$2.21\text{x}10^{-2}$	$1.65\text{x}10^{-1}$	0.71
46.7	$5.47\text{x}10^{-2}$	$3.02\text{x}10^{-1}$	0.61
64.2	$1.04\text{x}10^{-1}$	$3.96\text{x}10^{-1}$	0.49
82.1	$1.69\text{x}10^{-1}$	$8.20\text{x}10^{-2}$	0.33
100.4	$2.32\text{x}10^{-1}$	$3.33\text{x}10^{-2}$	0.17
119.1	$2.81\text{x}10^{-1}$	$9.70\text{x}10^{-3}$	0.045
138.3	$3.49\text{x}10^{-1}$	$3.40\text{x}10^{-3}$	0.0
Trial 1-6			
25.2	$1.65\text{x}10^{-2}$	$7.50\text{x}10^{-3}$	0.74
37.4	$3.67\text{x}10^{-2}$	$9.95\text{x}10^{-2}$	0.66
53.3	$7.46\text{x}10^{-2}$	$2.02\text{x}10^{-1}$	0.56
69.2	$1.26\text{x}10^{-1}$	$2.72\text{x}10^{-1}$	0.44
85.1	$1.90\text{x}10^{-1}$	$1.56\text{x}10^{-1}$	0.27
100.9	$2.41\text{x}10^{-1}$	$1.14\text{x}10^{-1}$	0.145
116.7	$2.84\text{x}10^{-1}$	$7.69\text{x}10^{-2}$	0.035
132.4	$3.38\text{x}10^{-1}$	$3.63\text{x}10^{-2}$	0.0
148.1	$4.07\text{x}10^{-1}$	$2.83\text{x}10^{-2}$	0.0
163.6	$4.78\text{x}10^{-1}$	$5.90\text{x}10^{-3}$	0.0
179.0	$5.45\text{x}10^{-1}$	$1.30\text{x}10^{-3}$	0.0
Trial 1-7			
25.2	$1.67\text{x}10^{-2}$	$1.03\text{x}10^{-2}$	0.74
37.4	$3.67\text{x}10^{-2}$	$1.17\text{x}10^{-1}$	0.66
53.3	$7.46\text{x}10^{-2}$	$3.33\text{x}10^{-1}$	0.56
64.2	$1.26\text{x}10^{-1}$	$2.74\text{x}10^{-1}$	0.44
85.1	$1.90\text{x}10^{-1}$	$1.39\text{x}10^{-1}$	0.27
100.9	$2.41\text{x}10^{-1}$	$7.47\text{x}10^{-2}$	0.145
116.7	$2.84\text{x}10^{-1}$	$2.74\text{x}10^{-2}$	0.035
132.4	$3.38\text{x}10^{-1}$	$7.90\text{x}10^{-3}$	0.0
148.1	$4.07\text{x}10^{-1}$	$1.56\text{x}10^{-2}$	0.0

TABLE 2-12 (Continued)

Mean Drop Diameter (μm)	Settling Velocity (m/sec)	Mass Fraction ϕ_n	Reflection Coefficient γ_n
		Trial 2-2R	
17.0	$7.47\text{x}10^{-3}$	$9.80\text{x}10^{-3}$	0.81
29.7	$2.28\text{x}10^{-2}$	$9.55\text{x}10^{-2}$	0.70
46.7	$5.63\text{x}10^{-2}$	$3.36\text{x}10^{-1}$	0.61
64.2	$1.06\text{x}10^{-1}$	$3.35\text{x}10^{-1}$	0.485
82.1	$1.74\text{x}10^{-1}$	$1.22\text{x}10^{-1}$	0.315
100.4	$2.37\text{x}10^{-1}$	$6.75\text{x}10^{-2}$	0.155
119.1	$2.87\text{x}10^{-1}$	$2.57\text{x}10^{-2}$	0.030
138.3	$3.58\text{x}10^{-1}$	$9.70\text{x}10^{-3}$	0.0
		Trial 2-3	
17.0	$7.34\text{x}10^{-3}$	$1.50\text{x}10^{-2}$	0.81
29.7	$2.24\text{x}10^{-2}$	$1.82\text{x}10^{-1}$	0.71
46.7	$5.54\text{x}10^{-2}$	$4.09\text{x}10^{-1}$	0.61
64.2	$1.05\text{x}10^{-1}$	$3.19\text{x}10^{-1}$	0.50
82.1	$1.71\text{x}10^{-1}$	$4.38\text{x}10^{-2}$	0.295
100.4	$2.34\text{x}10^{-1}$	$3.12\text{x}10^{-2}$	0.165

categories. The reflection coefficients were determined from Figure 2-8 of the ISC Model User's Guide.

2.3.2 Meteorological Data

Extensive meteorological data were collected during the trials reported by Boyle, et al. (1975). Wind speed and wind direction were measured at six levels on a 98-meter tower for Trials 1-5, 1-6, and 1-7 and at three levels on a 32-meter tower for Trials 2-2R and 2-3. PIBAL and rawinsonde soundings were made for each trial to determine the depth of the mixing layer and the vertical profiles of wind speed and wind direction. Observations of cloud cover and ambient air temperature were also made for each trial. With the exception of the Pasquill stability category, all of the meteorological input parameters required by the ISC Model short-term computer program ISCST are provided in the report by Boyle, et al.

Table 2-13 lists the meteorological inputs for the trials described by Boyle, et al. The cloud cover and wind data given by Boyle, et al. were used to estimate the Pasquill stability category for each trial following the Turner (1964) procedures. Because the wind speeds in Table 2-13 are at the effective emission heights, the wind-profile exponent was set equal to zero for all trials. The ambient air temperatures and vertical potential temperature gradients during the various trials are not shown in Table 2-13 because the ISC Model does not require these parameters to calculate deposition for volume sources.

2.3.3 Calculation Procedures and Results

The source data given in Section 2.3.1 and the meteorological data given in Section 2.3.2 were used with the ISC Model short-term computer program ISCST in the Rural Mode to calculate, for each trial, values of the total deposition at various distances normal to the line

TABLE 2-13

METEOROLOGICAL PARAMETERS FOR THE BOYLE, _ET AL_. (1975) EXPERIMENTS

Meteorological Parameter	Trial				
	1-5	1-6	1-7	2-2R	2-3
Average Flow Vector* (deg)	150	120	125	135	140
Mean Wind Speed** (m/sec)	3.0	1.0	1.8	4.0	4.2
Mixing Height (m)	[illegible]50	150	400	350	500
Pasquill Stability Category	B	B	C	C	C

*Direction toward which the wind is blowing.

**Mean wind speed at the effective emission height.

source. For each trial, calculations were made for receptors along three parallel lines that corresponded to the sampling lines (see Figures 2-1 and 2-2). The calculated deposition values at points equidistant from the line source were averaged to obtain representative deposition values (the observed data were averaged by Boyle, et al. in a similar manner). We then plotted the calculated total deposition values for each trial versus distance from the line source for comparison with the observed deposition profile. The calculated and observed deposition profiles for the five trials are shown in Figures 2-3 through 2-7. In general, the profiles generated by the ISC Model are in good agreement with the observed profiles. Specific differences between the calculated and observed profiles are discussed below.

Figure 2-3 compares the calculated and observed deposition profiles for Trial 1-5. In general, the calculated and observed deposition values are within a factor of 2 at all downwind distances. The highest calculated and observed deposition values occur at the first sampling distance. There is a secondary maximum in the observed deposition profile between about 4 and 8 kilometers that is attributable to the downward reflection of smaller droplets at the top of the surface mixing layer. This effect is also reproduced by the ISC Model, although there are differences in the calculated and observed magnitudes and locations of the secondary maximum. (All droplets that mix to the top of the surface mixing layer are assumed by the ISC Model to be reflected downward, but droplets that mix to the ground surface may or may not be reflected upward, depending on the value of the surface reflection coeffient.)

Figure 2-4 compares the calculated and observed deposition profiles for Trial 1-6. The ISC Model generates a deposition profile which approximately matches the shape of the observed profile. However, the overall correspondence between the calculated and observed deposition profiles is not as good as in the case of Trial 1-5. It should be noted that the ability of the ISC Model to duplicate the observed deposition

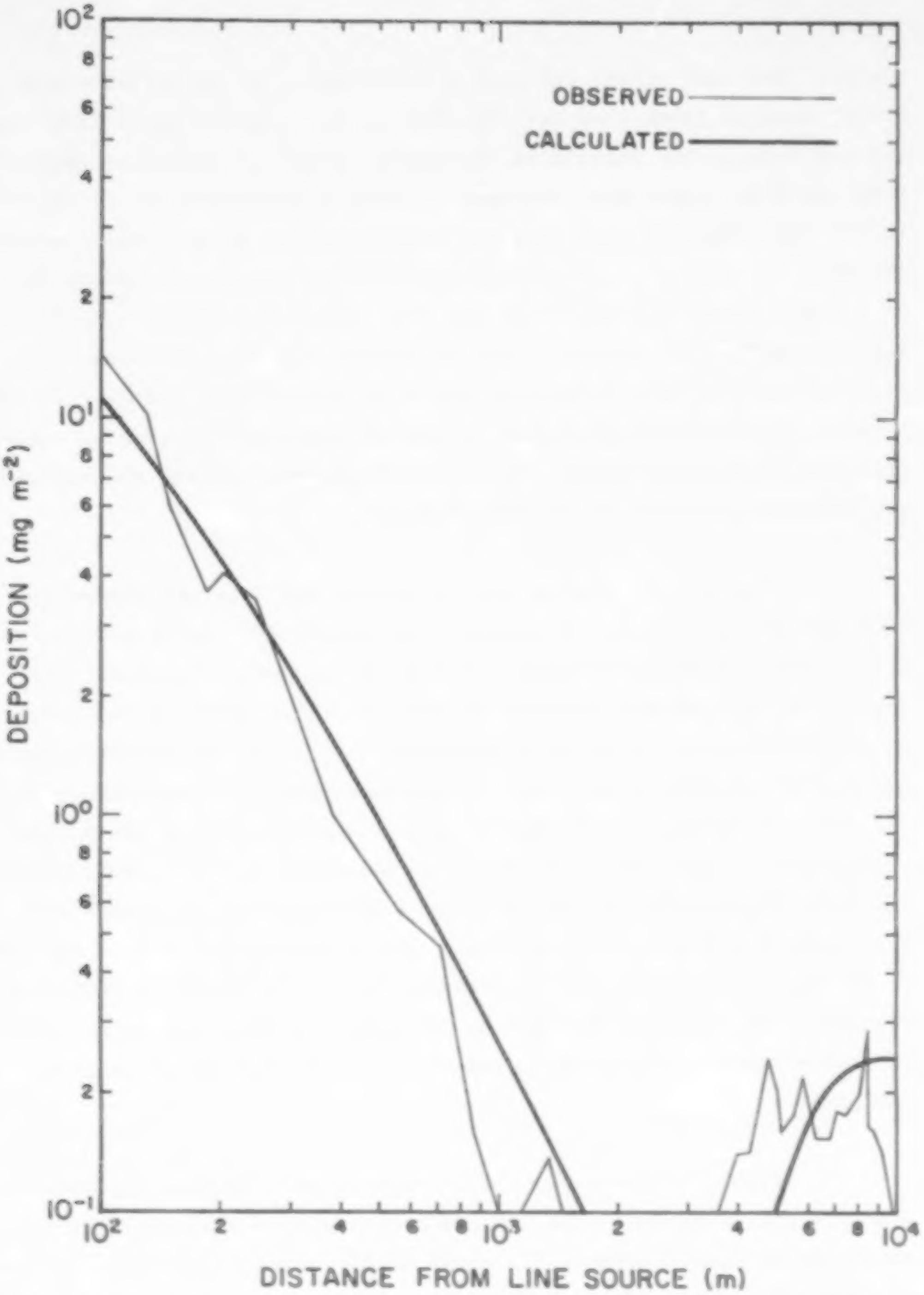

FIGURE 2-3. Observed and calculated deposition profiles for Boyle, et al. (1975) Trial 1-5.

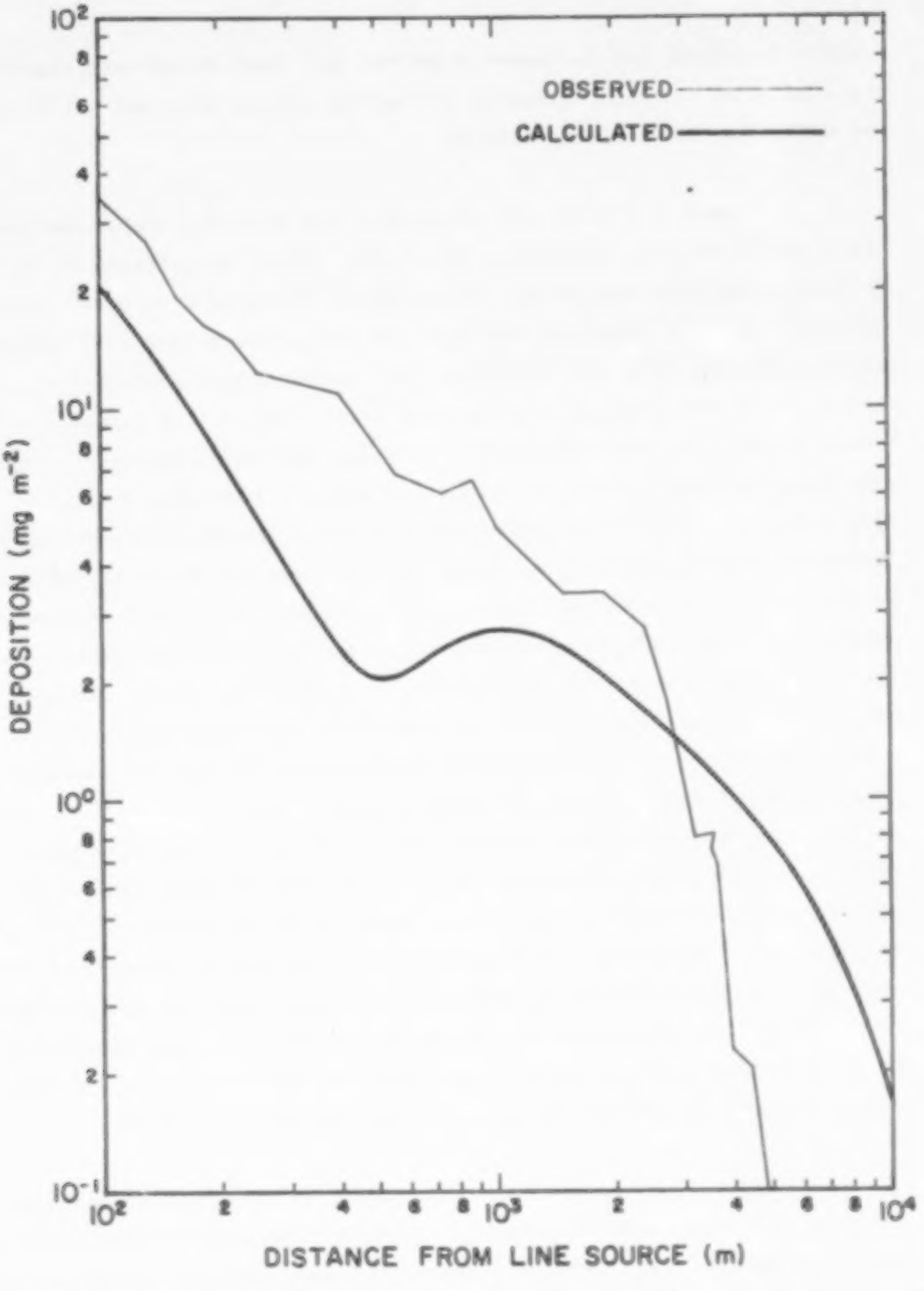

FIGURE 2-4. Observed and calculated deposition profiles for Boyle, et al. (1975) Trial 1-6.

profile for Trial 1-6 is hampered by the fact that there were significant shifts in the wind direction during the period when the oil spray was affecting the sampling network.

Figure 2-5 shows the calculated and observed deposition profiles for Trial 1-7. Following the Turner (1964) definitions of the Pasquill stability categories, the slightly unstable C category existed during Trial 1-7. However, the standard deviation of the wind azimuth angle σ_A during Trial 1-7 indicates that meteorological conditions during Trial 1-7 probably corresponded to the unstable B category. Consequently, ISC Model deposition profiles for both stability categories are shown in Figure 2-5. At downwind distances less than about 1 kilometer, the calculated deposition profiles are principally determined by the gravitational settling of large droplets and are minimally affected by atmospheric turbulence. Thus, there is a generally good agreement within the first kilometer between the observed deposition profile and the two calculated deposition profiles. If the C stability category is assumed to have existed during the trial, the ISC Model calculates a secondary maximum in the deposition profile that is farther downwind and lower in magnitude than the observed secondary maximum. If the B stability category is assumed to have existed during the trial, the agreement between the ISC Model deposition profile and the observed profile is significantly improved at the longer downwind distances where the only droplets still available for deposition are the smaller droplets which are significantly affected by both gravitational settling and atmospheric turbulence. The calculated and observed deposition values generally agree to within a factor of 2 at all downwind distances if the B stability category is assumed to have occurred during Trial 1-7.

Figure 2-6 compares the calculated and observed deposition profiles for Trial 2-2R. The DC-7B aircraft flew approximately into the mean wind during Trial 2-2R, and deposition was measured on both sides of the flight path. For the area to the right of the flight path, the ISC Model deposition profile is within a factor of 2 of the observed

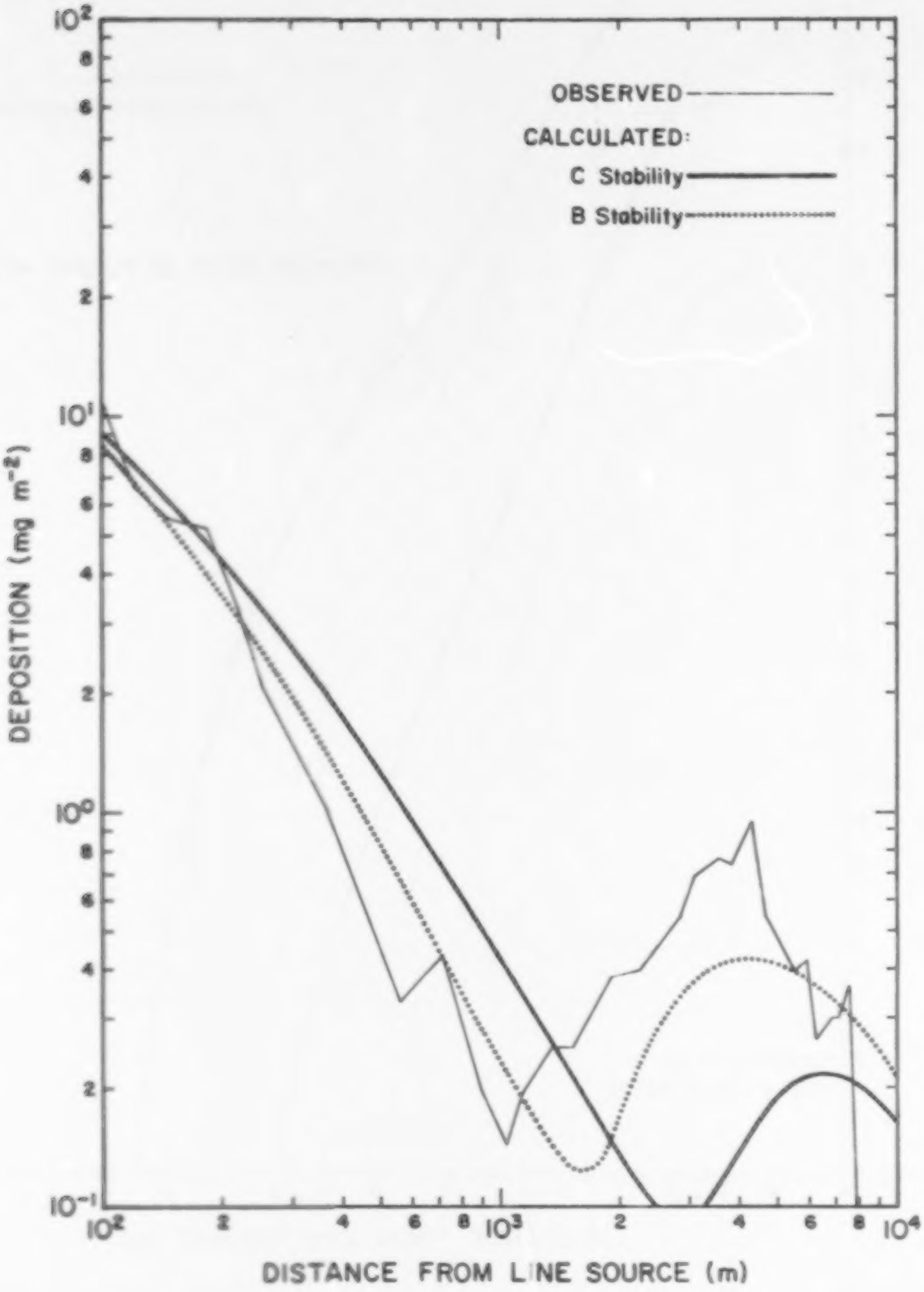

FIGURE 2-5. Observed and calculated deposition profiles for Boyle, et al. (1975) Trial 1-7.

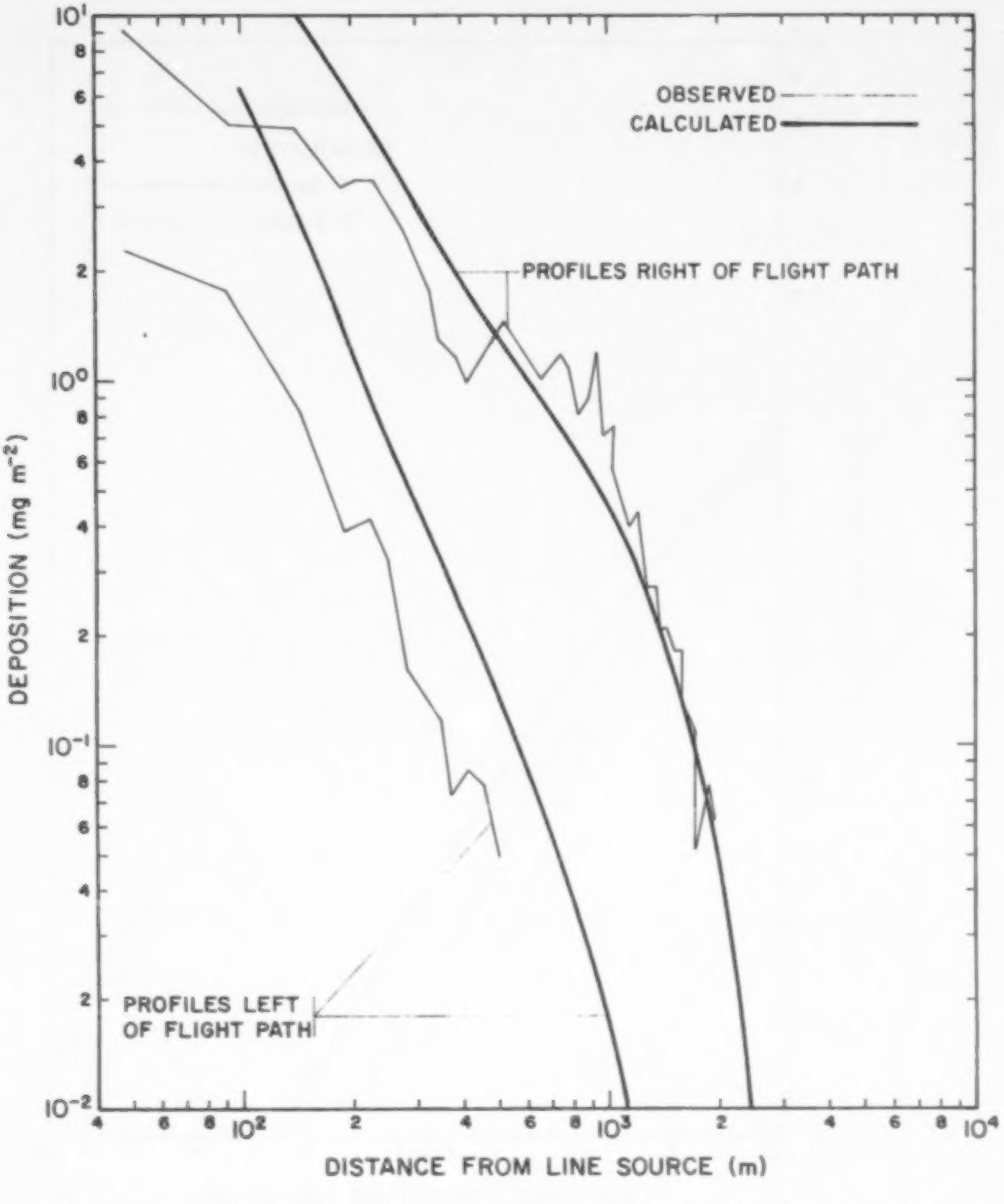

FIGURE 2-6. Observed and calculated deposition profiles for Boyle, et al (1975) Trial 2-2R.

profile at distances of more than about 200 meters normal to the flight path. The ISC Model overestimates the deposition within about 200 meters. For the area to the left of the flight path, the ISC Model calculates deposition values that are higher than the observed values at all distances normal to the flight path.

Figure 2-7 compares the calculated and observed deposition profiles for Trial 2-3. As in the case of Trial 2-2R, the DC-7B aircraft flew almost directly into the mean wind, and the deposition was measured on both sides of the flight path. For the area to the right of the flight path, the ISC Model yields calculated deposition values beyond about 200 meters that are within a factor of 2 of the observed values. However, the ISC Model overpredicts the deposition in the area to the left of the flight path. In both Trials 2-3 and 2-2R, the component of the mean wind normal to the flight path was blowing from left to right, causing the highest calculated and observed deposition values to occur to the right of the flight path. The performance of the ISC Model for these two trials is good for the area to the right of the flight path and poor for the area to the left of the flight path. The ISC Model does not accurately account for deposition in the area upwind of the line source because deposition in this area is principally determined by the complex interaction of the wind and the aircraft wake vortices.

Table 2-14 summarizes the comparisons of concurrent calculated and observed deposition values at 100 and 500 meters from the release line for the Boyle, et al. experiments. We point out that the calculated and observed deposition values are near the center of the line source where edge effects are unimportant. Also, Table 2-14 considers only the deposition to the right of the flight path for Trials 2-2R and 2-3 because the ISC Model cannot account for deposition upwind of the flight path for these trials. The MR and RMSE values in Table 2-14 show that the uncertainties in the model calculations tend to increase with distance from the line source. This result is explained by the fact that deposition near the source was principally determined by the gravitational settling

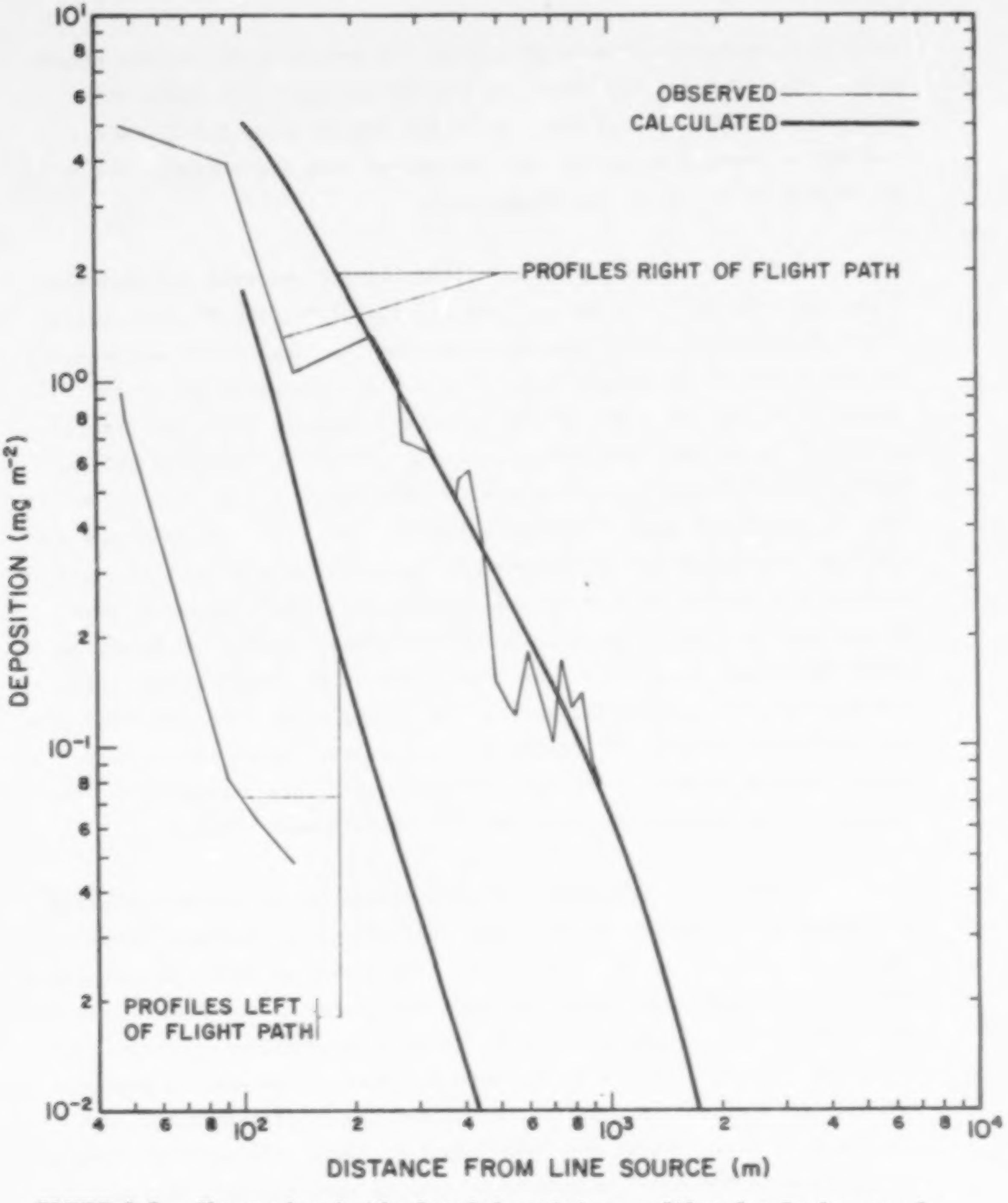

FIGURE 2-7. Observed and calculated deposition profiles for Boyle, et al. (1975) Trial 2-3.

TABLE 2-14

SUMMARY OF THE RESULTS OF THE ISC MODEL CALCULATIONS FOR THE BOYLE, ET AL. (1975) DEPOSITION EXPERIMENTS*

Distance from Line Source (m)	MR of Deposition Values	RMSE of Deposition Values	% Within a Factor of 2
100m	0.91 (0.90)**	1.89 (1.90)**	80 (80)**
500m	1.78 (1.92)**	2.33 (2.13)**	60 (80)**

*The sample size is 5.

**The numbers enclosed by parentheses assume that B stability rather than C stability existed during Trial 1-7.

of the larger droplets. At longer distances from the source, deposition was determined by smaller droplets which were affected by both gravitational settling and atmospheric turbulence.

SECTION 3

TESTS OF THE AERODYNAMIC WAKE EFFECTS OPTION

The published results of three diffusion experiments and the source, meteorological and air quality data for an existing industrial source complex were used to test the aerodynamic building wake effects option of the ISC Model. The calculations for each data set were first performed without using the building wake effects, distance-dependent plume rise and stack-tip downwash options to provide a reference for judging the effectiveness of these ISC Model features. The distance-dependent plume rise option was then used in combination with the building wake effects option in the ISC Model calculations for buoyant stack emissions because: (1) The building wake effects option was specifically designed for use in combination with distance-dependent plume rise equations, and (2) Sensitivity analyses performed during the development of the ISC Model showed that the use of the final plume rise option in combination with the building wake effects option often yielded zero or effectively zero calculated concentrations within the building wake region (i.e., within ten building heights or widths downwind, depending on the critical length scale). The third set of ISC Model calculations for buoyant stack emissions involved the combination of the distance-dependent plume rise, building wake effects and stack-tip downwash options.

The published diffusion experiments used to test the building wake effects option of the ISC Model consisted of the elevated, slightly buoyant tracer releases at Millstone Nuclear Power Station described by Johnson, et al. (1975), the ground-level tracer releases downwind of the MTR-ETR Complex at the National Reactor Testing Station described by Islitzer (1965), and the elevated, non-buoyant tracer releases at CANDU Nuclear Power Generating Station described by Munn and Cole (1967). Additionally, DOW Chemical USA provided to EPA for use in this study concurrent source, meteorological and air quality data for the DOW Michigan Division plant in Midland, Michigan (Brown, 1979a and 1979b and Abrams, 1978 and 1979). The three published data sets and the DOW data provide direct tests of the building wake effects option of the ISC Model. The Millstone and DOW data sets also provide direct tests of the ISC Model's representation of the physical separation of sources and indirect tests of the model's generalized (distance-dependent) plume rise equations and the stack-tip downwash option. The application of the ISC Model to the Johnson, et al. (1975), Islitzer (1965), Munn and Cole (1967), and DOW data sets is discussed in Sections 3.1, 3.2, 3.3 and 3.4, respectively.

3.1 MILLSTONE NUCLEAR POWER STATION TRACER EXPERIMENTS (JOHNSON, ET AL., 1975)

Johnson, et al. (1975) present the results of gaseous tracer experiments that were conducted at the Millstone Nuclear Power Station in southeastern Connecticut during the fall of 1974. Figure 3-1 is a map of the area surrounding the Millstone Station, which is located in Waterford, Connecticut on the tip of a small peninsula that extends into Long Island Sound. Sulfur hexafluoride (SF_6) gas was released from the reactor building main vent and dibromodifluoromethane (Freon-12B2) gas was released from three of the ten vents on the adjacent turbine building. Air samples were taken with bag samplers along arcs at nominal downwind distances of 350, 800 and 1500 meters from the reactor building main vent. The angular spacing between samplers was approximately 6 degrees. The sampler locations are shown by the + symbols in Figure 3-1. The results of 36 releases of SF_6 and 26 releases of Freon-12B2 are presented in the report by Johnson, et al. For each experiment, a non-linear least-squares regression technique was used to fit a Gaussian-shaped curve to the concentrations observed along each sampling arc. An estimate of the centerline concentration for each experiment at each distance was then derived from the fitted curves. These estimates are presented by Johnson, et al. in normalized form $\chi\bar{u}/Q$, where χ is the centerline concentration in micrograms per cubic meter, Q is the source emission

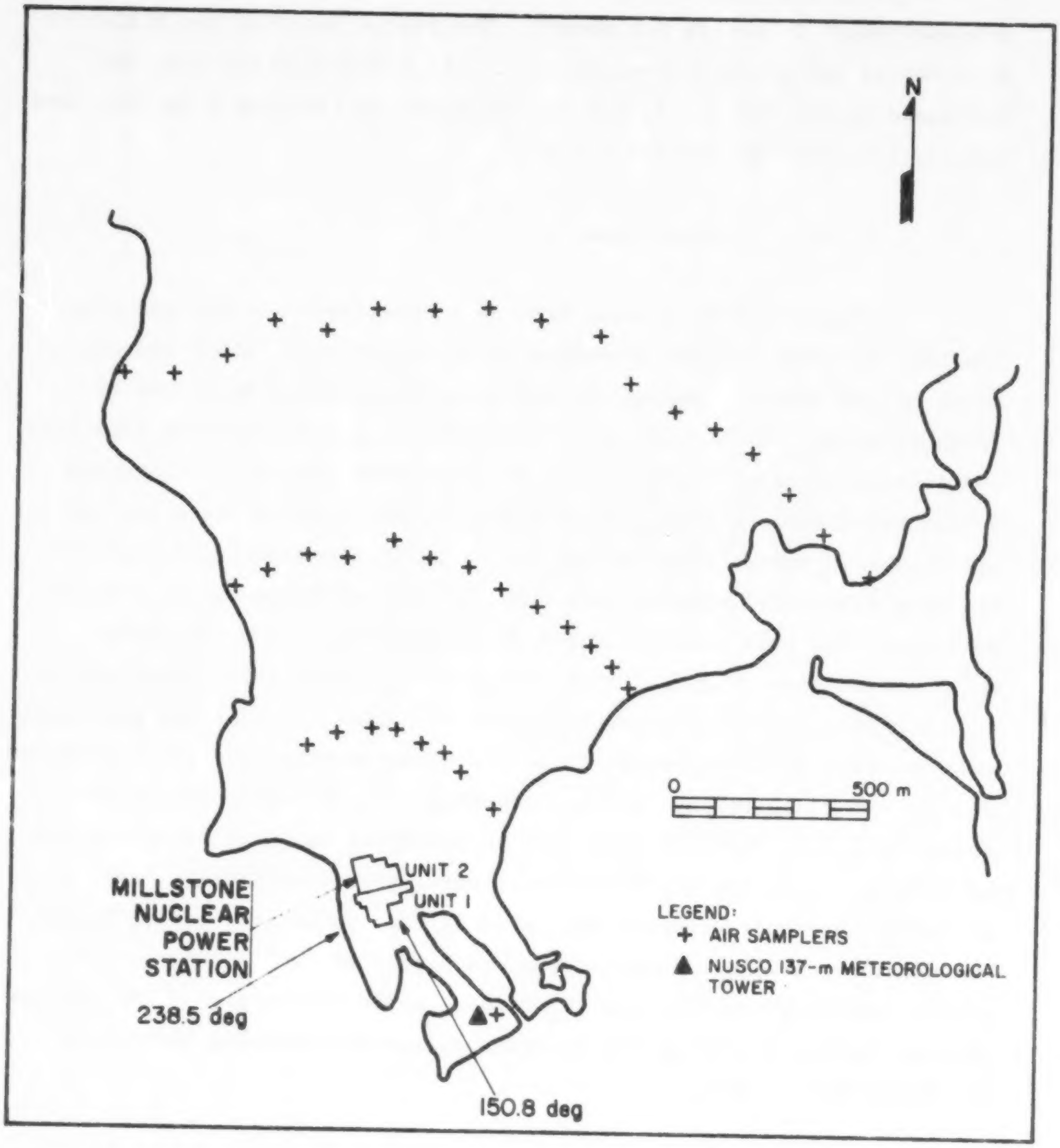
N
0
500 m
UNIT 2
UNIT 1
MILLSTONE
NUCLEAR
POWER
STATION
238.5 deg
150.8 deg
LEGEND:
+ AIR SAMPLERS
▲ NUSCO 137-m METEOROLOGICAL TOWER

FIGURE 3-1. Map of the area surrounding the Millstone Nuclear Power Station. The + symbols show the sampling locations used in the experiments described by Johnson, et al. (1975) and the ▲ symbol shows the location of the 137-meter meteorological tower.

rate in grams per second, and $\bar{u}$ is the hourly mean wind speed at the release height in meters per second. The source data for the Millstone experiments are given in Section 3.1.1, the meteorological data are discussed in Section 3.1.2, and the ISC Model calculation procedures and results are given in Section 3.1.3

3.1.1 Source Data

Figure 3-2 is a scale drawing of the Millstone Nuclear Power Station; building heights in meters above ground level (AGL) are also shown in the figure. During the diffusion experiments described by Johnson, et al. (1975), SF_6 and Freon-12B2 gases were injected into four ventilation ducts at the Millstone Nuclear Power Station. Thirty-six 1-hour releases were conducted in which SF_6 was injected into the reactor building main vent. Also, during 26 of the 36 experiments, Freon-12B2 was simultaneously injected into three of the ten vents on the turbine building. The exit velocities and exit temperatures for the vents, which varied from trial to trial, are given in Table 3-1. The physical vent locations and dimensions are given in Table 3-2. For the rectangular vent on the reactor building, Table 3-2 gives an effective stack diameter that is the diameter of a circular opening with the same area as the vent. It should be noted that, in the ISC Model calculations described in Section 3.1.3, the SF_6 experiments were modeled separately, and different coordinate systems were used in the two sets of calculations. The origin of the coordinate system was placed at the location of the reactor building vent for the SF_6 trials, while the origin of the coordinate system was placed at the location of turbine building Vent E for the Freon-12B2 trials.

The location of the Millstone Nuclear Power Station at the southern end of a small peninsula restricted the Millstone diffusion experiments to wind directions from south-southeast through south-southwest, and the majority of the experiments were conducted with south-southwest winds. Thus, the turbine building was generally upwind

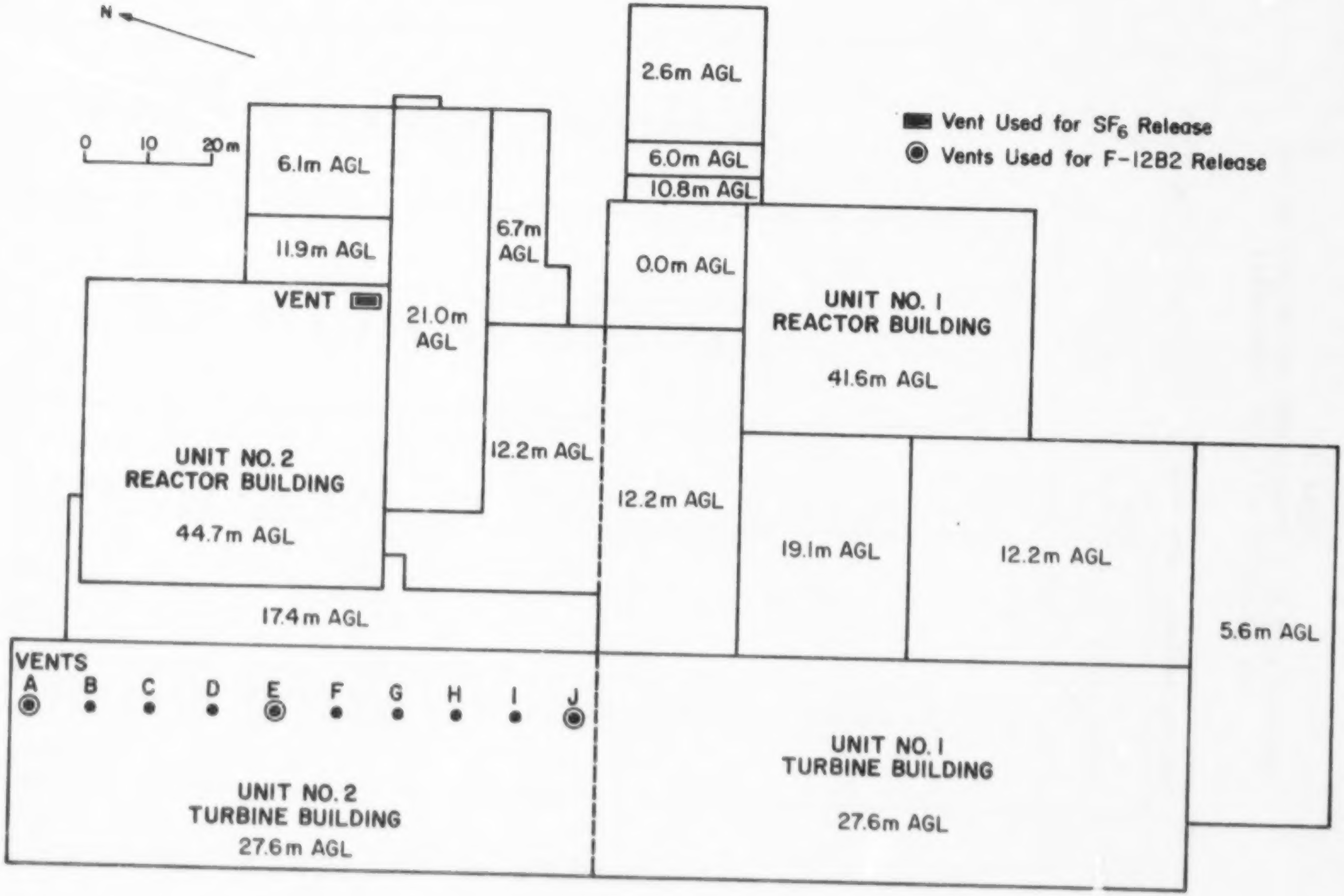
N
0
10
20m
6.1m AGL
11.9m AGL
VENT
21.0m AGL
6.7m AGL
2.6m AGL
6.0m AGL
10.8m AGL
0.0m AGL
UNIT NO. 1 REACTOR BUILDING
41.6m AGL
Vent Used for SF6 Release
Vents Used for F-12B2 Release
UNIT NO. 2 REACTOR BUILDING
44.7m AGL
12.2m AGL
12.2m AGL
19.1m AGL
12.2m AGL
5.6m AGL
17.4m AGL
VENTS
A
B
C
D
E
F
G
H
I
J
UNIT NO. 2 TURBINE BUILDING
27.6m AGL
UNIT NO. 1 TURBINE BUILDING
27.6m AGL

FIGURE 3-2. Layout of the Millstone Nuclear Power Station showing the locations of the emission points for the diffusion experiments conducted by Johnson, et al. (1975). Building heights are given in meters above ground level (AGL).

TABLE 3-1

BUILDING VENT EXIT TEMPERATURES AND VELOCITIES FOR THE MILLSTONE DIFFUSION EXPERIMENTS

Trial Number	Reactor Building Main Vent		Turbine Building Vents	
	Exit Temperature (°K)	Exit Velocity (m/sec)	Exit Temperature (°K)	Exit Velocity (m/sec)
1	294.2	8.7		
2	293.7	8.7		
3	292.7	8.7		
4	293.0	8.7		
5	291.1	8.3		
6	291.5	8.3		
8	294.5	8.1		
9	294.8	8.1		
10	294.0	8.1		
11	295.9	8.7	293.2	10.5
12	295.8	8.7	293.7	10.5
13	296.3	8.7	293.6	10.5
14	295.4	8.7	293.5	10.5
15	295.4	8.7	306.1	10.5
16	296.7	8.7	293.6	10.5
17	295.9	8.6	293.8	10.5
18	295.8	8.7	293.5	10.5
28	295.7	6.2	296.6	10.5
29	296.0	4.6	296.0	10.5
30	296.0	4.6	295.3	10.5
31	295.9	4.6	294.9	10.5
32	295.7	4.6	294.7	10.5
36	294.9	6.3	293.9	10.5
45	294.0	8.5	291.7	10.5
46	294.1	8.5	291.6	10.5
47	294.1	8.4	291.6	10.5
48	294.1	8.5	291.7	10.5
49	294.2	8.4	291.6	10.5
50	294.4	8.5	292.6	10.5
51	294.9	8.4	293.1	10.5
52	294.5	8.6	293.6	10.5
53	294.1	8.7	293.1	10.5
54	293.2	8.7	293.5	10.5
57	293.5	8.6	292.7	10.5
58	293.5	8.5	292.7	10.5
59	293.4	8.6		

TABLE 3-2

PHYSICAL BUILDING VENT PARAMETERS FOR THE MILLSTONE EXPERIMENTS

Vent	Height of Vent (m AGL)	Effective Stack Diameter (m)	X-Coord.* (m)	Y-Coord.* (m)
Reactor Building	48.3	2.12	0	0
Turbine Building				
Vent A	29.1	1.40	-10.9	37.5
Vent E	29.1	1.40	0	0
Vent J	29.1	1.40	13.1	-45.1

*The origin of the calculation grid for the SF_6 releases from the reactor building main vent is at the location of the vent, while the origin of the calculation grid for the Freon-12B2 releases from the turbine building vents is at the location of Vent E (see Figure 3-2).

of the reactor building, which was the dominant building at the Millstone station during the experiments described by Johnson, et al. The reactor building is 44.7 meters high and 47 meters square in the horizontal. These building dimensions were used in the ISC Model calculations for all trials, including the Freon-12B2 releases from the turbine building.

It is important to note that the emission height to building height ratio is less than 1.2 for all four of the vents used in the Millstone diffusion experiments. Also, the building width to building height ratio is greater than 1 and less than 5. Thus, the Millstone experiments provide a test of the building wake effects option for the special case of a squat building with an emission height to building height ratio less than 1.2. The modified vertical dispersion coefficient σ_z' is a function of the building height and the modified lateral dispersion coefficient σ_y' is a function of the building height and crosswind width. Because of the horizontal symmetry of the reactor building, the use by the ISC Model of a single effective building width (defined by the diameter of a circle with equal horizontal area) does not significantly affect the accuracy of the model calculations for any trial (see page 2-39 of the ISC Model User's Guide).

3.1.2 Meteorological Data

Johnson, et al. (1975) give the mean wind speed, mean wind direction, ambient air temperature, and potential temperature gradient for each of the 36 diffusion trials. Wind speed and direction measurements are reported for the 10.0-, 43.3-, 114- and 136-meter levels of an onsite meteorological tower (see Figure 3-1). The winds measured at the 43.3-meter level were used in the ISC Model calculations as the reference level mean wind speeds and flow vectors. We also used the wind-speed measurements at the four tower levels with a logarithmic least-squares regression technique to calculate a wind-profile exponent p for each trial. The values of the vertical potential temperature gradient and ambient air temperature given by Johnson, et al. were used directly as ISC Model inputs. (The ambient air temperatures were measured at the 19.5-meter tower level, while the vertical potential temperature gradients were based on the temperature differences between the 136- and 10-meter tower levels.)

We estimated the Pasquill stability category for each trial using the Turner (1964) criteria, which are based on wind speed and solar radiation (insolation). Insolation indices were determined for each trial on the basis of the date and time of the trial and the cloud cover data reported by Johnson, et al. Cloud cover amount is given by Johnson, et al. in tenths of the total sky covered, while cloud height is reported as low, middle or high. We assumed low clouds to be at heights less than 7,000 feet (2,133 meters) and middle and high clouds to be above 7,000 feet. We used the mean wind speed at the 10-meter tower level during each trial with the corresponding insolation index to determine the Pasquill stability category for the trial. The 10-meter wind speeds were used because airport wind measurements, which are used in the Turner (1964) stability classification scheme, are at that approximate height. Also, the wind measurement height used in the original Pasquill (1961) scheme is 10 meters. Table 3-3 gives all of the parameters that were used to determine the Pasquill stability categories along with the corresponding stability categories estimated for the various trials. The neutral D stability category existed during 31 of the 36 trials, slightly unstable (C stability) conditions existed during one trial, and stable (E stability) conditions existed during four trials.

The hourly meteorological inputs to the ISC Model short-term computer program ISCST are listed in Table 3-4 for each of the Millstone trials. These parameters were developed following the procedures discussed above. The wind speeds in Table 3-4 are the wind speeds at the 43.3-meter tower level, the wind measurement height nearest the emission height. Consequently, the wind system measurement height Z_1 was set

TABLE 3-3

PARAMETERS USED TO DETERMINE PASQUILL STABILITY CATEGORIES FOR THE MILLSTONE TRIALS

Trial Number	Date	Time (EST)	Cloud Cover		Net Radiation Index	10-Meter Mean Wind Speed (m/sec)	Pasquill Stability Category
			Amount (Tenths)	Height*			
1	12 Oct	0800	10	Low	0	7.2	D
2	12 Oct	0900	10	Low	0	6.6	D
3	12 Oct	1000	10	Low	0	6.4	D
4	12 Oct	1100	10	Low	0	6.9	D
5	14 Oct	0900	7	High	2	4.8	C
6	14 Oct	1000	8	Low	1	4.5	D
8	15 Oct	0800	10	High	1	6.8	D
9	15 Oct	0900	10	High	1	5.2	D
10	15 Oct	1000	10	High	1	6.2	D
11	25 Oct	0700	5	-	1	7.9	D
12	25 Oct	0800	5	-	1	8.5	D
13	25 Oct	0900	5	-	2	8.3	D
14	25 Oct	1000	10	Low	0	9.5	D
15	25 Oct	1100	10	Low	0	10.3	D
16	25 Oct	1200	10	Low	0	10.1	D
17	25 Oct	1300	10	Low	0	10.2	D
18	25 Oct	1400	10	Low	0	9.9	D
28	31 Oct	1700	0	-	1	3.0	D
29	31 Oct	1800	0	-	-2	3.7	E
30	31 Oct	1900	5	-	-1	2.9	E
31	31 Oct	2000	5	-	-1	3.1	E
32	31 Oct	2100	5	-	-1	3.1	E
36	4 Nov	0700	10	Low	1	3.7	D
45	14 Nov	0300	0	-	-2	7.2	D
46	14 Nov	0400	7	Middle	-1	8.1	D
47	14 Nov	0500	7	Middle	-1	9.5	D
48	14 Nov	0600	7	Middle	-1	9.2	D
49	14 Nov	0700	8	High	-1	9.5	D
50	14 Nov	0800	8	High	1	9.8	D
51	14 Nov	0900	8	High	2	10.3	D
52	14 Nov	1000	4	-	2	11.2	D
53	14 Nov	1100	4	-	2	10.9	D
54	14 Nov	1200	4	-	2	10.6	D
57	20 Nov	0200	10	Middle	-1	3.6	D
58	20 Nov	0300	10	Middle	-1	3.6	D
59	20 Nov	0400	10	Low	0	3.4	D

*Heights were not reported for amounts less than or equal to five tenths.

TABLE 3-4

METEOROLOGICAL INPUT PARAMETERS FOR THE MILLSTONE TRIALS

Trial Number	Average Flow Vector* (deg)	43.3-Meter Mean Wind Speed (m/sec)	Ambient Air Temperature (°K)	Wind Profile Exponent	Potential Temperature Gradient (°K/m)	Pasquill Stability Category
1	025	7.9	287	0.053	0.000	D
2	029	7.3	288	0.063	0.000	D
3	028	7.2	288	0.064	0.000	D
4	034	7.9	289	0.074	0.000	D
5	327	6.5	285	0.130	0.000	C
6	329	6.0	286	0.099	0.000	D
8	031	9.3	290	0.246	0.007	D
9	049	7.6	291	0.284	0.008	D
10	052	8.7	291	0.279	0.010	D
11	016	8.6	284	0.052	0.000	D
12	011	9.2	284	0.057	0.000	D
13	017	9.2	285	0.048	0.000	D
14	022	10.9	286	0.067	0.000	D
15	024	11.8	286	0.067	0.000	D
16	017	11.5	286	0.062	0.000	D
17	023	11.8	286	0.078	0.000	D
18	027	11.5	286	0.090	0.000	D
28	022	3.8	287	0.201	0.014	D
29	034	4.6	286	0.188	0.009	E
30	036	3.4	286	0.124	0.003	E
31	043	3.5	286	0.171	0.006	E
32	047	3.7	286	0.234	0.008	E
36	048	5.2	287	0.289	0.003	D
45	018	7.7	282	0.050	0.000	D
46	008	8.7	283	0.056	0.000	D
47	023	10.4	283	0.050	0.000	D
48	016	10.2	284	0.049	0.000	D
49	011	10.4	284	0.044	0.000	D
50	012	10.8	284	0.051	0.000	D
51	009	11.4	285	0.057	0.000	D
52	006	12.6	285	0.058	0.000	D
53	004	12.5	285	0.062	0.000	D
54	003	12.5	285	0.076	0.000	D
57	355	4.4	284	0.142	0.000	D
58	332	4.1	284	0.107	0.000	D
59	330	4.1	284	0.151	0.000	D

*Direction toward which the wind is blowing.

equal to 43.3 meters in the ISC Model calculations. Table 3-4 does not include any mixing height estimates. Because of the low emission heights, the relatively short distances to the sampling arcs and the meteorological conditions during the various trials, it is unlikely that the restriction on vertical mixing at the top of the surface mixing layer significantly affected the observed concentrations during any of the trials. We therefore assumed unrestricted vertical mixing in the ISC Model calculations for all of the trials.

3.1.3 Calculation Procedures and Results

The source data discussed in Section 3.1.1 and the meteorological data discussed in Section 3.1.2 were used with the ISC Model short-term computer program ISCST in the Rural Mode to calculate, for each Millstone diffusion experiment, the centerline tracer concentration χ divided by the emission rate Q at the downwind distance of each sampling arc. Concentrations were calculated without any building wake effects or distance-dependent plume rise and with building wake effects for the following combinations of ISC Model options:

- Case A -- Distance-dependent plume rise and building wake effects options
- Case B -- Distance-dependent plume rise, building wake effects and stack-tip downwash options

Additionally, concentrations were calculated under the assumption of surface-based emissions affected by building wakes (Case C) because of visual observations by Johnson, et al. (1975) that the plume often was intermittently entrained into the building's cavity zone and effectively acted as a ground-level source during these periods. All of the calculated centerline concentrations were multiplied by the mean wind speed $\bar{u}$ at 43.3 meters to obtain normalized centerline concentrations $\chi\bar{u}/Q$, the form in which the results of the Millstone experiments are presented by Johnson, et al.

The calculated and observed normalized centerline concentrations for the SF_6 trials at downwind distances of 350, 800 and 1500 meters are listed in Tables 3-5, 3-6 and 3-7, respectively. Similarly, the calculated and observed normalized centerline concentrations for the Freon trials at the three sampling distances are listed in Tables 3-8, 3-9 and 3-10. We point out that our comparisons of the normalized centerline concentrations given in Tables 6 and 7 of the report by Johnson, et al. with the detailed results presented in Appendix C of their report revealed several typographical errors in their Table 6. Thus, the observed concentrations in Tables 3-5 through 3-7 of this report differ in some cases from the corresponding concentrations given in Table 6 of the Johnson, et al. report.

The majority of the Millstone experiments were conducted under very similar meteorological conditions (moderate or strong south-southwest winds in combination with neutral stability). Thus, the ISC Model used unmodified (no building wake effects) or modified (with building wake effects) Pasquill-Gifford dispersion coefficients for the neutral D Pasquill stability category in the majority of the concentration calculations for the Millstone experiments. Because each of the calculated centerline concentrations was multiplied by the mean wind speed and divided by the emission rate for comparison with the corresponding observed normalized centerline concentration given by Johnson, et al., the calculated normalized concentrations are essentially the same for the majority of trials. The turbulent intensities associated with the Pasquill-Gifford dispersion coefficients are the median values for the various Pasquill stability categories and do not necessarily correspond to the actual turbulent intensities during any of the Millstone experiments. Consequently, the trial-to-trial differences in observed normalized concentrations are larger than the trial-to-trial differences in calculated normalized concentrations.

TABLE 3-5

COMPARISON OF OBSERVED AND CALCULATED NORMALIZED CENTERLINE CONCENTRATIONS FOR THE MILLSTONE SF_6 EXPERIMENTS AT 350 METERS DOWNWIND

Trial Number	Normalized Centerline Concentration $\chi\bar{u}/Q$ (10^{-6} m^{-2})					Ratio of Calculated and Observed Concentrations			
	Observed	Calculated				No Building	With Building		
		No Building	With Building						
			Case A	Case B	Case C		Case A	Case B	Case C
1	310	0	125	104	203	0.00	0.40	0.34	0.65
2	230	0	125	103	203	0.00	0.54	0.45	0.88
3	216	0	126	131	203	0.00	0.58	0.61	0.94
4	221	0	138	112	226	0.00	0.62	0.51	1.02
5	107	25	78	80	190	0.23	0.73	0.74	1.78
6	129	0	117	119	190	0.00	0.91	0.92	1.47
8	230	0	94	101	226	0.00	0.41	0.44	0.98
9	262	0	108	90	211	0.00	0.41	0.34	0.81
10	269	0	90	97	211	0.00	0.34	0.36	0.78
11	477	0	122	102	203	0.00	0.26	0.21	0.43
12	465	0	99	106	211	0.00	0.21	0.23	0.45
13	411	0	99	105	203	0.00	0.24	0.26	0.49
14	487	0	103	111	203	0.00	0.21	0.23	0.42
15	359	1	104	113	203	0.00	0.29	0.31	0.57
16	499	0	103	111	203	0.00	0.21	0.22	0.41
17	442	1	104	113	203	0.00	0.24	0.26	0.46
18	313	1	103	112	203	0.00	0.33	0.36	0.65
28	195	0	75	75	211	0.00	0.38	0.38	1.08
29	207	0	69	74	218	0.00	0.33	0.36	1.05

TABLE 3-5 (Continued)

Trial Number	Normalized Centerline Concentration $\chi\bar{u}/Q$ (10^{-6} m^{-2})					Ratio of Calculated and Observed Concentrations			
	Observed	Calculated				No Building	With Building		
		No Building	With Building						
			Case A	Case B	Case C		Case A	Case B	Case C
30	119	0	92	95	226	0.00	0.78	0.80	1.90
31	201	0	96	99	218	0.00	0.48	0.49	1.08
32	138	0	102	107	218	0.00	0.74	0.78	1.58
36	86*	0	87	72	211	0.00	1.02	0.84	2.45
45	331	0	119	99	203	0.00	0.36	0.30	0.61
46	569	0	99	105	211	0.00	0.17	0.18	0.37
47	598	0	103	111	211	0.00	0.17	0.19	0.35
48	434	0	103	111	211	0.00	0.24	0.26	0.49
49	467	0	104	112	211	0.00	0.22	0.24	0.45
50	470	0	104	112	211	0.00	0.22	0.24	0.45
51	520	0	106	114	211	0.00	0.20	0.22	0.41
52	463	0	107	116	211	0.00	0.23	0.25	0.46
53	454	0	107	116	211	0.00	0.24	0.26	0.46
54	539	0	107	117	211	0.00	0.20	0.22	0.39
57	73	0	100	100	197	0.00	1.37	1.37	2.70
58	65	0	99	99	203	0.00	1.52	1.52	3.12
59	37	0	96	96	190	0.00	2.59	2.59	5.14
Mean Ratio (MR)						0.00	0.33	0.33	0.66

*Plume centerline may have been off the sampling grid.

TABLE 3-6

COMPARISON OF OBSERVED AND CALCULATED NORMALIZED CENTERLINE CONCENTRATIONS FOR THE MILLSTONE SF_6 EXPERIMENTS AT 800 METERS DOWNWIND

Trial Number	Normalized Centerline Concentration $\chi\bar{u}/Q$ (10^{-6} m^{-2})					Ratio of Calculated and Observed Concentrations			
	Observed	Calculated				No Building	With Building		
		No Building	With Building				Case A	Case B	Case C
			Case A	Case B	Case C				
1	130	25	63	56	86	0.19	0.48	0.43	0.66
2	108	25	63	56	86	0.23	0.58	0.52	0.80
3	70	25	63	64	86	0.36	0.90	0.92	1.23
4	97	27	64	57	86	0.28	0.66	0.59	0.89
5	40	37	34	34	45	0.93	0.85	0.86	1.12
6	39	27	56	56	77	0.69	1.43	1.44	1.98
8	40	7	46	48	86	0.18	1.16	1.21	2.15
9	25	7	50	45	85	0.30	2.00	1.81	3.40
10	85	10	46	49	85	0.12	0.55	0.57	1.00
11	169	24	60	55	84	0.14	0.36	0.32	0.50
12	141	25	53	55	83	0.18	0.38	0.39	0.59
13	164	25	54	56	84	0.15	0.33	0.34	0.51
14	147	29	55	58	84	0.19	0.37	0.39	0.57
15	157	29	57	59	86	0.18	0.36	0.38	0.55
16	186	29	55	58	84	0.15	0.30	0.31	0.45
17	196	28	56	59	86	0.14	0.29	0.30	0.44
18	141	28	56	59	86	0.20	0.40	0.42	0.61
28	40	5	42	42	84	0.12	1.06	1.06	2.10
29	118	0	39	42	101	0.00	0.33	0.35	0.86

TABLE 3-6 (Continued)

Trial Number	Normalized Centerline Concentration $\chi\bar{u}/Q$ (10^{-6} m-2)					Ratio of Calculated and Observed Concentrations			
	Observed	Calculated				No Building	With Building		
		No Building	With Building				Case A	Case B	Case C
			Case A	Case B	Case C				
30	73	0	38	39	101	0.00	0.52	0.53	1.38
31	77	0	46	47	101	0.00	0.60	0.61	1.31
32	137	0	51	52	101	0.00	0.37	0.38	0.74
36	48*	1	39	35	85	0.02	0.80	0.73	1.77
45	153	21	61	55	86	0.14	0.40	0.36	0.56
46	140	25	53	55	83	0.18	0.38	0.39	0.59
47	170	27	55	57	84	0.16	0.32	0.34	0.49
48	157	28	55	57	84	0.18	0.35	0.36	0.53
49	146	28	55	57	84	0.19	0.38	0.39	0.57
50	164	28	55	57	84	0.17	0.33	0.35	0.51
51	134	29	55	58	84	0.22	0.41	0.43	0.63
52	170	30	55	59	84	0.18	0.33	0.35	0.49
53	162	31	55	57	82	0.19	0.34	0.35	0.51
54	161	32	55	58	82	0.20	0.34	0.36	0.51
57	75	16	51	51	80	0.21	0.69	0.69	1.07
58	50	13	52	52	83	0.27	1.05	1.05	1.66
59	23	15	49	49	78	0.67	2.15	2.15	3.40
Mean Ratio (MR)						0.18	0.46	0.46	0.74

*Plume centerline may have been off the sampling grid.

TABLE 3-7

COMPARISON OF OBSERVED AND CALCULATED NORMALIZED CENTERLINE CONCENTRATIONS FOR THE MILLSTONE SF_6 EXPERIMENTS AT 1500 METERS DOWNWIND

Trial Number	Normalized Centerline Concentration $\chi\bar{u}/Q$ (10^{-6} m^{-2})					Ratio of Calculated and Observed Concentrations			
	Observed	Calculated				No Building	With Building		
		No Building	With Building				Case A	Case B	Case C
			Case A	Case B	Case C				
1	41	32	35	33	46	0.79	0.86	0.81	1.12
2	67	32	35	33	46	0.48	0.52	0.49	0.68
3	25	33	35	35	45	1.30	1.39	1.41	1.80
4	44	34	35	33	45	0.76	0.80	0.75	1.03
5	11	20	18	18	20	1.85	1.59	1.60	1.85
6	8	31	36	36	48	3.94	4.53	4.55	6.05
8	52	19	26	27	45	0.37	0.51	0.52	0.87
9	30	19	27	26	44	0.63	0.92	0.88	1.47
10	62	22	27	28	44	0.35	0.43	0.45	0.71
11	69	31	35	33	46	0.45	0.51	0.48	0.67
12	36	31	30	31	42	0.86	0.84	0.86	1.17
13	32	32	33	34	46	1.01	1.03	1.06	1.45
14	44	34	33	34	46	0.77	0.76	0.78	1.05
15	73	34	33	34	46	0.47	0.45	0.47	0.63
16	72	34	33	35	46	0.47	0.47	0.48	0.65
17	41	34	33	34	46	0.84	0.81	0.84	1.12
18	49	34	33	34	45	0.69	0.67	0.69	0.92
28	24*	15	25	25	44	0.64	1.06	1.06	1.84
29	26	4	27	28	62	0.14	1.04	1.09	2.38

*Sampler location where maximum was observed was significantly off plume centerline (see Johnson, _et al._, 1975, p. 48).

TABLE 3-7 (Continued)

Trial Number	Normalized Centerline Concentration $\chi\bar{u}/Q$ (10^{-6} m^{-2})					Ratio of Calculated and Observed Concentrations			
	Observed	Calculated				No Building	With Building		
		No Building	With Building						
			Case A	Case B	Case C		Case A	Case B	Case C
30	23	1	23	23	62	0.04	0.98	1.00	2.70
31	39	2	28	29	61	0.02	0.72	0.73	1.57
32	34	3	30	31	61	0.01	0.89	0.92	1.81
36	17	9	21	20	44	0.51	1.21	1.15	2.59
45	59	30	34	32	46	0.51	0.58	0.55	0.78
46	61	31	31	31	43	0.51	0.50	0.51	0.70
47	52	33	33	34	46	0.64	0.64	0.66	0.89
48	55	34	33	34	46	0.61	0.61	0.63	0.85
49	53	32	31	32	42	0.61	0.58	0.60	0.80
50	41	33	32	34	45	0.81	0.79	0.82	1.09
51	56	33	31	32	42	0.59	0.55	0.57	0.75
52	55	34	31	33	42	0.61	0.57	0.59	0.77
53	58	34	32	33	43	0.58	0.55	0.57	0.74
54	54	34	32	33	43	0.63	0.59	0.61	0.80
57	29	24	30	30	43	0.84	1.03	1.03	1.49
58	12	24	30	30	43	1.98	2.48	2.48	3.59
59	8*	24	33	33	49	2.94	4.13	4.13	6.14
Mean Ratio (MR)						0.62	0.73	0.74	1.09

*Sampler location where maximum was observed was significantly off plume centerline (see Johnson, et al., 1975, p.48)

TABLE 3-8

COMPARISON OF OBSERVED AND CALCULATED NORMALIZED CENTERLINE CONCENTRATIONS FOR THE MILLSTONE FREON EXPERIMENTS AT 350 METERS DOWNWIND

Trial Number	Normalized Centerline Concentration $\chi\bar{u}/Q$ $(10^{-6}\ m^{-2})$					Ratio of Calculated and Observed Concentrations			
	Observed	Calculated				No Building	With Building		
		No Building	With Building				Case A	Case B	Case C
			Case A	Case B	Case C				
11	302	40	130	132	190	0.13	0.43	0.44	0.63
12	387	48	133	135	134	0.12	0.34	0.35	0.48
13	307	33	139	141	211	0.11	0.45	0.46	0.69
14	332	48	128	131	190	0.14	0.39	0.39	0.57
15	382	37	124	127	190	0.10	0.32	0.33	0.50
16	321	52	133	136	190	0.16	0.41	0.42	0.59
17	418	50	129	131	190	0.12	0.31	0.31	0.45
18	404	47	125	128	190	0.12	0.31	0.32	0.47
28	228	1	89	89	190	0.00	0.39	0.39	0.83
29	212	0	84	84	190	0.00	0.39	0.39	0.90
30	131	0	65	65	190	0.00	0.49	0.49	1.45
31	187	0	67	67	197	0.00	0.36	0.36	1.05
32	125	0	71	71	197	0.00	0.57	0.57	1.58
36	192*	0	82	82	178	0.00	0.43	0.43	0.93
45	201	35	127	127	190	0.17	0.63	0.63	0.95
46	306	45	138	140	190	0.15	0.45	0.46	0.62
47	282	44	126	128	190	0.16	0.45	0.45	0.67
48	245	48	133	135	190	0.20	0.54	0.55	0.78
49	419	52	137	140	190	0.12	0.33	0.33	0.45
50	203	51	137	140	190	0.25	0.67	0.69	0.94

*Plume centerline may have been off the sampling grid.

TABLE 3-8 (Continued)

Trial Number	Normalized Centerline Concentration $\chi\bar{u}/Q$ (10^{-6} m^{-2})					Ratio of Calculated and Observed Concentrations			
	Observed	Calculated				No Building	With Building		
		No Building	With Building						
			Case A	Case B	Case C		Case A	Case B	Case C
51	155	56	140	144	190	0.36	0.90	0.93	1.23
52	173	64	140	144	184	0.37	0.81	0.83	1.06
53	184	65	142	146	184	0.36	0.77	0.79	1.00
54	169	66	144	147	184	0.39	0.85	0.87	1.09
57	218	21	135	135	184	0.10	0.62	0.62	0.84
58	173	11	143	143	211	0.06	0.83	0.83	1.22
Mean Ratio (MR)						0.14	0.47	0.48	0.74

TABLE 3-9

COMPARISON OF OBSERVED AND CALCULATED NORMALIZED CENTERLINE CONCENTRATIONS FOR THE MILLSTONE FREON EXPERIMENTS AT 800 METERS DOWNWIND

Trial Number	Normalized Centerline Concentration $\chi\bar{u}/Q$ (10^{-6} m^{-2})					Ratio of Calculated and Observed Concentrations			
	Observed	Calculated				No Building	With Building		
		No Building	With Building				Case A	Case B	Case C
			Case A	Case B	Case C				
11	115	88	66	67	80	0.77	0.58	0.58	0.70
12	169	91	69	69	82	0.54	0.41	0.41	0.48
13	107	91	69	69	83	0.85	0.64	0.65	0.77
14	133	93	68	68	81	0.70	0.51	0.51	0.61
15	165	87	67	68	82	0.53	0.41	0.41	0.50
16	162	95	68	69	81	0.59	0.42	0.43	0.50
17	233	95	69	70	82	0.41	0.29	0.30	0.35
18	132	94	68	69	82	0.71	0.52	0.52	0.62
28	46	30	55	55	81	0.64	1.19	1.19	1.76
29	112	4	56	56	96	0.00	0.50	0.50	0.86
30	60	0	40	40	97	0.00	0.66	0.66	1.62
31	82	1	49	49	97	0.00	0.59	0.59	1.18
32	79	2	53	53	97	0.03	0.67	0.67	1.23
36	89*	14	48	48	81	0.16	0.54	0.54	0.91
45	121	85	66	66	81	0.70	0.55	0.55	0.67
46	125	91	68	69	81	0.73	0.55	0.55	0.65
47	137	91	67	68	81	0.66	0.49	0.49	0.59
48	109	93	68	69	81	0.85	0.62	0.63	0.74
49	141	95	68	69	81	0.67	0.49	0.49	0.57
50	74	95	68	69	81	1.28	0.93	0.94	1.09

*Plume centerline may have been off the sampling grid.

TABLE 3-9 (Continued)

Trial Number	Normalized Centerline Concentration $\chi\bar{u}/Q$ (10^{-6} m^{-2})					Ratio of Calculated and Observed Concentrations			
	Observed	Calculated				No Building	With Building		
		No Building	With Building				Case A	Case B	Case C
			Case A	Case B	Case C				
51	99	96	68	69	80	0.97	0.69	0.70	0.81
52	137	99	70	71	81	0.72	0.51	0.52	0.59
53	148	100	71	72	82	0.68	0.48	0.49	0.55
54	129	99	70	71	80	0.77	0.54	0.55	0.62
57	86	72	65	65	77	0.84	0.75	0.75	0.90
58	37	69	64	64	78	1.86	1.73	1.73	2.11
Mean Ratio (MR)						0.62	0.55	0.55	0.72

TABLE 3-10

COMPARISON OF OBSERVED AND CALCULATED NORMALIZED CENTERLINE CONCENTRATIONS FOR THE MILLSTONE FREON EXPERIMENTS AT 1500 METERS DOWNWIND

Trial Number	Normalized Centerline Concentration $\chi\bar{u}/Q$ (10^{-6} m^{-2})					Ratio of Calculated and Observed Concentrations			
	Observed	Calculated				No Building	With Building		
		No Building	With Building						
			Case A	Case B	Case C		Case A	Case B	Case C
11	70	52	37	37	42	0.75	0.53	0.53	0.60
12	46	54	38	38	43	1.18	0.83	0.83	0.93
13	35	56	39	39	44	1.59	1.11	1.12	1.26
14	74	57	39	40	44	0.77	0.53	0.54	0.60
15	55	57	40	41	46	1.04	0.73	0.74	0.83
16	108	58	40	41	45	0.54	0.37	0.38	0.41
17	76	57	39	40	44	0.75	0.52	0.52	0.58
18	45	57	40	40	44	1.27	0.88	0.89	0.98
28	12*	35	34	34	44	2.91	2.83	2.83	3.68
29	29	20	39	39	60	0.68	1.36	1.36	2.08
30	43	5	29	29	61	0.12	0.68	0.68	1.42
31	51	12	35	35	61	0.24	0.69	0.69	1.20
32	41	16	38	38	61	0.40	0.94	0.94	1.49
36	57	26	31	31	44	0.45	0.54	0.54	0.77
45	62	56	40	40	45	0.90	0.64	0.64	0.73
46	77	54	38	38	43	0.70	0.50	0.50	0.56
47	66	57	40	40	45	0.86	0.60	0.60	0.68
48	56	54	38	38	42	0.97	0.68	0.68	0.76
49	72	54	38	38	42	0.75	0.53	0.53	0.59
50	48	54	38	38	42	1.13	0.79	0.80	0.88

*Sampler location where maximum was observed was significantly off the plume centerline (see Johnson, et al., 1975, p. 48).

TABLE 3-10 (Continued)

Trial Number	Normalized Centerline Concentration $\chi\bar{u}/Q$ (10^{-6} m^{-2})					Ratio of Calculated and Observed Concentrations			
	Observed	Calculated				No Building	With Building		
		No Building	With Building				Case A	Case B	Case C
			Case A	Case B	Case C				
51	55	55	38	38	42	1.00	0.69	0.70	0.77
52	85	56	39	39	43	0.66	0.46	0.46	0.50
53	68	56	39	39	43	0.83	0.57	0.58	0.63
54	54	57	39	40	43	1.05	0.72	0.73	0.79
57	35	50	38	38	43	1.44	1.10	1.10	1.24
58	26	49	37	37	43	1.87	1.44	1.44	1.66
Mean Ratio (MR)						0.84	0.68	0.68	0.83

Table 3-11 summarizes the comparisons of the concurrent calculated and observed maximum centerline concentrations for the Millstone diffusion experiments. Because the equation for the root mean square error (RMSE) given in Section 1.3 cannot be applied to zero concentrations, the normalized centerline concentration was set equal to 1×10^{-6} per square meter for the cases with zero calculated concentrations in order to estimate the RMSE. As shown by Table 3-11, if the building wake effects option is not exercised (equivalent to current modeling techniques), the mean ratio (MR) of calculated to observed concentrations indicates that the model, on the average, underestimates the concentrations observed in the building wake region (i.e., at the 350-meter sampling arc) by an order of magnitude or more. The model's performance, as indicated by both the MR and the RMSE, is significantly improved if building wake effects are included in the model calculations for Cases A and B (the elevated releases). However, the MR indicates that the model has a systematic tendency to underestimate concentrations at all three sampling arcs for Cases A and B. The assumption of surface-based emissions affected by building wakes (Case C) yields the best overall model performance.

In addition to emission rate, wind speed and mixing height, the basic components of a Gaussian plume model are the effective emission height and the lateral and vertical dispersion coefficients. The emission rates and wind speeds are known with a relatively high degree of confidence for Millstone diffusion experiments, and the restriction on vertical mixing at the top of the surface mixing layer is unlikely to have affected the observed concentrations. Thus, the fact that the ISC Model tends to underpredict concentrations near the source for Cases A and B may be attributed to one or more of the following factors:

- The ISC Model may not accurately describe lateral plume spread (σ_y)
- The ISC Model may not accurately describe vertical plume spread (σ_z)

TABLE 3-11

SUMMARY OF THE RESULTS OF THE ISC MODEL CALCULATIONS FOR THE MILLSTONE DIFFUSION EXPERIMENTS (JOHNSON, ET AL., 1975)

Tracer	Sampling Distance (m)		
	350	800	1500
(a) Mean Ratio (MR) of Calculated to Observed Concentrations			
SF_6*			
No Buildings	0.00	0.18	0.62
Buildings: Case A	0.33	0.46	0.73
Buildings: Case B	0.33	0.46	0.74
Buildings: Case C	0.66	0.74	1.09
Freon-12B2**			
No Buildings	0.14	0.62	0.84
Buildings: Case A	0.47	0.55	0.68
Buildings: Case B	0.48	0.55	0.68
Buildings: Case C	0.74	0.72	0.83
(b) Root Mean Square Error (RMSE)			
SF_6*			
No Buildings	259.90	9.38	2.88
Buildings: Case A	3.17	2.31	1.79
Buildings: Case B	3.09	2.28	1.78
Buildings: Case C	2.06	1.83	1.88
Freon-12B2**			
No Buildings	19.76	5.07	1.94
Buildings: Case A	2.20	1.89	1.69
Buildings: Case B	2.12	1.88	1.68
Buildings: Case C	1.53	1.64	1.64
(c) Percent Within a Factor of 2			
SF_6*			
No Buildings	0	8	67
Buildings: Case A	31	42	83
Buildings: Case B	28	42	78
Buildings: Case C	56	86	83
Freon-12B2**			
No Buildings	0	77	81
Buildings: Case A	38	73	88
Buildings: Case B	38	73	88
Buildings: Case C	85	88	88

*The sample size is 36.
**The sample size is 26.

- The ISC Model may not accurately predict the effective emission height (H)

Of the three possible sources of error, lateral plume spread is the simplest to evaluate because σ_y may be estimated from the data given by Johnson, et al. The other two possible sources of error are far more difficult to evaluate because no vertical concentration profiles are available for the Millstone experiments. Additionally, because the H/σ_z ratio appears in the Vertical Term of the concentration equation, no direct procedure for the estimation of σ_z is known if H is unknown, and vice versa.

Johnson, et al. used a nonlinear least-square regression technique to fit a Gaussian-shaped curve to the observed concentrations at each of the three sampling arcs for each trial. Although the fitted curves are shown in Appendix C of the report by Johnson, et al., the fitted σ_y values are not listed in their report. We contacted Johnson to obtain the fitted σ_y values. However, the fitted σ_y values had not been located at the time of the preparation of this report. Consequently, we graphically estimated the σ_y value at each sampling distance for each SF_6 trial using the definition for a Gaussian distribution that the distance between the locations on a Gaussian curve of concentrations equal to 10 percent of the centerline concentration is 4.3 σ_y. (We did not attempt to estimate σ_y values for the Freon trials because these trials involved simultaneous releases from multiple vents.)

Table 3-12 compares the calculated σ_y values for the neutral D and slightly unstable C stability categories with the mean observed (fitted) σ_y values for the trials conducted under conditions of D stability, the stability category associated with about 89 percent of all trials. We point out that the σ_y values calculated for C stability in the Rural Mode in Table 3-12 also correspond to the σ_y values calculated for D stability in Urban Mode 2. Also, the calculated σ_y values at 350 meters are the same for the D and C stability categories because the

TABLE 3-12

COMPARISONS OF CALCULATED σ_y VALUES AND OBSERVED MEAN σ_y VALUES FOR THE SF_6 TRIALS CONDUCTED UNDER NEUTRAL (D STABILITY) CONDITIONS

Downwind Distance (m)	Mean Observed σ_y (m)	Calculated σ_y (m)		$\frac{\text{Calculated } \sigma_y}{\text{Observed } \sigma_y}$	
		D Stability	C Stability	D Stability	C Stability
350	44.5	33.0	33.0	0.74	0.74
800	87.5	63.6	84.2	0.73	0.96
1500	139.5	106.7	149.8	0.76	1.07

modified dispersion coefficients calculated by the ISC Model within the wake region are independent of stability. For the effective crosswind building width h_w of 53 meters used in the ISC Model calculations, the model underestimates lateral plume spread by about 25 percent at all downwind distances if turbulent intensities corresponding to the D stability category are assumed to have occurred during the trials. If turbulent intensities corresponding to the C stability category are assumed to have occurred during the trials, the model underestimates σ_y by about 25 percent at 350 meters and closely matches the observed mean σ_y values at 800 and 1500 meters. It is also possible to solve for the value of h_w that forces the calculated σ_y in the Rural Mode under D stability to match the observed mean σ_y value at each sampling arc. This value ranges from about 86 meters at 350 meters downwind to about 153 meters at 1500 meters downwind.

Our comparison of calculated and observed σ_y values for the SF_6 trials may be summarized as follows:

- Because the σ_y values used in the model calculations are about 25 percent lower than the corresponding mean observed σ_y values at the three sampling arcs, the ISC Model's tendency to underestimate concentrations near the source cannot be attributed to overestimations of lateral plume spread

- The calculated σ_y values can be forced to match the observed σ_y values by varying the effective crosswind building width h_w, but no single value of h_w yields calculated σ_y values that match the mean observed σ_y values at all downwind distances

We conclude from these results that the discrepancies between calculated and observed centerline concentrations near the source are primarily attributable to errors in the calculated plume heights H and/or in the calculated vertical dispersion coefficients σ_z.

Figure 3-3 illustrates the visual observations of plume behavior reported by Johnson, et al. for the Millstone diffusion experiments. When the exit velocity V_s to mean wind speed $\bar{u}$ ratio was less than or equal to about 0.9 (Mode I), complete entrainment of the plume into the building's cavity zone appeared to occur with the plume effectively acting as a ground-level source. On the other hand, when the $V_s/\bar{u}$ ratio was greater than or equal to about 5 (Mode II), the plume remained elevated and appeared to be unaffected by downwash into the cavity zone. However, most of the time the plume appeared to be in a condition of partial entrainment (Mode III) in which portions of the plume would intermittently become entrained into the cavity zone. The prevalent mode during the Millstone experiments was Mode III. It follows from Figure 3-3 that the hourly average effective emission height during most of the trials probably was intermediate between the release height and the ground surface.

As discussed above, the majority of the Millstone diffusion experiments were conducted under very similar meteorological conditions (moderate or strong south-southwest winds in combination with the neutral Pasquill D stability category). Also, the upwind fetch was over water. Thus, the Millstone data set may represent a unique combination of source and meteorological parameters. Additionally, the turbulent intensities, especially the vertical turbulent intensities, measured during the Millstone experiments generally were smaller than the median turbulent intensities implicit in the Pasquill-Gifford dispersion coefficients used by the ISC Model. Because vertical plume expansion is reduced if these smaller vertical turbulent intensities apply, site-specific turbulent intensities may account for the ISC Model's tendency to underestimate centerline concentrations when surface-based emissions are assumed (Case C).

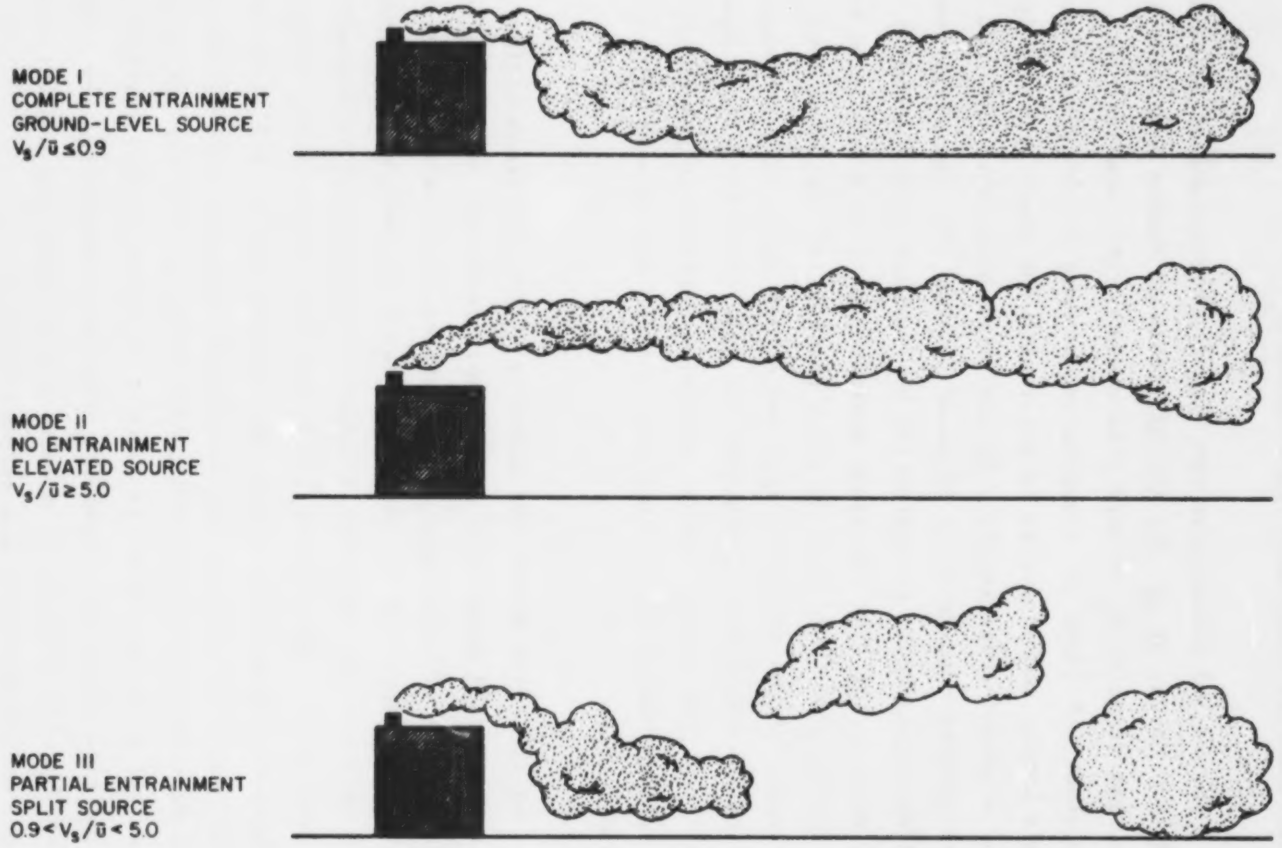
MODE I
COMPLETE ENTRAINMENT
GROUND-LEVEL SOURCE
$V_s/\bar{u} \leq 0.9$
MODE II
NO ENTRAINMENT
ELEVATED SOURCE
$V_s/\bar{u} \geq 5.0$
MODE III
PARTIAL ENTRAINMENT
SPLIT SOURCE
$0.9 < V_s/\bar{u} < 5.0$

FIGURE 3-3. Illustration of the three types of plume behavior observed by Johnson, et al. (1975) during the Millstone diffusion experiments.

3.2 ISLITZER (1965) TRACER RELEASES

Islitzer (1965) presents the results of tracer tests conducted at the Materials Test Reactor Engineering Test Reactor (MTR-ETR) Complex of the National Reactor Testing Station in Idaho. Uranine dye in solution, which was used as the tracer, was released from near ground-level at the downwind edge of the main reactor building, which is shown in Figure 3-4. High volume (hi-vol) air samplers were placed at four downwind distances ranging from the wake region (nominal downwind distance of 118 meters) to 850 meters from the tracer source. The small filled circles in Figure 3-4 show the locations of the hi-vol samplers and the filled square shows the release point. The results of the tracer tests given by Islitzer include estimates of the normalized centerline concentration χ/Q for each test at each sampling distance and the lateral plume spread σ_y at each of the first three sampling distances. No σ_y estimates are given for the 850-meter sampling distance because the 850-meter sampler array was too narrow to allow accurate estimates of plume width. The source data for the Islitzer tracer releases are discussed in Section 3.2.1, the meteorological data are given in Section 3.2.2, and the ISC Model calculation procedures and results are described in Section 3.2.3.

3.2.1 Source Data

The tracer source for the Islitzer (1965) tests was a non-buoyant, ground-level point source with only minimal vertical momentum. Excluding building dimensions, the only ISC Model source input parameter required for a surface-based, non-buoyant source is the emission rate. However, it is not necessary to know the actual emission rates for the Islitzer tests because the tracer concentrations are reported in the normalized form χ/Q, where χ is the estimated centerline concentration in grams per cubic meter and Q is the tracer emission rate in grams per second.

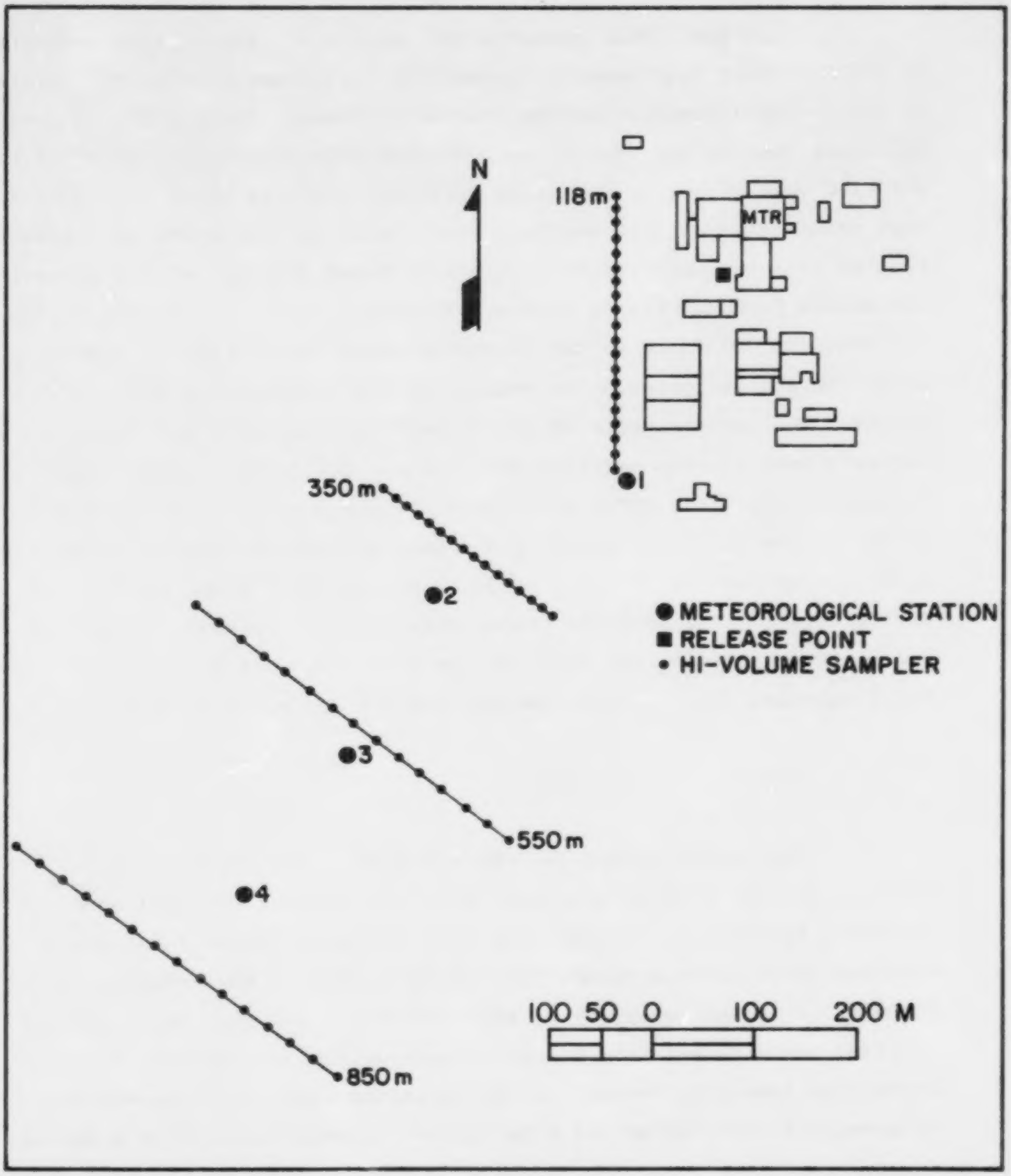
N
118m
MTR
350m
550m
850m
1
2
3
4
● METEOROLOGICAL STATION
■ RELEASE POINT
• HI-VOLUME SAMPLER
100 50 0 100 200 M

FIGURE 3-4. Experimental layout for the Islitzer (1965) diffusion experiments.

As shown by Figure 3-4, the tracer release point was immediately downwind of the main MTR building, which is 24.4 meters high and 45 meters square in the horizontal. The remainder of the MTR-ETR Complex consists of a number of smaller buildings with heights ranging from 6 to 18 meters. (No elevations are given by Islitzer for the individual buildings other than the MTR building.) If the aerodynamic wakes and eddies generated by the MTR building are assumed for modeling purposes to have had the primary effect on the initial dispersion of the tracer, the ISC Model will modify both the vertical and lateral dispersion coefficients for the Islitzer tests. The modified vertical dispersion coefficient σ_z' is a function of the MTR building height and the modified lateral dispersion coefficient σ_y' is a function of the MTR building height and crosswind width. On the other hand, if the aerodynamic wakes and eddies generated by the entire MTR-ETR Complex are assumed to have affected the initial dispersion of the tracer, Figure 3-4 indicates that the effective crosswind width h_w is more than 5 times the MTR building height h_b. The ISC Model uses either Equation (2-31) or Equation (2-33) in the ISC Model User's Guide to calculate the modified lateral dispersion coefficient when the h_w/h_b ratio exceeds 5. As discussed on page 2-38 of the ISC Model User's Guide, Equation (2-33) generally is considered to be more appropriate than Equation (2-31). Consequently, we used Equation (2-33) in the set of ISC Model calculations which considered the effects of the building wakes of the entire MTR-ETR Complex. The modified lateral dispersion coefficient σ_y' defined by Equation (2-33) is a function of the building height, but not of the building width.

3.2.2 Meteorological Data

Wind speed and wind direction were measured during the Islitzer (1965) tests at the four locations downwind from the release point shown by the large filled circles in Figure 3-4. In addition to wind speed and direction, the standard deviations of horizontal (σ_A) and vertical

(σ_E) wind directions were measured. No measurements were made of the undisturbed winds upwind of the MTR-ETR Complex.

Measurements of mixing height are not reported by Islitzer. However, because of the relatively short sampling distances and because of the presence of the MTR-ETR Complex upwind of the test area, we assumed that the surface mixing layer was sufficiently deep that reflection from the top of the mixing layer did not significantly affect the measured ground-level tracer concentrations.

The meteorological data given by Islitzer are not sufficient to determine the Pasquill stability categories for the tests using the Turner (1964) method, the stability classification scheme routinely used with the ISC Model. Specifically, insolation data, the times of the tests and the cloud cover data for the tests are not provided. However, measurements of two other meteorological parameters, the vertical temperature gradient (ΔT) and the standard deviation of the wind direction angle (σ_A), can be used to estimate the Pasquill stability categories following criteria established by the Atomic Energy Commission (1972). The AEC criteria for determining stability categories from ΔT and σ_A measurements are given in Table 3-13.

The meteorological inputs for the Islitzer tracer tests are given in Table 3-14. As shown by the table, the Pasquill stability categories determined for a given test by the ΔT and σ_A methods differ by as many as six stability categories. Therefore, ISC Model calculations were performed for both sets of stability categories. We point out that, with the exception of Test 7, the very unstable A Pasquill stability category is indicated for all tests by one or both of the stability classification schemes. Thus, it is entirely possible that A stability existed during all tests except Test 7. The mean wind speed at the emission height during each test is also given in Table 3-14. The other ISC Model meteorological input parameters are not required to model the Islitzer tests. For example, the ambient air temperature and the vertical

TABLE 3-13

ATOMIC ENERGY COMMISSION (1972) PASQUILL STABILITY CLASSIFICATION CRITERIA

Pasquill Stability Category	Standard Deviation of Horizontal Wind Direction* σ_A (deg)	Temperature Change with Height ΔT (^{o}C/100m)
A	25.0	<-1.9
B	20.0	-1.9 to -1.7
C	15.0	-1.7 to -1.5
D	10.0	-1.5 to -0.5
E	5.0	-0.5 to 1.5
F	2.5	1.5 to 4.0
G	1.7	> 4.0

*Values are averages for each category.

TABLE 3-14

METEOROLOGICAL DATA FOR THE ISLITZER (1965) TESTS

Test Number	Pasquill Stability Category		Mean Wind Speed at Release Height (m/sec)
	AEC: ΔT	AEC: σ_A	
3	A	A	3.1
4	A	A	3.1
5	C	A	3.1
6	A	C	2.7
7	G	D	4.5
8	A	C	3.1
9	A	C	3.1
10	G	A	2.2
11	A	C	2.2
12	A	C	2.7
13	A	B	1.8

potential temperature gradient, which are used to compute plume rise, are not needed because the tracer source was non-buoyant. Similarly, the wind-profile exponent, which is used to adjust the wind speed from the measurement height to the release height, is not required because the emission height, the wind sensors and the hi-vol samplers were all at approximately the same elevation.

3.2.3 Calculation Procedures and Results

The source data presented in Section 3.2.1 and the meteorological data given in Section 3.2.2 were used with the ISC Model short-term computer program ISCST in the Rural Mode to calculate 1-hour average ground-level centerline tracer concentrations for comparison with the centerline concentrations estimated by Islitzer (1965) from the observed tracer concentrations. Values of lateral plume spread σ_y were also calculated for comparison with the measured values of σ_y. The ISC Model calculations were performed under the assumption of no building wake effects and under the assumption that building wakes affected initial tracer dispersion. As explained below, the results of the lateral plume spread calculations within the building wake region (i.e., at the 118-meter sampling distance) were used to estimate the appropriate building dimensions for use in the ISC Model calculations for the Islitzer tests.

The first sampling distance of 118 meters is within the building wake region of both the MTR building alone and the entire MTR-ETR Complex. Table 3-15 compares the observed values of the lateral dispersion coefficient σ_y at 118 meters for the Islitzer tests with the corresponding coefficients calculated in the absence of any building wake effects and with the MTR building and the MTR-ETR Complex defining the effects of building wakes on lateral plume spread. The calculated σ_y values in the absence of any building wake effects are based on the stability categories defined by the ΔT and σ_A stability classification schemes. Also, for the reasons given in Section 3.2.2 above, a third set of σ_y

TABLE 3-15

COMPARISON OF CALCULATED AND OBSERVED σ_y VALUES AT 118 METERS FOR THE ISLITZER (1965) TESTS FOR THE ΔT AND σ_A STABILITY CLASSIFICATION SCHEMES AND FOR A STABILITY

Test No.	Observed σ_y (m)	Calculated σ_y (m)				
		No. Bldgs.			MTR Bldg.	MTR-ETR Complex
		ΔT	σ_A	A Stability		
3	54.5	31.2	31.2	31.2	20.8	45.7
4	58.2	31.2	31.2	31.2	20.8	45.7
5	55.1	14.5	31.2	31.2	20.8	45.7
6	47.4	31.2	14.5	31.2	20.8	45.7
7	24.8	4.7	9.6	31.2	20.8	45.7
8	55.7	31.2	14.5	31.2	20.8	45.7
9	43.4	31.2	14.5	31.2	20.8	45.7
10	50.0	4.7	31.2	31.2	20.8	45.7
11	44.5	31.2	14.5	31.2	20.8	45.7
12	54.4	31.2	14.5	31.2	20.8	45.7
13	49.5	31.2	21.2	31.2	20.8	45.7

values calculated without any building wake effects assumes that A stability existed during all of the tests (with the possible exception of Test 7). The σ_y values calculated by the ISC Model within the wake region are independent of atmospheric stability if building wake effects are included in the calculations. As shown by Table 3-15, the modified σ_y values attributable to the effects of the aerodynamic wake of the MTR building alone are smaller than the point source σ_y values at 118 meters for the A and B stability categories. However, the modified σ_y values attributable to the effects of the aerodynamic wake of the entire MTR-ETR Complex exceed the point source σ_y values for A and B stabilities and are in good agreement with the observed values for all tests except Test 7. We therefore assumed that the building wakes affecting tracer dispersion during the Islitzer tests were determined by the entire MTR-ETR Complex.

Table 3-16 compares the calculated and observed normalized centerline concentrations at the 118-meter sampling distance for the Islitzer tests. In the absence of building wake effects, the best correspondence between calculated and observed concentrations is obtained if A stability is assumed to have existed during all of the tests. However, the ISC Model overpredicts the observed concentrations by an average factor of 1.94 for A stability with no building wake effects. If the effects of the building wakes for the entire MTR-ETR Complex are included in the calculations, the model overpredicts the observed centerline concentrations by an average factor of only 1.09.

The observed σ_y values at 350 and 550 meters for the Islitzer tests are compared with the corresponding values calculated using the ΔT and σ_A stability classification schemes in Tables 3-17 and 3-18, respectively. (It is important to note that the σ_y values calculated with building wake effects included are not independent of atmospheric stability at 350 and 550 meters because these distances are beyond the building wake region.) The largest differences between calculated and observed σ_y values in Tables 3-17 and 3-18 occur when a stability category other

TABLE 3-16

COMPARISON OF CALCULATED AND OBSERVED NORMALIZED CENTERLINE GROUND-LEVEL CONCENTRATIONS AT 118 METERS FOR THE ISLITZER (1965) TESTS FOR THE ΔT AND σ_A STABILITY CLASSIFICATION SCHEMES AND FOR A STABILITY

Test No.	Normalized Concentration χ/Q (10^{-6} sec/m^3)					Ratio of Calculated and Observed Concentrations			
	Observed	Calculated							
		No Buildings			MTR-ETR Complex	No Buildings			MTR-ETR Complex
		ΔT	σ_A	A Stability		ΔT	σ_A	A Stability	
3	77.9	198	198	198	112	2.54	2.54	2.54	1.44
4	77.4	198	198	198	112	2.56	2.56	2.56	1.45
5	62.6	817	198	198	112	13.05	3.16	3.16	1.79
6	127.0	228	938	228	128	1.80	7.39	1.80	1.01
7	349.0	5,602	1,378	137	77	16.05	3.95	0.39	0.22
8	116.0	198	817	198	112	1.71	7.04	1.71	0.97
9	122.0	198	817	198	112	1.62	6.70	1.62	0.92
10	57.1	11,459	280	280	158	200.68	4.90	4.90	2.77
11	77.8	280	1,151	280	158	3.60	14.79	3.60	2.03
12	129.0	228	938	228	128	1.77	7.27	1.77	0.99
13	86.1	342	673	342	193	3.97	7.82	3.97	2.24
				Mean Ratio (MR)		15.41	6.22	1.94	1.09

TABLE 3-17

COMPARISON OF THE OBSERVED σ_y VALUES AT 350 AND 550 METERS FOR THE ISLITZER (1965) TESTS WITH THE CORRESPONDING σ_y VALUES CALCULATED USING THE ΔT STABILITY CLASSIFICATION SCHEME

Test No.	350 m Downwind			550 m Downwind			Ratio of Calculated and Observed σ_y Values			
	Observed σ_y (m)	Calculated σ_y (m)		Observed σ_y (m)	Calculated σ_y (m)		350 m		550 m	
		No Buildings	MTR-ETR Complex		No Buildings	MTR-ETR Complex	No Buildings	MTR-ETR Complex	No Buildings	MTR-ETR Complex
3	86.3	82.3	82.3	149.0	123.0	123.0	0.95	0.95	0.83	0.83
4	88.9	82.3	82.3	138.0	123.0	123.0	0.93	0.93	0.89	0.89
5	71.0	39.5	65.5	193.0	59.8	84.9	0.56	0.92	0.31	0.44
6	66.3	82.3	82.3	125.1	123.0	123.0	1.24	1.24	0.98	0.98
8	67.0	82.3	82.3	103.2	123.0	123.0	1.23	1.23	1.19	1.19
9	58.5	82.3	82.3	125.0	123.0	123.0	1.41	1.41	0.98	0.98
10	58.1	12.9	57.7	111.2	19.6	63.5	0.22	0.99	0.18	0.57
12	63.8	82.3	82.3	98.8	123.0	123.0	1.29	1.29	1.24	1.24
					Mean Ratio (MR)		0.98	1.10	0.78	0.85

TABLE 3-18

COMPARISON OF THE OBSERVED σ_y VALUES AT 350 AND 550 METERS FOR THE ISLITZER (1965) TESTS WITH THE CORRESPONDING σ_y VALUES CALCULATED USING THE σ_A STABILITY CLASSIFICATION SCHEME

Test No.	350 m Downwind			550 m Downwind			Ratio of Calculated and Observed σ_y Values			
	Observed σ_y (m)	Calculated σ_y (m)		Observed σ_y (m)	Calculated σ_y (m)		350 m		550 m	
		No Buildings	MTR-ETR Complex		No Buildings	MTR-ETR Complex	No Buildings	MTR-ETR Complex	No Buildings	MTR-ETR Complex
3	86.3	82.3	82.3	149.0	123.0	123.0	0.95	0.95	0.83	0.83
4	88.9	82.3	82.3	138.0	123.0	123.0	0.93	0.93	0.89	0.89
5	71.0	82.3	82.3	193.0	123.0	123.0	1.16	1.16	0.64	0.64
6	66.3	39.5	65.5	125.1	59.8	84.9	0.60	0.99	0.48	0.68
8	67.0	39.5	65.5	103.2	59.8	84.9	0.59	0.98	0.58	0.82
9	58.5	39.5	65.5	125.0	59.8	84.9	0.68	1.12	0.48	0.68
10	58.1	82.3	82.3	111.2	123.0	123.0	1.42	1.42	1.11	1.11
12	63.8	39.5	65.5	98.8	59.8	84.9	0.62	1.03	0.61	0.86
					Mean Ratio (MR)		0.87	1.06	0.70	0.80

than the very unstable A Pasquill stability category is assumed in the model calculations. Because it is entirely possible that A stability occurred during all of the Islitzer tests with the possible exception of Test 7 for which no observed σ_y values are available at 350 and 550 meters, Table 3-19 compares the observed σ_y values at 350 and 550 meters with the corresponding values calculated for A stability. Inspection of Table 3-19 shows that the calculated effects of building wakes on lateral dispersion at 350 and 550 meters are negligible in comparison with the calculated effects of atmospheric turbulence if A stability is assumed. The overall correspondence between calculated and observed σ_y values at 350 and 550 meters is about the same for the ΔT and σ_A stability classification schemes and if A stability is assumed for all tests, both with and without the inclusion of building wake effects in the model calculations.

The observed normalized centerline concentrations at 350, 550 and 850 meters for the Islitzer tests are compared with the corresponding concentrations calculated using the ΔT and σ_A stability classification schemes in Tables 3-20 and 3-21, respectively. Additionally, Table 3-22 compares the observed concentrations at 350, 550 and 850 meters with the corresponding concentrations calculated under the assumption that all of the tests were conducted during periods of A stability. Inspection of Tables 3-20 through 3-22 shows that the best overall model performance at 350, 550 and 850 meters is obtained if it is assumed that A stability existed during all trials. At these distances, the calculated effects of atmospheric turbulence for A stability are far more important than the calculated effects of building wakes. Thus, the inclusion of building wake effects in the calculations does not significantly improve the ISC Model's performance for the Islitzer tests except within the building wake region.

Table 3-23 summarizes the comparisons of concurrent calculated and observed centerline concentrations for the Islitzer tests assuming that the

TABLE 3-19

COMPARISON OF OBSERVED σ_y VALUES AT 350 AND 550 METERS FOR THE ISLIZTER (1965) TESTS WITH THE CORRESPONDING σ_y VALUES CALCULATED UNDER THE ASSUMPTION OF A STABILITY DURING ALL TESTS

Test No.	Lateral Plume Spread σ_y (m)				Ratio of Calculated and Observed σ_y Values	
	350m		550m			
	Observed	Calculated*	Observed	Calculated*	350m	550 m
3	86.3	82.3	149.0	123.0	0.95	0.83
4	88.9	82.3	138.0	123.0	0.93	0.89
5	71.0	82.3	193.0	123.0	1.16	0.64
6	66.3	82.3	125.1	123.0	1.24	0.98
8	67.0	82.3	103.2	123.0	1.23	1.19
9	58.5	82.3	125.0	123.0	1.41	0.98
10	58.1	82.3	111.2	123.0	1.42	1.11
12	63.8	82.3	98.8	123.0	1.29	1.24
				Mean Ratio (MR)	1.18	0.94

*Calculated σ_y values are the same both with and without building wake effects.

TABLE 3-20

COMPARISON OF THE OBSERVED NORMALIZED CENTERLINE CONCENTRATIONS AT 350, 550 AND 850 METERS FOR THE ISLITZER (1965) TESTS WITH THE CORRESPONDING CONCENTRATIONS CALCULATED USING THE ΔT STABILITY CLASSIFICATION SCHEME

Test No.	Normalized Concentration χ/Q (10^{-6} sec/m^3)									Ratio of Calculated and Observed Concentrations					
	350 m			550 m			850 m			350 m		550 m		850 m	
	Obs.	Calculated		Obs.	Calculated		Obs.	Calculated		No Bldgs	MTR-ETR Complex	No Bldgs	MTR-ETR Complex	No Bldgs	MTR-ETR Complex
		No Bldgs	MTR-ETR Complex		No Bldg	MTR-ETR Complex		No Bldgs	MTR-ETR Complex						
3	5.83	21.2	21.2	2.66	6.5	5.8	0.85	1.8	1.6	3.64	3.64	2.44	2.18	2.12	1.88
4	9.64	21.2	21.2	4.19	6.5	5.8	MSG	1.8	1.6	2.20	2.20	1.55	1.38	-	-
5	5.99	111.1	44.1	2.30	48.6	25.6	1.96	21.9	14.1	18.55	7.36	21.13	11.13	11.17	7.19
6	20.60	24.3	24.3	5.69	7.5	6.7	3.09	2.0	1.9	1.18	1.18	1.32	1.18	0.65	0.61
8	19.70	21.2	21.2	7.53	6.5	5.8	3.29	1.8	1.6	1.08	1.08	0.86	0.77	0.55	0.49
9	17.80	21.2	21.2	8.29	6.5	5.8	3.25	1.8	1.6	1.19	1.19	0.78	0.70	0.55	0.49
10	9.88	1760.9	84.5	3.96	815.6	74.9	0.93	396.8	63.7	178.23	8.55	205.96	18.91	426.67	68.49
11	9.93	29.8	29.8	4.13	9.2	8.2	2.37	2.5	2.3	3.00	3.00	2.23	1.99	1.05	0.97
12	20.10	24.3	24.3	10.80	7.5	6.7	5.51	2.0	1.9	1.21	1.21	0.69	0.62	0.36	0.34
13	14.80	36.4	36.4	4.96	11.2	10.0	3.29	3.0	2.8	2.46	2.46	2.26	2.02	0.91	0.85
Mean Ratio (MR)										15.43	2.44	16.98	2.85	17.67	3.73

TABLE 3-21

COMPARISON OF THE OBSERVED NORMALIZED CENTERLINE CONCENTRATIONS AT 350, 550 AND 850 METERS FOR THE ISLITZER (1965) TESTS WITH THE CORRESPONDING CONCENTRATIONS CALCULATED USING THE σ_A STABILITY CLASSIFICATION SCHEME

Test No.	Normalized Concentration X/Q (10^{-6} sec/m^3)									Ratio of Calculated and Observed Concentrations					
	350 m			550 m			850 m			350 m		550 m		850 m	
	Obs.	Calculated		Obs.	Calculated		Obs.	Calculated		No Bldgs	MTR-ETR Complex	No Bldgs	MTR-ETR Complex	No Bldgs	MTR-ETR Complex
		No Bldgs	MTR-ETR Complex		No Bldgs	MTR-ETR Complex		No Bldgs	MTR-ETR Complex						
3	5.83	21.2	21.2	2.66	6.5	5.8	0.85	1.8	1.6	3.64	3.64	2.44	2.18	2.12	1.88
4	9.64	21.2	21.2	4.19	6.5	5.8	MSG	1.8	1.6	2.20	2.20	1.55	1.38	-	-
5	5.99	21.2	21.2	2.30	6.5	5.8	1.96	1.8	1.6	3.54	3.54	2.83	2.52	0.92	0.82
6	20.60	127.5	50.6	5.69	55.8	29.4	3.09	25.2	16.2	6.19	2.46	9.81	5.17	8.16	5.24
8	19.70	111.1	44.1	7.53	48.6	25.6	3.29	21.9	14.1	5.64	2.24	6.45	3.40	6.66	4.29
9	17.80	111.1	44.1	8.29	48.6	25.6	3.25	21.9	14.1	6.24	2.48	5.86	3.09	6.74	4.34
10	9.88	29.8	29.8	3.96	9.2	8.2	0.93	2.5	2.3	3.02	3.02	2.32	2.07	2.69	2.47
11	9.93	156.5	62.1	4.13	68.4	36.1	2.37	30.9	19.9	15.76	6.25	16.56	8.74	13.04	8.40
12	20.10	127.5	50.6	10.80	55.8	29.4	5.51	25.2	19.9	6.34	2.52	5.17	2.72	4.57	3.61
13	14.80	84.0	62.4	4.96	34.6	27.7	3.29	14.5	12.5	5.68	4.22	6.98	5.58	4.41	3.80
									Mean Ratio (MR)	6.04	3.03	6.25	3.66	5.94	4.21

TABLE 3-22

COMPARISON OF THE OBSERVED NORMALIZED CENTERLINE CONCENTRATIONS AT 350, 550 AND 850 METERS FOR THE ISLITZER (1965) TESTS WITH THE CORRESPONDING CONCENTRATIONS CALCULATED UNDER THE ASSUMPTION OF A STABILITY DURING ALL TESTS

Test No.	Normalized Concentration X/Q (10^{-6} sec/m^3)									Ratio of Calculated and Observed Concentrations					
	350 m			550 m			850 m			350 m		550 m		850 m	
	Obs.	Calculated		Obs.	Calculated		Obs.	Calculated		No Bldgs	MTR-ETR Complex	No Bldgs	MTR-ETR Complex	No Bldgs	MTR-ETR Complex
		No Bldg.	MTR-ETR Complex		No Bldg.	MTR-ETR Complex		No Bldg.	MTR-ETR Complex						
3	5.83	21.2	21.2	2.66	6.5	5.8	0.85	1.8	1.6	3.64	3.64	2.44	2.18	2.12	1.88
4	9.64	21.2	21.2	4.19	6.5	5.8	MSG	1.8	1.6	2.20	2.20	1.55	1.38	-	-
5	5.99	21.2	21.2	2.30	6.5	5.8	1.96	1.8	1.6	3.54	3.54	2.83	2.52	0.92	0.82
6	20.60	24.3	24.3	5.69	7.5	6.7	3.09	2.0	1.9	1.18	1.18	1.32	1.18	0.65	0.61
8	19.70	21.2	21.2	7.53	6.5	5.8	3.29	1.8	1.6	1.08	1.08	0.86	0.77	0.55	0.49
9	17.80	21.2	21.2	8.29	6.5	5.8	3.25	1.8	1.6	1.19	1.19	0.78	0.70	0.55	0.49
10	9.88	29.8	29.8	3.96	9.2	8.2	0.93	2.5	2.3	3.02	3.02	2.32	2.07	2.69	2.47
11	9.93	29.8	29.8	4.13	9.2	8.2	2.37	2.5	2.3	3.00	3.00	2.23	1.99	1.05	0.97
12	20.10	24.3	24.3	10.80	7.5	6.7	5.51	2.0	1.9	1.21	1.21	0.69	0.62	0.36	0.34
13	14.80	36.4	36.4	4.96	11.2	10.0	3.29	3.0	2.8	2.46	2.46	2.26	2.02	0.91	0.85
							Mean Ratio (MR)			1.87	1.87	1.41	1.26	0.78	0.72

TABLE 3-23

SUMMARY OF THE RESULTS OF THE ISC MODEL CALCULATIONS FOR THE ISLITZER (1965) TESTS ASSUMING A STABILITY FOR ALL TESTS

Downwind Distance (m)	No. of Valid Samples	MR of Centerline Concentrations		RMSE of Centerline Concentrations		% Within Factor of 2	
		No Bldgs	Bldgs	No Bldgs	Bldgs	No Bldgs	Bldgs
118	11	1.94	1.09	2.74	1.97	36	64
350	10	1.87	1.87	2.34	2.34	40	40
550	10	1.41	1.26	1.94	1.82	50	60
850	9	0.78	0.72	1.86	1.90	67	50

Pasquill A stability category existed during all of the tests. Under this assumption, the concentrations calculated at the 350-, 550- and 850-meter sampling distances are primarily determined by atmospheric turbulence and are not significantly affected by building wake effects. However, as noted above, the 118-meter sampling distance is within the wake region of the MTR-ETR Complex where the calculated concentrations are entirely determined by building wake effects. As shown by the MR in Table 3-23, the inclusion of building wake effects in the model calculations improves the average correspondence between calculated and observed concentrations by almost a factor of 2. Also, the RMSE is decreased from 2.7 to 2.0, and the number of calculated concentrations within a factor of 2 of the corresponding observed concentrations is almost doubled.

3.3 MUNN AND COLE (1967) TRACER RELEASES

Munn and Cole (1967) present the results of eleven tracer releases conducted at the CANDU Nuclear Power Generating Station at Douglas Point, Ontario. Uranine dye, which was used as the tracer, was released from the top of a 46-meter stack while the station was under construction. Several large buildings which were located near the stack might be expected to affect the dispersion of the tracer. Five to seven portable samplers were placed in a single arc at downwind distances that differed from trial to trial. For six of the eleven trials, the samplers were placed within three building heights of one or more of the large buildings of the complex. These trials are not included in this analysis because the ISC Model does not estimate concentrations within three building heights of a building (i.e., within the cavity zone). Munn and Cole give only the maximum observed normalized concentration for each trial. The sampling array was too small to estimate either centerline concentrations or plume widths. The source data for the Munn and Cole (1967) tracer releases are discussed in Section 3.3.1, the meteorological data are given in Section 3.3.2, and the ISC Model calculation procedures and results are described in Section 3.3.3.

3.3.1 Source Data

Figure 3-5 shows the experimental layout for the tracer releases at the CANDU Nuclear Generating Station described by Munn and Cole (1967). The heights above ground level of the buildings at the CANDU Nuclear Generating Station are labeled in meters in Figure 3-5. The tracer source for each of the Munn and Cole trials was a non-buoyant release from the top of the 46-meter stack (chimney) shown in Figure 3-5. Although Munn and Cole do not give the tracer emission rates for the various trials, the emission rates are not required for use in testing the ISC Model because the observed concentrations are given in the normalized form χ/Q, where χ is the maximum observed concentration in grams per cubic meter and Q is the tracer emission rate in grams per second. The tallest building at the CANDU Station was the reactor building, which is 44 meters high and 43 meters in diameter. The tracer release point was about 45 meters from the reactor building, but was not either directly upwind or directly downwind of the reactor building during any of the five trials analyzed in this section. The next largest building was the turbine building, which is 28 meters high, 55 meters long and 46 meters wide. The tracer release point was about 70 meters from the turbine building and was downwind of the turbine building during two of the five trials. The stack used as the tracer release platform is located on the end of the third large building at the CANDU Station, which is 12 meters high, 65 meters long and 40 meters wide.

Two sets of building dimensions were used in the ISC Model calculations for the Munn and Cole trials. The first set of building dimensions corresponded to the reactor building and consisted of a building height h_b of 44 meters and an effective building width h_w of 43 meters. The second set of building dimensions assumed that the building wakes of the entire complex affected the dispersion of the tracer. The building height h_b for the second set of building dimensions was set equal to the height of the tallest building (the 44-meter reactor building)

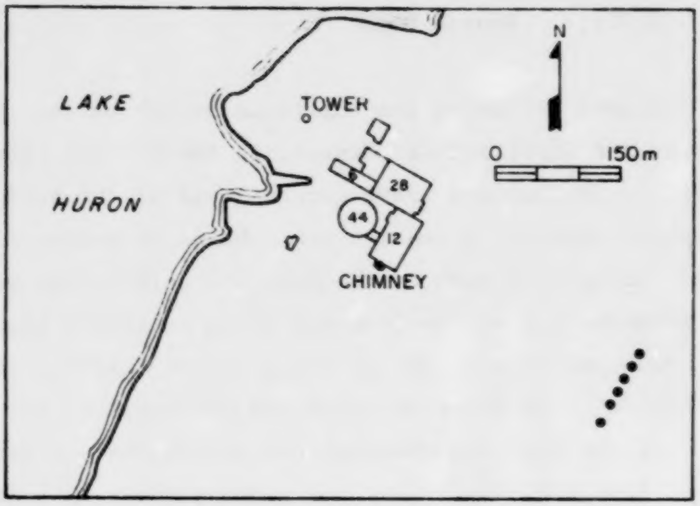
LAKE
HURON
TOWER
N
0
150m
5
28
44
12
CHIMNEY

(a) Munn and Cole (1967) Trials 2, 3 and 12

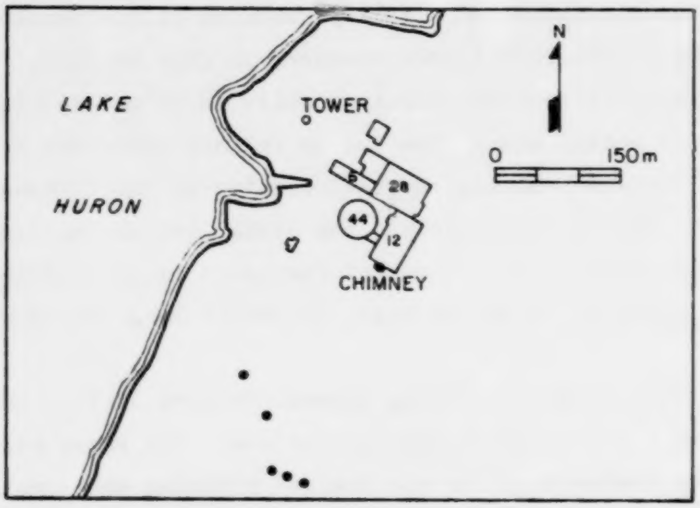
LAKE
HURON
TOWER
N
0
150m
5
28
44
12
CHIMNEY

(b) Munn and Cole (1967) Trials 39 and 40

FIGURE 3-5. Experimental layout for (a) Trials 2, 3 and 12 (west-northwest winds) and (b) Trials 39 and 40 (north-northeast winds) reported by Munn and Cole (1967). Building elevations are shown in meters above ground level (AGL). The filled circles show the sampler locations and the chimney shows the emission point.

and the effective crosswind width h_w of the source complex was estimated from Figure 3-5 to be about 100 meters for all five trials. Because the stack height to building height ratio is only about 1.05 for both sets of building dimensions, the ISC Model modifies both the vertical and lateral dispersion coefficients. The modified vertical dispersion coefficient σ_z' for the first set of building dimensions is a function of both h_b and h_w, while the modified vertical dispersion coefficient for the second set of building dimensions is a function of h_b alone. Similarly, the modified lateral dispersion coefficient σ_y' for the first set of building dimensions is a function of h_w alone, while the modified lateral dispersion coefficient for the second set of building dimensions is a function of both h_w and h_b.

3.3.2 Meteorological Data

The only meteorological data given by Munn and Cole (1967) are the mean wind speeds and wind directions measured on a 24-meter tower located near the source. (The wind speeds are listed in Table 3-24 in Section 3.3.3.) It was therefore necessary to estimate the remaining ISC Model meteorological input parameters. Because the trials were conducted on summer days with wind speeds greater than or equal to 3.6 meters per second, we assumed that the mixing heights during the trials were sufficiently deep so that the restriction on vertical growth at the top of the surface mixing layer did not affect the observed concentrations. The ambient air temperature and vertical potential temperature gradient, which are used by the ISC Model to calculate plume rise, were not required as inputs because the tracer emissions were non-buoyant with essentially no initial vertical momentum. All of the samplers were located within the building wake, and the ISC Model yields concentration estimates that are independent of stability within the wake. Consequently, it was not necessary to know the Pasquill stability category for the two sets of calculations that included building wake effects. The neutral D stability category was arbitrarily assumed to apply during all trials in the set of calculations without wake effects. The default value of the wind-profile exponent for D stability (0.25) was used in all of the model calculations.

3.3.3 Calculation Procedures and Results

The source data presented in Section 3.3.1 and the meteorological data discussed in Section 3.3.2 were used with the ISC Model short-term computer program ISCST in the Rural Mode to calculate ground-level centerline concentrations at the distances of the highest observed concentrations under the following assumptions:

- Building wakes did not affect tracer dispersion
- The aerodynamic wakes and eddies formed by the reactor building alone affected tracer dispersion
- The aerodynamic wakes and eddies formed by all of the buildings of the CANDU Station affected tracer dispersion

The results of these calculations are summarized in Table 3-24. For each trial, the table gives the highest observed normalized concentration, the corresponding normalized centerline concentrations calculated under the three assumptions about building wake effects listed above, and the ratios of the calculated and observed concentrations.

It is important to note that the ISC Model was used to calculate centerline concentrations for each trial, while the highest observed concentrations in Table 3-24 were not necessarily measured at the plume centerline. Thus, the calculated concentrations in Table 3-24 should be greater than or equal to the highest observed concentrations if the ISC Model is accurately simulating the actual dispersion of the tracer. Trial 12 is probably an example of a case in which the maximum observed

TABLE 3-24

COMPARISON OF THE MAXIMUM OBSERVED CONCENTRATIONS FOR THE MUNN AND COLE (1967) TRIALS WITH THE CORRESPONDING CENTERLINE CONCENTRATIONS CALCULATED UNDER THREE DIFFERENT ASSUMPTIONS ABOUT BUILDING WAKE EFFECTS

Trial Number	24-Meter Wind Speed (m/sec)	Highest Normalized Concentration χ/Q (10^{-6} sec/m^3)				Ratio of Calculated and Observed Concentrations		
		Observed	Calculated			No Bldg	Reactor Bldg	All Bldgs
			No Bldg	Reactor Bldg	All Bldgs			
2	4.9	15.6	0.30	25.9	15.2	0.02	1.66	0.97
3	3.6	11.9	0.36	35.5	20.7	0.03	2.98	1.74
12	6.7	0.2	0.00	23.1	12.2	0.00	115.50	61.00
39	8.9	5.4	0.00	20.1	9.3	0.00	3.72	1.72
40	8.5	21.8	0.04	16.4	9.2	0.00	0.75	0.42
				Mean Ratio (MR)*		0.01	1.79	0.99

*The MR values exclude Trial 12 for the reasons given in the text.

concentration was measured some distance from the actual plume centerline. For this trial, the highest observed concentration is about two orders of magnitude lower than both of the calculated centerline concentrations with building wake effects included. Also, the highest observed concentrations for Trials 2 and 3, which were conducted under meteorological conditions similar to those of Trial 12, are about two orders of magnitude larger than the highest observed concentration for Trial 12. Because of this strong implication that the highest observed concentration for Trial 12 is about two orders of magnitude lower than the actual plume centerline concentration, the Trial 12 results are excluded from the MR given at the bottom of Table 3-24.

Table 3-25 summarizes the results of the comparisons of the calculated centerline concentrations and the corresponding maximum observed concentrations for the four Munn and Cole trials we determined were suitable for use for the reasons given above. The results presented in Table 3-25 illustrate the sensitivity of concentrations calculated in the wake region to different assumptions about the buildings with wakes affecting initial plume dispersion. However, whether or not the reactor building or all buildings are assumed to have affected initial plume dispersion, the overall model performance is significantly improved by the inclusion of building wake effects in the model calculations.

3.4 DOW MIDLAND, MICHIGAN PLANT DATA

DOW Chemical USA currently uses a Supplementary Control System (SCS) at its Michigan Division plant in Midland, Michigan to maintain the National Ambient Air Quality Standards (NAAQS) for sulfur dioxide (SO_2). (A Supplementary Control System curtails SO_2 emissions whenever meteorological conditions conducive to high ground-level concentrations occur or are anticipated.) Figure 3-6, a map of the Midland area, shows the locations of DOW's West and South Power Houses, which are the

TABLE 3-25

SUMMARY OF THE RESULTS OF THE ISC MODEL CALCULATIONS FOR THE MUNN AND COLE (1967) TRIALS*

Case	Mean Ratio of Calculated to Observed Concentrations (MR)	Root Mean Square Error (RMSE)	% of Centerline Concentrations within a Factor of 2 of Highest Observed Concentrations
No Buildings	0.01	176.84	0
Reactor Building	1.79	2.47	50
All Buildings	0.99	1.79	75

*Sample size is 4.

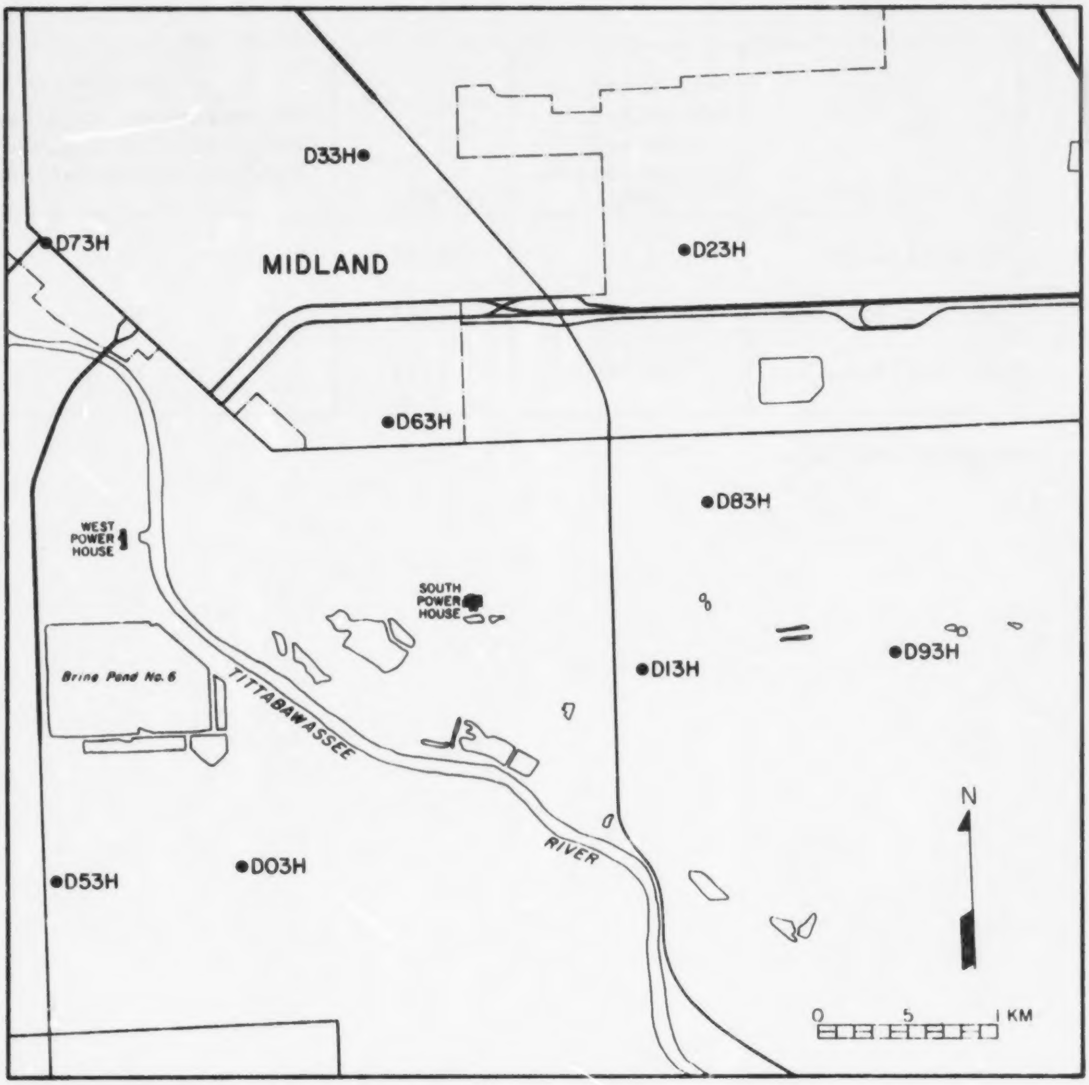
D33H
D73H
MIDLAND
D23H
D63H
D83H
WEST POWER HOUSE
SOUTH POWER HOUSE
Brine Pond No. 6
TITTABAWASSEE
RIVER
D13H
D93H
N
D53H
D03H
0
.5
1 KM

FIGURE 3-6. Map of the area surrounding the West and South Power Houses at the DOW Midland, Michigan plant. The filled circles show the locations of the continuous SO_2 air quality monitors.

primary sources of SO_2 emissions in the Midland area. The filled circles in the figure show the locations of the nine continuous SO_2 air quality monitors in the vicinity of the DOW plant. The stack height to building height ratios at both power houses are less than 1.8 and the stack exit velocities are relatively low. Consequently, DOW and the Michigan Department of Natural Resources (DNR) believe that the aerodynamic wakes and eddies formed by the power house buildings have an adverse effect on the dispersion of the plumes from the power house stacks. Because DOW operates an SCS at the Midland plant, detailed and concurrent emissions, meteorological and air quality data are available for the plant. The DOW Michigan Division provided these data to EPA for use in testing the ISC Model building wake effects option. The DOW source data are discussed in Section 3.4.1, the meteorological inputs for 90 selected cases are given in Section 3.4.2, and the ISC Model calculation procedures and results are described in Section 3.4.3.

3.4.1 Source Data

DOW's meteorological consultant, Environmental Research and Technology, Inc. (ERT), provided magnetic tapes containing hourly emissions, meteorological and air quality data for the Midland plant during the period 10 November 1975 through 27 September 1976 (Abrams, 1978 and 1979). We analyzed the meteorological and air quality data to isolate hours when meteorological conditions were favorable for adverse building wake effects. The selection criteria were as follows:

- A 1-hour SO_2 concentration greater than or equal to 0.25 parts per million (ppm) at one or more of the SO_2 monitors shown in Figure 3-6

- A 10-meter wind speed greater than or equal to 6.17 meters per second (12 knots)

The basis for the first selection criterion was that we wished to model the hours with the highest observed SO_2 concentrations. The two reasons for the second selection criterion were: (1) Adverse building wake effects are most likely during periods of moderate or strong winds, and (2) Following the Turner (1964) definitions of the Pasquill stability categories, the neutral D stability category is almost always associated with 10-meter wind speeds greater than or equal to 6.17 meters per second (no cloud cover data were available to estimate stability using the Turner approach).

Table 3-26 gives the dates, Julian Days and hours of the 90 cases selected for use in testing the building wake effects option of the ISC Model. It is important to note that, in addition to the West and South Power Houses, the DOW Midland plant has two package boilers that are normally used as peak load units. One of the package boilers was in operation during 25 of the 90 cases (Cases 5, 6, 7, 8, 9, 10, 14, 15, 16, 17, 18, 19, 20, 21, 22, 23, 24, 25, 26, 27, 29, 30, 31, 32 and 33) and both package boilers were in operation during Case 13. The package boiler SO_2 emissions are small in comparison with the SO_2 emissions from the power houses. For example, the maximum contribution of the package boiler emissions to the total SO_2 emissions from the DOW plant for the 90 cases listed in Table 3-26 is 6.5 percent (Case 13). Consequently, the air quality impact of emissions from the package boilers was assumed in this study to be negligible in comparison with the impact of emissions from the power houses.

Scale drawings of the West and South Power Houses are shown in Figures 3-7 and 3-8, respectively. These figures, which are based on DOW plant layouts dated 23 February 1979, indicate structure elevations in meters above ground level (AGL). The stack height for Units 13, 19 and 20 is 56 meters, while the height of the single stack serving Units 9 and 12 is 48 meters. The stack height for all stacks at the South Power House is 54 meters. The building dimensions derived from Figures 3-7 and 3-8 and assumed in the ISC Model calculations are listed in Table 3-27. The stack height to building height ratio for each stack at

TABLE 3-26

HOURS SELECTED FOR TESTING THE ISC MODEL AT THE DOW MIDLAND PLANT

Case Number	Date	Julian Day	Hour*
1	10 November 1975	314	0100
2			0200
3			0500
4			1300
5			2300
6			2400
7	12 November 1975	316	1700
8	20 November 1975	324	1200
9			1300
10	21 November 1975	325	0800
11	22 November 1975	326	1500
12			1600
13	1 December 1975	335	0400
14	16 December 1975	350	1500
15			1900
16			2000
17			2100
18	17 December 1975	351	0400
19			0700
20			1000
21	18 December 1975	352	1100
22			1300
23	20 December 1975	354	1200
24			1300
25			1400
26			1600
27			1700
28			2400
29	3 January 1976	003	0100
30			1100
31	5 January 1976	005	1300
32	8 January 1976	008	1600
33			1700
34	14 January 1976	014	0300
35			0400
36			0500
37			0600
38			0700
39			0800
40			2100

TABLE 3-26 (Continued)

Case Number	Date	Julian Day	Hour*
41	14 January 1976	014	2200
42	28 January 1976	028	1600
43			1700
44	7 February 1976	038	2400
45	8 February 1976	039	0100
46			0200
47	11 February 1976	042	1200
48	12 February 1976	043	0900
49	15 February 1976	046	1700
50			1800
51			1900
52	18 February 1976	049	1700
53			1800
54			1900
55	21 February 1976	052	1300
56			1500
57			1600
58	5 March 1976	065	1000
59			1100
60			1500
61	6 March 1976	066	2400
62	7 March 1976	067	0200
63			1400
64			1500
65			1700
66	13 March 1976	073	1200
67	14 March 1976	074	1300
68			1900
69			2000
70			2400
71	24 March 1976	084	0200
72			0300
73			0400
74	3 April 1976	094	1800
75			2000
76			2300
77	4 April 1976	095	0200
78	5 April 1976	096	1600
79			1700
80	15 April 1976	106	0200

TABLE 3-26 (Continued)

Case Number	Date	Julian Day	Hour*
81	16 April 1976	107	1200
82	18 April 1976	109	1000
83	22 April 1976	113	0600
84			0700
85			0800
86	1 May 1976	122	2200
87	3 May 1976	124	1200
88	5 May 1976	126	0200
89	12 June 1976	164	2400
90	7 July 1976	189	1800

*Depending on the day of the year, times are in Eastern Standard Time (EST) or Eastern Daylight Time (EDT) as used by the DOW Midland Plant's Supplementary Control System (SCS).

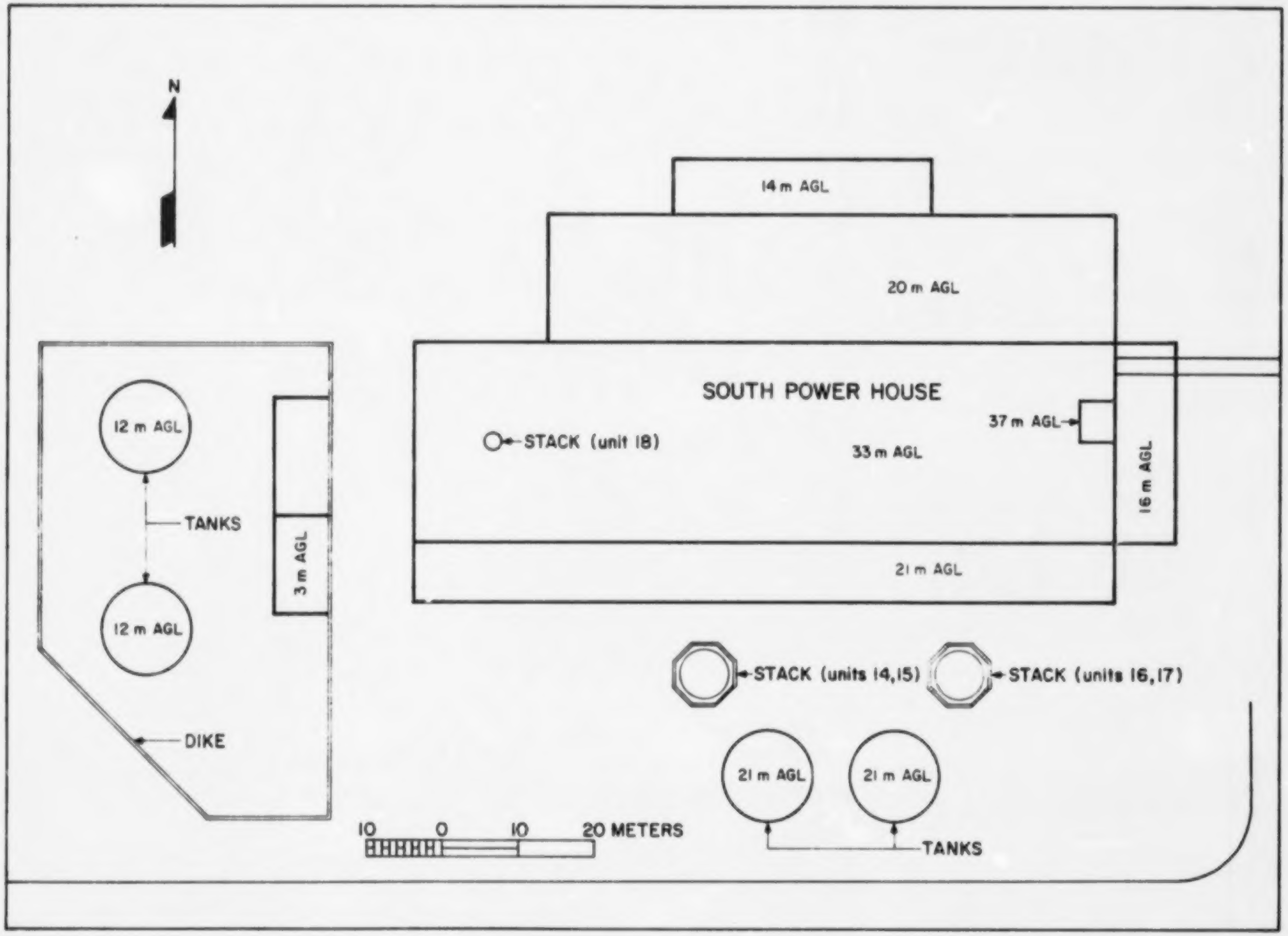
N
14 m AGL
20 m AGL
SOUTH POWER HOUSE
STACK (unit 18)
33 m AGL
37 m AGL
16 m AGL
21 m AGL
12 m AGL
TANKS
12 m AGL
3 m AGL
DIKE
STACK (units 14,15)
STACK (units 16,17)
21 m AGL
21 m AGL
TANKS
10 0 10 20 METERS

FIGURE 3-7. Layout of the South Power House at the DOW Midland, Michigan plant. Structure elevations are shown in meters above ground level (AGL).

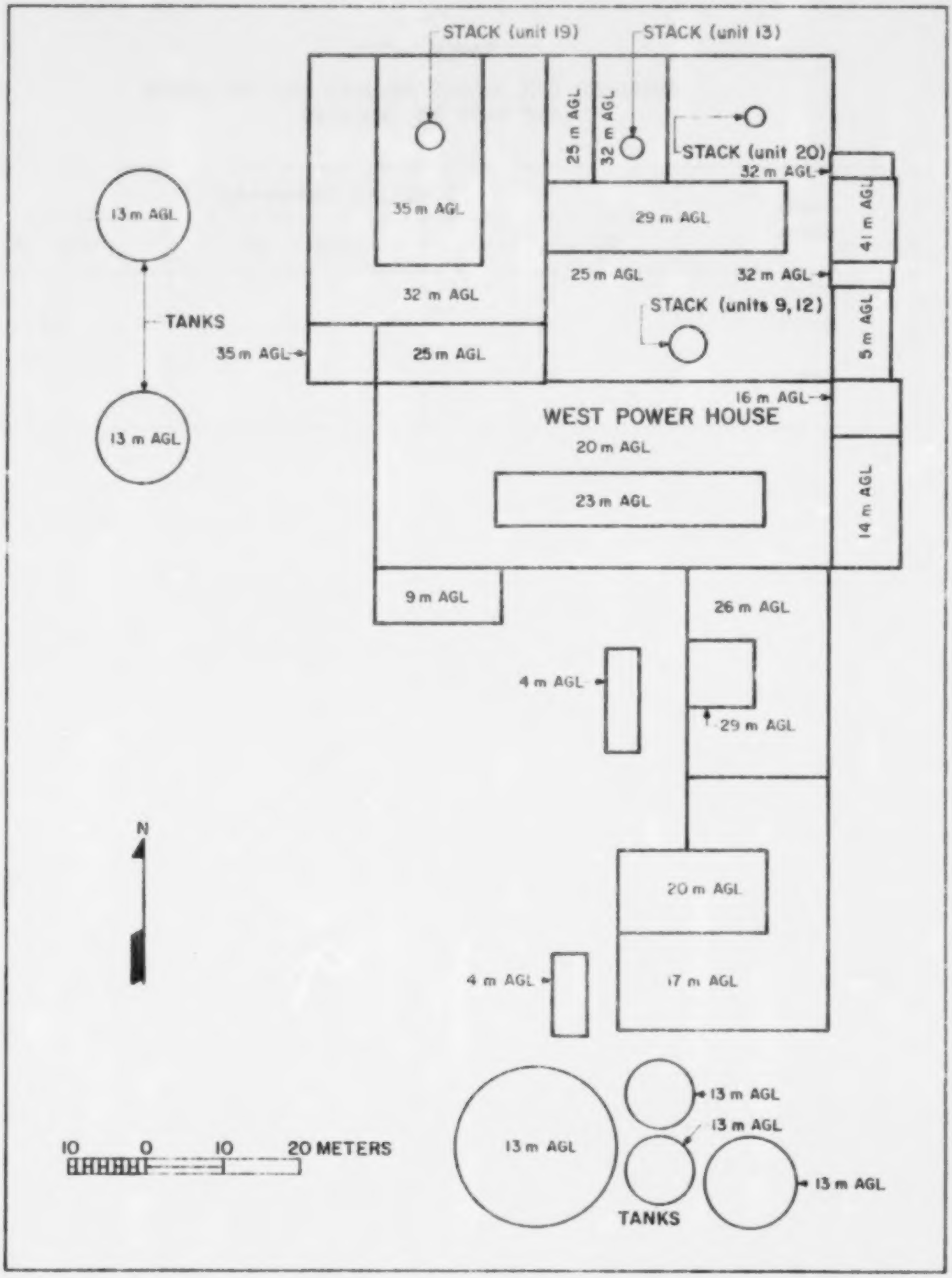
STACK (unit 19)
STACK (unit 13)
25 m AGL
32 m AGL
STACK (unit 20)
32 m AGL
35 m AGL
29 m AGL
41 m AGL
13 m AGL
TANKS
25 m AGL
32 m AGL
32 m AGL
STACK (units 9, 12)
35 m AGL
25 m AGL
5 m AGL
16 m AGL
WEST POWER HOUSE
13 m AGL
20 m AGL
23 m AGL
14 m AGL
9 m AGL
26 m AGL
4 m AGL
29 m AGL
N
20 m AGL
4 m AGL
17 m AGL
13 m AGL
13 m AGL
10 0 10 20 METERS
13 m AGL
13 m AGL
TANKS

FIGURE 3-8. Layout of the West Power House at the DOW Midland, Michigan plant. Structure elevations are shown in meters above ground level (AGL).

TABLE 3-27

BUILDING DIMENSIONS ASSUMED FOR THE SOUTH AND WEST POWERHOUSES

Power House	Building Dimensions		
	Height (m)	Length (m)	Width (m)
South	33	90	25
West	32	70	70

each power house exceeds 1.2. Also, the building width to building height ratio is between 1 and 5 for each power house. Thus, the ISC Model building wake effects option will modify only the vertical dispersion coefficient σ_z, and the critical building scale for each power house is the height scale.

The stack and full-load source data, excluding SO_2 emission rates, are listed for the South and West Power Houses in Tables 3-28 and 3-29, respectively. These data were developed from the plant layouts and additional information provided by DOW (Brown, 1979a and 1979b). The DOW emissions data tape (Abrams, 1979) included the following parameters for each stack for each hour:

- HHV -- fuel heat content in British Thermal Units (BTU) per pound
- SPC — fuel sulfur content in percent
- LOAD -- load in thousands of pounds of steam per hour

Based on the information provided by Abrams (1979), the hourly SO_2 emission rate in grams per second is given by

$$Q(\text{g/sec}) = \frac{0.86 \times C1 \times LOAD \times SPC}{EFF \times HHV} \qquad (3\text{-}1)$$

where C1 is a constant, EFF is the boiler efficiency in percent and 0.86 is a units conversion factor. Table 3-30 lists the values of C1 and EFF provided by Abrams (1979). The hourly stack exit velocity in meters per

TABLE 3-28
STACK AND FULL-LOAD SOURCE DATA FOR THE SOUTH POWER HOUSE

Parameter	Parameter Value		
	Units 14 & 15	Units 16 & 17	Unit 18
Stack Height (m)	53.5	53.5	53.9
Stack Inner Diameter (m)	4.57	4.57	3.28
Stack Exit Temperature (^{o}K)	408.0	408.0	419.4
Stack Exit Velocity at Full Load (m/sec)	9.32	9.32	10.05
Full load (10^{3} lb steam/hr)	720	720	400
UTM X Coordinate (m)	724,590	724,620	724,550
UTM Y Coordiante (m)	4,830,620	4,830,620	4,830,660

TABLE 3-29
STACK AND FULL-LOAD SOURCE DATA FOR THE WEST POWER HOUSE

Parameter	Parameter Value			
	Unit 19	Unit 13	Unit 20	Units 9 & 12
Stack Height (m)	55.5	56.0	55.5	47.9
Stack Inner Diameter (m)	3.79	2.47	2.43	4.42
Stack Exit Temperature (^{o}K)	411.1	416.7	422.2	416.7
Stack Exit Velocity at Full Load (m/sec)	10.96	14.18	18.01	5.17
Full Load (10^{3} lb steam/hr)	625	360	400	400
UTM X Coordinate (m)	722,620	722,630	722,650	722,640
UTM Y Coordinate (m)	4,831,070	4,831,070	4,831,070	4,831,040

TABLE 3-30

PARAMETERS USED TO CALCULATE SO_2 EMISSION RATES

Unit(s)	C1 (Watts/10^3 lb steam)	EFF (%)
13	342, 810	90
18	342, 810	89
19	342, 810	89
20	342, 810	90
9 & 12	342, 810	85
14 & 15	342, 810	91
16 & 17	342, 810	91

second is given by Brown (1979b) as

$$V_s(\text{m/sec}) = V_s\{\text{Max}\}\left(\frac{\text{LOAD}}{\text{LOAD }\{\text{Max}\}}\right) \tag{3-2}$$

where $V_s\{\text{Max}\}$ is the exit velocity in meters per second at full load (LOAD {Max}). Tables 3-28 and 3-29 give the values of $V_s\{\text{Max}\}$ and LOAD{Max} for the various stacks at the South and West Power Houses.

The stack exit velocities and SO_2 emission rates calculated for the various stacks at the South and West Power Houses during the selected cases identified in Table 3-26 are presented in Tables 3-31 and 3-32. Inspection of Tables 3-31 and 3-32 shows that there is no case chosen for model testing in which all of the boilers at the South and West Power Houses were in simultaneous operation. The emissions data tape gives non-zero values of HHV and LOAD for Unit 18, but zero values of SPC (fuel sulfur content). Consequently, Unit 18 was assumed to have had zero SO_2 emissions.

3.4.2 Meteorological Data

The source of the meteorological data used by the DOW Midland plant's SCS is a 91.5-meter meteorological tower located near SO_2 monitor D03H in Figure 3-6. The meteorological tower, which is adjacent to a nuclear power plant currently under construction, is owned by a power company rather than by DOW or its meteorological consultant. Insofar as possible, the meteorological inputs used in the ISC Model calculations for the DOW plant were developed from the tower meteorological measurements.

TABLE 3-31

HOURLY STACK EXIT VELOCITIES AND SO_2 EMISSION RATES FOR THE SOUTH POWER HOUSE DURING THE SELECTED DOW CASES

Case No.	Units 14 and 15		Units 16 and 17		Unit 18	
	Exit Velocity (m/sec)	SO_2 Emission Rate (g/sec)	Exit Velocity (m/sec)	SO_2 Emission Rate (g/sec)	Exit Velocity (m/sec)	SO_2 Emission Rate (g/sec)
1	5.9	491.4	4.2	348.8	0	0
2	5.2	429.8	3.8	319.7	0	0
3	5.7	478.4	4.2	346.7	0	0
4	8.4	697.6	2.5	33.6	0	0
5	6.5	540.0	3.7	49.5	0	0
6	6.5	540.0	3.7	49.5	0	0
7	8.3	695.5	4.2	349.9	0	0
8	8.3	690.1	0	0	0	0
9	8.3	695.5	0	0	0	0
10	8.4	700.9	0	0	0	0
11	8.3	694.4	3.9	53.0	0	0
12	8.3	694.4	3.9	53.0	0	0
13	4.4	368.3	3.5	47.2	0	0
14	8.6	718.1	4.3	357.5	0	0
15	8.6	718.1	4.3	357.5	0	0
16	8.6	718.1	4.3	357.5	0	0
17	8.6	718.1	4.3	357.5	0	0
18	8.6	718.1	4.3	357.5	0	0
19	8.8	734.3	4.2	351.0	0	0
20	8.7	722.5	4.2	349.9	0	0
21	8.3	695.5	4.6	61.3	0	0
22	8.6	718.1	4.6	61.3	0	0
23	8.1	671.7	2.8	230.0	0	0
24	8.1	671.7	4.1	338.0	0	0
25	8.3	691.1	3.9	324.0	0	0
26	8.3	691.1	3.9	324.0	0	0
27	6.9	572.4	3.9	52.3	0	0
28	4.3	359.6	4.5	60.8	0	0
29	8.0	665.2	4.0	53.3	0	0
30	7.9	660.9	4.0	54.3	0	0
31	3.9	324.0	8.2	680.3	0	0
32	0	0	8.1	672.8	0	0
33	0	0	8.1	672.8	0	0
34	4.4	370.4	8.1	671.7	0	0
35	4.4	370.4	8.1	671.7	0	0

TABLE 3-31 (Continued)

Case No.	Units 14 and 15		Units 16 and 17		Unit 18	
	Exit Velocity (m/sec)	SO_2 Emission Rate (g/sec)	Exit Velocity (m/sec)	SO_2 Emission Rate (g/sec)	Exit Velocity (m/sec)	SO_2 Emission Rate (g/sec)
36	4.4	370.4	8.1	671.7	0	0
37	4.5	375.8	8.2	685.7	0	0
38	4.5	375.8	8.2	685.7	0	0
39	4.5	375.8	8.2	680.3	0	0
40	4.4	369.3	8.8	730.0	0	0
41	4.4	368.3	8.8	735.4	0	0
42	4.4	369.3	4.1	339.1	0	0
43	4.4	369.3	4.1	54.7	0	0
44	8.8	408.6	4.4	59.2	0	0
45	8.8	408.6	4.4	59.2	0	0
46	8.8	408.6	4.4	59.2	0	0
47	8.2	382.2	4.1	54.5	0	0
48	9.0	418.8	4.3	58.4	0	0
49	8.6	397.2	3.8	51.7	0	0
50	8.6	400.2	3.8	51.7	0	0
51	8.0	369.0	4.3	57.5	0	0
52	8.4	388.8	4.1	55.4	0	0
53	6.9	321.6	4.6	61.5	0	0
54	6.9	321.6	4.6	61.5	0	0
55	8.4	391.2	4.6	61.8	0	0
56	6.5	65.7	4.6	61.3	0	0
57	5.7	58.0	4.5	61.0	0	0
58	8.0	668.5	4.1	345.6	0	0
59	8.2	687.9	4.3	57.5	0	0
60	8.2	685.7	4.4	59.2	0	0
61	5.0	413.6	8.3	694.4	0	0
62	5.0	413.6	8.3	112.0	0	0
63	4.1	345.6	8.8	118.4	0	0
64	2.6	216.0	8.8	118.4	0	0
65	2.2	185.7	8.9	119.3	0	0
66	8.7	723.5	7.8	104.5	0	0
67	8.7	723.5	8.2	109.7	0	0
68	8.6	721.4	8.2	110.3	0	0
69	8.6	719.2	8.2	110.8	0	0
70	8.7	722.5	8.2	111.0	0	0
71	8.9	740.8	8.5	712.7	0	0
72	8.9	740.8	8.5	115.0	0	0
73	8.9	740.8	8.0	108.0	0	0
74	8.5	711.7	4.4	365.0	0	0

TABLE 3-31 (Continued)

Case No.	Units 14 and 15		Units 16 and 17		Unit 18	
	Exit Velocity (m/sec)	SO_2 Emission Rate (g/sec)	Exit Velocity (m/sec)	SO_2 Emission Rate (g/sec)	Exit Velocity (m/sec)	SO_2 Emission Rate (g/sec)
75	8.5	711.7	4.4	365.0	0	0
76	8.5	706.3	4.5	378.0	0	0
77	8.4	697.6	4.3	58.5	0	0
78	8.5	708.4	4.2	352.1	0	0
79	8.5	708.4	4.2	352.1	0	0
80	8.8	737.6	4.3	58.5	0	0
81	8.5	708.4	4.2	203.8	0	0
82	8.3	695.5	4.2	56.4	0	0
83	4.5	374.7	8.6	716.0	0	0
84	4.5	374.7	8.6	716.0	0	0
85	4.5	374.7	8.6	716.0	0	0
86	4.5	378.0	8.3	691.1	0	0
87	4.3	356.4	8.5	114.1	0	0
88	3.8	314.3	8.1	108.3	0	0
89	4.2	346.7	4.5	371.5	0	0
90	8.9	745.1	3.1	41.8	0	0

TABLE 3-32

HOURLY STACK EXIT VELOCITIES AND SO_2 EMISSION RATES FOR THE WEST POWER HOUSE DURING THE SELECTED DOW CASES

Case No.	Unit 19		Unit 13		Unit 20		Units 9 and 12	
	Exit Velocity (m/sec)	SO_2 Emission Rate (g/sec)	Exit Velocity (m/sec)	SO_2 Emission Rate (g/sec)	Exit Velocity (m/sec)	SO_2 Emission Rate (g/sec)	Exit Velocity (m/sec)	SO_2 Emission Rate (g/sec)
1	0	0	0	0	15.2	369.1	0	0
2	0	0	0	0	14.4	348.3	0	0
3	0	0	0	0	16.9	410.6	0	0
4	0	0	0	0	14.7	355.0	0	0
5	0	0	0	0	13.8	334.1	0	0
6	0	0	0	0	11.8	285.0	0	0
7	0	0	0	0	14.5	350.5	2.5	35.6
8	0	0	0	0	15.8	384.4	3.0	42.7
9	0	0	0	0	16.3	395.3	3.0	42.7
10	0	0	0	0	17.5	424.8	6.1	87.8
11	0	0	12.0	333.0	13.5	329.8	4.8	69.7
12	0	0	12.0	333.0	15.6	378.9	4.4	64.0
13	0	0	7.9	35.2	15.0	363.6	4.7	67.1
14	0	0	12.4	344.0	14.6	354.9	0	0
15	0	0	12.4	344.0	0	0	0	0
16	0	0	12.4	344.0	0	0	0	0
17	0	0	12.4	344.0	0	0	0	0
18	0	0	12.4	344.0	0	0	0	0
19	0	0	13.3	368.0	0	0	0	0
20	0	0	13.3	369.1	0	0	0	0
21	0	0	13.8	61.8	0	0	0	0
22	0	0	8.4	37.5	16.6	402.9	0	0
23	0	0	13.2	58.8	12.6	305.7	1.6	22.6
24	0	0	13.2	58.8	12.6	305.7	1.6	22.6
25	0	0	11.8	52.8	12.6	305.7	1.3	18.6
26	0	0	11.8	327.6	12.6	305.7	2.6	37.3

TABLE 3-32 (Continued)

Case No.	Unit 19		Unit 13		Unit 20		Units 9 and 12	
	Exit Velocity (m/sec)	SO_2 Emission Rate (g/sec)	Exit Velocity (m/sec)	SO_2 Emission Rate (g/sec)	Exit Velocity (m/sec)	SO_2 Emission Rate (g/sec)	Exit Velocity (m/sec)	SO_2 Emission Rate (g/sec)
27	0	0	11.8	327.6	14.4	349.4	2.6	37.3
28	0	0	12.8	354.9	15.0	363.6	2.7	39.2
29	8.6	544.4	0	0	0	0	1.8	26.1
30	8.2	513.4	0	0	0	0	2.0	28.5
31	9.1	574.2	0	0	0	0	3.6	51.3
32	10.4	653.7	3.2	88.4	0	0	2.2	31.7
33	9.0	566.4	10.5	291.5	0	0	2.2	31.7
34	9.0	568.7	12.5	347.2	0	0	1.2	17.9
35	9.0	568.7	12.5	347.2	0	0	1.2	17.9
36	9.0	568.7	12.5	347.2	0	0	1.2	17.9
37	8.7	549.9	12.1	336.3	0	0	1.7	25.0
38	8.7	549.9	11.7	326.5	0	0	1.7	25.0
39	9.1	573.1	10.7	295.9	0	0	2.0	28.2
40	8.6	541.0	12.6	348.3	0	0	1.3	18.8
41	8.5	533.3	12.5	347.2	0	0	1.4	20.0
42	9.5	596.3	12.9	357.1	0	0	4.1	59.7
43	9.5	596.3	12.9	57.6	0	0	4.1	59.7
44	8.6	543.3	0	0	0	0	2.7	38.8
45	9.3	584.1	0	0	0	0	2.7	38.8
46	9.9	623.9	0	0	0	0	2.7	38.8
47	8.4	528.9	13.0	361.4	0	0	1.2	16.6
48	9.0	564.2	12.6	56.5	0	0	2.8	40.7
49	8.6	542.2	12.2	339.6	0	0	1.0	14.9
50	8.8	554.3	11.7	52.3	0	0	1.0	14.9
51	5.6	355.5	12.2	54.4	0	0	2.1	30.8
52	9.0	567.5	12.6	56.2	0	0	2.2	32.3
53	6.7	422.9	12.6	56.2	0	0	2.2	32.3
54	5.4	339.0	12.6	56.2	0	0	2.2	32.2

TABLE 3-32 (Continued)

Case No.	Unit 19		Unit 13		Unit 20		Units 9 and 12	
	Exit Velocity (m/sec)	SO_2 Emission Rate (g/sec)	Exit Velocity (m/sec)	SO_2 Emission Rate (g/sec)	Exit Velocity (m/sec)	SO_2 Emission Rate (g/sec)	Exit Velocity (m/sec)	SO_2 Emission Rate (g/sec)
55	4.0	250.6	9.4	42.1	0	0	2.8	41.0
56	3.6	227.5	12.9	57.8	0	0	2.9	42.3
57	3.7	233.0	13.1	58.6	0	0	2.9	42.3
58	3.9	244.0	12.9	57.8	0	0	2.7	38.4
59	0.8	50.8	13.0	58.1	0	0	3.7	52.8
60	2.1	134.7	13.0	58.1	0	0	4.0	58.4
61	9.3	584.1	6.9	30.8	0	0	3.7	54.1
62	5.2	330.2	11.7	52.3	0	0	3.7	54.1
63	9.5	596.3	9.8	44.0	0	0	3.9	55.9
64	9.5	596.3	9.8	44.0	0	0	3.2	46.6
65	9.2	578.6	8.7	38.9	0	0	3.3	48.1
66	8.6	541.0	3.2	14.1	0	0	0.8	11.2
67	8.4	530.0	3.2	14.1	0	0	0.8	11.2
68	7.5	474.8	3.2	14.4	0	0	0.8	11.2
69	7.3	458.2	4.8	21.7	0	0	0.8	12.1
70	4.8	300.3	8.6	38.7	0	0	1.1	15.5
71	4.9	309.2	0	0	0	0	2.1	29.8
72	4.9	309.2	0	0	0	0	2.1	29.8
73	4.9	309.2	0	0	0	0	2.1	29.8
74	7.2	452.7	4.8	21.5	0	0	3.0	43.3
75	6.3	394.2	4.8	21.5	0	0	3.9	55.6
76	6.4	403.0	4.2	18.7	0	0	1.7	24.4
77	6.9	437.3	7.7	34.3	0	0	0	0
78	6.3	394.2	7.7	34.5	0	0	0	0
79	6.9	437.3	7.7	34.5	0	0	0	0
80	0	0	0	0	15.0	364.7	0	0
81	0	0	0	0	14.3	347.2	0	0
82	6.2	389.8	0	0	0	0	0	0
83	6.9	436.2	0	0	0	0	0	0

TABLE 3-32 (Continued)

Case No.	Unit 19		Unit 13		Unit 20		Units 9 and 12	
	Exit Velocity (m/sec)	SO_2 Emission Rate (g/sec)	Exit Velocity (m/sec)	SO_2 Emission Rate (g/sec)	Exit Velocity (m/sec)	SO_2 Emission Rate (g/sec)	Exit Velocity (m/sec)	SO_2 Emission Rate (g/sec)
84	6.9	436.2	0	0	0	0	0	0
85	6.9	436.2	0	0	0	0	0	0
86	0	0	0	0	14.0	338.5	0	0
87	0	0	0	0	16.2	392.0	0	0
88	0	0	0	0	15.6	378.9	0	0
89	0	0	0	0	14.9	362.5	0	0
90	0	0	0	0	16.2	393.1	0	0

Table 3-33 lists the hourly meteorological inputs for the 90 DOW cases selected for testing the ISC Model. Although the 60-meter level of the meteorological tower is the wind measurement height nearest to the stack height, we selected the wind data from the 91.5-meter tower level for use in the model calculations because we believe that the 91.5-meter wind directions are more likely to be representative of wind directions at plume height than the 60-meter wind directions. (The ISC Model uses a wind-profile power law expression to account for vertical wind-speed shear, but does not account for vertical wind-direction shear.) The tower 91.5-meter hourly wind directions are reversed 180 degrees in Table 3-33 to obtain the average flow vectors required for input to the ISCST program, the tower 91.5-meter wind speeds are converted to meters per second from miles per hour and the 91.5-meter ambient air temperatures are converted to degrees Kelvin from degrees Celsius. Following the Turner (1964) definitions of the Pasquill stability categories, the D category existed during all of the hours selected for model testing with the possible exception of Case 87 when the C category might have occurred. Because only three tower levels were available for calculating wind-profile exponents, the ISC Model default values were used in the model calculations. Additionally, the ISC Model default values for the vertical potential temperature gradient were used in the calculations. In the absence of onsite mixing height measurements, the average of the early morning and afternoon mean annual mixing heights given by Holzworth (1972) for Flint, Michigan was assigned to all hours.

3.4.3 Calculation Procedures and Results

The ISC Model short-term program ISCST was used with the source data discussed in Section 3.4.1 and the meteorological inputs listed in Table 3-33 to calculate 1-hour average ground-level SO_2 concentrations at the locations of the SO_2 monitors shown in Figure 3-6 for the 90 cases identified in Table 3-26. The Universal Transverse Mercator (UTM) coordinates of the SO_2 monitors are listed in Table 3-34. The ISC Model

TABLE 3-33

HOURLY METEOROLOGICAL INPUTS FOR THE SELECTED DOW CASES

Case No.	Average Flow Vector*(deg)	91.5-Meter Mean Wind Speed (m/sec)	Mixing Height (m)	Ambient Air Temperature (^oK)	Pasquill Stability Category
1	346	10.94	937	290	D
2	350	11.38	937	291	D
3	344	11.96	937	289	D
4	065	19.69	937	280	D
5	078	10.40	937	281	D
6	077	10.31	937	280	D
7	073	9.15	937	279	D
8	328	9.29	937	286	D
9	330	10.00	937	287	D
10	031	8.53	937	276	D
11	087	8.21	937	275	D
12	086	8.21	937	275	D
13	082	10.45	937	268	D
14	044	8.35	937	272	D
15	042	8.44	937	272	D
16	033	9.46	937	272	D
17	031	9.15	937	272	D
18	112	8.62	937	270	D
19	105	10.13	937	266	D
20	111	7.41	937	265	D
21	111	8.97	937	262	D
22	115	9.11	937	262	D
23	247	10.36	937	272	D
24	245	11.65	937	271	D
25	234	12.54	937	270	D
26	235	11.92	937	270	D
27	230	11.56	937	270	D
28	194	9.60	937	268	D
29	081	8.79	937	272	D
30	067	9.15	937	271	D
31	033	9.02	937	263	D
32	084	11.74	937	262	D
33	078	10.58	937	262	D
34	107	9.20	937	271	D
35	108	8.71	937	271	D
36	118	10.94	937	270	D
37	114	8.93	937	269	D
38	114	9.42	937	268	D

*Direction toward which the wind is blowing.

TABLE 3-33 (Continued)

Case No.	Average Flow Vector*(deg)	91.5-Meter Mean Wind Speed (m/sec)	Mixing Height (m)	Ambient Air Temperature (°K)	Pasquill Stability Category
39	107	8.97	937	268	D
40	099	9.02	937	266	D
41	106	9.42	937	266	D
42	028	10.36	937	267	D
43	032	10.09	937	268	D
44	073	11.07	937	271	D
45	076	11.70	937	272	D
46	077	11.74	937	272	D
47	109	11.52	937	273	D
48	031	10.80	937	275	D
49	071	12.41	937	284	D
50	073	12.99	937	284	D
51	078	12.54	937	284	D
52	064	11.88	937	279	D
53	074	13.17	937	276	D
54	077	13.84	937	275	D
55	234	10.89	937	274	D
56	226	9.51	937	274	D
57	229	11.07	937	274	D
58	066	17.50	937	272	D
59	068	18.57	937	272	D
60	071	18.30	937	272	D
61	091	10.18	937	273	D
62	106	12.14	937	271	D
63	102	12.23	937	271	D
64	109	12.86	937	271	D
65	121	12.46	937	271	D
66	067	11.16	937	275	D
67	079	10.13	937	274	D
68	079	10.18	937	276	D
69	074	10.31	937	275	D
70	108	11.34	937	274	D
71	028	11.12	937	281	D
72	029	11.65	937	280	D
73	027	11.29	937	281	D
74	226	15.80	937	278	D
75	231	14.38	937	277	D
76	230	13.75	937	276	D
77	228	13.84	937	277	D

*Direction toward which the wind is blowing.

TABLE 3-33 (Continued)

Case No.	Average Flow Vector*(deg)	91.5-Meter Mean Wind Speed (m/sec)	Mixing Height (m)	Ambient Air Temperature (°K)	Pasquill Stability Category
78	094	8.62	937	285	D
79	104	8.93	937	285	D
80	029	11.65	937	292	D
81	066	10.49	937	294	D
82	027	9.24	937	294	D
83	062	11.34	937	283	D
84	071	10.76	937	282	D
85	070	9.91	937	282	D
86	103	8.08	937	287	D
87	109	8.39	937	277	D
88	028	13.04	937	284	D
89	325	9.55	937	295	D
90	090	9.33	937	300	D

*Direction toward which the wind is blowing.

TABLE 3-34

UNIVERSAL TRANSVERSE MERCATOR (UTM) COORDINATES OF THE SO_2 MONITORS IN THE VICINITY OF THE DOW MIDLAND PLANT

Monitor ID No.	Monitor Name	UTM X Coordinate (m)	UTM Y Coordinate (m)
D23H	Abbott Road	725,790	4,832,660
D33H	Eastlawn	724,010	4,833,190
D63H	Austin St.	724,140	4,831,680
D53H	Bullock Creek	722,270	4,829,100
D73H	Ellsworth St.	722,230	4,832,690
D83H	Kent St.	725,920	4,831,230
D93H	Waldo Rd.	726,960	4,830,380
D03H	Nuclear Site	723,310	4,829,190
D13H	14SB (State Monitor)	725,550	4,830,290

calculations were performed using the six combinations of model options outlined in Table 3-35. On the basis of a site survey of the DOW Midland plant, Urban Mode 2 was included in the model calculations (Combinations 4, 5 and 6 in Table 3-35) because the presence of numerous large roughness elements (buildings) at the plant indicated the possibility of enhanced turbulent intensities in the vicinity of the plant.

We point out that, because the DOW data were compiled from routine records of plant operations, the uncertainties in the source, meteorological and air quality data for the DOW data set tend to be larger than for the three sets of published diffusion experiments discussed in Sections 3.1, 3.2 and 3.3. Additionally, uncertainties about the mean transport wind directions, which are not present in the data from the diffusion experiments because the locations of the plume centerlines were defined by the monitoring networks, cannot be removed from the DOW data set. (See Ellis and Liu (1980) for a discussion of the sensitivity of short-term concentrations calculated at fixed monitor locations to slight uncertainties about the transport wind direction.) Thus, the RMSE values for the DOW data set are expected to be much larger than for the diffusion experiments. Similarly, the percent of calculated concentrations within a factor of 2 of the corresponding observed concentrations is expected to be much smaller for the DOW data set than for the diffusion experiments.

Table 3-36 compares the calculated and observed 1-hour ground-level SO_2 concentrations for Combination 1 in Table 3-35. Because of the uncertainties about the SO_2 background and the effects of the package boiler emissions, Table 3-36 considers only monitors with observed 1-hour SO_2 concentrations greater than or equal to 0.10 ppm. Similarly, the observed concentrations greater than or equal to 0.10 ppm are compared with the corresponding concentrations calculated by the ISC Model for Combinations 2 through 6 in Table 3-37 through 3-41.

TABLE 3-35

COMBINATIONS OF ISC MODEL OPTIONS APPLIED TO THE DOW DATA SET

Combination	ISC Model Mode		Plume Rise		Building Wake Effects		Stack-Tip Downwash	
	Rural	Urban 2	Final	Distance Dependent	Yes	No	Yes	No
1	X		X			X		X
2	X			X	X			X
3	X			X	X		X	
4		X	X			X		X
5		X		X	X			X
6		X		X	X		X	

TABLE 3-36

COMPARISON OF CALCULATED AND OBSERVED 1-HOUR SO_2 CONCENTRATIONS FOR THE DOW CASES FOR COMBINATION 1 IN TABLE 3-35

Case No.	Year/ Julian Day	Hour	Monitor	Observed Concentration (ppm)	Calculated Concentration (ppm)	Ratio of Calculated and Observed Concentrations
1	75/314	0100	D33H	0.36	0.20	0.56
			D63H	0.11	0.00	0.00
			D73H	0.12	0.05	0.42
2	75/314	0200	D33H	0.26	0.15	0.58
			D73H	0.13	0.03	0.23
3	75/314	0500	D63H	0.49	0.01	0.02
4	75/314	1300	D63H	0.14	0.06	0.43
			D83H	0.27	0.09	0.33
5	75/314	2300	D63H	0.28	0.00	0.00
			D83H	0.19	0.03	0.16
6	75/314	2400	D63H	0.30	0.00	0.00
			D83H	0.15	0.00	0.00
7	75/316	1700	D63H	0.12	0.01	0.08
			D83H	0.33	0.00	0.00
8	75/324	1200	D63H	0.39	0.00	0.00
9	75/324	1300	D63H	0.55	0.00	0.00
10	75/325	0800	D23H	0.27	0.03	0.11
11	75/326	1500	D63H	0.27	0.00	0.00
12	75/326	1600	D63H	0.30	0.00	0.00
			D83H	0.13	0.17	1.31
13	75/335	0400	D63H	0.30	0.00	0.00
			D83H	0.12	0.04	0.33
14	75/350	1500	D23H	0.38	0.00	0.00
			D33H	0.12	0.00	0.00
15	75/350	1900	D23H	0.30	0.00	0.00
16	75/350	2000	D23H	0.27	0.08	0.30
17	75/350	2100	D23H	0.29	0.10	0.34
			D33H	0.10	0.07	0.70
18	75/351	0400	D13H	0.28	0.01	0.04
			D93H	0.23	0.00	0.00
19	75/351	0700	D13H	0.14	0.09	0.64
			D93H	0.25	0.02	0.08
20	75/351	1000	D13H	0.35	0.02	0.06
21	75/352	1100	D13H	0.25	0.00	0.00
			D83H	0.11	0.00	0.00
22	75/352	1300	D13H	0.31	0.00	0.00
23	75/354	1200	D53H	0.25	0.00	0.00
24	75/354	1300	D03H	0.36	0.00	0.00
			D53H	0.10	0.01	0.10

TABLE 3-36 (Continued)

Case No.	Year/ Julian Day	Hour	Monitor	Observed Concentration (ppm)	Calculated Concentration (ppm)	Ratio of Calculated and Observed Concentrations
25	75/354	1400	D03H	0.65	0.00	0.00
26	75/354	1600	D03H	0.49	0.00	0.00
27	75/354	1700	D03H	0.44	0.06	0.14
28	75/354	2400	D53H	0.35	0.08	0.23
29	76/003	0100	D63H	0.26	0.00	0.00
			D83H	0.23	0.02	0.09
30	76/003	1100	D63H	0.28	0.03	0.11
			D83H	0.20	0.07	0.35
31	76/005	1300	D23H	0.30	0.07	0.23
32	76/008	1600	D63H	0.27	0.00	0.00
			D83H	0.14	0.11	0.79
33	76/008	1700	D63H	0.30	0.00	0.00
			D83H	0.10	0.01	0.10
34	76/014	0300	D13H	0.37	0.16	0.43
			D93H	0.20	0.01	0.05
35	76/014	0400	D13H	0.26	0.12	0.46
			D93H	0.21	0.01	0.05
36	76/014	0500	D13H	0.33	0.00	0.00
			D93H	0.18	0.00	0.00
37	76/014	0600	D13H	0.50	0.01	0.02
38	76/014	0700	D13H	0.59	0.01	0.02
			D93H	0.30	0.00	0.00
39	76/014	0800	D93H	0.34	0.01	0.03
40	76/014	2100	D13H	0.21	0.04	0.19
			D93H	0.48	0.26	0.54
41	76/014	2200	D13H	0.33	0.18	0.55
			D93H	0.21	0.03	0.14
42	76/028	1600	D23H	0.32	0.13	0.41
43	76/028	1700	D23H	0.44	0.08	0.18
			D33H	0.19	0.10	0.53
44	76/038	2400	D63H	0.47	0.02	0.04
			D83H	0.15	0.00	0.00
45	76/039	0100	D63H	0.45	0.00	0.00
			D83H	0.18	0.00	0.00
46	76/039	0200	D63H	0.47	0.00	0.00
			D83H	0.16	0.00	0.00
47	76/042	1200	D13H	0.40	0.11	0.28
			D93H	0.16	0.00	0.00
48	76/043	0900	D33H	0.26	0.10	0.38
49	76/046	1700	D23H	0.22	0.02	0.09
			D63H	0.29	0.10	0.34

TABLE 3-36 (Continued)

Case No.	Year/ Julian Day	Hour	Monitor	Observed Concentration (ppm)	Calculated Concentration (ppm)	Ratio of Calculated and Observed Concentrations
50	76/046	1800	D63H	0.81	0.03	0.04
			D83H	0.23	0.00	0.00
51	76/046	1900	D63H	0.42	0.00	0.00
			D83H	0.18	0.00	0.00
52	76/049	1700	D63H	0.40	0.04	0.10
			D83H	0.15	0.02	0.13
53	76/049	1800	D63H	0.29	0.03	0.10
			D83H	0.15	0.00	0.00
54	76/049	1900	D63H	0.28	0.01	0.04
			D83H	0.16	0.00	0.00
55	76/052	1300	D03H	0.39	0.00	0.00
56	76/052	1500	D03H	0.28	0.01	0.04
57	76/052	1600	D03H	0.29	0.00	0.00
58	76/065	1000	D63H	0.11	0.09	0.82
			D83H	0.34	0.13	0.38
59	76/065	1100	D83H	0.29	0.06	0.21
60	76/065	1500	D63H	0.12	0.07	0.58
			D83H	0.26	0.02	0.08
61	76/066	2400	D13H	0.12	0.00	0.00
			D93H	0.31	0.06	0.19
62	76/067	0200	D13H	0.27	0.13	0.48
			D93H	0.15	0.02	0.13
63	76/067	1400	D13H	0.34	0.11	0.32
			D93H	0.11	0.12	1.09
64	76/067	1500	D13H	0.32	0.10	0.31
65	76/067	1700	D13H	0.29	0.00	0.00
66	76/073	0200	D63H	0.26	0.06	0.23
			D83H	0.12	0.01	0.08
67	76/074	1300	D63H	0.25	0.00	0.00
			D83H	0.10	0.01	0.10
68	76/074	1900	D63H	0.29	0.00	0.00
			D83H	0.17	0.01	0.06
69	76/074	2000	D63H	0.28	0.02	0.07
			D83H	0.11	0.00	0.00
70	76/074	2400	D13H	0.16	0.08	0.50
			D93H	0.25	0.00	0.00
71	76/084	0200	D23H	0.30	0.12	0.40
72	76/084	0300	D23H	0.35	0.08	0.23
73	76/084	0400	D23H	0.30	0.05	0.17
74	76/094	1800	D03H	0.26	0.11	0.42
75	76/094	2000	D03H	0.27	0.01	0.04
76	76/094	2300	D03H	0.59	0.02	0.03

TABLE 3-36 (Continued)

Case No.	Year/ Julian Day	Hour	Monitor	Observed Concentration (ppm)	Calculated Concentration (ppm)	Ratio of Calculated and Observed Concentrations
77	76/095	0200	D03H	0.27	0.02	0.07
78	76/096	1600	D13H	0.30	0.00	0.00
			D93H	0.16	0.14	0.88
79	76/096	1700	D13H	0.60	0.11	0.18
			D93H	0.16	0.05	0.31
80	76/106	0200	D23H	0.64	0.10	0.16
81	76/107	1200	D63H	0.10	0.05	0.50
			D83H	0.26	0.04	0.15
82	76/109	1000	D23H	0.35	0.05	0.14
83	76/113	0600	D63H	0.15	0.01	0.07
			D83H	0.36	0.04	0.11
84	76/113	0700	D63H	0.21	0.04	0.19
			D83H	0.31	0.02	0.06
85	76/113	0800	D63H	0.25	0.04	0.16
			D83H	0.31	0.02	0.06
86	76/122	2200	D13H	0.25	0.07	0.28
87	76/124	1200	D13H	0.27	0.04	0.15
88	76/126	0200	D23H	0.29	0.09	0.31
89	76/164	2400	D63H	0.28	0.00	0.00
90	76/189	1800	D13H	0.30	0.00	0.00
			D93H	0.10	0.02	0.20
					Mean Ratio (MR)	0.15

TABLE 3-37

COMPARISON OF CALCULATED AND OBSERVED 1-HOUR SO_2 CONCENTRATIONS FOR THE DOW CASES FOR COMBINATION 2 IN TABLE 3-35

Case No.	Year/ Julian Day	Hour	Monitor	Observed Concentration (ppm)	Calculated Concentration (ppm)	Ratio of Calculated and Observed Concentrations
1	75/314	0100	D33H	0.36	0.28	0.78
			D63H	0.11	0.01	0.09
			D73H	0.12	0.14	0.17
2	75/314	0200	D33H	0.26	0.20	0.77
			D73H	0.13	0.07	0.54
3	75/314	0500	D63H	0.49	0.05	0.10
4	75/314	1300	D63H	0.14	0.11	0.79
			D83H	0.27	0.24	0.89
5	75/314	2300	D63H	0.28	0.00	0.00
			D83H	0.19	0.00	0.00
6	75/314	2400	D63H	0.30	0.01	0.03
			D83H	0.15	0.00	0.00
7	75/316	1700	D63H	0.12	0.05	0.42
			D83H	0.33	0.02	0.06
8	75/324	1200	D63H	0.39	0.00	0.00
9	75/324	1300	D63H	0.55	0.02	0.04
10	75/325	0800	D23H	0.27	0.09	0.33
11	75/326	1500	D63H	0.27	0.00	0.00
12	75/326	1600	D63H	0.30	0.00	0.00
			D83H	0.13	0.23	1.77
13	75/335	0400	D63H	0.30	0.00	0.00
			D83H	0.12	0.05	0.42
14	75/350	1500	D23H	0.38	0.00	0.00
			D33H	0.12	0.00	0.00
15	75/350	1900	D23H	0.30	0.00	0.00
16	75/350	2000	D23H	0.27	0.17	0.63
17	75/350	2100	D23H	0.29	0.22	0.76
			D33H	0.10	0.11	1.10
18	75/351	0400	D13H	0.28	0.11	0.39
			D93H	0.23	0.00	0.00
19	75/351	0700	D13H	0.14	0.03	0.21
			D93H	0.25	0.03	0.12
20	75/351	1000	D13H	0.35	0.09	0.26
21	75/352	1100	D13H	0.25	0.04	0.16
			D83H	0.11	0.00	0.00
22	75/352	1300	D13H	0.31	0.02	0.06
23	75/354	1200	D53H	0.25	0.00	0.00

TABLE 3-37 (Continued)

Case No.	Year/ Julian Day	Hour	Monitor	Observed Concentration (ppm)	Calculated Concentration (ppm)	Ratio of Calculated and Observed Concentrations
24	75/354	1300	D03H	0.36	0.00	0.00
			D53H	0.10	0.02	0.20
25	75/354	1400	D03H	0.65	0.00	0.00
26	75/354	1600	D03H	0.49	0.00	0.00
27	75/354	1700	D03H	0.44	0.02	0.05
28	75/354	2400	D53H	0.35	0.18	0.51
29	76/003	0100	D63H	0.26	0.00	0.00
			D83H	0.23	0.03	0.13
30	76/003	1100	D63H	0.28	0.13	0.46
			D83H	0.20	0.09	0.45
31	76/005	1300	D23H	0.30	0.15	0.50
32	76/008	1600	D63H	0.27	0.00	0.00
			D83H	0.14	0.13	0.93
33	76/008	1700	D63H	0.30	0.01	0.03
			D83H	0.10	0.01	0.10
34	76/014	0300	D13H	0.37	0.35	0.95
			D93H	0.20	0.02	0.10
35	76/014	0400	D13H	0.26	0.30	1.15
			D93H	0.21	0.01	0.05
36	76/014	0500	D13H	0.33	0.02	0.06
			D93H	0.18	0.00	0.00
37	76/014	0600	D13H	0.50	0.07	0.14
38	76/014	0700	D13H	0.59	0.08	0.14
			D93H	0.30	0.00	0.00
39	76/014	0800	D93H	0.34	0.02	0.06
40	76/014	2100	D13H	0.21	0.06	0.29
			D93H	0.48	0.36	0.75
41	76/014	2200	D13H	0.33	0.35	1.06
			D93H	0.21	0.03	0.14
42	76/028	1600	D23H	0.32	0.22	0.69
43	76/028	1700	D23H	0.44	0.14	0.32
			D33H	0.19	0.17	0.89
44	76/038	2400	D63H	0.47	0.07	0.15
			D83H	0.15	0.01	0.07
45	76/039	0100	D63H	0.45	0.02	0.04
			D83H	0.18	0.00	0.00
46	76/039	0200	D63H	0.47	0.01	0.02
			D83H	0.16	0.00	0.00
47	76/042	1200	D13H	0.40	0.22	0.55
			D93H	0.16	0.00	0.00
48	76/043	0900	D33H	0.26	0.16	0.62

TABLE 3-37 (Continued)

Case No.	Year/ Julian Day	Hour	Monitor	Observed Concentration (ppm)	Calculated Concentration (ppm)	Ratio of Calculated and Observed Concentrations
49	76/046	1700	D23H	0.22	0.02	0.09
			D63H	0.29	0.25	0.86
50	76/046	1800	D63H	0.81	0.09	0.11
			D83H	0.23	0.01	0.04
51	76/046	1900	D63H	0.42	0.01	0.02
			D83H	0.18	0.00	0.00
52	76/049	1700	D63H	0.40	0.12	0.30
			D83H	0.15	0.10	0.67
53	76/049	1800	D63H	0.29	0.06	0.21
			D83H	0.15	0.01	0.07
54	76/049	1900	D63H	0.28	0.01	0.04
			D83H	0.16	0.00	0.00
55	76/052	1300	D03H	0.39	0.00	0.00
56	76/052	1500	D03H	0.28	0.02	0.07
57	76/052	1600	D03H	0.29	0.01	0.03
58	76/065	1000	D63H	0.11	0.15	1.36
			D83H	0.34	0.36	1.06
59	76/065	1100	D83H	0.29	0.18	0.62
60	76/065	1500	D63H	0.12	0.09	0.75
			D83H	0.26	0.07	0.27
61	76/066	2400	D13H	0.12	0.00	0.00
			D93H	0.31	0.12	0.39
62	76/067	0200	D13H	0.27	0.27	1.00
			D93H	0.15	0.02	0.13
63	76/067	1400	D13H	0.34	0.17	0.50
			D93H	0.11	0.14	1.27
64	76/067	1500	D13H	0.32	0.27	0.84
65	76/067	1700	D13H	0.29	0.00	0.00
66	76/073	0200	D63H	0.26	0.17	0.65
			D83H	0.12	0.13	1.08
67	76/074	1300	D63H	0.25	0.00	0.00
			D83H	0.10	0.01	0.10
68	76/074	1900	D63H	0.29	0.00	0.00
			D83H	0.17	0.01	0.06
69	76/074	2000	D63H	0.28	0.05	0.18
			D83H	0.11	0.01	0.09
70	76/074	2400	D13H	0.16	0.20	1.25
			D93H	0.25	0.00	0.00
71	76/084	0200	D23H	0.30	0.25	0.83
72	76/084	0300	D23H	0.35	0.17	0.49
73	76/084	0400	D23H	0.30	0.11	0.37

TABLE 3-37 (Continued)

Case No.	Year/ Julian Day	Hour	Monitor	Observed Concentration (ppm)	Calculated Concentration (ppm)	Ratio of Calculated and Observed Concentrations
74	76/094	1800	D03H	0.26	0.20	0.77
75	76/094	2000	D03H	0.27	0.02	0.07
76	76/094	2300	D03H	0.59	0.03	0.05
77	76.095	0200	D03H	0.27	0.05	0.19
78	76/096	1600	D13H	0.30	0.00	0.00
			D93H	0.16	0.26	1.63
79	76/096	1700	D13H	0.60	0.22	0.37
			D93H	0.16	0.06	0.38
80	76/106	0200	D23H	0.64	0.18	0.28
81	76/107	1200	D63H	0.10	0.13	1.30
			D83H	0.26	0.24	0.92
82	76/109	1000	D23H	0.35	0.11	0.31
83	76/113	0600	D63H	0.15	0.04	0.27
			D83H	0.36	0.21	0.58
84	76/113	0700	D63H	0.21	0.12	0.57
			D83H	0.31	0.08	0.26
85	76/113	0800	D63H	0.25	0.13	0.52
			D83H	0.31	0.11	0.35
86	76/122	2200	D13H	0.25	0.14	0.56
87	76/124	1200	D13H	0.27	0.16	0.59
88	76/126	0200	D23H	0.29	0.13	0.45
89	76/164	2400	D63H	0.28	0.00	0.00
90	76/189	1800	D13H	0.30	0.00	0.00
			D93H	0.10	0.05	0.50
					Mean Ratio (MR)	0.31

TABLE 3-38

COMPARISON OF CALCULATED AND OBSERVED 1-HOUR SO_2 CONCENTRATIONS FOR THE DOW CASES FOR COMBINATION 3 IN TABLE 3-35

Case No.	Year/ Julian Day	Hour	Monitor	Observed Concentration (ppm)	Calculated Concentration (ppm)	Ratio of Calculated and Observed Concentrations
1	75/314	0100	D33H	0.36	0.34	0.94
			D63H	0.11	0.02	0.18
			D73H	0.12	0.14	0.17
2	75/314	0200	D33H	0.26	0.24	0.92
			D73H	0.13	0.07	0.54
3	75/314	0500	D63H	0.49	0.07	0.14
4	75/314	1300	D63H	0.14	0.12	0.86
			D83H	0.27	0.31	1.15
5	75/314	2300	D63H	0.28	0.00	0.00
			D83H	0.19	0.00	0.00
6	75/314	2400	D63H	0.30	0.01	0.03
			D83H	0.15	0.00	0.00
7	75/316	1700	D63H	0.12	0.05	0.42
			D83H	0.33	0.03	0.09
8	75/324	1200	D63H	0.39	0.01	0.03
9	75/324	1300	D63H	0.55	0.02	0.04
10	75/325	0800	D23H	0.27	0.10	0.37
11	75/326	1500	D63H	0.27	0.00	0.00
12	75/326	1600	D63H	0.30	0.00	0.00
			D83H	0.13	0.23	1.77
13	75/335	0400	D63H	0.30	0.00	0.00
			D83H	0.12	0.05	0.42
14	75/350	1500	D23H	0.38	0.00	0.00
			D33H	0.12	0.00	0.00
15	75/350	1900	D23H	0.30	0.00	0.00
16	75/350	2000	D23H	0.27	0.20	0.74
17	75/350	2100	D23H	0.29	0.26	0.90
			D33H	0.10	0.11	1.10
18	75/351	0400	D13H	0.28	0.16	0.57
			D93H	0.23	0.00	0.00
19	75/351	0700	D13H	0.14	0.25	1.79
			D93H	0.25	0.03	0.12
20	75/351	1000	D13H	0.35	0.12	0.34
21	75/352	1100	D13H	0.25	0.06	0.24
			D83H	0.11	0.00	0.00
22	75/352	1300	D13H	0.31	0.02	0.06

TABLE 3-38 (Continued)

Case No.	Year/ Julian Day	Hour	Monitor	Observed Concentration (ppm)	Calculated Concentration (ppm)	Ratio of Calculated and Observed Concentrations
23	75/354	1200	D53H	0.25	0.00	0.00
24	75/354	1300	D03H	0.36	0.00	0.00
			D53H	0.10	0.02	0.20
25	75/354	1400	D03H	0.65	0.00	0.00
26	75/354	1600	D03H	0.49	0.00	0.00
27	75/354	1700	D03H	0.44	0.02	0.05
28	75/354	2400	D53H	0.35	0.18	0.51
29	76/003	0100	D63H	0.26	0.00	0.00
			D83H	0.23	0.03	0.13
30	76/003	1100	D63H	0.28	0.15	0.54
			D83H	0.20	0.11	0.55
31	76/005	1300	D23H	0.30	0.18	0.60
32	76/008	1600	D63H	0.27	0.00	0.00
			D83H	0.14	0.14	1.00
33	76/008	1700	D63H	0.30	0.01	0.03
			D83H	0.10	0.01	0.10
34	76/014	0300	D13H	0.37	0.41	1.11
			D93H	0.20	0.02	0.10
35	76/014	0400	D13H	0.26	0.36	1.38
			D93H	0.21	0.01	0.05
36	76/014	0500	D13H	0.33	0.02	0.06
			D93H	0.18	0.00	0.00
37	76/014	0600	D13H	0.50	0.10	0.20
38	76/014	0700	D13H	0.59	0.11	0.19
			D93H	0.30	0.00	0.00
39	76/014	0800	D93H	0.34	0.02	0.06
40	76/014	2100	D13H	0.21	0.07	0.33
			D93H	0.48	0.39	0.81
41	76/014	2200	D13H	0.33	0.40	1.21
			D93H	0.21	0.03	0.14
42	76/028	1600	D23H	0.32	0.26	0.81
43	76/028	1700	D23H	0.44	0.17	0.39
			D33H	0.19	0.18	0.95
44	76/038	2400	D63H	0.47	0.08	0.17
			D83H	0.15	0.01	0.07
45	76/039	0100	D63H	0.45	0.02	0.04
			D83H	0.18	0.00	0.00
46	76/039	0200	D63H	0.47	0.01	0.02
			D83H	0.16	0.00	0.00
47	76/042	1200	D13H	0.40	0.26	0.65
			D93H	0.16	0.00	0.00

TABLE 3-38 (Continued)

Case No.	Year/ Julian Day	Hour	Monitor	Observed Concentration (ppm)	Calculated Concentration (ppm)	Ratio of Calculated and Observed Concentrations
48	76/043	0900	D33H	0.26	0.17	0.65
49	76/046	1700	D23H	0.22	0.02	0.09
			D63H	0.29	0.29	1.00
50	76/046	1800	D63H	0.81	0.11	0.14
			D83H	0.23	0.02	0.09
51	76/046	1900	D63H	0.42	0.01	0.02
			D83H	0.18	0.01	0.06
52	76/049	1700	D63H	0.40	0.14	0.35
			D83H	0.15	0.13	0.87
53	76/049	1800	D63H	0.29	0.07	0.24
			D83H	0.15	0.01	0.07
54	76/049	1900	D63H	0.28	0.01	0.04
			D83H	0.16	0.00	0.00
55	76/052	1300	D03H	0.39	0.00	0.00
56	76/052	1500	D03H	0.28	0.03	0.11
57	76/052	1600	D03H	0.29	0.01	0.03
58	76/065	1000	D63H	0.11	0.17	1.55
			D83H	0.34	0.47	1.38
59	76/065	1100	D83H	0.29	0.24	0.83
60	76/065	1500	D63H	0.12	0.11	0.92
			D83H	0.26	0.10	0.38
61	76/066	2400	D13H	0.12	0.00	0.00
			D93H	0.31	0.14	0.45
62	76/067	0200	D13H	0.27	0.34	1.26
			D93H	0.15	0.02	0.13
63	76/067	1400	D13H	0.34	0.20	0.59
			D93H	0.11	0.15	1.36
64	76/067	1500	D13H	0.32	0.35	1.09
65	76/067	1700	D13H	0.29	0.00	0.00
66	76/073	0200	D63H	0.26	0.19	0.73
			D83H	0.12	0.16	1.33
67	76/074	1300	D63H	0.25	0.00	0.00
			D83H	0.10	0.01	0.10
68	76/074	1900	D63H	0.29	0.00	0.00
			D83H	0.17	0.01	0.06
69	76/074	2000	D63H	0.28	0.06	0.21
			D83H	0.11	0.01	0.09
70	76/074	2400	D13H	0.16	0.24	1.50
			D93H	0.25	0.00	0.00
71	76/084	0200	D23H	0.30	0.29	0.97

TABLE 3-38 (Continued)

Case No.	Year/ Julian Day	Hour	Monitor	Observed Concentration (ppm)	Calculated Concentration (ppm)	Ratio of Calculated and Observed Concentrations
72	76/084	0300	D23H	0.35	0.19	0.54
73	76/084	0400	D23H	0.30	0.13	0.43
74	76/094	1800	D03H	0.26	0.25	0.96
75	76/094	2000	D03H	0.27	0.02	0.07
76	76/094	2300	D03H	0.59	0.04	0.07
77	76/095	0200	D03H	0.27	0.06	0.22
78	76/096	1600	D13H	0.30	0.00	0.00
			D93H	0.16	0.30	1.88
79	76/096	1700	D13H	0.60	0.26	0.43
			D93H	0.16	0.07	0.44
80	76/106	0200	D23H	0.64	0.21	0.33
81	76/107	1200	D63H	0.10	0.13	1.30
			D83H	0.26	0.30	1.15
82	76/109	1000	D23H	0.35	0.12	0.34
83	76/113	0600	D63H	0.15	0.05	0.33
			D83H	0.36	0.28	0.78
84	76/113	0700	D63H	0.21	0.14	0.67
			D83H	0.31	0.11	0.35
85	76/113	0800	D63H	0.25	0.15	0.60
			D83H	0.31	0.14	0.45
86	76/122	2200	D13H	0.25	0.15	0.60
87	76/124	1200	D13H	0.27	0.21	0.78
88	76/126	0200	D23H	0.29	0.16	0.55
89	76/164	2400	D63H	0.28	0.01	0.04
90	76/189	1800	D13H	0.30	0.00	0.00
			D93H	0.10	0.06	0.60
					Mean Ratio (MR)	0.37

TABLE 3-39

COMPARISON OF CALCULATED AND OBSERVED 1-HOUR SO_2 CONCENTRATIONS FOR THE DOW CASES FOR COMBINATION 4 IN TABLE 3-35

Case No.	Year/ Julian Day	Hour	Monitor	Observed Concentration (ppm)	Calculated Concentration (ppm)	Ratio of Calculated and Observed Concentrations
1	75/314	0100	D33H	0.36	0.22	0.61
			D63H	0.11	0.10	0.91
			D73H	0.12	0.16	1.33
2	75/314	0200	D33H	0.26	0.17	0.65
			D73H	0.13	0.11	0.85
3	75/314	0500	D63H	0.49	0.16	0.33
4	75/314	1300	D63H	0.14	0.10	0.71
			D83H	0.27	0.22	0.81
5	75/314	2300	D63H	0.28	0.03	0.11
			D83H	0.19	0.03	0.16
6	75/314	2400	D63H	0.30	0.04	0.13
			D83H	0.15	0.04	0.27
7	75/316	1700	D63H	0.12	0.12	1.00
			D83H	0.33	0.15	0.45
8	75/324	1200	D63H	0.39	0.05	0.13
9	75/324	1300	D63H	0.55	0.09	0.16
10	75/325	0800	D23H	0.27	0.19	0.70
11	75/326	1500	D63H	0.27	0.00	0.00
12	75/326	1600	D63H	0.30	0.00	0.00
			D83H	0.13	0.18	1.38
13	75/335	0400	D63H	0.30	0.01	0.03
			D83H	0.12	0.06	0.50
14	75/350	1500	D23H	0.38	0.01	0.03
			D33H	0.12	0.03	0.25
15	75/350	1900	D23H	0.30	0.03	0.10
16	75/350	2000	D23H	0.27	0.27	1.00
17	75/350	2100	D23H	0.29	0.31	1.07
			D33H	0.10	0.10	1.00
18	75/351	0400	D13H	0.28	0.21	0.75
			D93H	0.23	0.01	0.04
19	75/351	0700	D13H	0.14	0.27	1.93
			D93H	0.25	0.10	0.40
20	75/351	1000	D13H	0.35	0.18	0.51
21	75/352	1100	D13H	0.25	0.10	0.40
			D83H	0.11	0.00	0.00
22	75/352	1300	D13H	0.31	0.07	0.23
23	75/354	1200	D53H	0.25	0.04	0.16
24	75/354	1300	D03H	0.36	0.00	0.00
			D53H	0.10	0.07	0.70

TABLE 3-39 (Continued)

Case No.	Year/ Julian Day	Hour	Monitor	Observed Concentration (ppm)	Calculated Concentration (ppm)	Ratio of Calculated and Observed Concentrations
25	75/354	1400	D03H	0.65	0.03	0.05
26	75/354	1600	D03H	0.49	0.02	0.04
27	75/354	1700	D03H	0.44	0.07	0.16
28	75/354	2400	D53H	0.35	0.25	0.71
29	76/003	0100	D63H	0.26	0.01	0.04
			D83H	0.23	0.07	0.30
30	76/003	1100	D63H	0.28	0.21	0.75
			D83H	0.20	0.21	1.05
31	76/005	1300	D23H	0.30	0.25	0.83
32	76/008	1600	D63H	0.27	0.00	0.00
			D83H	0.14	0.11	0.79
33	76/008	1700	D63H	0.30	0.07	0.23
			D83H	0.10	0.05	0.50
34	76/014	0300	D13H	0.37	0.41	1.11
			D93H	0.20	0.08	0.40
35	76/014	0400	D13H	0.26	0.39	1.50
			D93H	0.21	0.05	0.24
36	76/014	0500	D13H	0.33	0.10	0.30
			D93H	0.18	0.00	0.00
37	76/014	0600	D13H	0.50	0.20	0.40
38	76/014	0700	D13H	0.59	0.21	0.36
			D93H	0.30	0.00	0.00
39	76/014	0800	D93H	0.34	0.08	0.24
40	76/014	2100	D13H	0.21	0.16	0.76
			D93H	0.48	0.39	0.81
41	76/014	2200	D13H	0.33	0.39	1.18
			D93H	0.21	0.10	0.48
42	76/028	1600	D23H	0.32	0.21	0.66
43	76/028	1700	D23H	0.44	0.13	0.30
			D33H	0.19	0.19	1.00
44	76/038	2400	D63H	0.47	0.15	0.32
			D83H	0.15	0.06	0.40
45	76/039	0100	D63H	0.45	0.08	0.18
			D83H	0.18	0.04	0.22
46	76/039	0200	D63H	0.47	0.07	0.15
			D83H	0.16	0.03	0.19
47	76/042	1200	D13H	0.40	0.25	0.63
			D93H	0.16	0.02	0.13
48	76/043	0900	D33H	0.26	0.16	0.62
49	76/046	1700	D23H	0.22	0.05	0.23
			D63H	0.29	0.31	1.07

TABLE 3-39 (Continued)

Case No.	Year/ Julian Day	Hour	Monitor	Observed Concentration (ppm)	Calculated Concentration (ppm)	Ratio of Calculated and Observed Concentrations
50	76/046	1800	D63H	0.81	0.16	0.20
			D83H	0.23	0.07	0.30
51	76/046	1900	D63H	0.42	0.04	0.10
			D83H	0.18	0.03	0.17
52	76/049	1700	D63H	0.40	0.19	0.48
			D83H	0.15	0.15	1.00
53	76/049	1800	D63H	0.29	0.12	0.41
			D83H	0.15	0.05	0.33
54	76/049	1900	D63H	0.28	0.05	0.18
			D83H	0.16	0.03	0.19
55	76/052	1300	D03H	0.39	0.01	0.03
56	76/052	1500	D03H	0.28	0.04	0.14
57	76/052	1600	D03H	0.29	0.02	0.07
58	76/065	1000	D63H	0.11	0.11	1.00
			D83H	0.34	0.34	1.00
59	76/065	1100	D83H	0.29	0.21	0.72
60	76/065	1500	D63H	0.12	0.08	0.67
			D83H	0.26	0.14	0.54
61	76/066	2400	D13H	0.12	0.01	0.08
			D93H	0.31	0.24	0.77
62	76/067	0200	D13H	0.27	0.25	0.93
			D93H	0.15	0.04	0.27
63	76/067	1400	D13H	0.34	0.20	0.59
			D93H	0.11	0.13	1.18
64	76/067	1500	D13H	0.32	0.25	0.78
65	76/067	1700	D13H	0.29	0.02	0.07
66	76/073	0200	D63H	0.26	0.21	0.81
			D83H	0.12	0.24	2.00
67	76/074	1300	D63H	0.25	0.03	0.12
			D83H	0.10	0.04	0.40
68	76/074	1900	D63H	0.29	0.03	0.10
			D83H	0.17	0.04	0.24
69	76/074	2000	D63H	0.28	0.12	0.43
			D83H	0.11	0.08	0.73
70	76/074	2400	D13H	0.16	0.23	1.44
			D93H	0.25	0.03	0.12
71	76/084	0200	D23H	0.30	0.35	1.17
72	76/084	0300	D23H	0.35	0.21	0.60
73	76/084	0400	D23H	0.30	0.18	0.60
74	76/094	1800	D03H	0.26	0.23	0.88
75	76/094	2000	D03H	0.27	0.09	0.33
76	76/094	2300	D03H	0.59	0.12	0.20

TABLE 3-39 (Continued)

Case No.	Year/ Julian Day	Hour	Monitor	Observed Concentration (ppm)	Calculated Concentration (ppm)	Ratio of Calculated and Observed Concentrations
77	76/095	0200	D03H	0.27	0.12	0.44
78	76/096	1600	D13H	0.30	0.02	0.07
			D93H	0.16	0.35	2.19
79	76/096	1700	D13H	0.60	0.28	0.47
			D93H	0.16	0.15	0.94
80	76/106	0200	D23H	0.64	0.20	0.31
81	76/107	1200	D63H	0.10	0.15	1.50
			D83H	0.26	0.35	1.35
82	76/109	1000	D23H	0.35	0.18	0.51
83	76/113	0600	D63H	0.15	0.10	0.67
			D83H	0.36	0.35	0.97
84	76/113	0700	D63H	0.21	0.16	0.76
			D83H	0.31	0.24	0.77
85	76/113	0800	D63H	0.25	0.18	0.72
			D83H	0.31	0.27	0.87
86	76/122	2200	D13H	0.25	0.21	0.84
87	76/124	1200	D13H	0.27	0.22	0.81
88	76/126	0200	D23H	0.29	0.10	0.34
89	76/164	2400	D63H	0.28	0.06	0.21
90	76/189	1800	D13H	0.30	0.00	0.00
			D93H	0.10	0.14	1.40
					Mean Ratio (MR)	0.48

TABLE 3-40

COMPARISON OF CALCULATED AND OBSERVED 1-HOUR SO_2 CONCENTRATIONS FOR THE DOW CASES FOR COMBINATION 5 IN TABLE 3-35

Case No.	Year/ Julian Day	Hour	Monitor	Observed Concentration (ppm)	Calculated Concentration (ppm)	Ratio of Calculated and Observed Concentrations
1	75/314	0100	D33H	0.36	0.21	0.58
			D63H	0.11	0.12	1.09
			D73H	0.12	0.16	1.33
2	75/314	0200	D33H	0.26	0.16	0.62
			D73H	0.13	0.11	0.85
3	75/314	0500	D63H	0.49	0.20	0.41
4	75/314	1300	D63H	0.14	0.09	0.64
			D83H	0.27	0.22	0.81
5	75/314	2300	D63H	0.28	0.03	0.11
			D83H	0.19	0.04	0.21
6	75/314	2400	D63H	0.30	0.04	0.13
			D83H	0.15	0.04	0.27
7	75/316	1700	D63H	0.12	0.12	1.00
			D83H	0.33	0.18	0.55
8	75/324	1200	D63H	0.39	0.08	0.21
9	75/324	1300	D63H	0.55	0.13	0.24
10	75/325	0800	D23H	0.27	0.20	0.74
11	75/326	1500	D63H	0.27	0.00	0.00
12	75/326	1600	D63H	0.30	0.00	0.00
			D83H	0.13	0.18	1.38
13	75/335	0400	D63H	0.30	0.01	0.03
			D83H	0.12	0.06	0.50
14	75/350	1500	D23H	0.38	0.01	0.03
			D33H	0.12	0.03	0.25
15	75/350	1900	D23H	0.30	0.03	0.10
16	75/350	2000	D23H	0.27	0.27	1.00
17	75/350	2100	D23H	0.29	0.31	1.07
			D33H	0.10	0.10	1.00
18	75/351	0400	D13H	0.28	0.39	1.39
			D93H	0.23	0.01	0.04
19	75/351	0700	D13H	0.14	0.41	2.93
			D93H	0.25	0.09	0.36
20	75/351	1000	D13H	0.35	0.35	1.00
21	75/352	1100	D13H	0.25	0.21	0.84
			D83H	0.11	0.00	0.00
22	75/352	1300	D13H	0.31	0.15	0.48
23	75/354	1200	D53H	0.25	0.03	0.12
24	75/354	1300	D03H	0.36	0.00	0.00
			D53H	0.10	0.07	0.70

TABLE 3-40 (Continued)

Case No.	Year/ Julian Day	Hour	Monitor	Observed Concentration (ppm)	Calculated Concentration (ppm)	Ratio of Calculated and Observed Concentrations
25	75/354	1400	D03H	0.65	0.03	0.05
26	75/354	1600	D03H	0.49	0.02	0.04
27	75/354	1700	D03H	0.44	0.07	0.16
28	75/354	2400	D53H	0.35	0.24	0.69
29	76/003	0100	D63H	0.26	0.02	0.08
			D83H	0.23	0.06	0.26
30	76/003	1100	D63H	0.28	0.23	0.82
			D83H	0.20	0.26	1.30
31	76/005	1300	D23H	0.30	0.25	0.83
32	76/008	1600	D63H	0.27	0.00	0.00
			D83H	0.14	0.11	0.79
33	76/008	1700	D63H	0.30	0.08	0.27
			D83H	0.10	0.05	0.50
34	76/014	0300	D13H	0.37	0.59	1.59
			D93H	0.20	0.07	0.35
35	76/014	0400	D13H	0.26	0.58	2.23
			D93H	0.21	0.05	0.24
36	76/014	0500	D13H	0.33	0.16	0.48
			D93H	0.18	0.00	0.00
37	76/014	0600	D13H	0.50	0.34	0.68
38	76/014	0700	D13H	0.59	0.35	0.59
			D93H	0.30	0.00	0.00
39	76/014	0800	D93H	0.34	0.07	0.21
40	76/014	2100	D13H	0.21	0.20	0.95
			D93H	0.48	0.39	0.81
41	76/014	2200	D13H	0.33	0.55	1.67
			D93H	0.21	0.10	0.48
42	76/028	1600	D23H	0.32	0.20	0.63
43	76/028	1700	D23H	0.44	0.12	0.27
			D33H	0.19	0.18	0.95
44	76/038	2400	D63H	0.47	0.16	0.34
			D83H	0.15	0.07	0.47
45	76/039	0100	D63H	0.45	0.09	0.20
			D83H	0.18	0.04	0.22
46	76/039	0200	D63H	0.47	0.07	0.15
			D83H	0.16	0.04	0.25
47	76/042	1200	D13H	0.40	0.31	0.78
			D93H	0.16	0.02	0.13
48	76/043	0900	D33H	0.26	0.16	0.62
49	76/046	1700	D23H	0.22	0.04	0.18
			D63H	0.29	0.31	1.07
50	76/046	1800	D63H	0.81	0.16	0.20
			D83H	0.23	0.07	0.30

TABLE 3-40 (Continued)

Case No.	Year/ Julian Day	Hour	Monitor	Observed Concentration (ppm)	Calculated Concentration (ppm)	Ratio of Calculated and Observed Concentrations
51	76/046	1900	D63H	0.42	0.04	0.10
			D83H	0.18	0.03	0.17
52	76/049	1700	D63H	0.40	0.20	0.50
			D83H	0.15	0.17	1.13
53	76/049	1800	D63H	0.29	0.12	0.41
			D83H	0.15	0.05	0.33
54	76/049	1900	D63H	0.28	0.05	0.18
			D83H	0.16	0.03	0.19
55	76/052	1300	D03H	0.39	0.01	0.03
56	76/052	1500	D03H	0.28	0.04	0.14
57	76/052	1600	D03H	0.29	0.02	0.07
58	76/065	1000	D63H	0.11	0.11	1.00
			D83H	0.34	0.34	1.00
59	76/065	1100	D83H	0.29	0.21	0.72
60	76/065	1500	D63H	0.12	0.07	0.58
			D83H	0.26	0.14	0.54
61	76/066	2400	D13H	0.12	0.01	0.08
			D93H	0.31	0.23	0.74
62	76/067	0200	D13H	0.27	0.32	1.19
			D93H	0.15	0.04	0.27
63	76/067	1400	D13H	0.34	0.23	0.68
			D93H	0.11	0.12	1.09
64	76/067	1500	D13H	0.32	0.29	0.91
65	76/067	1700	D13H	0.29	0.02	0.07
66	76/073	0200	D63H	0.26	0.22	0.85
			D83H	0.12	0.29	2.42
67	76/074	1300	D63H	0.25	0.03	0.12
			D83H	0.10	0.05	0.50
68	76/074	1900	D63H	0.29	0.03	0.10
			D83H	0.17	0.04	0.24
69	76/074	2000	D63H	0.28	0.12	0.43
			D83H	0.11	0.10	0.91
70	76/074	2400	D13H	0.16	0.36	2.25
			D93H	0.25	0.02	0.08
71	76/084	0200	D23H	0.30	0.34	1.13
72	76/084	0300	D23H	0.35	0.20	0.57
73	76/084	0400	D23H	0.30	0.18	0.60
74	76/094	1800	D03H	0.26	0.23	0.88
75	76/094	2000	D03H	0.27	0.08	0.30
76	76/094	2300	D03H	0.59	0.12	0.20
77	76/095	0200	D03H	0.27	0.12	0.44

TABLE 3-40 (Continued)

Case No.	Year/ Julian Day	Hour	Monitor	Observed Concentration (ppm)	Calculated Concentration (ppm)	Ratio of Calculated and Observed Concentrations
78	76/096	1600	D13H	0.30	0.03	0.10
			D93H	0.16	0.35	2.19
79	76/096	1700	D13H	0.60	0.42	0.70
			D93H	0.16	0.15	0.94
80	76/106	0200	D23H	0.64	0.20	0.31
81	76/107	1200	D63H	0.10	0.16	1.60
			D83H	0.26	0.39	1.50
82	76/109	1000	D23H	0.35	0.18	0.51
83	76/113	0600	D63H	0.15	0.10	0.67
			D83H	0.36	0.39	1.08
84	76/113	0700	D63H	0.21	0.17	0.81
			D83H	0.31	0.27	0.87
85	76/113	0800	D63H	0.25	0.19	0.76
			D83H	0.31	0.32	1.03
86	76/122	2200	D13H	0.25	0.33	1.32
87	76/124	1200	D13H	0.27	0.32	1.19
88	76/126	0200	D23H	0.29	0.10	0.34
89	76/164	2400	D63H	0.28	0.07	0.25
90	76/189	1800	D13H	0.30	0.00	0.00
			D93H	0.10	0.14	1.40
					Mean Ratio (MR)	0.54

TABLE 3-41

COMPARISON OF CALCULATED AND OBSERVED 1-HOUR SO_2 CONCENTRATIONS FOR THE DOW CASES FOR COMBINATION 6 in TABLE 3-35

Case No.	Year/ Julian Day	Hour	Monitor	Observed Concentration (ppm)	Calculated Concentration (ppm)	Ratio of Calculated and Observed Concentrations
1	75/314	0100	D33H	0.36	0.21	0.58
			D63H	0.11	0.14	1.27
			D73H	0.12	0.16	1.33
2	75/314	0200	D33H	0.26	0.16	0.62
			D73H	0.13	0.11	0.85
3	75/314	0500	D63H	0.49	0.22	0.45
4	75/314	1300	D63H	0.14	0.10	0.71
			D83H	0.27	0.24	0.89
5	75/314	2300	D83H	0.28	0.03	0.11
			D83H	0.19	0.04	0.21
6	75/314	2400	D63H	0.30	0.04	0.13
			D83H	0.15	0.04	0.27
7	75/316	1700	D63H	0.12	0.12	1.00
			D83H	0.33	0.19	0.58
8	75/324	1200	D63H	0.39	0.09	0.23
9	75/324	1300	D63H	0.55	0.15	0.27
10	75/325	0800	D23H	0.27	0.20	0.74
11	75/326	1500	D63H	0.27	0.00	0.00
12	75/326	1600	D63H	0.30	0.00	0.00
			D83H	0.13	0.18	1.38
13	75/335	0400	D63H	0.30	0.01	0.03
			D83H	0.12	0.06	0.50
14	75/350	1500	D23H	0.38	0.01	0.03
			D33H	0.12	0.03	0.25
15	75/350	1900	D23H	0.30	0.03	0.10
16	75/350	2000	D23H	0.27	0.28	1.04
17	75/350	2100	D23H	0.29	0.32	1.10
			D33H	0.10	0.10	1.00
18	75/351	0400	D13H	0.28	0.44	1.57
			D93H	0.23	0.01	0.04
19	75/351	0700	D13H	0.14	0.46	3.29
			D93H	0.25	0.10	0.40
20	75/351	1000	D13H	0.35	0.38	1.09
21	75/352	1100	D13H	0.25	0.24	0.96
			D83H	0.11	0.00	0.00
22	75/352	1300	D13H	0.31	0.16	0.52
23	75/354	1200	D53H	0.25	0.04	0.16

TABLE 3-41 (Continued)

Case No.	Year/ Julian Day	Hour	Monitor	Observed Concentration (ppm)	Calculated Concentration (ppm)	Ratio of Calculated and Observed Concentrations
24	75/354	1300	D03H	0.36	0.00	0.00
			D53H	0.10	0.07	0.70
25	75/354	1400	D03H	0.65	0.03	0.05
26	75/354	1600	D03H	0.49	0.02	0.04
27	75/354	1700	D03H	0.44	0.07	0.16
28	75/354	2400	D53H	0.35	0.24	0.69
29	76/003	0100	D63H	0.26	0.02	0.08
			D83H	0.23	0.07	0.30
30	76/003	1100	D63H	0.28	0.24	0.86
			D83H	0.20	0.28	1.40
31	76/005	1300	D23H	0.30	0.26	0.87
32	76/008	1600	D63H	0.27	0.00	0.00
			D83H	0.14	0.11	0.79
33	76/008	1700	D63H	0.30	0.08	0.27
			D83H	0.10	0.06	0.60
34	76/014	0300	D13H	0.37	0.65	1.76
			D93H	0.20	0.08	0.40
35	76/014	0400	D13H	0.26	0.64	2.46
			D93H	0.21	0.05	0.24
36	76/014	0500	D13H	0.33	0.19	0.58
			D93H	0.18	0.00	0.00
37	76/014	0600	D13H	0.50	0.38	0.76
38	76/014	0700	D13H	0.59	0.40	0.68
			D93H	0.30	0.00	0.00
39	76/014	0800	D93H	0.34	0.08	0.24
40	76/014	2100	D13H	0.21	0.21	1.00
			D93H	0.48	0.40	0.83
41	76/014	2200	D13H	0.33	0.60	1.82
			D93H	0.21	0.10	0.48
42	76/028	1600	D23H	0.32	0.21	0.66
43	76/028	1700	D23H	0.44	0.13	0.30
			D33H	0.19	0.18	0.95
44	76/038	2400	D63H	0.47	0.16	0.34
			D83H	0.15	0.08	0.53
45	76/039	0100	D63H	0.45	0.09	0.20
			D83H	0.18	0.04	0.22
46	76/039	0200	D63H	0.47	0.07	0.15
			D83H	0.16	0.04	0.25
47	76/042	1200	D13H	0.40	0.34	0.85
			D93H	0.16	0.02	0.13
48	76/043	0900	D33H	0.26	0.16	0.62

TABLE 3-41 (Continued)

Case No.	Year/ Julian Day	Hour	Monitor	Observed Concentration (ppm)	Calculated Concentration (ppm)	Ratio of Calculated and Observed Concentrations
49	76/046	1700	D23H	0.22	0.05	0.23
			D63H	0.29	0.32	1.10
50	76/046	1800	D63H	0.81	0.17	0.21
			D83H	0.23	0.08	0.35
51	76/046	1900	D63H	0.42	0.04	0.10
			D83H	0.18	0.03	0.17
52	76/049	1700	D63H	0.40	0.21	0.53
			D83H	0.15	0.18	1.20
53	76/049	1800	D63H	0.29	0.12	0.41
			D83H	0.15	0.06	0.40
54	76/049	1900	D63H	0.28	0.05	0.18
			D83H	0.16	0.03	0.19
55	76/052	1300	D03H	0.39	0.01	0.03
56	76/052	1500	D03H	0.28	0.04	0.14
57	76/052	1600	D03H	0.29	0.02	0.07
58	76/065	1000	D63H	0.11	0.11	1.00
			D83H	0.34	0.38	1.12
59	76/065	1100	D83H	0.29	0.23	0.79
60	76/065	1500	D63H	0.12	0.08	0.67
			D83H	0.26	0.16	0.62
61	76/066	2400	D13H	0.12	0.01	0.08
			D93H	0.31	0.24	0.77
62	76/067	0200	D13H	0.27	0.36	1.33
			D93H	0.15	0.04	0.27
63	76/067	1400	D13H	0.34	0.26	0.76
			D93H	0.11	0.13	1.18
64	76/067	1500	D13H	0.32	0.32	1.00
65	76/067	1700	D13H	0.29	0.03	0.10
66	76/073	0200	D63H	0.26	0.23	0.88
			D83H	0.12	0.31	2.58
67	76/074	1300	D63H	0.25	0.04	0.16
			D83H	0.10	0.05	0.50
68	76/074	1900	D63H	0.29	0.03	0.10
			D83H	0.17	0.05	0.29
69	76/074	2000	D63H	0.28	0.13	0.46
			D83H	0.11	0.10	0.91
70	76/074	2400	D13H	0.16	0.40	2.50
			D93H	0.25	0.03	0.12
71	76/084	0200	D23H	0.30	0.35	1.17
72	76/084	0300	D23H	0.35	0.21	0.60
73	76/084	0400	D23H	0.30	0.18	0.60

TABLE 3-41 (Continued)

Case No.	Year/ Julian Day	Hour	Monitor	Observed Concentration (ppm)	Calculated Concentration (ppm)	Ratio of Calculated and Observed Concentrations
74	76/094	1800	D03H	0.26	0.24	0.92
75	76/094	2000	D03H	0.27	0.09	0.33
76	76/094	2300	D03H	0.59	0.12	0.20
77	76/095	0200	D03H	0.27	0.12	0.44
78	76/096	1600	D13H	0.30	0.03	0.10
			D93H	0.16	0.36	2.25
79	76/096	1700	D13H	0.60	0.47	0.78
			D93H	0.16	0.15	0.94
80	76/106	0200	D23H	0.64	0.20	0.31
81	76/107	1200	D63H	0.10	0.16	1.60
			D83H	0.26	0.42	1.62
82	76/109	1000	D23H	0.35	0.19	0.54
83	76/113	0600	D63H	0.15	0.11	0.73
			D83H	0.36	0.43	1.19
84	76/113	0700	D63H	0.21	0.18	0.86
			D83H	0.31	0.29	0.94
85	76/113	0800	D63H	0.25	0.20	0.80
			D83H	0.31	0.34	1.10
86	76/122	2200	D13H	0.25	0.36	1.44
87	76/124	1200	D13H	0.27	0.36	1.33
88	76/126	0200	D23H	0.29	0.10	0.34
89	76/164	2400	D63H	0.28	0.08	0.29
90	76/189	1800	D13H	0.30	0.00	0.00
			D93H	0.10	0.14	1.40
					Mean Ratio (MR)	0.58

Table 3-42 summarizes the results of comparisons of concurrent calculated and observed 1-hour SO_2 concentrations for the 143 observed concentrations greater than or equal to 0.10 ppm during the 90 hours selected for model testing. Because the equation for the RMSE cannot be applied to zero concentrations, the concentration was set equal to 0.01 ppm for all cases with zero calculated concentrations. (The threshold and accuracy of the SO_2 monitors are about 0.01 ppm.) Whether or not building wake effects are included in the ISC Model calculations, the correspondence between calculated and observed concentrations obtained in Urban Mode 2 is superior to that obtained in the Rural Mode. This result supports the hypothesis of enhanced turbulence at the DOW plant. Although the building wake effects and stack-tip downwash options improve the model's performance in both the Rural Mode and Urban Mode 2, the MR values suggest that there may be errors in the model inputs or a bias in the model towards underestimating concentrations for the DOW data set.

We are not certain that the MR, RMSE and percentage error bands are the most appropriate measures of model performance for the DOW data set because the density of the DOW monitoring network is inadequate to determine the locations of the plume centerlines. The current Guideline on Air Quality Models (EPA, 1978) suggests that, as an alternative to direct comparisons of concurrent calculated and observed concentrations, short-term dispersion models may be evaluated by comparing the upper percentiles of the calculated and observed concentration frequency distributions. Additionally, Turner (1979) observes that a comparison of the maximum concentration observed at any point with the maximum concentration calculated at any point is of interest for regulatory purposes. We therefore used Tables 3-36 and 3-41 to generate the cumulative frequency distributions of calculated and observed hourly SO_2 concentrations for the DOW data set shown in Figure 3-9. We point out that the concentrations calculated by the ISC Model for model option Combination 1 are the same as calculated by conventional modeling techniques (for example the MPTER Model). As shown by Figure 3-9, the upper end of the observed

TABLE 3-42

SUMMARY OF THE RESULTS OF THE ISC MODEL CALCULATIONS FOR THE DOW DATA SET FOR SIX COMBINATIONS OF ISC MODEL OPTIONS*

ISC Model Option Combination Number	ISC Model Mode	Briggs (1973) Stack-Tip Downwash	Bldg. Wake Effects	Measures of Model Performance		
				MR	RMSE	% Within Factor of 2
1	Rural	No	No	0.15	12.37	10
2	Rural	No	Yes	0.31	8.79	29
3	Rural	Yes	Yes	0.37	8.34	34
4	Urban 2	No	No	0.48	4.55	46
5	Urban 2	No	Yes	0.54	4.43	48
6	Urban 2	Yes	Yes	0.58	4.19	49

*The sample size is 143.

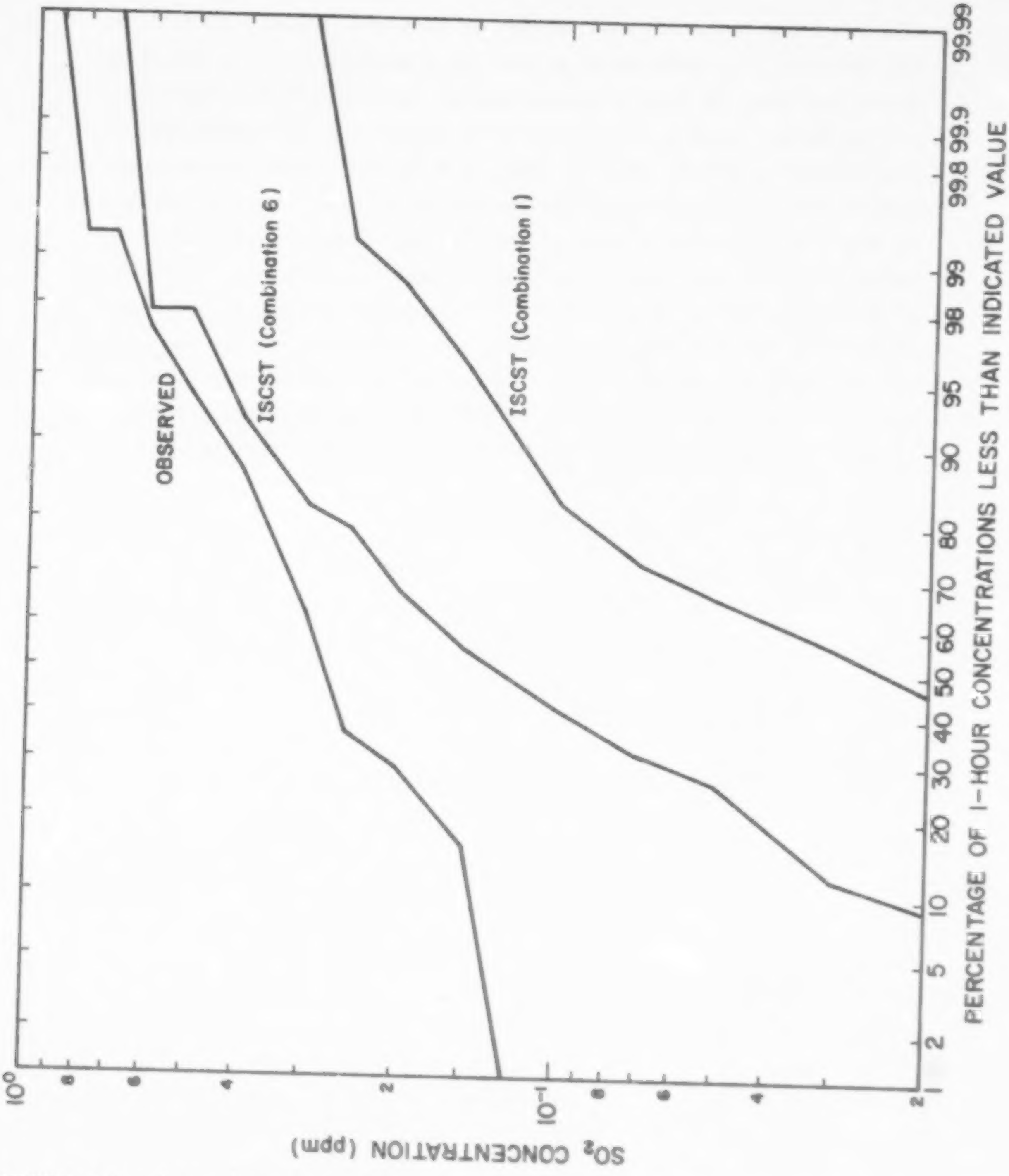

FIGURE 3-9. Comparison of calculated and observed cumulative 1-hour SO_2 concentration frequency distributions for the DOW data set.

concentration frequency distribution is much more closely matched by the ISC Model for Combination 6 than for Combination 1. It should be emphasized that the hourly concentrations used to form the observed concentration frequency distribution in Figure 3-9 were restricted to concentrations greater than or equal to 0.10 ppm. Thus, the observed concentration frequency distribution reflects the presence at the monitor of emissions from one or both of the DOW power houses during every hour. However, if the wind directions used as input to the model are assumed to be representative of the winds defining plume trajectories during every hour, the wind directions imply that emissions from one or both of the DOW power houses were not present at the monitors during every hour. Thus, it is not unexpected that the ISC Model underpredicts the lower end of the observed concentration frequency distribution in Figure 3-9.

SECTION 4

SUGGESTIONS FOR MODEL IMPROVEMENT

The results of the ISC Model calculations described in Section 3 for the DOW and Millstone (Johnson, et al., 1975) data sets indicate that the model's building wake effects option may have a systematic tendency to underestimate the concentrations produced in a building's wake region by buoyant or slightly buoyant stack emissions subject to building wake effects. In addition to the emission rate, the wind speed and the mixing height, the basic components of a Gaussian plume model are the effective emission height and the lateral and vertical dispersion coefficients. Although the uncertainties in the DOW emissions are unknown, the emissions for the Millstone data set are estimated by Johnson, et al. to be accurate to within about 5 percent. Also, the wind speeds are known with a relatively high degree of confidence for both the Millstone and DOW data sets, and the restriction on vertical mixing at the top of the surface mixing layer is unlikely to have affected the observed concentrations for either data set. Additionally, the Islitzer (1965) and Millstone data sets do not reveal any systematic errors in the lateral dispersion coefficients calculated by the ISC Model in the wake region. It follows that the apparent systematic tendency toward underpredictions in the wake region results from errors in the effective emission heights, the vertical dispersion coefficients or both. Consequently, modifications that might improve the ISC Model's performance include adjustments in the effective emission heights to account for the effects of downwash and the use of different vertical dispersion coefficients.

Of the various data sets used to test the ISC Model, the following features are unique to the Millstone data set: (1) The Millstone experiments involved slightly buoyant releases from a squat building with a stack height to building height ratio less than 1.2, and (2) Visual observations indicated that the plume was in a condition of partial entrainment in which portions of the plume were intermittently entrained into the building's cavity zone and effectively acted as a ground-level source. Thus, we suggest the following change in the way that the ISC model calculates effective emission heights for insignificantly buoyant emissions from stacks located on or adjacent to squat buildings with stack height to building height ratios less than 1.2:

$$H\{x\} = \left\{ \begin{array}{lll} h + \Delta h\{x\} & ; & h + \Delta h_m\{2h_b\} \geq 1.2\ h_b \\ \\ 0 & ; & h + \Delta h_m\{2h_b\} < 1.2\ h_b \end{array} \right\} \qquad (4\text{-}1)$$

where

$H\{x\}$ = effective emission height at downwind distance x

h = physical stack height

$\Delta h\{x\}$ = plume rise due to momentum and/or buoyancy at downwind distance x, calculated by Equation (2-4) or Equation (2-7) in the ISC Model User's Guide

$\Delta h_m\{2h_b\}$ = plume rise due to momentum alone at a downwind distance of $2h_b$, where h_b is the building height

We point out that the addition of Equation (4-1) to the ISC Model will have no effects on the model's performance for the DOW data set because the stack height to building height ratios exceed 1.2. However, the addition of Equation (4-1) to the ISC Model will yield essentially the same model performance for the Millstone data set as obtained for Case C (see Table 3-11 in Section 3.1.3). As explained above, we believe that the model's tendency to underestimate concentrations for Case C, as indicated by the mean ratio (MR) of calculated to observed concentrations, may be attributed to vertical turbulent intensities that are smaller than the median values associated with Pasquill-Gifford vertical dispersion coefficients.

Briggs (1969), Fay, et al., (1970) and other developers of plume rise equations have expressed the belief that their plume rise equations may not be applicable when the ratio of the stack exit velocity to the mean wind speed is less than about 1.5 because of downwash of the plume into the low pressure region in the lee of the stack. Additionally, Briggs (1969, p. 6) points out that these adverse effects may be abated for stacks with low Froude numbers on the order of unity. Bjorklund and Bowers (1979) conclude from an analysis of the Bringfelt (1968) plume rise data that the effects of stack-tip downwash on buoyant plume rise are insignificant for stacks with Froude numbers (as defined by Briggs, 1969) less than 1.0 and, depending on the stack, may or may not be important for stacks with Froude numbers between 1.0 and 3.0. For stacks with Froude numbers greater than 3.0, Bjorklund and Bowers conclude that stack-tip downwash significantly affects buoyant plume rise when the ratio of the stack exit velocity to the mean wind speed at stack height is less than about 1.5.

To account for the effects of stack-tip downwash, Cramer, et al. (1975) multiplied the unmodified plume rise Δh by the semi-empirical correction factor

$$f = \begin{cases} 1 & ; \quad \bar{u}\{h\} \leq V_s/1.5 \\ \left(\dfrac{3\, V_s - 3\, \bar{u}\{h\}}{V_s} \right) & ; \quad V_s/1.5 < \bar{u}\{h\} < V_s \\ 0 & ; \quad \bar{u}\{h\} \geq V_s \end{cases} \qquad (4\text{-}2)$$

where V_s is the stack exit velocity and $\bar{u}\{h\}$ is the mean wind speed at stack height. As shown by Equation (4-2), plume rise is precluded when the wind speed at stack height equals or exceeds the stack exit velocity. The development of Equation (4-2) is discussed in Appendix G of the report by Bjorklund and Bowers. Because the full-load Froude numbers for the DOW stacks exceed 3.0, the substitution in the ISC Model of Equation (4-2) for the Briggs (1973) stack-tip downwash correction currently used by the model might improve the model's performance for the DOW data set if stack-tip downwash is the cause of the ISC Model's apparent tendency to underpredict concentrations for the data set.

Scire and Schulman (1980) propose a "downwash radius" correction to the Briggs plume rise equations to account for the effects of building wakes on initial entrainment and hence on buoyant plume rise. If momentum effects are considered, the generalized solution to Equation (12) in the paper by Scire and Schulman is of the form (Dumbauld, et al., 1973)

$$\Delta h\{x\} = \left[M\{x\} + B\{x\} + \left(\frac{R_o}{\beta}\right)^3 \right]^{1/3} - \frac{R_o}{\beta} \qquad (4\text{-}3)$$

where M{x} is the momentum term at downwind distance x, B{x} is the buoyancy term, R_o is the "downwash radius" and β is the entrainment coefficient. (See Equations (2-4) and (2-7) in the ISC Model User's Guide for definitions of M{x} and B{x}). On the basis of the results of wind tunnel experiments (Huber and Snyder, 1976), Scire and Schulman hypothesize that R_o is approximately equal to the building height h_b. The addition of Equation (4-3) to the ISC Model might also improve the performance of the model for the DOW data set if the effects of building wakes on buoyant plume rise are the cause of the model's apparent tendency to underestimate concentrations for the data set. However, it is important to note that Equation (4-3) is not applicable to free standing stacks and thus cannot account for the effects on buoyant plume rise of stack-tip downwash.

As a test of the Cramer, et al. (1975) stack-tip downwash correction, we substituted Equation (4-2) for the Briggs (1973) stack-tip downwash correction in the ISCST program and repeated the ISC Model calculations for the DOW data set. Concentrations were calculated in both the Rural Mode and Urban Mode 2 using the distance-dependent plume rise and building wake effects options. Because of the uncertainties about whether or not Equation (4-2) should be applied to stacks with Froude numbers less than 3.0, Equation (4-2) was first applied to all stacks during each hour and then was applied only to stacks with Froude numbers greater than or equal to 3.0 during each hour. (The Froude numbers for the various stacks varied significantly from hour to hour.) Similarly, as a test of the Scire and Schulman (1980) "downwash radius" correction, we converted the plume rise equations in the ISCST program to the form of Equation (4-3) and repeated the ISC Model calculations for the DOW data set. The concentration calculations for the Scire and Schulman "downwash radius" correction were also made in both the Rural Mode and Urban Mode 2 using the distance-dependent plume rise and building wake effects options. The results of the ISC Model calculations for the Cramer, _et al_. stack-tip downwash correction are given in Tables 4-1 through 4-4 and the results of the calculations for the Scire and Schulman "downwash radius" correction are given in Tables 4-5 and 4-6.

Table 4-7 summarizes the results of the various ISC Model calculations for the DOW data set. In both the Rural Mode and Urban Mode 2, the overall performance of the ISC Model - as indicated by the mean ratio (MR) of calculated to observed concentrations, the root mean square error (RMSE) and the percentage error bands - is significantly improved by both the Cramer, _et al_. stack-tip downwash correction and the Scire and Schulman "downwash radius" correction. However, as discussed in Section 3.4.3, the correspondence between the upper percentiles of the calculated and observed concentration frequency distributions may be a better measure of model performance for the DOW data set than the MR, RMSE and percentage error bands because the density of the DOW monitoring network is inadequate to determine the locations of the plume centerlines.

Figures 4-1 and 4-2 compare the observed 1-hour SO_2 concentration cumulative frequency distribution for the DOW data set with the concentration frequency distributions calculated by the ISC Model using the Cramer, _et al_. stack-tip downwash correction for all stacks and for

TABLE 4-1

COMPARISON OF CALCULATED AND OBSERVED 1-HOUR SO$_2$ CONCENTRATIONS FOR THE DOW CASES FOR COMBINATION 2 IN TABLE 3-35 AND THE CRAMER, ET AL. (1975) STACK-TIP DOWNWASH CORRECTION FOR ALL STACKS

Case No.	Year/ Julian Day	Hour	Monitor	Observed Concentration (ppm)	Calculated Concentration (ppm)	Ratio of Calculated and Observed Concentrations
1	75/314	0100	D33H	0.36	0.65	1.81
			D63H	0.11	0.07	0.64
			D73H	0.12	0.14	1.17
2	75/314	0200	D33H	0.26	0.41	1.58
			D73H	0.13	0.08	0.62
3	75/314	0500	D63H	0.49	0.21	0.43
4	75/314	1300	D63H	0.14	0.20	1.43
			D83H	0.27	0.60	2.22
5	75/314	2300	D63H	0.28	0.00	0.00
			D83H	0.19	0.01	0.05
6	75/314	2400	D63H	0.30	0.01	0.03
			D83H	0.15	0.01	0.07
7	75/316	1700	D63H	0.12	0.06	0.50
			D83H	0.33	0.19	0.58
8	75/324	1200	D63H	0.39	0.09	0.23
9	75/324	1300	D63H	0.55	0.27	0.49
10	75/325	0800	D23H	0.27	0.49	1.81
11	75/326	1500	D63H	0.27	0.00	0.00
12	75/326	1600	D63H	0.30	0.00	0.00
			D83H	0.13	0.26	2.00
13	75/335	0400	D63H	0.30	0.00	0.00
			D83H	0.12	0.06	0.50
14	75/350	1500	D23H	0.38	0.00	0.00
			D33H	0.12	0.00	0.00
15	75/350	1900	D23H	0.30	0.00	0.00
16	75/350	2000	D23H	0.27	0.78	2.89
17	75/350	2100	D23H	0.29	0.96	3.31
			D33H	0.10	0.11	1.10
18	75/351	0400	D13H	0.28	1.29	4.61
			D93H	0.23	0.00	0.00
19	75/351	0700	D13H	0.14	1.51	10.78
			D93H	0.25	0.06	0.24
20	75/351	1000	D13H	0.35	1.10	3.14
21	75/352	1100	D13H	0.25	1.19	4.76
			D83H	0.11	0.00	0.00
22	75/352	1300	D13H	0.31	0.37	1.19
23	75/354	1200	D53H	0.25	0.01	0.04

TABLE 4-1 (Continued)

Case No.	Year/ Julian Day	Hour	Monitor	Observed Concentration (ppm)	Calculated Concentration (ppm)	Ratio of Calculated and Observed Concentrations
24	75/354	1300	D03H	0.36	0.00	0.00
			D53H	0.10	0.05	0.50
25	75/354	1400	D03H	0.65	0.00	0.00
26	75/354	1600	D03H	0.49	0.00	0.00
27	75/354	1700	D03H	0.44	0.06	0.14
28	75/354	2400	D53H	0.35	0.20	0.57
29	76/003	0100	D63H	0.26	0.00	0.00
			D83H	0.23	0.07	0.30
30	76/003	1100	D63H	0.28	0.76	2.71
			D83H	0.20	1.15	5.75
31	76/005	1300	D23H	0.30	0.73	2.43
32	76/008	1600	D63H	0.27	0.00	0.00
			D83H	0.14	0.29	2.07
33	76/008	1700	D63H	0.30	0.03	0.10
			D83H	0.10	0.02	0.20
34	76/014	0300	D13H	0.37	2.54	6.86
			D93H	0.20	0.03	0.15
35	76/014	0400	D13H	0.26	2.32	8.92
			D93H	0.21	0.01	0.05
36	76/014	0500	D13H	0.33	0.19	0.58
			D93H	0.18	0.00	0.00
37	76/014	0600	D13H	0.50	1.11	2.22
38	76/014	0700	D13H	0.59	1.30	2.20
			D93H	0.30	0.00	0.00
39	76/014	0800	D93H	0.34	2.31	6.79
40	76/014	2100	D13H	0.21	0.18	0.86
			D93H	0.48	0.98	2.04
41	76/014	2200	D13H	0.33	1.94	5.88
			D93H	0.21	0.06	0.29
42	76/028	1600	D23H	0.32	0.57	1.78
43	76/028	1700	D23H	0.44	0.38	0.86
			D33H	0.19	0.50	2.63
44	76/038	2400	D63H	0.47	0.31	0.66
			D83H	0.15	0.08	0.53
45	76/039	0100	D63H	0.45	0.08	0.18
			D83H	0.18	0.01	0.06
46	76/039	0200	D63H	0.47	0.04	0.09
			D83H	0.16	0.01	0.06
47	76/042	1200	D13H	0.40	1.12	2.80
			D93H	0.16	0.00	0.00
48	76/043	0900	D33H	0.26	0.44	1.69

TABLE 4-1 (Continued)

Case No.	Year/ Julian Day	Hour	Monitor	Observed Concentration (ppm)	Calculated Concentration (ppm)	Ratio of Calculated and Observed Concentrations
49	76/046	1700	D23H	0.22	0.04	0.18
			D63H	0.29	0.69	2.38
50	76/046	1800	D63H	0.81	0.28	0.35
			D83H	0.23	0.07	0.30
51	76/046	1900	D63H	0.42	0.01	0.02
			D83H	0.18	0.01	0.06
52	76/049	1700	D63H	0.40	0.42	1.05
			D83H	0.15	0.57	3.80
53	76/049	1800	D63H	0.29	0.15	0.52
			D83H	0.15	0.03	0.20
54	76/049	1900	D63H	0.28	0.02	0.07
			D83H	0.16	0.10	0.06
55	76/052	1300	D03H	0.39	0.00	0.00
56	76/052	1500	D03H	0.28	0.10	0.36
57	76/052	1600	D03H	0.29	0.02	0.07
58	76/065	1000	D63H	0.11	0.24	2.18
			D83H	0.34	0.92	2.71
59	76/065	1100	D83H	0.29	0.51	1.76
60	76/065	1500	D63H	0.12	0.14	1.17
			D83H	0.26	0.21	0.81
61	76/066	2400	D13H	0.12	0.00	0.00
			D93H	0.31	0.46	1.48
62	76/067	0200	D13H	0.27	0.98	3.63
			D93H	0.15	0.03	0.20
63	76/067	1400	D13H	0.34	0.47	1.38
			D93H	0.11	0.27	2.45
64	76/067	1500	D13H	0.32	0.80	2.50
65	76/067	1700	D13H	0.29	0.01	0.03
66	76/073	0200	D63H	0.26	0.68	2.62
			D83H	0.12	1.09	9.08
67	76/074	1300	D63H	0.25	0.01	0.04
			D83H	0.10	0.02	0.20
68	76/074	1900	D63H	0.29	0.01	0.03
			D83H	0.17	0.02	0.12
69	76/074	2000	D63H	0.28	0.19	0.68
			D83H	0.11	0.09	0.82
70	76/074	2400	D13H	0.16	1.78	11.13
			D93H	0.25	0.01	0.04
71	76/084	0200	D23H	0.30	1.09	3.63
72	76/084	0300	D23H	0.35	0.68	1.94
73	76/084	0400	D23H	0.30	0.48	1.60

TABLE 4-1 (Continued)

Case No.	Year/ Julian Day	Hour	Monitor	Observed Concentration (ppm)	Calculated Concentration (ppm)	Ratio of Calculated and Observed Concentrations
74	76/094	1800	D03H	0.26	0.47	1.81
75	76/094	2000	D03H	0.27	0.05	0.19
76	76/094	2300	D03H	0.59	0.09	0.15
77	76/095	0200	D03H	0.27	0.17	0.63
78	76/096	1600	D13H	0.30	0.00	0.00
			D93H	0.16	0.89	5.56
79	76/096	1700	D13H	0.60	1.17	1.95
			D93H	0.16	0.16	1.00
80	76/106	0200	D23H	0.64	0.63	0.98
81	76/107	1200	D63H	0.10	0.13	1.30
			D83H	0.26	1.39	5.35
82	76/109	1000	D23H	0.35	0.48	1.37
83	76/113	0600	D63H	0.15	0.14	0.93
			D83H	0.36	1.15	3.19
84	76/113	0700	D63H	0.21	0.42	2.00
			D83H	0.31	0.48	1.55
85	76/113	0800	D63H	0.25	0.54	2.16
			D83H	0.31	0.76	2.45
86	76/122	2200	D13H	0.25	0.55	2.20
87	76/124	1200	D13H	0.27	1.12	4.15
88	76/126	0200	D23H	0.29	0.26	0.90
89	76/164	2400	D63H	0.28	0.02	0.07
90	76/189	1800	D13H	0.30	0.00	0.00
			D93H	0.10	0.18	1.80
					Mean Ratio (MR)	1.42

TABLE 4-2

COMPARISON OF CALCULATED AND OBSERVED 1-HOUR SO_2 CONCENTRATIONS FOR THE DOW CASES FOR COMBINATION 5 IN TABLE 3-35 AND THE CRAMER, ET AL. (1975) STACK-TIP DOWNWASH CORRECTION FOR ALL STACKS

Case No.	Year/ Julian Day	Hour	Monitor	Observed Concentration (ppm)	Calculated Concentration (ppm)	Ratio of Calculated and Observed Concentrations
1	75/314	0100	D33H	0.36	0.24	0.67
			D63H	0.11	0.23	2.09
			D73H	0.12	0.16	1.33
2	75/314	0200	D33H	0.26	0.18	0.69
			D73H	0.13	0.11	0.85
3	75/314	0500	D63H	0.49	0.34	0.69
4	75/314	1300	D63H	0.14	0.11	0.79
			D83H	0.27	0.30	1.11
5	75/314	2300	D63H	0.28	0.03	0.11
			D83H	0.19	0.05	0.26
6	75/314	2400	D63H	0.30	0.04	0.13
			D83H	0.15	0.07	0.47
7	75/316	1700	D63H	0.12	0.13	1.08
			D83H	0.33	0.36	1.09
8	75/324	1200	D63H	0.39	0.25	0.64
9	75/324	1300	D63H	0.55	0.39	0.71
10	75/325	0800	D23H	0.27	0.28	1.04
11	75/326	1500	D63H	0.27	0.00	0.00
12	75/326	1600	D63H	0.30	0.00	0.00
			D83H	0.13	0.18	1.38
13	75/335	0400	D63H	0.30	0.01	0.03
			D83H	0.12	0.06	0.50
14	75/350	1500	D23H	0.38	0.02	0.05
			D33H	0.12	0.03	0.25
15	75/350	1900	D23H	0.30	0.04	0.13
16	75/350	2000	D23H	0.27	0.38	1.41
17	75/350	2100	D23H	0.29	0.43	1.48
			D33H	0.10	0.10	1.00
18	75/351	0400	D13H	0.28	1.19	4.25
			D93H	0.23	0.01	0.04
19	75/351	0700	D13H	0.14	1.22	8.71
			D93H	0.25	0.12	0.48
20	75/351	1000	D13H	0.35	0.95	2.71
21	75/352	1100	D13H	0.25	0.93	3.72
			D83H	0.11	0.00	0.00
22	75/352	1300	D13H	0.31	0.58	1.87
23	75/354	1200	D53H	0.25	0.04	0.16

TABLE 4-2 (Continued)

Case No.	Year/ Julian Day	Hour	Monitor	Observed Concentration (ppm)	Calculated Concentration (ppm)	Ratio of Calculated and Observed Concentrations
24	75/354	1300	D03H	0.36	0.00	0.00
			D53H	0.10	0.08	0.80
25	75/354	1400	D03H	0.65	0.04	0.06
26	75/354	1600	D03H	0.49	0.03	0.06
27	75/354	1700	D03H	0.44	0.10	0.23
28	75/354	2400	D53H	0.35	0.25	0.71
29	76/003	0100	D63H	0.26	0.03	0.12
			D83H	0.23	0.08	0.35
30	76/003	1100	D63H	0.28	0.39	1.39
			D83H	0.20	0.61	3.05
31	76/005	1300	D23H	0.30	0.37	1.23
32	76/008	1600	D63H	0.27	0.01	0.04
			D83H	0.14	0.12	0.86
33	76/008	1700	D63H	0.30	0.12	0.40
			D83H	0.10	0.08	0.80
34	76/014	0300	D13H	0.37	1.65	4.46
			D93H	0.20	0.09	0.45
35	76/014	0400	D13H	0.26	1.63	6.27
			D93H	0.21	0.07	0.33
36	76/014	0500	D13H	0.33	0.46	1.39
			D93H	0.18	0.00	0.00
37	76/014	0600	D13H	0.50	1.15	2.30
38	76/014	0700	D13H	0.59	1.19	2.02
			D93H	0.30	0.00	0.00
39	76/014	0800	D93H	0.34	0.09	0.26
40	76/014	2100	D13H	0.21	0.42	2.00
			D93H	0.48	0.51	1.06
41	76/014	2200	D13H	0.33	1.43	4.33
			D93H	0.21	0.13	0.62
42	76/028	1600	D23H	0.32	0.25	0.78
43	76/028	1700	D23H	0.44	0.16	0.36
			D33H	0.19	0.23	1.21
44	76/038	2400	D63H	0.47	0.24	0.51
			D83H	0.15	0.14	0.93
45	76/039	0100	D63H	0.45	0.14	0.31
			D83H	0.18	0.07	0.39
46	76/039	0200	D63H	0.47	0.11	0.23
			D83H	0.16	0.06	0.38
47	76/042	1200	D13H	0.40	0.66	1.65
			D93H	0.16	0.02	0.13
48	76/043	0900	D33H	0.26	0.19	0.73

TABLE 4-2 (Continued)

Case No.	Year/ Julian Day	Hour	Monitor	Observed Concentration (ppm)	Calculated Concentration (ppm)	Ratio of Calculated and Observed Concentrations
49	76/046	1700	D23H	0.22	0.05	0.23
			D63H	0.29	0.42	1.45
50	76/046	1800	D63H	0.81	0.22	0.27
			D83H	0.23	0.12	0.52
51	76/046	1900	D63H	0.42	0.05	0.12
			D83H	0.18	0.04	0.22
52	76/049	1700	D63H	0.40	0.29	0.73
			D83H	0.15	0.30	2.00
53	76/049	1800	D63H	0.29	0.15	0.52
			D83H	0.15	0.08	0.53
54	76/049	1900	D63H	0.28	0.06	0.21
			D83H	0.16	0.04	0.25
55	76/052	1300	D03H	0.39	0.02	0.05
56	76/052	1500	D03H	0.28	0.06	0.21
57	76/052	1600	D03H	0.29	0.03	0.10
58	76/065	1000	D63H	0.11	0.13	1.18
			D83H	0.34	0.47	1.38
59	76/065	1100	D83H	0.29	0.29	1.00
60	76/065	1500	D63H	0.12	0.08	0.67
			D83H	0.26	0.20	0.77
61	76/066	2400	D13H	0.12	0.01	0.08
			D93H	0.31	0.31	1.00
62	76/067	0200	D13H	0.27	0.60	2.22
			D93H	0.15	0.05	0.33
63	76/067	1400	D13H	0.34	0.38	1.12
			D93H	0.11	0.14	1.27
64	76/067	1500	D13H	0.32	0.46	1.44
65	76/067	1700	D13H	0.29	0.05	0.17
66	76/073	0200	D63H	0.26	0.34	1.31
			D83H	0.12	0.58	4.83
67	76/074	1300	D63H	0.25	0.06	0.24
			D83H	0.10	0.07	0.70
68	76/074	1900	D63H	0.29	0.05	0.17
			D83H	0.17	0.07	0.41
69	76/074	2000	D63H	0.28	0.19	0.68
			D83H	0.11	0.21	1.91
70	76/074	2400	D13H	0.16	1.05	6.56
			D93H	0.25	0.03	0.12
71	76/084	0200	D23H	0.30	0.47	1.57
72	76/084	0300	D23H	0.35	0.28	0.80
73	76/084	0400	D23H	0.30	0.24	0.80

TABLE 4-2 (Continued)

Case No.	Year/ Julian Day	Hour	Monitor	Observed Concentration (ppm)	Calculated Concentration (ppm)	Ratio of Calculated and Observed Concentrations
74	76/094	1800	D03H	0.26	0.28	1.08
75	76/094	2000	D03H	0.27	0.11	0.41
76	76/094	2300	D03H	0.59	0.15	0.25
77	76/095	0200	D03H	0.27	0.16	0.59
78	76/096	1600	D13H	0.30	0.06	0.20
			D93H	0.16	0.46	2.88
79	76/096	1700	D13H	0.60	1.08	1.80
			D93H	0.16	0.19	1.19
80	76/106	0200	D23H	0.64	0.26	0.41
81	76/107	1200	D63H	0.10	0.16	1.60
			D83H	0.26	0.70	2.69
82	76/109	1000	D23H	0.35	0.26	0.74
83	76/113	0600	D63H	0.15	0.15	1.00
			D83H	0.36	0.69	1.92
84	76/113	0700	D63H	0.21	0.24	1.14
			D83H	0.31	0.49	1.58
85	76/113	0800	D63H	0.25	0.28	1.12
			D83H	0.31	0.63	2.03
86	76/122	2200	D13H	0.25	0.82	3.28
87	76/124	1200	D13H	0.27	0.76	2.81
88	76/126	0200	D23H	0.29	0.12	0.41
89	76/164	2400	D63H	0.28	0.13	0.46
90	76/189	1800	D13H	0.30	0.01	0.03
			D93H	0.10	0.19	1.90
					Mean Ratio (MR)	1.02

TABLE 4-3

COMPARISON OF CALCULATED AND OBSERVED 1-HOUR SO_2 CONCENTRATIONS FOR THE DOW CASES FOR COMBINATION 2 IN TABLE 3-35 AND THE CRAMER, ET AL. (1975) STACK-TIP DOWNWASH CORRECTION FOR STACKS WITH FROUDE NUMBERS ABOVE 3.0

Case No.	Year/ Julian Day	Hour	Monitor	Observed Concentration (ppm)	Calculated Concentration (ppm)	Ratio of Calculated and Observed Concentrations
1	75/314	0100	D33H	0.36	0.28	0.78
			D63H	0.11	0.01	0.09
			D73H	0.12	0.14	1.17
2	75/314	0200	D33H	0.26	0.20	0.77
			D73H	0.13	0.08	0.62
3	75/314	0500	D63H	0.49	0.05	0.10
4	75/314	1300	D63H	0.14	0.20	1.43
			D83H	0.27	0.59	2.19
5	75/314	2300	D63H	0.28	0.00	0.00
			D83H	0.19	0.00	0.00
6	75/314	2400	D63H	0.30	0.01	0.03
			D83H	0.15	0.00	0.00
7	75/316	1700	D63H	0.12	0.05	0.42
			D83H	0.33	0.14	0.42
8	75/324	1200	D63H	0.39	0.09	0.23
9	75/324	1300	D63H	0.55	0.27	0.49
10	75/325	0800	D23H	0.27	0.49	1.81
11	75/326	1500	D63H	0.27	0.00	0.00
12	75/326	1600	D63H	0.30	0.00	0.00
			D83H	0.13	0.23	1.77
13	75/335	0400	D63H	0.30	0.00	0.00
			D83H	0.12	0.05	0.42
14	75/350	1500	D23H	0.38	0.00	0.00
			D33H	0.12	0.00	0.00
15	75/350	1900	D23H	0.30	0.00	0.00
16	75/350	2000	D23H	0.27	0.61	2.26
17	75/350	2100	D23H	0.29	0.71	2.45
			D33H	0.10	0.11	1.10
18	75/351	0400	D13H	0.28	0.57	2.04
			D93H	0.23	0.00	0.00
19	75/351	0700	D13H	0.14	1.17	8.36
			D93H	0.25	0.05	0.20
20	75/351	1000	D13H	0.35	0.13	0.37
21	75/352	1100	D13H	0.25	0.04	0.16
			D83H	0.11	0.00	0.00
22	75/352	1300	D13H	0.31	0.02	0.06
23	75/354	1200	D53H	0.25	0.00	0.00

TABLE 4-3 (Continued)

Case No.	Year/ Julian Day	Hour	Monitor	Observed Concentration (ppm)	Calculated Concentration (ppm)	Ratio of Calculated and Observed Concentrations
24	75/354	1300	D03H	0.36	0.00	0.00
			D53H	0.10	0.02	0.20
25	75/354	1400	D03H	0.65	0.00	0.00
26	75/354	1600	D03H	0.49	0.00	0.00
27	75/354	1700	D03H	0.44	0.02	0.05
28	75/354	2400	D53H	0.35	0.18	0.51
29	76/003	0100	D63H	0.26	0.00	0.00
			D83H	0.23	0.07	0.30
30	76/003	1100	D63H	0.28	0.74	2.64
			D83H	0.20	0.09	0.45
31	76/005	1300	D23H	0.30	0.15	0.50
32	76/008	1600	D63H	0.27	0.00	0.00
			D83H	0.14	0.28	2.00
33	76/008	1700	D63H	0.30	0.03	0.10
			D83H	0.10	0.02	0.20
34	76/014	0300	D13H	0.37	0.54	1.46
			D93H	0.20	0.02	0.10
35	76/014	0400	D13H	0.26	0.42	1.62
			D93H	0.21	0.01	0.05
36	76/014	0500	D13H	0.33	0.02	0.06
			D93H	0.18	0.00	0.00
37	76/014	0600	D13H	0.50	0.08	0.16
38	76/014	0700	D13H	0.59	0.09	0.15
			D93H	0.30	0.00	0.00
39	76/014	0800	D93H	0.34	0.02	0.06
40	76/014	2100	D13H	0.21	0.14	0.67
			D93H	0.48	0.79	1.65
41	76/014	2200	D13H	0.33	1.35	4.09
			D93H	0.21	0.06	0.29
42	76/028	1600	D23H	0.32	0.22	0.69
43	76/028	1700	D23H	0.44	0.14	0.32
			D33H	0.19	0.46	2.42
44	76/038	2400	D63H	0.47	0.30	0.64
			D83H	0.15	0.08	0.53
45	76/039	0100	D63H	0.45	0.08	0.18
			D83H	0.18	0.01	0.06
46	76/039	0200	D63H	0.47	0.04	0.09
			D83H	0.16	0.01	0.06
47	76/042	1200	D13H	0.40	1.04	2.60
			D93H	0.16	0.00	0.00
48	76/043	0900	D33H	0.26	0.43	1.65

TABLE 4-3 (Continued)

Case No.	Year/ Julian Day	Hour	Monitor	Observed Concentration (ppm)	Calculated Concentration (ppm)	Ratio of Calculated and Observed Concentrations
49	76/046	1700	D23H	0.22	0.04	0.18
			D63H	0.29	0.69	2.38
50	76/046	1800	D63H	0.81	0.28	0.35
			D83H	0.23	0.07	0.30
51	76/046	1900	D63H	0.42	0.01	0.02
			D83H	0.18	0.01	0.06
52	76/049	1700	D63H	0.40	0.41	1.03
			D83H	0.15	0.52	3.47
53	76/049	1800	D63H	0.29	0.07	0.24
			D83H	0.15	0.01	0.07
54	76/049	1900	D63H	0.28	0.01	0.04
			D83H	0.16	0.00	0.00
55	76/052	1300	D03H	0.39	0.00	0.00
56	76/052	1500	D03H	0.28	0.02	0.07
57	76/052	1600	D03H	0.29	0.01	0.03
58	76/065	1000	D63H	0.11	0.17	1.55
			D83H	0.34	0.36	1.06
59	76/065	1100	D83H	0.29	0.49	1.69
60	76/065	1500	D63H	0.12	0.11	0.92
			D83H	0.26	0.21	0.81
61	76/066	2400	D13H	0.12	0.00	0.00
			D93H	0.31	0.35	1.13
62	76/067	0200	D13H	0.27	0.41	1.52
			D93H	0.15	0.02	0.13
63	76/067	1400	D13H	0.34	0.36	1.06
			D93H	0.11	0.23	2.09
64	76/067	1500	D13H	0.32	0.57	1.78
65	76/067	1700	D13H	0.29	0.00	0.00
66	76/073	0200	D63H	0.26	0.67	2.58
			D83H	0.12	0.98	8.17
67	76/074	1300	D63H	0.25	0.01	0.04
			D83H	0.10	0.02	0.20
68	76/074	1900	D63H	0.29	0.01	0.03
			D83H	0.17	0.02	0.12
69	76/074	2000	D63H	0.28	0.05	0.18
			D83H	0.11	0.09	0.82
70	76/074	2400	D13H	0.16	1.72	10.75
			D93H	0.25	0.01	0.04
71	76/084	0200	D23H	0.30	1.09	3.63
72	76/084	0300	D23H	0.35	0.68	1.94
73	76/084	0400	D23H	0.30	0.48	1.60

TABLE 4-3 (Continued)

Case No.	Year/ Julian Day	Hour	Monitor	Observed Concentration (ppm)	Calculated Concentration (ppm)	Ratio of Calculated and Observed Concentrations
74	76/094	1800	D03H	0.26	0.39	1.50
75	76/094	2000	D03H	0.27	0.04	0.15
76	76/094	2300	D03H	0.59	0.07	0.12
77	76/095	0200	D03H	0.27	0.16	0.59
78	76/096	1600	D13H	0.30	0.00	0.00
			D93H	0.16	0.61	3.81
79	76/096	1700	D13H	0.60	0.66	1.10
			D93H	0.16	0.10	0.63
80	76/106	0200	D23H	0.64	0.60	0.94
81	76/107	1200	D63H	0.10	0.13	1.30
			D83H	0.26	1.18	4.54
82	76/109	1000	D23H	0.35	0.45	1.29
83	76/113	0600	D63H	0.15	0.04	0.27
			D83H	0.36	0.90	2.50
84	76/113	0700	D63H	0.21	0.12	0.57
			D83H	0.31	0.35	1.13
85	76/113	0800	D63H	0.25	0.13	0.52
			D83H	0.31	0.54	1.74
86	76/122	2200	D13H	0.25	0.26	1.04
87	76/124	1200	D13H	0.27	0.25	0.93
88	76/126	0200	D23H	0.29	0.18	0.62
89	76/164	2400	D63H	0.28	0.00	0.00
90	76/189	1800	D13H	0.30	0.00	0.00
			D93H	0.10	0.17	1.70
					Mean Ratio (MR)	0.83

TABLE 4-4

COMPARISON OF CALCULATED AND OBSERVED 1-HOUR SO_2 CONCENTRATIONS FOR THE DOW CASES FOR COMBINATION 5 IN TABLE 3-35 AND THE CRAMER *ET AL.* (1975) STACK-TIP DOWNWASH CORRECTION FOR STACKS WITH FROUDE NUMBERS ABOVE 3.0

Case No.	Year/ Julian Day	Hour	Monitor	Observed Concentration (ppm)	Calculated Concentration (ppm)	Ratio of Calculated and Observed Concentrations
1	75/314	0100	D33H	0.36	0.21	0.58
			D63H	0.11	0.12	1.09
			D73H	0.12	0.16	1.33
2	75/314	0200	D33H	0.26	0.16	0.62
			D73H	0.13	0.11	0.85
3	75/314	0500	D63H	0.49	0.20	0.41
4	75/314	1300	D63H	0.14	0.11	0.79
			D83H	0.27	0.30	1.11
5	75/314	2300	D63H	0.28	0.03	0.11
			D83H	0.19	0.04	0.21
6	75/314	2400	D63H	0.30	0.04	0.13
			D83H	0.15	0.04	0.27
7	75/316	1700	D63H	0.12	0.12	1.00
			D83H	0.33	0.31	0.94
8	75/324	1200	D63H	0.39	0.25	0.64
9	75/324	1300	D63H	0.55	0.39	0.71
10	75/325	0800	D23H	0.27	0.28	1.04
11	75/326	1500	D63H	0.27	0.00	0.00
12	75/326	1600	D63H	0.30	0.00	0.00
			D83H	0.13	0.18	1.38
13	75/335	1400	D63H	0.30	0.01	0.03
			D83H	0.12	0.06	0.50
14	75/350	1500	D23H	0.38	0.02	0.05
			D33H	0.12	0.03	0.25
15	75/350	1900	D23H	0.30	0.04	0.13
16	75/350	2000	D23H	0.27	0.36	1.33
17	75/350	2100	D23H	0.29	0.40	1.38
			D33H	0.10	0.10	1.00
18	75/351	0400	D13H	0.28	0.85	3.04
			D93H	0.23	0.01	0.04
19	75/351	0700	D13H	0.14	1.02	7.29
			D93H	0.25	0.12	0.48
20	75/351	1000	D13H	0.35	0.48	1.37
21	75/352	1100	D13H	0.25	0.21	0.84
			D83H	0.11	0.00	0.00
22	75/352	1300	D13H	0.31	0.15	0.48
23	75/354	1200	D53H	0.25	0.03	0.12

TABLE 4-4 (Continued)

Case No.	Year/ Julian Day	Hour	Monitor	Observed Concentration (ppm)	Calculated Concentration (ppm)	Ratio of Calculated and Observed Concentrations
24	75/354	1300	D03H	0.36	0.00	0.00
			D53H	0.10	0.07	0.70
25	75/354	1400	D03H	0.65	0.04	0.06
26	75/354	1600	D03H	0.49	0.03	0.06
27	75/354	1700	D03H	0.44	0.07	0.16
28	75/354	2400	D53H	0.35	0.24	0.69
29	76/003	0100	D63H	0.26	0.03	0.12
			D83H	0.23	0.07	0.30
30	76/003	1100	D63H	0.28	0.39	1.39
			D83H	0.20	0.26	1.30
31	76/005	1300	D23H	0.30	0.25	0.83
32	76/008	1600	D63H	0.27	0.01	0.04
			D83H	0.14	0.12	0.86
33	76/008	1700	D63H	0.30	0.12	0.40
			D83H	0.10	0.06	0.60
34	76/014	3000	D93H	0.37	0.61	1.65
			D93H	0.20	0.08	0.40
35	76/014	0400	D13H	0.26	0.60	2.31
			D93H	0.21	0.05	0.24
36	76/014	0500	D13H	0.33	0.16	0.48
			D93H	0.18	0.00	0.00
37	76/014	0600	D13H	0.50	0.35	0.70
38	76/014	0700	D13H	0.59	0.36	0.61
			D93H	0.30	0.00	0.00
39	76/014	0800	D93H	0.34	0.08	0.24
40	76/014	2100	D13H	0.21	0.33	1.57
			D93H	0.48	0.48	1.00
41	76/014	2200	D13H	0.33	1.16	3.52
			D93H	0.21	0.12	0.57
42	76/028	1600	D23H	0.32	0.20	0.63
43	76/028	1700	D23H	0.44	0.12	0.27
			D33H	0.19	0.22	1.16
44	76/038	2400	D63H	0.47	0.24	0.51
			D83H	0.15	0.14	0.93
45	76/039	0100	D63H	0.45	0.13	0.29
			D83H	0.18	0.07	0.39
46	76/039	0200	D63H	0.47	0.11	0.23
			D83H	0.16	0.06	0.38
47	76/042	1200	D13H	0.40	0.63	1.58
			D93H	0.16	0.02	0.13
48	76/043	0900	D33H	0.26	0.19	0.73

TABLE 4-4 (Continued)

Case No.	Year/ Julian Day	Hour	Monitor	Observed Concentration (ppm)	Calculated Concentration (ppm)	Ratio of Calculated and Observed Concentrations
49	76/046	1700	D23H	0.22	0.05	0.23
			D63H	0.29	0.42	1.45
50	76/046	1800	D63H	0.81	0.22	0.27
			D83H	0.23	0.11	0.48
51	76/046	1900	D63H	0.42	0.04	0.10
			D83H	0.18	0.04	0.22
52	76/049	1700	D63H	0.40	0.29	0.73
			D83H	0.15	0.29	1.93
53	76/049	1800	D63H	0.29	0.12	0.41
			D83H	0.15	0.05	0.33
54	76/049	1900	D63H	0.28	0.05	0.18
			D83H	0.16	0.03	0.19
55	76/052	1300	D03H	0.39	0.02	0.05
56	76/052	1500	D03H	0.28	0.04	0.14
57	76/052	1600	D03H	0.29	0.02	0.07
58	76/065	1000	D63H	0.11	0.11	1.00
			D83H	0.34	0.34	1.00
59	76/065	1100	D83H	0.29	0.29	1.00
60	76/065	1500	D63H	0.12	0.07	0.58
			D83H	0.26	0.20	0.77
61	76/066	2400	D13H	0.12	0.01	0.08
			D93H	0.31	0.29	0.94
62	76/067	0200	D13H	0.27	0.39	1.44
			D93H	0.15	0.04	0.27
63	76/067	1400	D13H	0.34	0.29	0.85
			D93H	0.11	0.13	1.18
64	76/067	1500	D13H	0.32	0.38	1.19
65	76/067	1700	D13H	0.29	0.04	0.14
66	76/073	0200	D63H	0.26	0.34	1.31
			D83H	0.12	0.54	4.50
67	76/074	1300	D63H	0.25	0.06	0.24
			D83H	0.10	0.07	0.70
68	76/074	1900	D63H	0.29	0.05	0.17
			D83H	0.17	0.07	0.41
69	76/074	2000	D63H	0.28	0.12	0.43
			D83H	0.11	0.21	1.91
70	76/074	2400	D13H	0.16	1.04	6.50
			D93H	0.25	0.03	0.12
71	76/084	0200	D23H	0.30	0.47	1.57
72	76/084	0300	D23H	0.35	0.28	0.80
73	76/084	0400	D23H	0.30	0.24	0.80

TABLE 4-4 (Continued)

Case No.	Year/ Julian Day	Hour	Monitor	Observed Concentration (ppm)	Calculated Concentration (ppm)	Ratio of Calculated and Observed Concentrations
74	76/094	1800	D03H	0.26	0.27	1.04
75	76/094	2000	D03H	0.27	0.10	0.37
76	76/094	2300	D03H	0.59	0.14	0.24
77	76/095	0200	D03H	0.27	0.16	0.59
78	76/096	1600	D13H	0.30	0.05	0.17
			D93H	0.16	0.43	2.69
79	76/096	1700	D13H	0.60	0.85	1.42
			D93H	0.16	0.17	1.06
80	76/106	0200	D23H	0.64	0.25	0.39
81	76/107	1200	D63H	0.10	0.16	1.60
			D83H	0.26	0.65	2.50
82	76/109	1000	D23H	0.35	0.25	0.71
83	76/113	0600	D63H	0.15	0.10	0.67
			D83H	0.36	0.62	1.72
84	76/113	0700	D63H	0.21	0.17	0.81
			D83H	0.31	0.43	1.39
85	76/113	0800	D63H	0.25	0.19	0.76
			D83H	0.31	0.54	1.74
86	76/122	2200	D13H	0.25	0.58	2.32
87	76/124	1200	D13H	0.27	0.40	1.48
88	76/126	0200	D23H	0.29	0.10	0.34
89	76/164	2400	D63H	0.28	0.07	0.25
90	76/189	1800	D13H	0.30	0.01	0.03
			D93H	0.10	0.18	1.80
					Mean Ratio (MR)	0.76

TABLE 4-5

COMPARISON OF CALCULATED AND OBSERVED 1-HOUR SO_2 CONCENTRATIONS FOR THE DOW CASES FOR COMBINATION 2 IN TABLE 3-35 AND THE SCIRE AND SCHULMAN (1980) "DOWNWASH RADIUS" CORRECTION

Case No.	Year/ Julian Day	Hour	Monitor	Observed Concentration (ppm)	Calculated Concentration (ppm)	Ratio of Calculated and Observed Concentrations
1	75/314	0100	D33H	0.36	0.55	1.53
			D63H	0.11	0.00	0.00
			D73H	0.12	0.37	3.08
2	75/314	0200	D33H	0.26	0.36	1.38
			D73H	0.13	0.17	1.31
3	75/314	0500	D63H	0.49	0.16	0.33
4	75/314	1300	D63H	0.14	0.19	1.36
			D83H	0.27	0.53	1.96
5	75/314	2300	D63H	0.28	0.01	0.04
			D83H	0.19	0.01	0.05
6	75/314	2400	D63H	0.30	0.01	0.03
			D83H	0.15	0.01	0.07
7	75/316	1700	D63H	0.12	0.15	1.25
			D83H	0.33	0.10	0.30
8	75/324	1200	D63H	0.39	0.03	0.08
9	75/324	1300	D63H	0.55	0.12	0.22
10	75/325	0800	D23H	0.27	0.35	1.30
11	75/326	1500	D63H	0.27	0.00	0.00
12	75/326	1600	D63H	0.30	0.00	0.00
			D83H	0.13	0.46	3.54
13	75/335	0400	D63H	0.30	0.00	0.00
			D83H	0.12	0.09	0.75
14	75/350	1500	D23H	0.38	0.00	0.00
			D33H	0.12	0.00	0.00
15	75/350	1900	D23H	0.30	0.00	0.00
16	75/350	2000	D23H	0.27	0.49	1.81
17	75/350	2100	D23H	0.29	0.65	2.24
			D33H	0.10	0.23	2.30
18	75/351	0400	D13H	0.28	0.73	2.61
			D93H	0.23	0.00	0.00
19	75/351	0700	D13H	0.14	0.79	5.64
			D93H	0.25	0.06	0.24
20	75/351	1000	D13H	0.35	0.63	1.80
21	75/352	1100	D13H	0.25	0.41	1.64
			D83H	0.11	0.00	0.00
22	75/352	1300	D13H	0.31	0.15	0.48
23	75/354	1200	D53H	0.25	0.01	0.04

TABLE 4-5 (Continued)

Case No.	Year/ Julian Day	Hour	Monitor	Observed Concentration (ppm)	Calculated Concentration (ppm)	Ratio of Calculated and Observed Concentrations
24	75/354	1300	D03H	0.36	0.00	0.00
			D53H	0.10	0.04	0.40
25	75/354	1400	D03H	0.65	0.00	0.00
26	75/354	1600	D03H	0.49	0.00	0.00
27	75/354	1700	D03H	0.44	0.04	0.09
28	75/354	2400	D53H	0.35	0.45	1.29
29	76/003	0100	D63H	0.26	0.00	0.00
			D83H	0.23	0.06	0.26
30	76/003	1100	D63H	0.28	0.46	1.64
			D83H	0.20	0.46	2.30
31	76/005	1300	D23H	0.30	0.44	1.47
32	76/008	1600	D63H	0.27	0.00	0.00
			D83H	0.14	0.23	1.64
33	76/008	1700	D63H	0.30	0.02	0.07
			D83H	0.10	0.01	0.10
34	76/014	0300	D13H	0.37	1.32	3.57
			D93H	0.20	0.03	0.15
35	76/014	0400	D13H	0.26	1.27	4.88
			D93H	0.21	0.01	0.05
36	76/014	0500	D13H	0.33	0.09	0.27
			D93H	0.18	0.00	0.00
37	76/014	0600	D13H	0.50	0.47	0.94
38	76/014	0700	D13H	0.59	0.49	0.83
			D93H	0.30	0.00	0.00
39	76/014	0800	D93H	0.34	0.03	0.09
40	76/014	2100	D13H	0.21	0.16	0.76
			D93H	0.48	0.81	1.69
41	76/014	2200	D13H	0.33	1.18	3.58
			D93H	0.21	0.06	0.29
42	76/028	1600	D23H	0.32	0.47	1.47
43	76/028	1700	D23H	0.44	0.30	0.68
			D33H	0.19	0.41	2.16
44	76/038	2400	D63H	0.47	0.21	0.45
			D83H	0.15	0.04	0.27
45	76/039	0100	D63H	0.45	0.05	0.11
			D83H	0.18	0.01	0.06
46	76/039	0200	D63H	0.47	0.03	0.06
			D83H	0.16	0.01	0.06
47	76/042	1200	D13H	0.40	0.70	1.75
			D93H	0.16	0.00	0.00
48	76/043	0900	D33H	0.26	0.35	1.35

TABLE 4-5 (Continued)

Case No.	Year/ Julian Day	Hour	Monitor	Observed Concentration (ppm)	Calculated Concentration (ppm)	Ratio of Calculated and Observed Concentrations
49	76/046	1700	D23H	0.22	0.03	0.14
			D63H	0.29	0.61	2.10
50	76/046	1800	D63H	0.81	0.23	0.28
			D83H	0.23	0.05	0.22
51	76/046	1900	D63H	0.42	0.01	0.02
			D83H	0.18	0.01	0.06
52	76/049	1700	D63H	0.40	0.33	0.83
			D83H	0.15	0.36	2.40
53	76/049	1800	D63H	0.29	0.13	0.45
			D83H	0.15	0.02	0.13
54	76/049	1900	D63H	0.28	0.02	0.07
			D83H	0.16	0.01	0.06
55	76/052	1300	D03H	0.39	0.00	0.00
56	76/052	1500	D03H	0.28	0.06	0.21
57	76/052	1600	D03H	0.29	0.02	0.07
58	76/065	1000	D63H	0.11	0.23	2.09
			D83H	0.34	0.80	2.35
59	76/065	1100	D83H	0.29	0.44	1.52
60	76/065	1500	D63H	0.12	0.13	1.08
			D83H	0.26	0.18	0.69
61	76/066	2400	D13H	0.12	0.00	0.00
			D93H	0.31	0.30	0.97
62	76/067	0200	D13H	0.27	0.74	2.74
			D93H	0.15	0.03	0.20
63	76/067	1400	D13H	0.34	0.37	1.09
			D93H	0.11	0.23	2.09
64	76/067	1500	D13H	0.32	0.63	1.97
65	76/067	1700	D13H	0.29	0.00	0.00
66	76/073	0200	D63H	0.26	0.48	1.85
			D83H	0.12	0.57	4.75
67	76/074	1300	D63H	0.25	0.01	0.04
			D83H	0.10	0.02	0.20
68	76/074	1900	D63H	0.29	0.01	0.03
			D83H	0.17	0.02	0.12
69	76/074	2000	D63H	0.28	0.14	0.50
			D83H	0.11	0.04	0.36
70	76/074	2400	D13H	0.16	0.86	5.38
			D93H	0.25	0.01	0.04
71	76/084	0200	D23H	0.30	0.71	2.37
72	76/084	0300	D23H	0.35	0.45	1.29
73	76/084	0400	D23H	0.30	0.32	1.07

TABLE 4-5 (Continued)

Case No.	Year/ Julian Day	Hour	Monitor	Observed Concentration (ppm)	Calculated Concentration (ppm)	Ratio of Calculated and Observed Concentrations
74	76/094	1800	D03H	0.26	0.41	1.58
75	76/094	2000	D03H	0.27	0.04	0.15
76	76/094	2300	D03H	0.59	0.08	0.14
77	76/095	0200	D03H	0.27	0.13	0.48
78	76/096	1600	D13H	0.30	0.00	0.00
			D93H	0.16	0.69	4.31
79	76/096	1700	D13H	0.60	0.74	1.23
			D93H	0.16	0.13	0.81
80	76/106	0200	D23H	0.64	0.46	0.72
81	76/107	1200	D63H	0.10	0.34	3.40
			D83H	0.26	0.85	3.27
82	76/109	1000	D23H	0.35	0.31	0.89
83	76/113	0600	D63H	0.15	0.11	0.73
			D83H	0.36	0.73	2.03
84	76/113	0700	D63H	0.21	0.32	1.52
			D83H	0.31	0.30	0.97
85	76/113	0800	D63H	0.25	0.39	1.56
			D83H	0.31	0.42	1.35
86	76/122	2200	D13H	0.25	0.48	1.92
87	76/124	1200	D13H	0.27	0.73	2.70
88	76/126	0200	D23H	0.29	0.23	0.79
89	76/164	2400	D63H	0.28	0.02	0.07
90	76/189	1800	D13H	0.30	0.00	0.00
			D93H	0.10	0.14	1.40
					Mean Ratio (MR)	0.92

TABLE 4-6

COMPARISON OF CALCULATED AND OBSERVED 1-HOUR SO_2 CONCENTRATIONS FOR THE DOW CASES FOR COMBINATION 5 IN TABLE 3-35 AND THE SCIRE AND SCHULMAN (1980) "DOWNWASH RADIUS" CORRECTION

Case No.	Year/ Julian Day	Hour	Monitor	Observed Concentration (ppm)	Calculated Concentration (ppm)	Ratio of Calculated and Observed Concentrations
1	75/314	0100	D33H	0.36	0.24	0.67
			D63H	0.11	0.20	1.82
			D73H	0.12	0.21	1.75
2	75/314	0200	D33H	0.26	0.18	0.69
			D73H	0.13	0.14	1.08
3	75/314	0500	D63H	0.49	0.31	0.63
4	75/314	1300	D63H	0.14	0.11	0.79
			D83H	0.27	0.29	1.07
5	75/314	2300	D63H	0.28	0.04	0.14
			D83H	0.19	0.05	0.26
6	75/314	2400	D63H	0.30	0.05	0.17
			D83H	0.15	0.06	0.40
7	75/316	1700	D63H	0.12	0.17	1.42
			D83H	0.33	0.29	0.88
8	75/324	1200	D63H	0.39	0.17	0.44
9	75/324	1300	D63H	0.55	0.28	0.51
10	75/325	0800	D23H	0.27	0.26	0.96
11	75/326	1500	D63H	0.27	0.00	0.00
12	75/326	1600	D63H	0.30	0.00	0.00
			D83H	0.13	0.20	1.54
13	75/335	0400	D63H	0.30	0.01	0.03
			D83H	0.12	0.06	0.50
14	75/350	1500	D23H	0.38	0.02	0.05
			D33H	0.12	0.03	0.25
15	75/350	1900	D23H	0.30	0.04	0.13
16	75/350	2000	D23H	0.27	0.35	1.30
17	75/350	2100	D23H	0.29	0.40	1.37
			D33H	0.10	0.11	1.10
18	75/351	0400	D13H	0.28	0.93	3.32
			D93H	0.23	0.01	0.04
19	75/351	0700	D13H	0.14	0.85	6.07
			D93H	0.25	0.11	0.44
20	75/351	1000	D13H	0.35	0.91	2.60
21	75/352	1100	D13H	0.25	0.58	2.32
			D83H	0.11	0.00	0.00
22	75/352	1300	D13H	0.31	0.39	1.26
23	75/354	1200	D53H	0.25	0.04	0.16

TABLE 4-6 (Continued)

Case No.	Year/ Julian Day	Hour	Monitor	Observed Concentration (ppm)	Calculated Concentration (ppm)	Ratio of Calculated and Observed Concentrations
24	75/354	1300	D03H	0.36	0.00	0.00
			D53H	0.10	0.08	0.80
25	75/354	1400	D03H	0.65	0.04	0.06
26	75/354	1600	D03H	0.49	0.03	0.06
27	75/354	1700	D03H	0.44	0.09	0.20
28	75/354	2400	D53H	0.35	0.31	0.89
29	76/003	0100	D63H	0.26	0.03	0.12
			D83H	0.23	0.08	0.35
30	76/003	1100	D63H	0.28	0.34	1.21
			D83H	0.20	0.45	2.25
31	76/005	1300	D23H	0.30	0.33	1.10
32	76/008	1600	D63H	0.27	0.01	0.04
			D83H	0.14	0.12	0.86
33	76/008	1700	D63H	0.30	0.11	0.37
			D83H	0.10	0.07	0.70
34	76/014	0300	D13H	0.37	1.16	3.14
			D93H	0.20	0.09	0.45
35	76/014	0400	D13H	0.26	1.19	4.58
			D93H	0.21	0.06	0.29
36	76/014	0500	D13H	0.33	0.34	1.03
			D93H	0.18	0.00	0.00
37	76/014	0600	D13H	0.50	0.79	1.58
38	76/014	0700	D13H	0.59	0.78	1.32
			D93H	0.30	0.00	0.00
39	76/014	0800	D93H	0.34	0.09	0.26
40	76/014	2100	D13H	0.21	0.34	1.62
			D93H	0.48	0.48	1.00
41	76/014	2200	D13H	0.33	1.08	3.27
			D93H	0.21	0.12	0.57
42	76/028	1600	D23H	0.32	0.24	0.75
43	76/028	1700	D23H	0.44	0.15	0.34
			D33H	0.19	0.22	1.16
44	76/038	2400	D63H	0.47	0.22	0.47
			D83H	0.15	0.11	0.73
45	76/039	0100	D63H	0.45	0.12	0.27
			D83H	0.18	0.06	0.33
46	76/039	0200	D63H	0.47	0.10	0.21
			D83H	0.16	0.05	0.31
47	76/042	1200	D13H	0.40	0.53	1.33
			D93H	0.16	0.02	0.13
48	76/043	0900	D33H	0.26	0.18	0.69

TABLE 4-6 (Continued)

Case No.	Year/ Julian Day	Hour	Monitor	Observed Concentration (ppm)	Calculated Concentration (ppm)	Ratio of Calculated and Observed Concentrations
49	76/046	1700	D23H	0.22	0.05	0.23
			D63H	0.29	0.41	1.41
50	76/046	1800	D63H	0.81	0.21	0.26
			D83H	0.23	0.10	0.43
51	76/046	1900	D63H	0.42	0.05	0.12
			D83H	0.18	0.04	0.22
52	76/049	1700	D63H	0.40	0.27	0.68
			D83H	0.15	0.26	1.73
53	76/049	1800	D63H	0.29	0.15	0.52
			D83H	0.15	0.07	0.47
54	76/049	1900	D63H	0.28	0.06	0.21
			D83H	0.16	0.04	0.25
55	76/052	1300	D03H	0.39	0.02	0.05
56	76/052	1500	D03H	0.28	0.05	0.18
57	76/052	1600	D03H	0.29	0.03	0.10
58	76/065	1000	D63H	0.11	0.12	1.09
			D83H	0.34	0.45	1.32
59	76/065	1100	D83H	0.29	0.28	0.97
60	76/065	1500	D63H	0.12	0.08	0.67
			D83H	0.26	0.19	0.73
61	76/066	2400	D13H	0.12	0.01	0.08
			D93H	0.31	0.29	0.94
62	76/067	0200	D13H	0.27	0.52	1.93
			D93H	0.15	0.05	0.33
63	76/067	1400	D13H	0.34	0.34	1.00
			D93H	0.11	0.14	1.27
64	76/067	1500	D13H	0.32	0.41	1.28
65	76/067	1700	D13H	0.29	0.04	0.14
66	76/073	0200	D63H	0.26	0.30	1.15
			D83H	0.12	0.47	3.92
67	76/074	1300	D63H	0.25	0.05	0.20
			D83H	0.10	0.06	0.60
68	76/074	1900	D63H	0.29	0.05	0.17
			D83H	0.17	0.06	0.35
69	76/074	2000	D63H	0.28	0.17	0.61
			D83H	0.11	0.16	1.45
70	76/074	2400	D13H	0.16	0.75	4.69
			D93H	0.25	0.03	0.12
71	76/084	0200	D23H	0.30	0.43	1.43
72	76/084	0300	D23H	0.35	0.25	0.71
73	76/084	0400	D23H	0.30	0.22	0.73

TABLE 4-6 (Continued)

Case No.	Year/ Julian Day	Hour	Monitor	Observed Concentration (ppm)	Calculated Concentration (ppm)	Ratio of Calculated and Observed Concentrations
74	76/094	1800	D03H	0.26	0.27	1.04
75	76/094	2000	D03H	0.27	0.10	0.37
76	76/094	2300	D03H	0.59	0.14	0.24
77	76/095	0200	D03H	0.27	0.15	0.56
78	76/096	1600	D13H	0.30	0.05	0.17
			D93H	0.16	0.44	2.75
79	76/096	1700	D13H	0.60	0.85	1.42
			D93H	0.16	0.18	1.13
80	76/106	0200	D23H	0.64	0.24	0.38
81	76/107	1200	D63H	0.10	0.21	2.10
			D83H	0.26	0.60	2.31
82	76/109	1000	D23H	0.35	0.23	0.66
83	76/113	0600	D63H	0.15	0.14	0.93
			D83H	0.36	0.60	1.67
84	76/113	0700	D63H	0.21	0.22	1.05
			D83H	0.31	0.41	1.32
85	76/113	0800	D63H	0.25	0.26	1.04
			D83H	0.31	0.51	1.65
86	76/122	2200	D13H	0.25	0.71	2.84
87	76/124	1200	D13H	0.27	0.62	2.30
88	76/126	0200	D23H	0.29	0.11	0.38
89	76/164	2400	D63H	0.28	0.12	0.43
90	76/189	1800	D13H	0.30	0.00	0.00
			D93H	0.10	0.18	1.80
					Mean Ratio (MR)	0.86

TABLE 4-7

SUMMARY OF THE RESULTS OF THE ISC MODEL CALCULATIONS FOR THE DOW DATA SET*

ISC Model Mode	Building Wake Effects	Stack-Tip Downwash		Scire and Schulman 1980 Downwash Radius	Measures of Model Performance		
		Briggs (1973)	Cramer, et al. (1975)		MR	RMSE	% Within a Factor of 2
Rural	No	No	No	No	0.15	12.37	10
Rural	Yes	No	No	No	0.31	8.79	29
Rural	Yes	Yes	No	No	0.37	8.34	34
Rural	Yes	No	Yes	No	1.42 (0.83)**	6.80 (7.47)**	31 (34)**
Rural	Yes	No	No	Yes	0.92	6.83	33
Urban 2	No	No	No	No	0.48	4.55	46
Urban 2	Yes	No	No	No	0.54	4.43	48
Urban 2	Yes	Yes	No	No	0.58	4.19	49
Urban 2	Yes	No	Yes	No	1.02 (0.76)**	4.00 (4.05)**	48 (50)**
Urban 2	Yes	No	No	Yes	0.86	3.94	48

* The sampling size is 143.

** The measures of performance enclosed by parentheses are based on the results of the calculations when the use of the Cramer, et al. (1975) stack-tip downwash option is restricted to stacks with Froude numbers greater than or equal to 3.0.

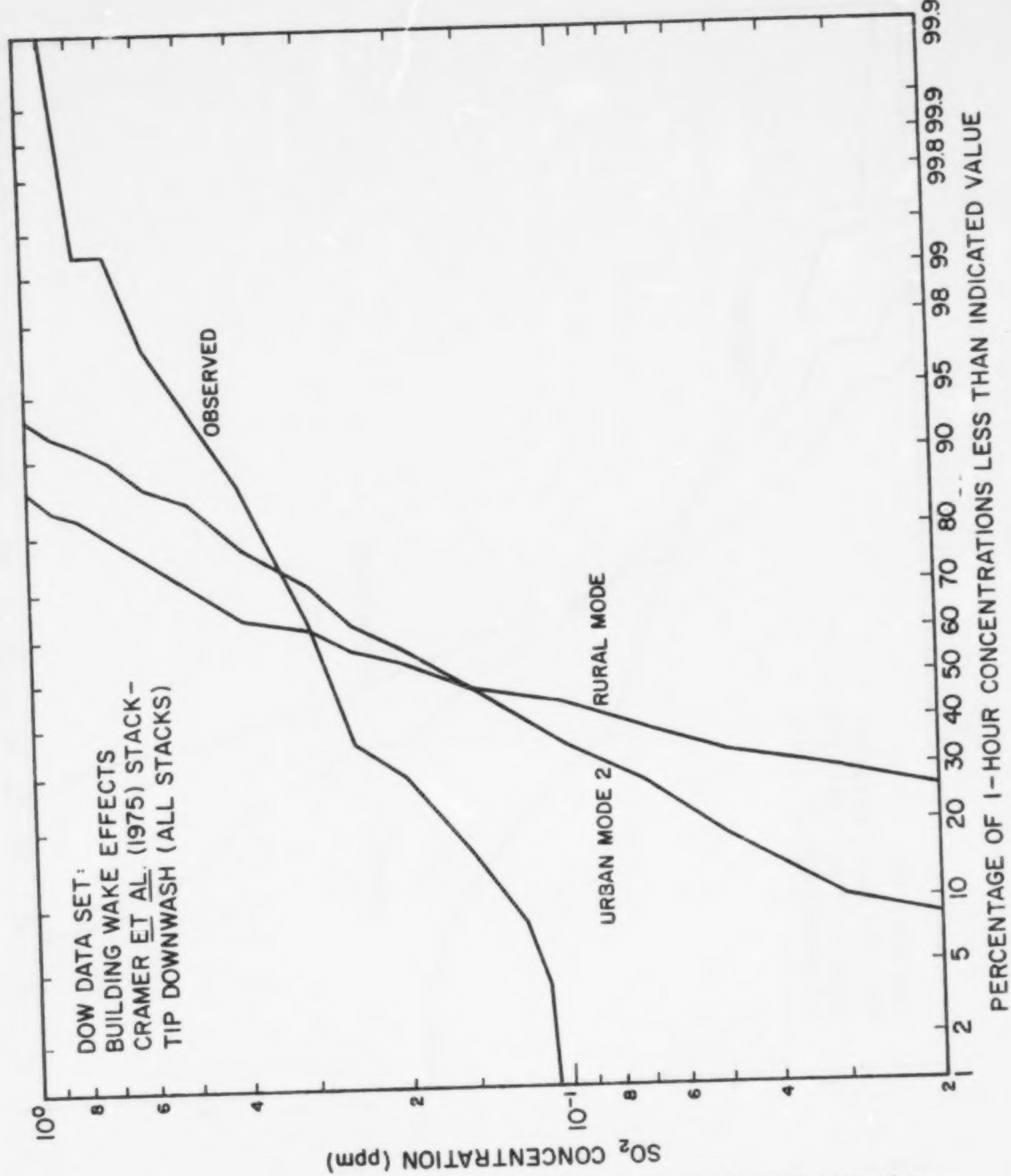

FIGURE 4-1. Comparison of the observed cumulative 1-hour SO_2 concentration frequency distribution for the DOW data set with the corresponding distributions calculated by the ISCST program in the Rural Mode and Urban Mode 2 using the Cramer, et al. (1975) stack-tip downwash correction for all stacks.

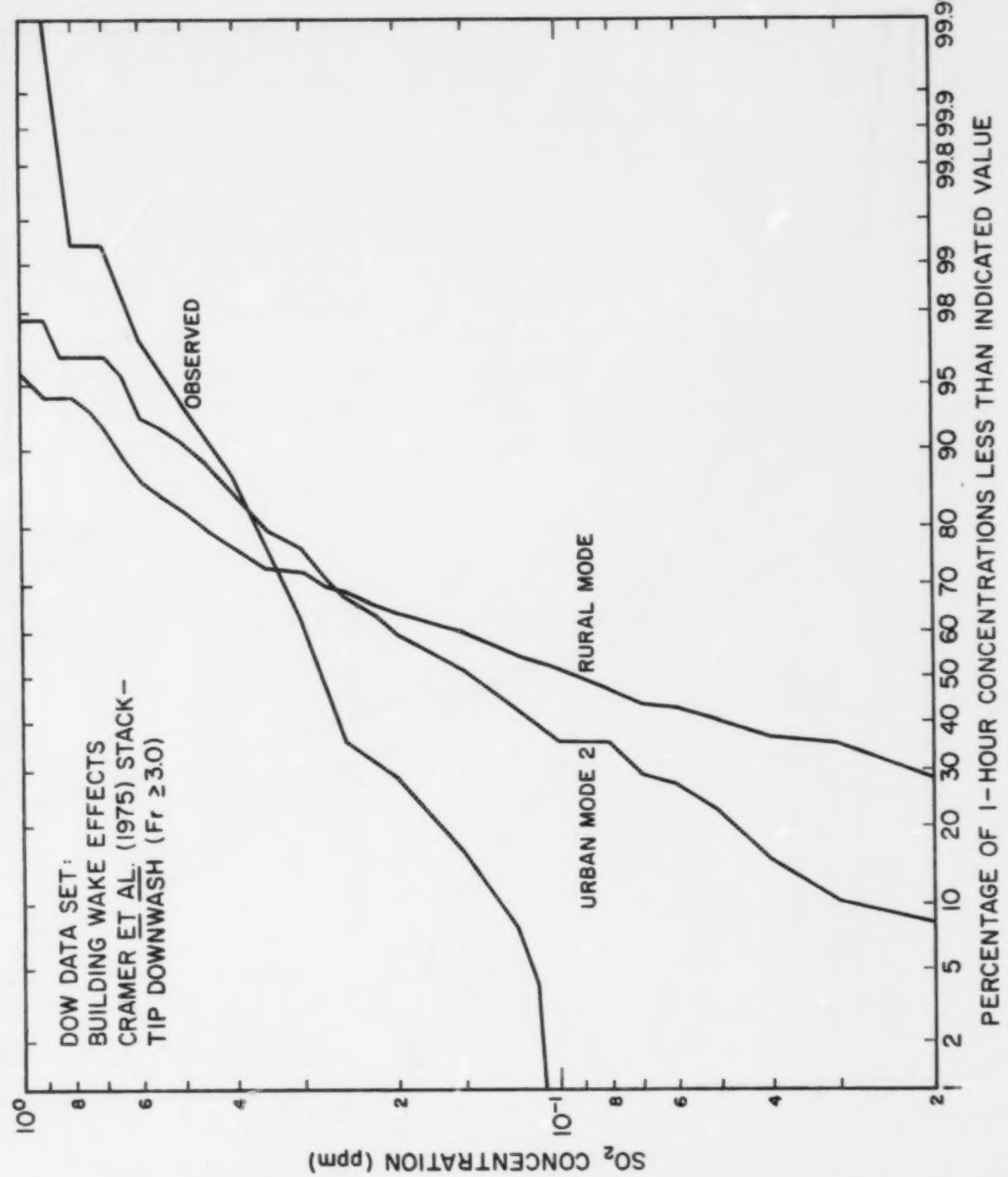

FIGURE 4-2. Comparison of the observed cumulative 1-hour SO_2 concentration frequency distribution for the DOW data set with the corresponding distributions calculated by the ISCST program in the Rural Mode and Urban Mode 2 using the Cramer, et al. (1975) stack-tip downwash correction for stacks with Froude numbers above 3.0.

stacks with Froude numbers (Fr) greater than or equal to 3.0, respectively. Similarly, Figure 4-3 compares the observed concentration frequency distribution with the distributions calculated by the ISC Model using the Scire and Schulman "downwash radius" correction. Inspection of Figures 4-1 through 4-3 shows that the Cramer, et al. stack-tip downwash correction in Urban Mode 2 for stacks with Froude numbers above 3.0 and the Scire and Schulman "downwash radius" correction in both the Rural Mode and Urban Mode 2 closely match the upper percentiles of the observed concentration distribution. However, as shown by Figure 3-9 in Section 3.4.3, the unmodified ISC Model also closely matches the upper percentiles of the observed concentration distribution for model option Combination 6. Thus, we cannot determine on the basis of the available information whether or not the Cramer, et al. stack-tip downwash correction or the Scire and Schulman "downwash radius" correction definitely improves the performance of the ISC model for the DOW data set.

We point out that comparisons of calculated and observed 1-hour concentration cumulative frequency distributions such as shown in Figures 4-1 through 4-3 generally should be restricted to hours with the same meteorological conditions and approximately the same emissions parameters. The DOW data set satisfies the first criterion because the meteorological conditions during all of the hours selected for model testing were neutral stability in combination with moderate or strong winds. However, the DOW data set does not satisfy the second criterion because of the highly variable SO_2 emission rates and exit velocites for the various stacks at the two DOW power houses (see Tables 3-31 and 3-32 in Section 3.4.1). Additionally, because of limitations in sample size for a given monitor, Figure 3-9 in Section 3.4.3 and Figures 4-1 through 4-3 are based on the calculated and observed concentrations for all monitors.

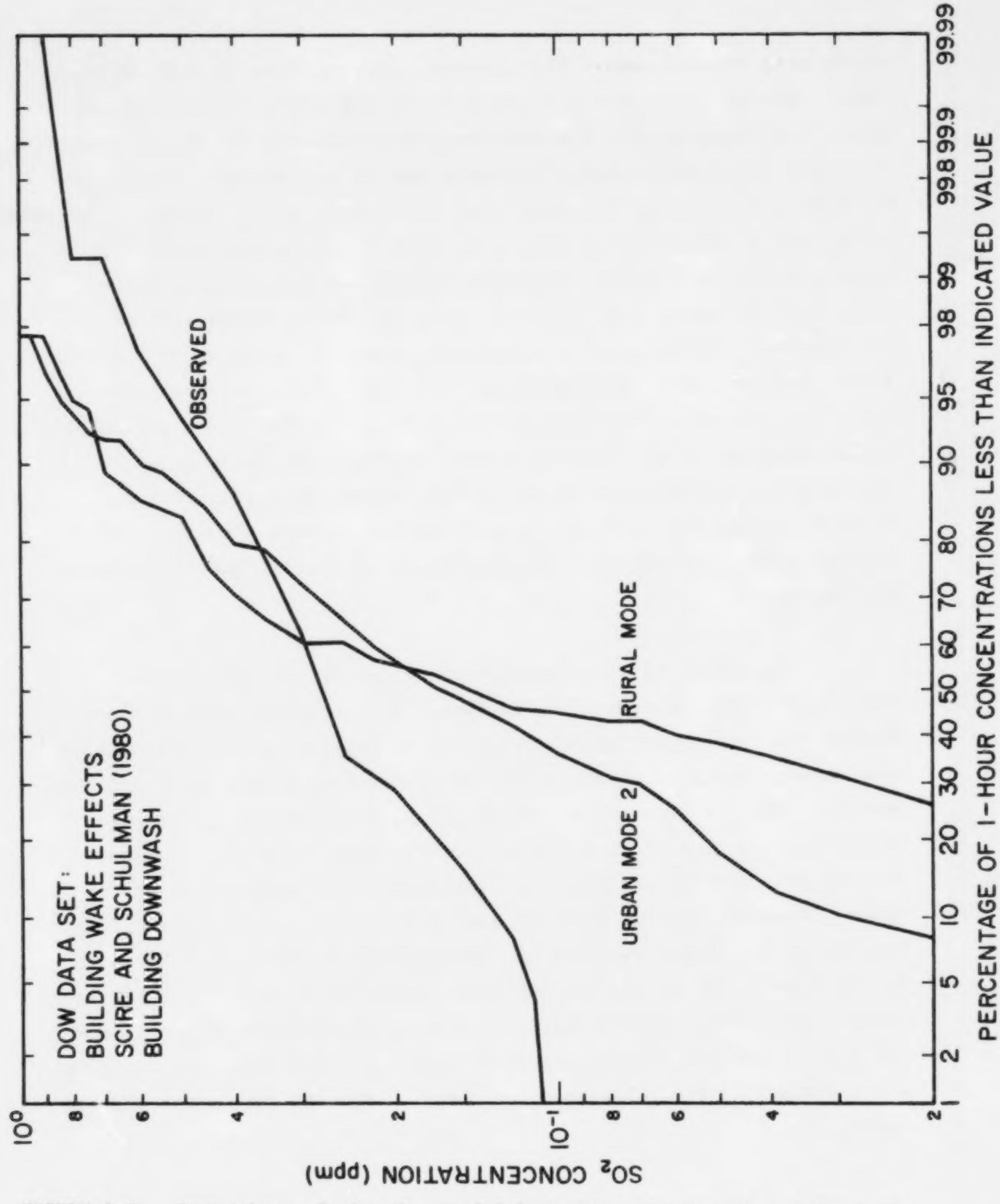

FIGURE 4-3. Comparison of the observed 1-hour SO_2 concentration frequency distribution for the DOW data set with the corresponding distributions calculated by the ISCST program in the Rural Mode and Urban Mode 2 using the Scire and Schulman (1980) "downwash radius" correction.

SECTION 5
CONCLUSIONS

The key features that distinguish the ISC Model from other generally available dispersion models are the gravitational settling/dry deposition option and the building wake effects option. We conclude from the tests of these key features described in Sections 2 and 3 that:

1. The gravitational settling/dry deposition option adds capabilities lacking in most current models, and the accuracy of this option for particulates with appreciable gravitational settling velocities appears to correspond to the approximate factor of 2 accuracy generally attributed to the results of short-term dispersion model calculations in the absence of complicating factors (AMS, 1978).

2. For plumes subject to building wake effects, the building wake effects option significantly improves the performance of the ISC Model over that of the corresponding models (CRSTER and MPTER) which do not consider building wake effects when used to calculate concentrations near the source.

However, the results of the model calculations for the Millstone data set (Johnson, et al., 1975) indicate that it may be desirable to modify the model to consider a reduction in plume height due to initial entrainment of insignificantly buoyant emissions into the cavity zone for stacks located on or adjacent to squat buildings with stack height to building height ratios less then 1.2.

If the mean ratio (MR) of calculated to observed concentrations, the root mean square error (RMSE) and the percentage error bands are used as measures of model performance for the DOW data set, the ISC Model appears to have a systematic tendency to underestimate the concentrations produced near the source by buoyant stack emissions subject to building wake effects. As discussed in Section 4, we added the Cramer, et al. (1975) stack-tip downwash correction and the Scire and Schulman (1980) "downwash radius" correction to special versions of the ISCST program and repeated the concentration calculations for the DOW data set. Both corrections improved the model's performance, as indicated by the MR, RMSE and percentage error bands. However, the MR, RMSE and percentage error bands may not be the most appropriate measures of model performance for the DOW data set because uncertainties about the locations of the plume centerlines arising from the uncertainties about the mean transport wind directions cannot be removed from the DOW data set as was done in the diffusion experiments where the locations of the plume centerlines could be determined from the dense monitoring networks. It is not possible, from a comparison of the calculated and observed concentration frequency distributions, to determine whether or not either of the two corrections significantly improves the model's performance for the DOW data set.

REFERENCES

Abrams, I. B., 1978: Private communication (22 December 1978 letter to J. F. Bowers, H. E. Cramer Company, Inc.).

Abrams, I. B., 1979: Private communication (26 February 1979 letter to J. F. Bowers, H. E. Cramer Company, Inc.).

American Meteorological Society, 1978: Accuracy of dispersion models: A position paper of the 1977 AMS Committee on Atmospheric Turbulence and Diffusion. Bulletin American Meteorological Society, 59, 1025-1026.

Atomic Energy Commission, 1972: On-site meteorological programs. U. S. AEC Regulatory Guide 1.23.

Bjorklund, J. R. and J. F. Bowers, 1979: User's instructions for the SHORTZ and LONGZ computer programs. Technical Report TR-79-131-01, H. E. Cramer Company, Inc., Salt Lake City, Utah.

Briggs, G. A., 1969: Plume Rise. Available as TID-25075 from Clearinghouse for Federal Scientific and Technical Information, Springfield Va., 80.

Briggs, G. A., 1971: Some recent analyses of plume rise observations. In Proceedings of the Second International Clean Air Congress, Academic Press, New York.

Briggs, G. A., 1973: Diffusion estimates for small emissions. ATDL Contribution File No. (Draft) 79, Air Resources Atmospheric Turbulence and Diffusion Laboratories, Oak Ridge, Tennessee.

Briggs, G. A., 1975: Plume rise predictions. Lectures on Air Pollution and Environmental Impact Analyses. American Meteorological Society, Boston, Massachusetts.

Bringfelt, B., 1968: Plume rise measurements at industrial chimneys. Atmospheric Environment, 3(6), 575-598.

Brown, J. M., 1979a: Private communication (Telephone conversation on 17 February 1979 with J. F. Bowers, H. E. Cramer Company, Inc.).

Brown, J. M., 1979b: Private communication (Telephone conversation on 7 March 1979 with J. F. Bowers, H. E. Cramer Company, Inc.).

Boyle, D. G., et al., 1975: DC-7B aircraft spray system for large-area insect control. DPG Document No. DPG-DR-C980A, U. S. Army Dugway Proving Ground, Dugway, Utah 84022.

REFERENCES (Continued)

Busse, A. D. and J. R. Zimmerman, 1973: User's guide for the Climatological Dispersion Model. EPA Report No. EPA-RA-73-024, U. S. Environmental Protection Agency, Research Triangle Park, North Carolina.

Cramer, H. E., H. V. Geary and J. F. Bowers, 1975: Diffusion-model calculations of long-term and short-term ground-level SO_2 concentrations in Allegheny County, Pennsylvania. H. E. Cramer Company Technical Report TR-75-102-01, prepared for the U. S. Environmental Protection Agency, Region III, Philadelphia, Pennsylvania. EPA Report 903/9-75-018. NTIS Accession No. PB-245262/AS.

Draxler, R. R., 1980: An improved Gaussian model for long-term average air concentration estimates. Atmospheric Environment, 14(5), 597-601.

Dumbauld, R. K., J. R. Bjorklund and J. F. Bowers, 1973: NASA/MSFC multilayer diffusion models and computer program for operational prediction of toxic fuel hazards. NASA Contractor Report NASA CR-129006. H. E. Cramer Company Technical Report prepared for National Aeronautics and Space Administration, George C. Marshall Space Flight Center, Alabama 35812.

Ellis, H. M. and P. C. Liu, 1980: Discussion: An air quality model performance assessment package. Atmospheric Environment, 14, 1113.

Environmental Protection Agency, 1969: Air Quality Display Model. Prepared by TRW Systems Group, Washington, D. C., available as PB 189-194 from the National Technical Information Service, Springfield, Virginia.

Environmental Protection Agency, 1977: User's manual for Single Source (CRSTER) Model. EPA Report No. EPA-450/2-77-013, U. S. Environmental Protection Agency, Research Triangle Park, North Carolina.

Environmental Protection Agency, 1978: Guideline on air quality models. EPA Report No. EPA-450/2-78-027, OAQPS No. 1.2-080, U. S. Environmental Protection Agency, Research Triangle Park, North Carolina.

Environmental Protection Agency, 1979: Industrial Source Complex (ISC) Dispersion Model user's guide. EPA Reports EPA-450/4-79-030 (Volume I) and EPA-450/4-79-031 (Volume II), U. S. Environmental Protection Agency, Research Triangle Park, North Carolina.

Fay, J. A., M. Escudier and D. P. Hoult, 1970: A correlation of field observations of plume rise. Journal of the Air Pollution Control Association, 20(6), 391-397.

REFERENCES (Continued)

Halitsky, J. H. and K. Woodard, 1974: Atmospheric diffusion experiments at a nuclear power plant site under light wind inversion conditions. Preprint Volume for the Symposium on Atmospheric Diffusion and Air Pollution, American Meteorological Society, Boston, Massachusetts.

Holzworth, G. C., 1972: Mixing heights, wind speeds and potential for urban air pollution throughout the contiguous United States. Publication No. AP-101, U. S. Environmental Protection Agency, Research Triangle Park, North Carolina.

Huber, A. H. and W. H. Snyder, 1976: Building wake effects on short stack effluents. Preprint Volume for the Third Symposium on Atmospheric Turbulence, Diffusion and Air Quality, American Meteorological Society, Boston, Massachusetts.

Islitzer, N. F., 1965: Aerodynamic effects of large reactor complexes upon atmospheric turbulence and diffusion. USAEC Report No. IDO-12041, U. S. Weather Bureau, Idaho Falls, Idaho.

Johnson, W. B., et al., 1975: Gas tracer study of roof-vent effluent diffusion at Millstone Nuclear Power Station. Atomic Industrial Forum, Inc. Report No. AIF/NESP-0076, prepared by Stanford Research Institute, Menlo Park, California.

Lee, R. F., M. T. Mills and R. W. Stern, 1975: Validation of a single source dispersion model. Paper presented at the 6th NATO/CCMS International Technical Meeting on Air Pollution Modeling, Frankfurt/Main, Germany, 24-26 September 1975.

McDonald, J. E., 1960: An aid to computation of terminal fall velocities of spheres. J. Met., 17, 463.

Munn, R. E. and A. F. W. Cole, 1967: Some strong-wind downwash diffusion measurements at Douglas Point, Ontario, Canada. Atmospheric Environment, 1, 601-604.

Pasquill, F., 1961: The estimation of the dispersion of windborne material. Meteorology Magazine, 90, 33-49.

Pierce, T. E. and D. B. Turner, 1980: User's guide for MPTER. EPA Report No. EPA-600/8-80-016, U. S. Environmental Protection Agency, Research Triangle Park, North Carolina.

Scire, J. S. and L. L. Schulman, 1980: Modeling Plume rise from low-level buoyant line and point sources. Preprint Volume for the Second Joint Conference on Applications of Air Pollution Meteorology, American Meteorological Society, Boston, Massachusetts.

REFERENCES (Continued)

Start, G. E., et al., 1977: Rancho Seco building wake effects on atmospheric diffusion. NOAA Technical Memorandum ERL ARL-64, Air Resources Laboratories, Idaho Falls, Idaho.

Stewart, R. E., 1968: Atmospheric diffusion of particulate matter released from an elevated source. Journal of Applied Meteorology, 7, 425-432.

Turner D. B., 1964: A diffusion model for an urban area. Journal of Applied Meteorology, 3(1), 83-91.

Turner, D. B., J. R. Zimmerman and A. D. Busse, 1972: An evaluation of some climatological dispersion models. Paper presented at the 3rd NATO/CCMS International Technical Meeting on Air Pollution Modeling, Paris, France, October 1972.

Turner, D. B., 1979: Atmospheric dispersion modeling: A critical review. Journal of the Air Pollution Control Association, 29(5), 502-519.

Walker, E. R., 1965: A particulate diffusion experiment. Journal of Applied Meteorology, 4, 614-621.

APPENDIX A

CALCULATED AND OBSERVED DEPOSITION PROFILES FOR THE WALKER (1965) AND STEWART (1968) EXPERIMENTS

This appendix contains the plots of calculated and observed deposition profiles for the Walker (1965) and Stewart (1965) deposition experiments that are discussed in Section 2. Figures A-1 through A-18 show the observed and calculated normalized crosswind integrated deposition (CWID) profiles for the Walker (1965) trials. Two calculated profiles are given for each trial. The mean layer wind speed $\bar{u}_L$ was used in the deposition calculations for the first profile and the mean wind speed at the height of emission $\bar{u}\{h\}$ was used in the deposition calculations for the second profile. The surface reflection coefficients γ_n used to calculate the deposition profiles shown in Figure A-1 through A-12 were taken from Figure 2-8 of the Industrial Source Complex (ISC) Model User's Guide (EPA, 1979). For the calculated profiles in Figures A-13 through A-18, it was assumed that there was no reflection at the ground surface ($\gamma_n = 0$). Figures A-19 through A-28 show the calculated non-dimensional crosswind integrated deposition profiles for the Stewart (1968) trials and the observed maximum non-dimensional crosswind integrated deposition values.

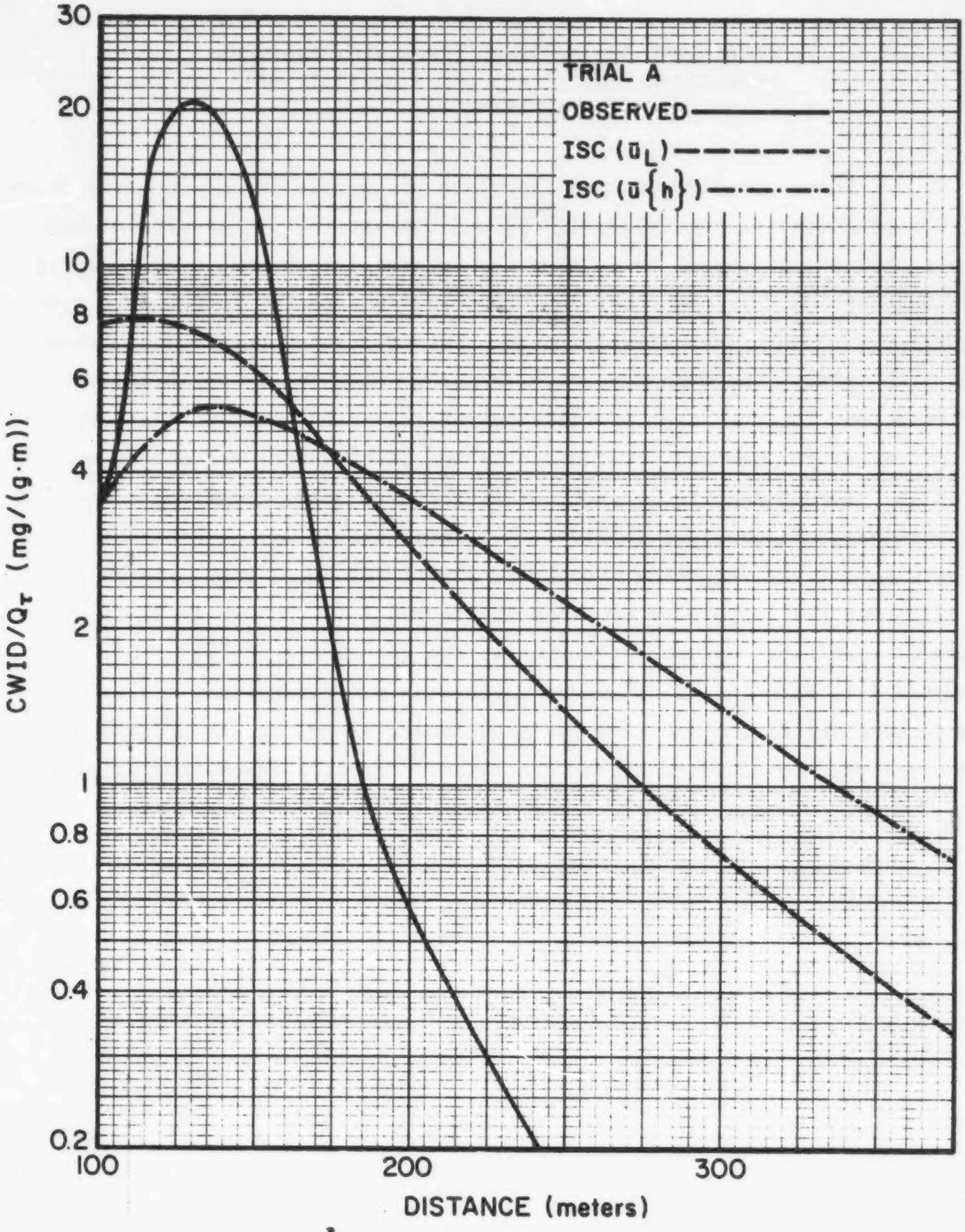

FIGURE A-1. Observed and calculated normalized crosswind integrated deposition versus distance for Walker Trial A.

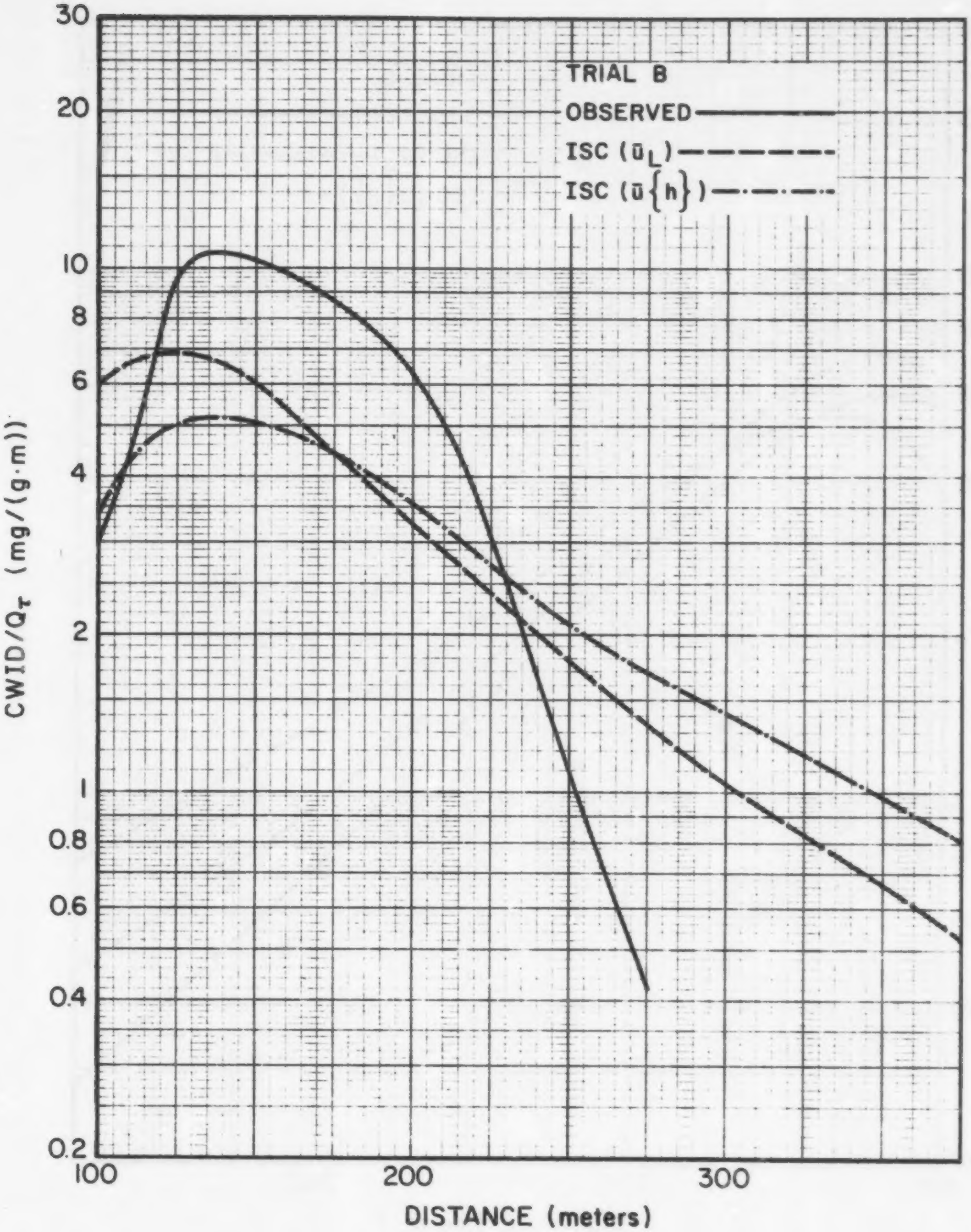

FIGURE A-2. Observed and calculated normalized crosswind integrated deposition versus distance for Walker Trial B.

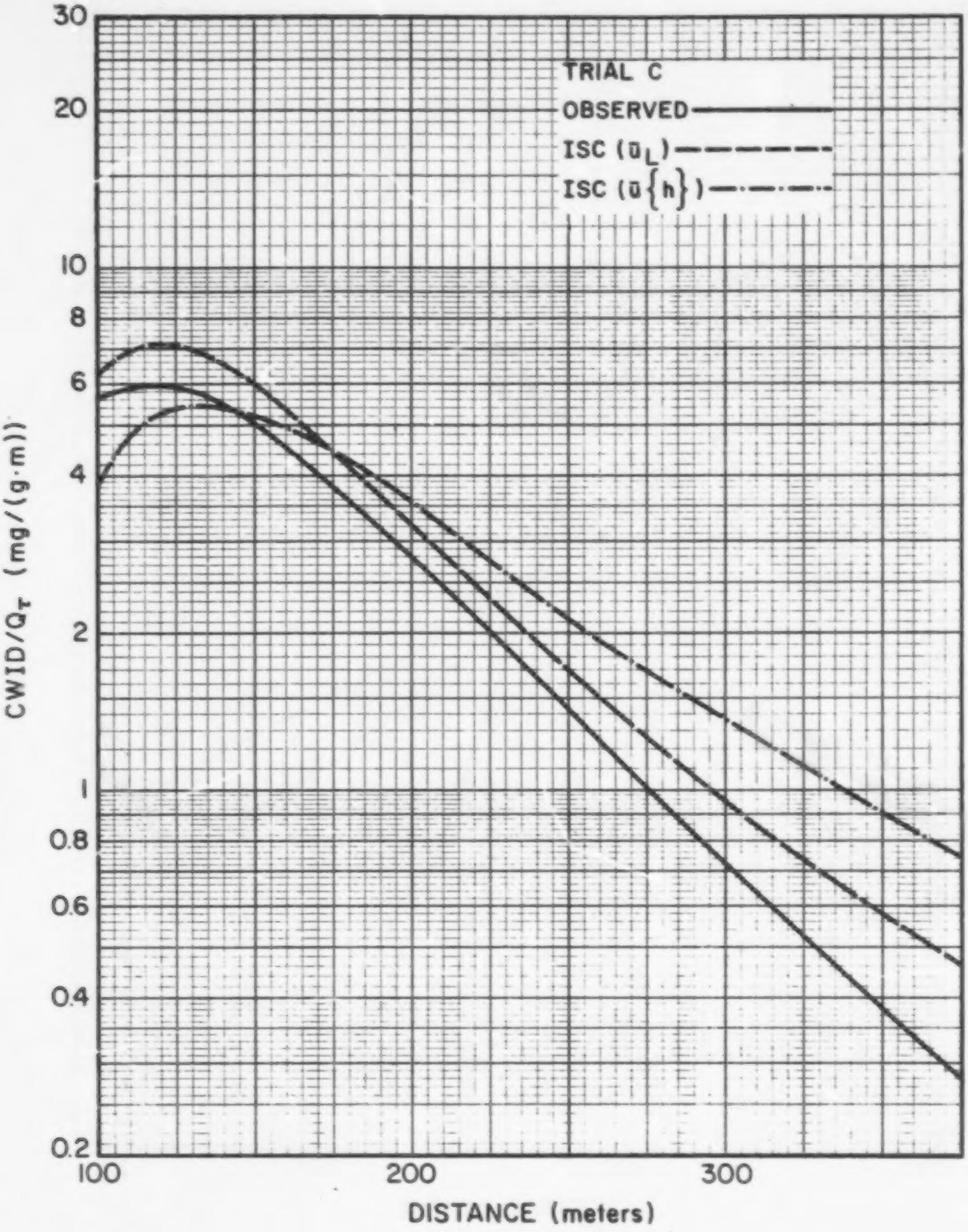

FIGURE A-3. Observed and calculated normalized crosswind integrated deposition versus distance for Walker Trial C.

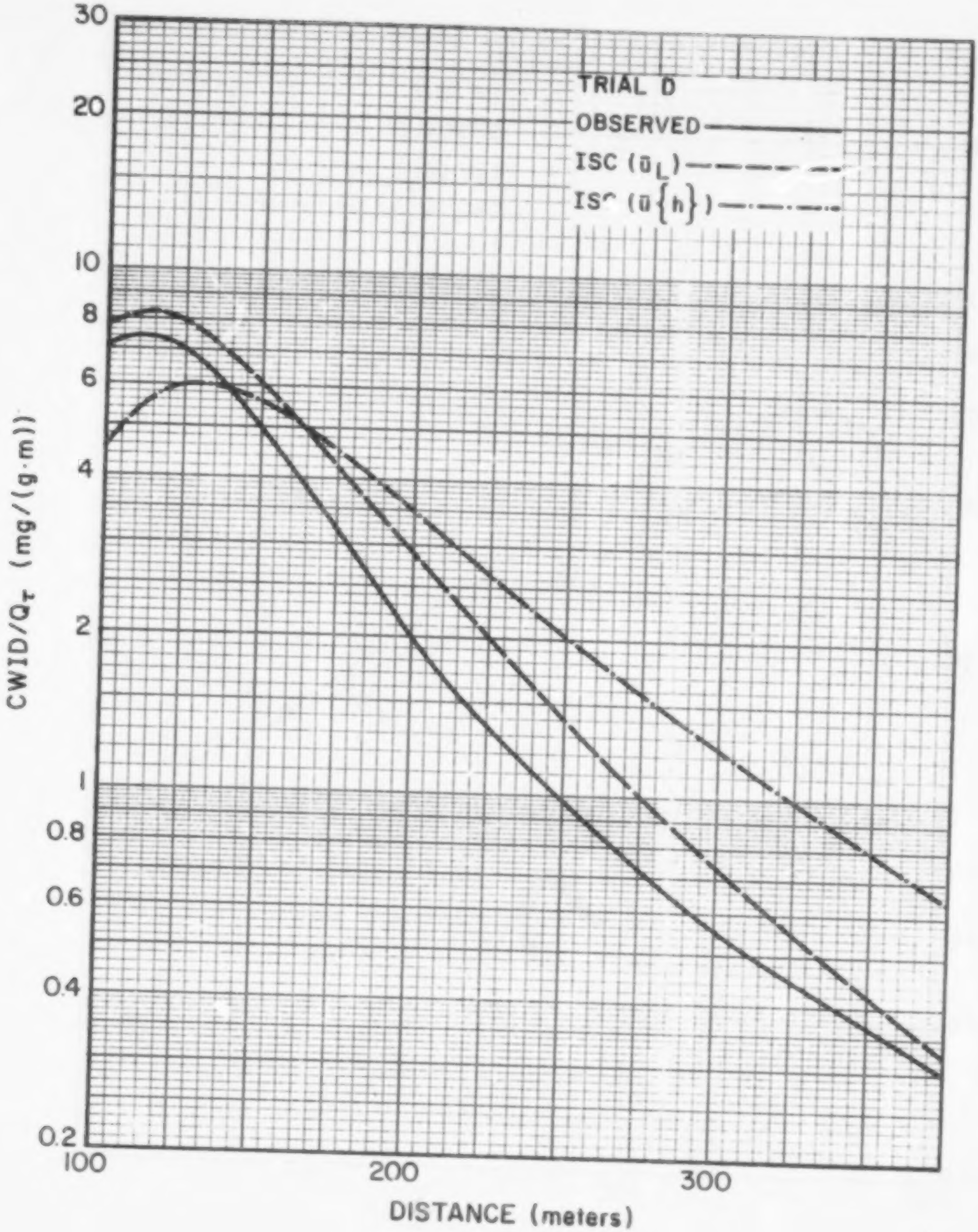

FIGURE A-4. Observed and calculated normalized crosswind integrated deposition versus distance for Walker Trial D.

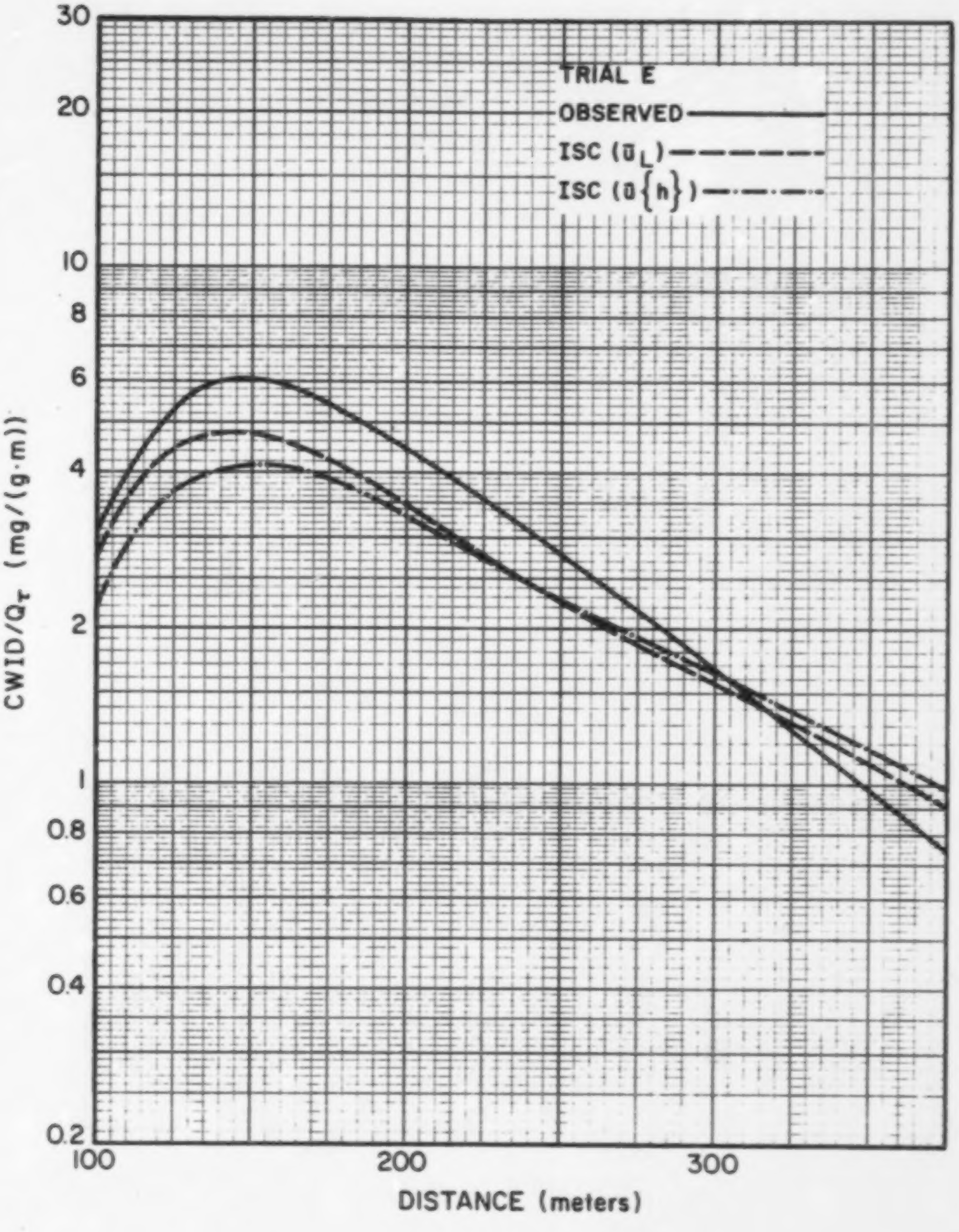

FIGURE A-5. Observed and calculated normalized crosswind integrated deposition versus distance for Walker Trial E.

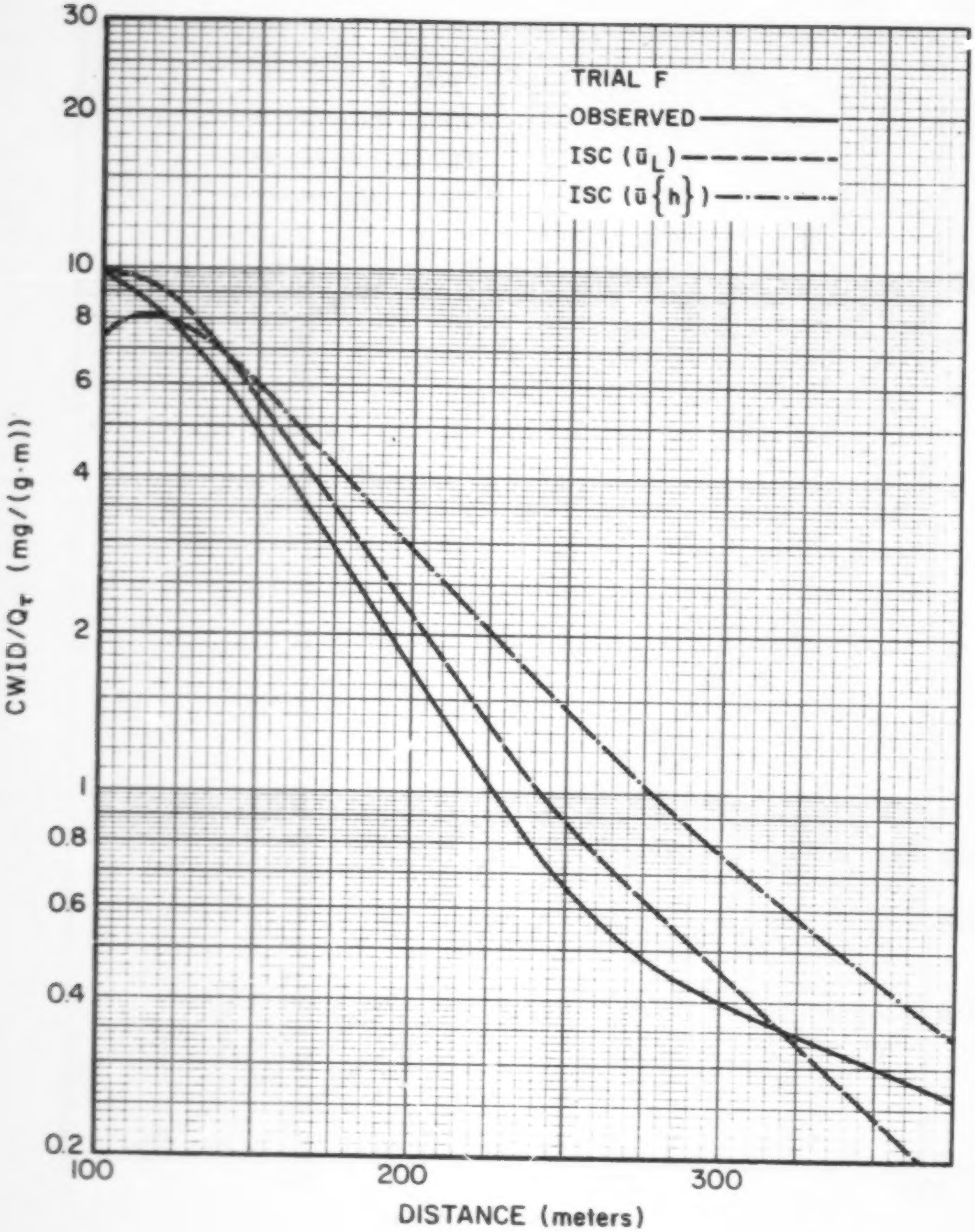

FIGURE A-6. Observed and calculated normalized crosswind integrated deposition versus distance for Walker Trial F.

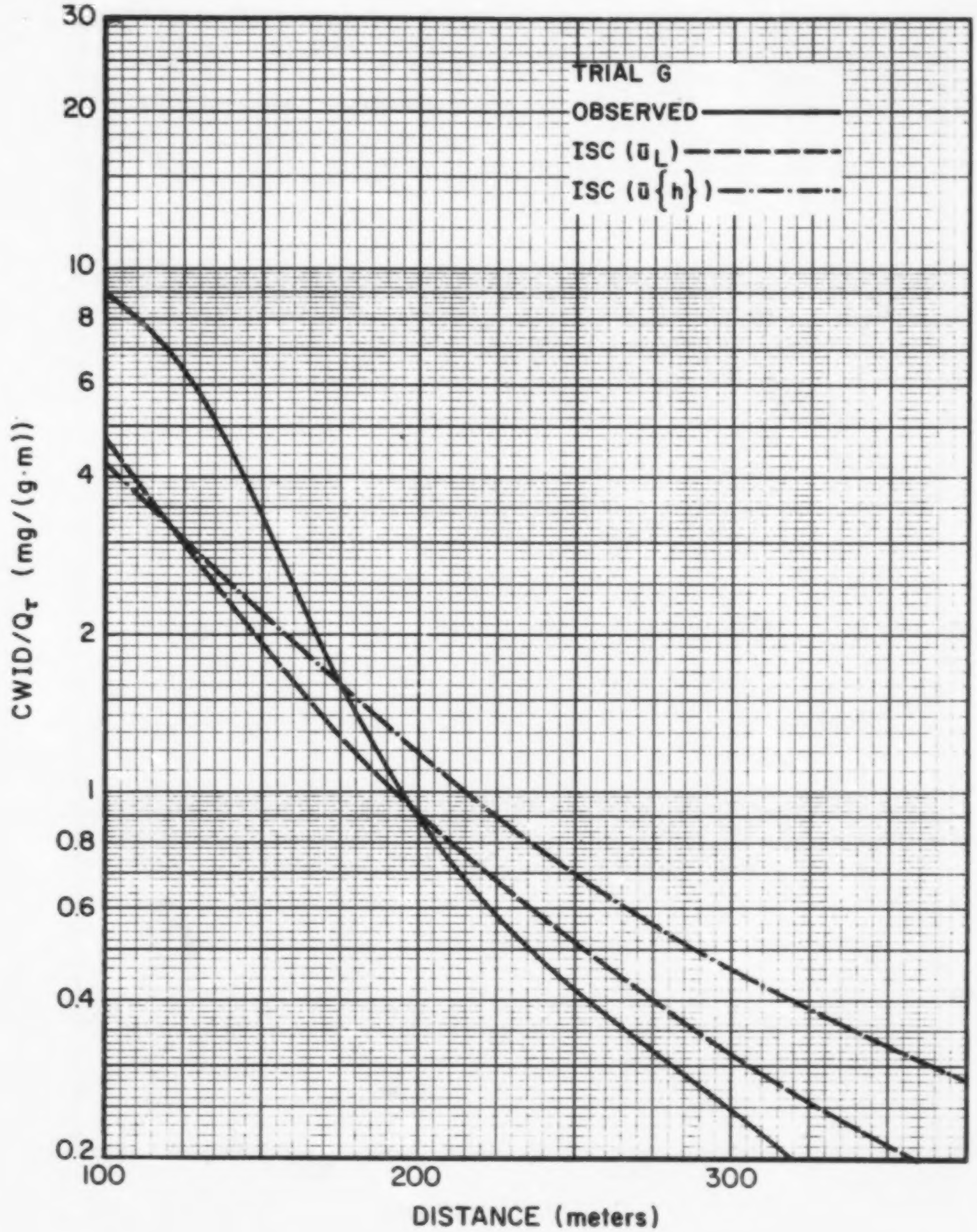

FIGURE A-7. Observed and calculated normalized crosswind integrated deposition versus distance for Walker Trial G.

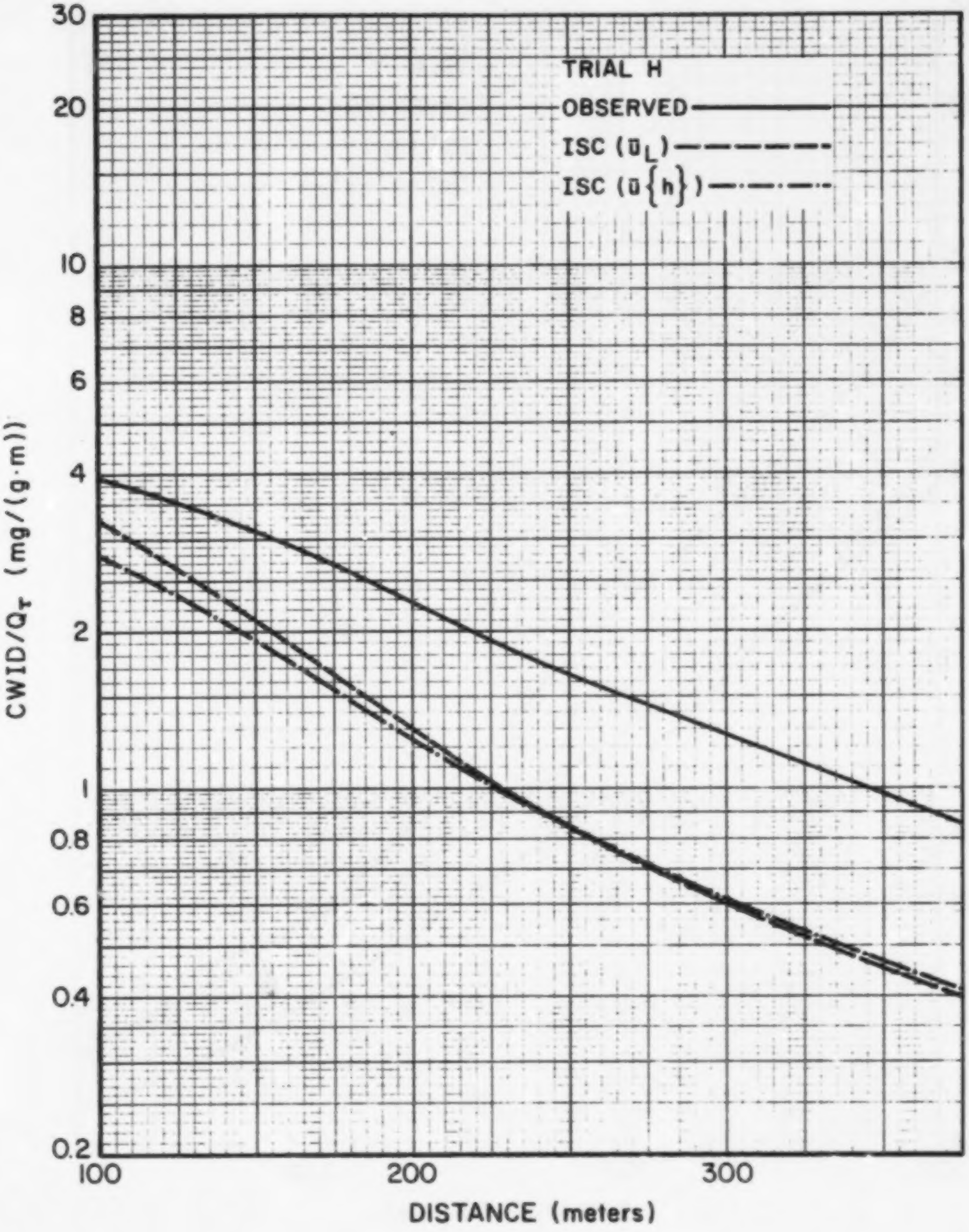

FIGURE A-8. Observed and calculated normalized crosswind integrated deposition versus distance for Walker Trial H.

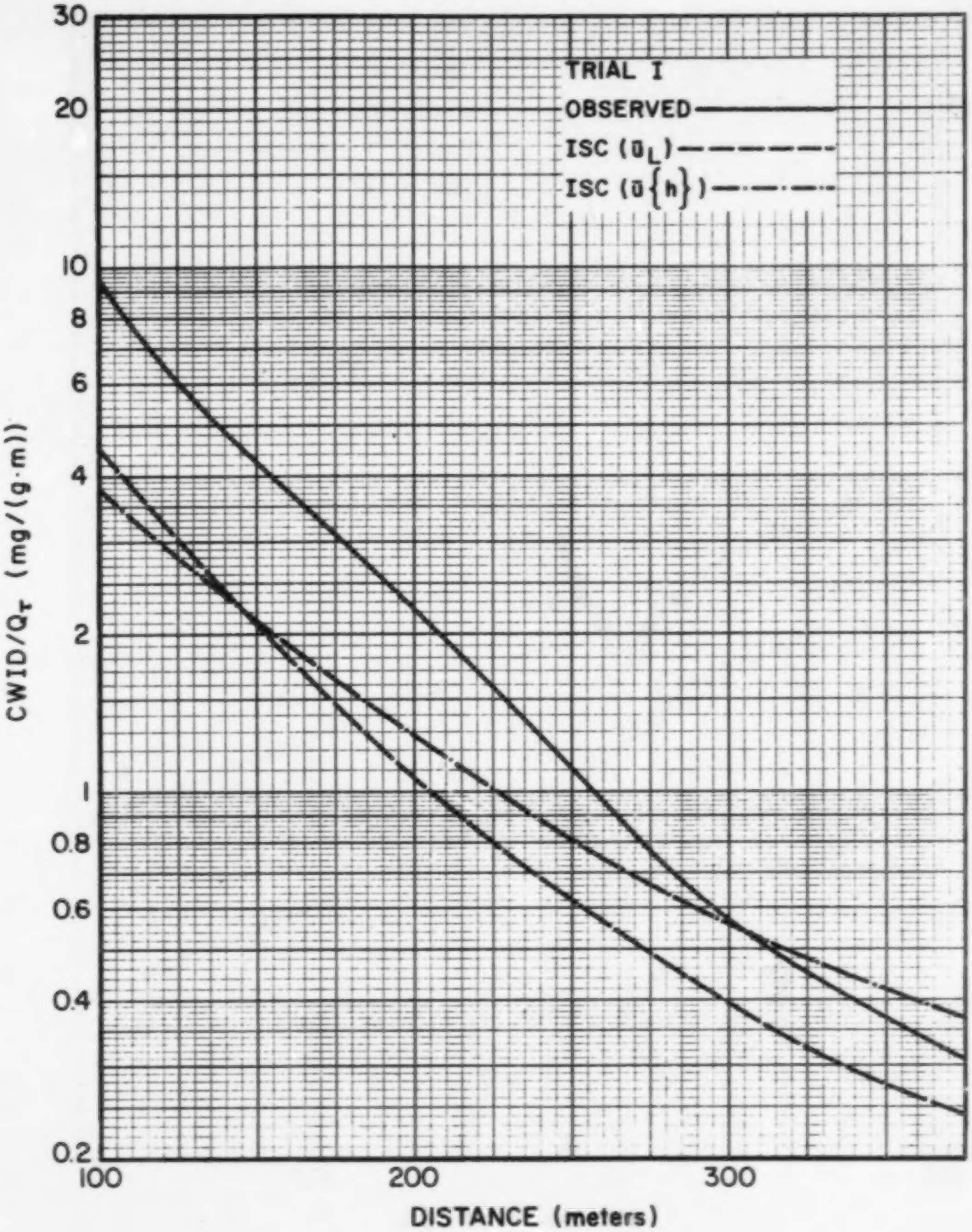

FIGURE A-9. Observed and calculated normalized crosswind integrated deposition versus distance for Walker Trial I.

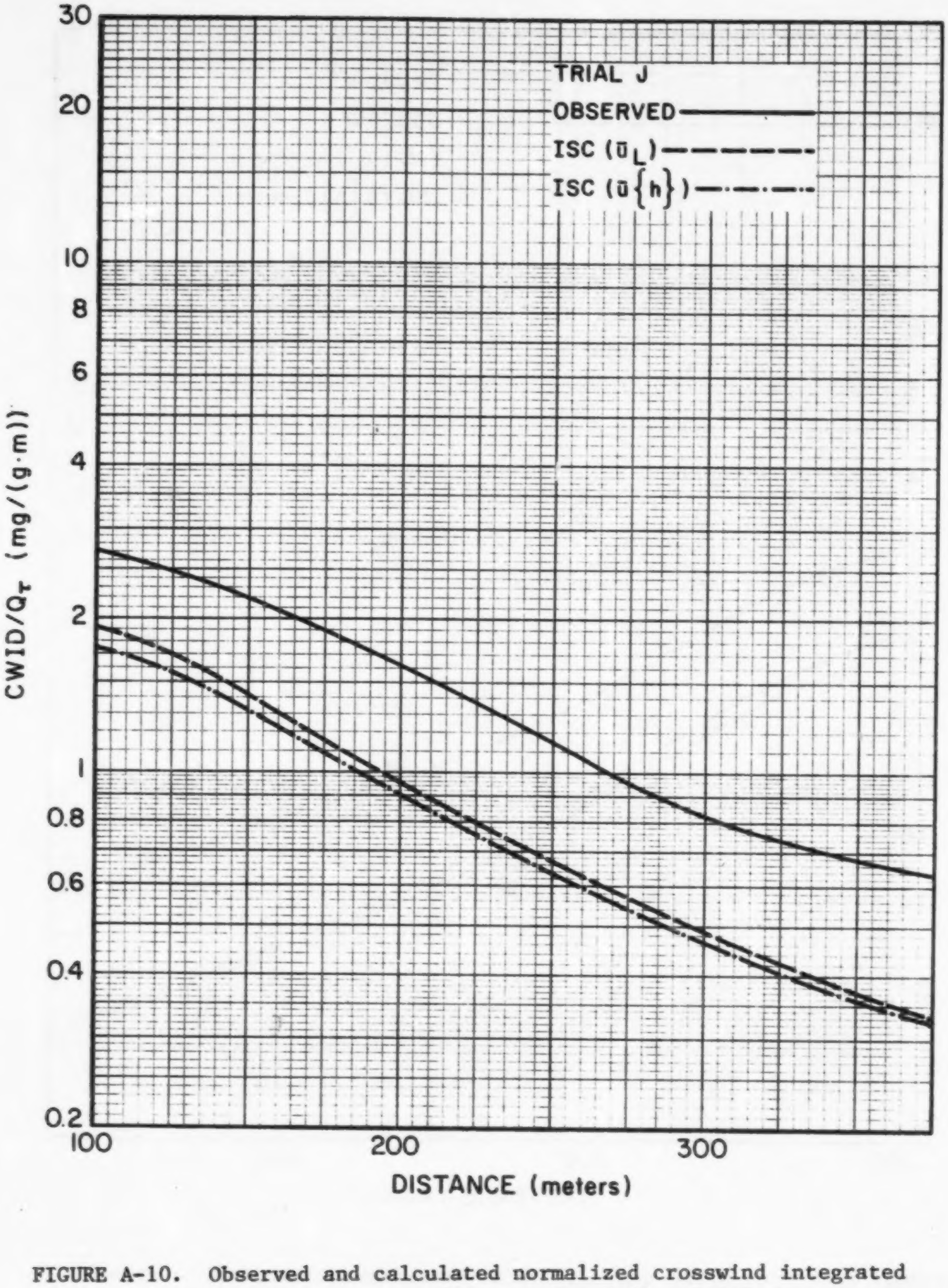

FIGURE A-10. Observed and calculated normalized crosswind integrated deposition versus distance for Walker Trial J.

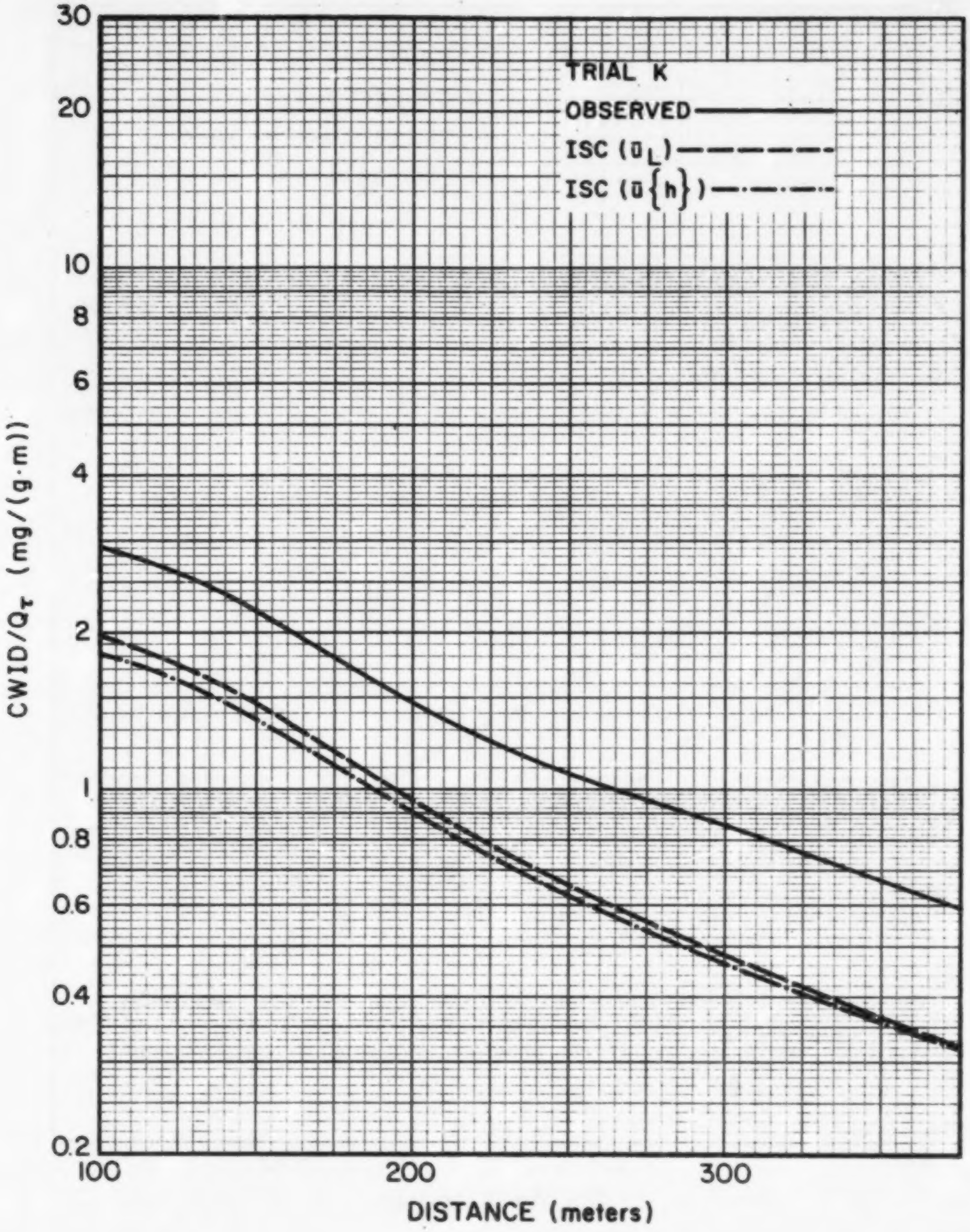

FIGURE A-11. Observed and calculated normalized crosswind integrated deposition versus distance for Walker Trial K.

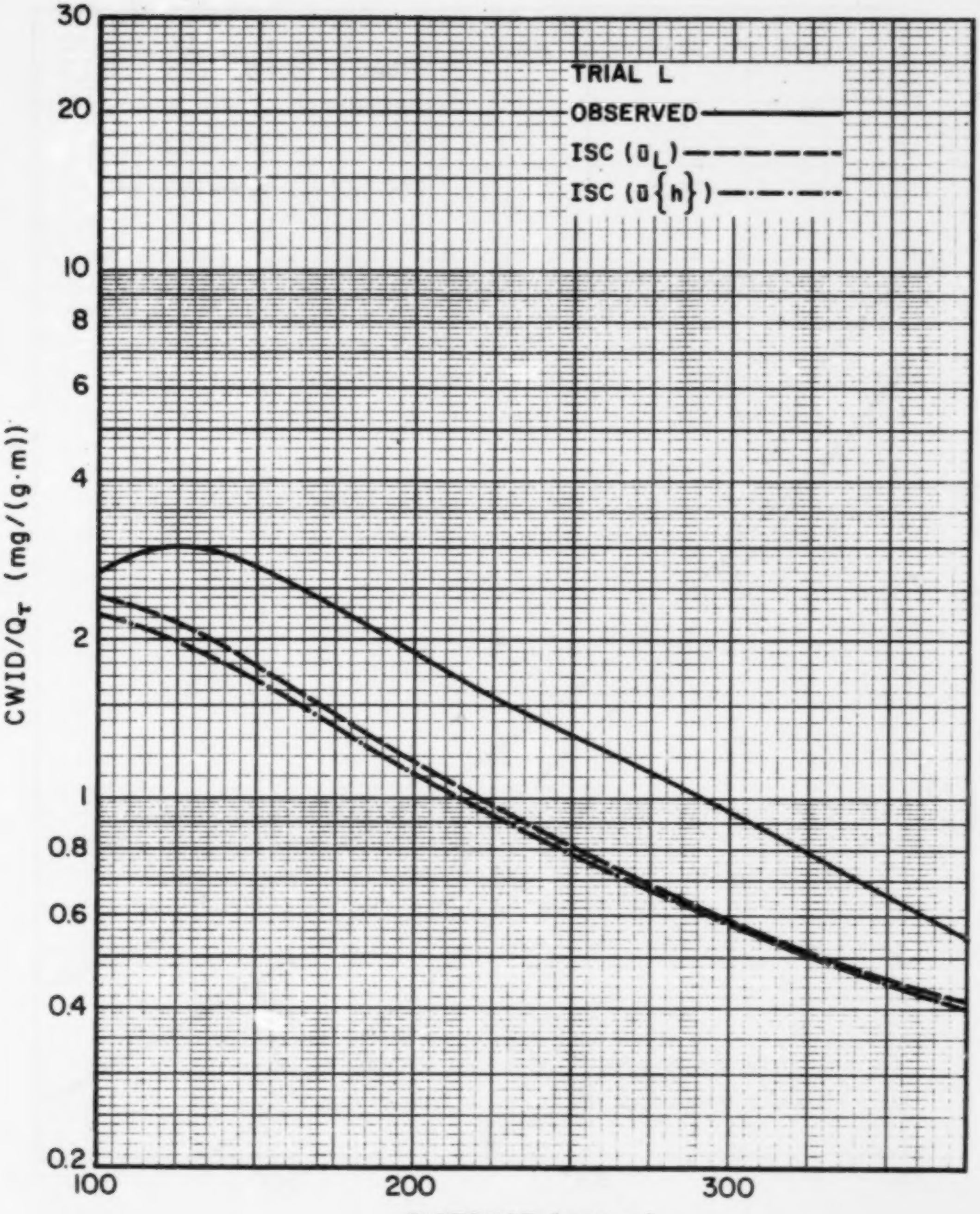

FIGURE A-12. Observed and calculated normalized crosswind integrated deposition versus distance for Walker Trial L.

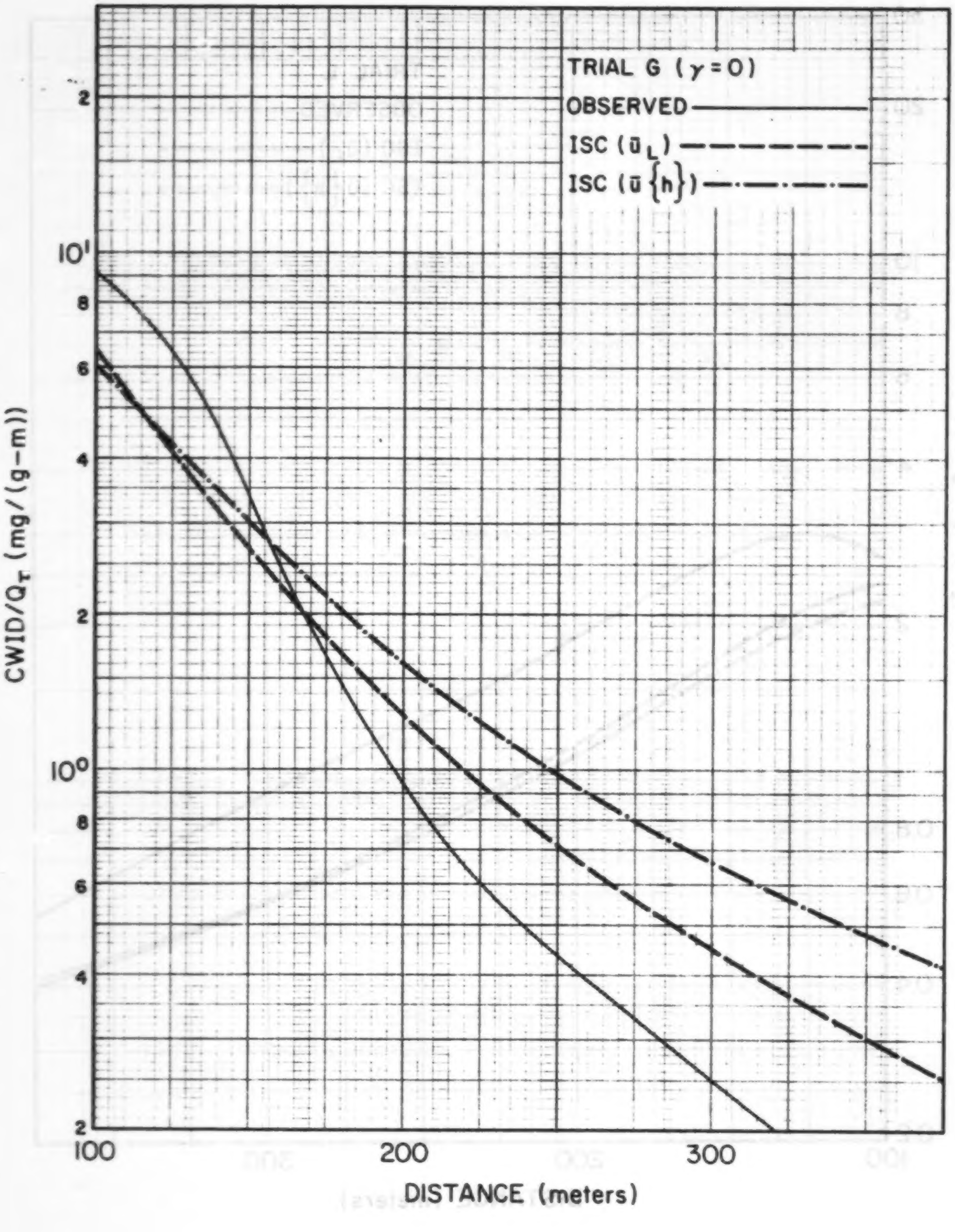

FIGURE A-13. Observed and calculated normalized crosswind integrated deposition versus distance for Walker Trial G with no reflection at the surface.

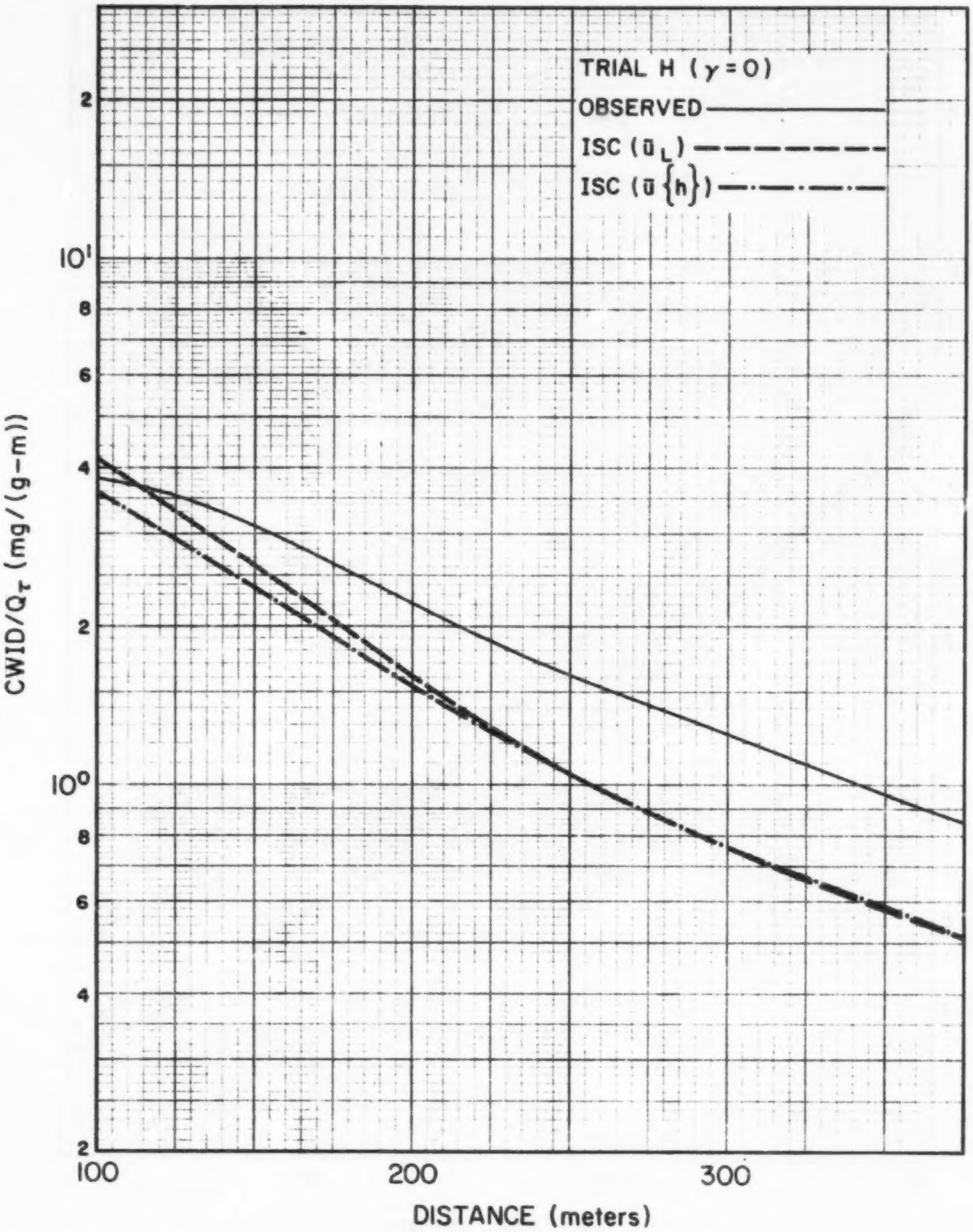

FIGURE A-14. Observed and calculated normalized crosswind integrated deposition versus distance for Walker Trial H with no reflection at the surface.

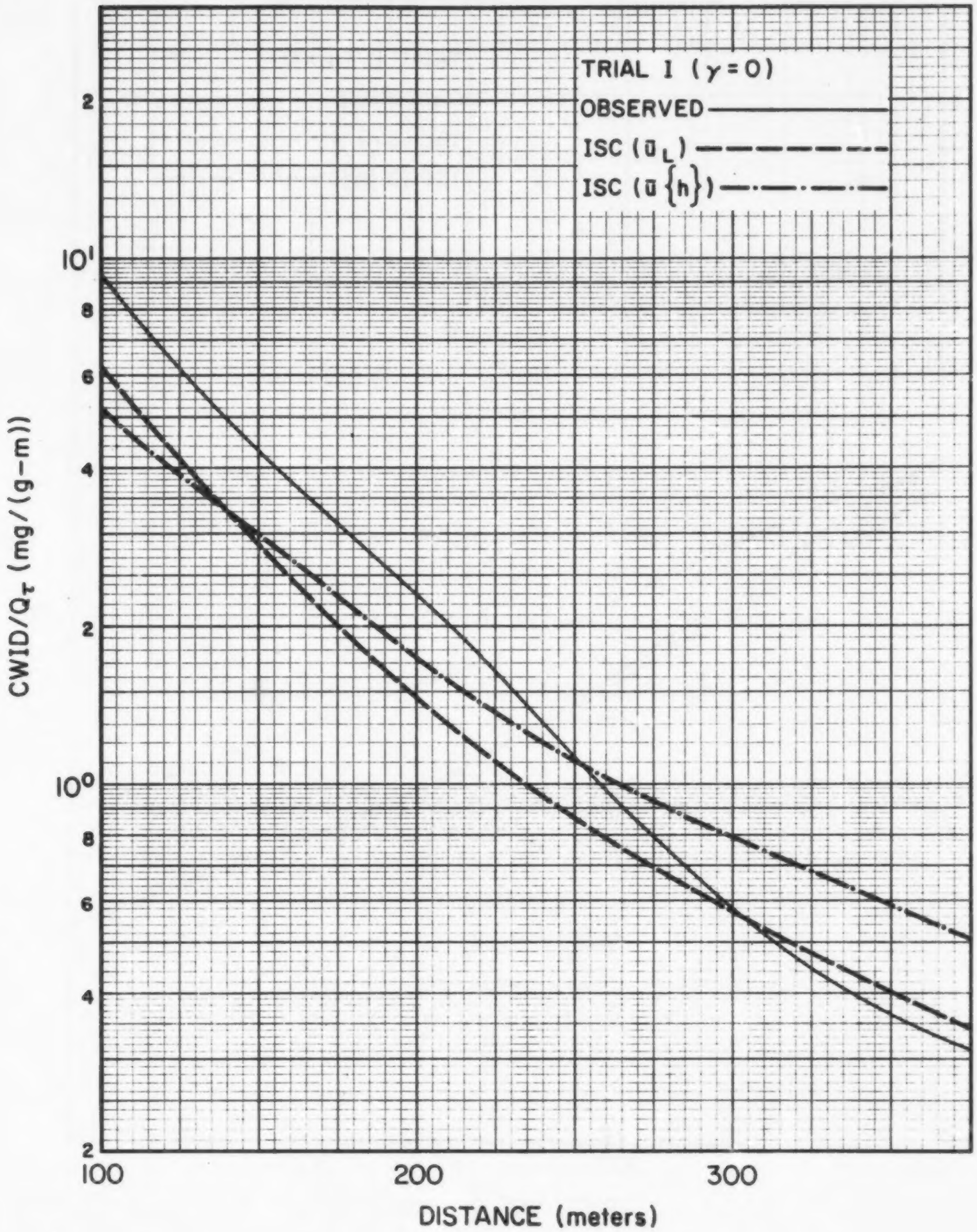

FIGURE A-15. Observed and calculated normalized crosswind integrated deposition versus distance for Walker Trial I with no reflection at the surface.

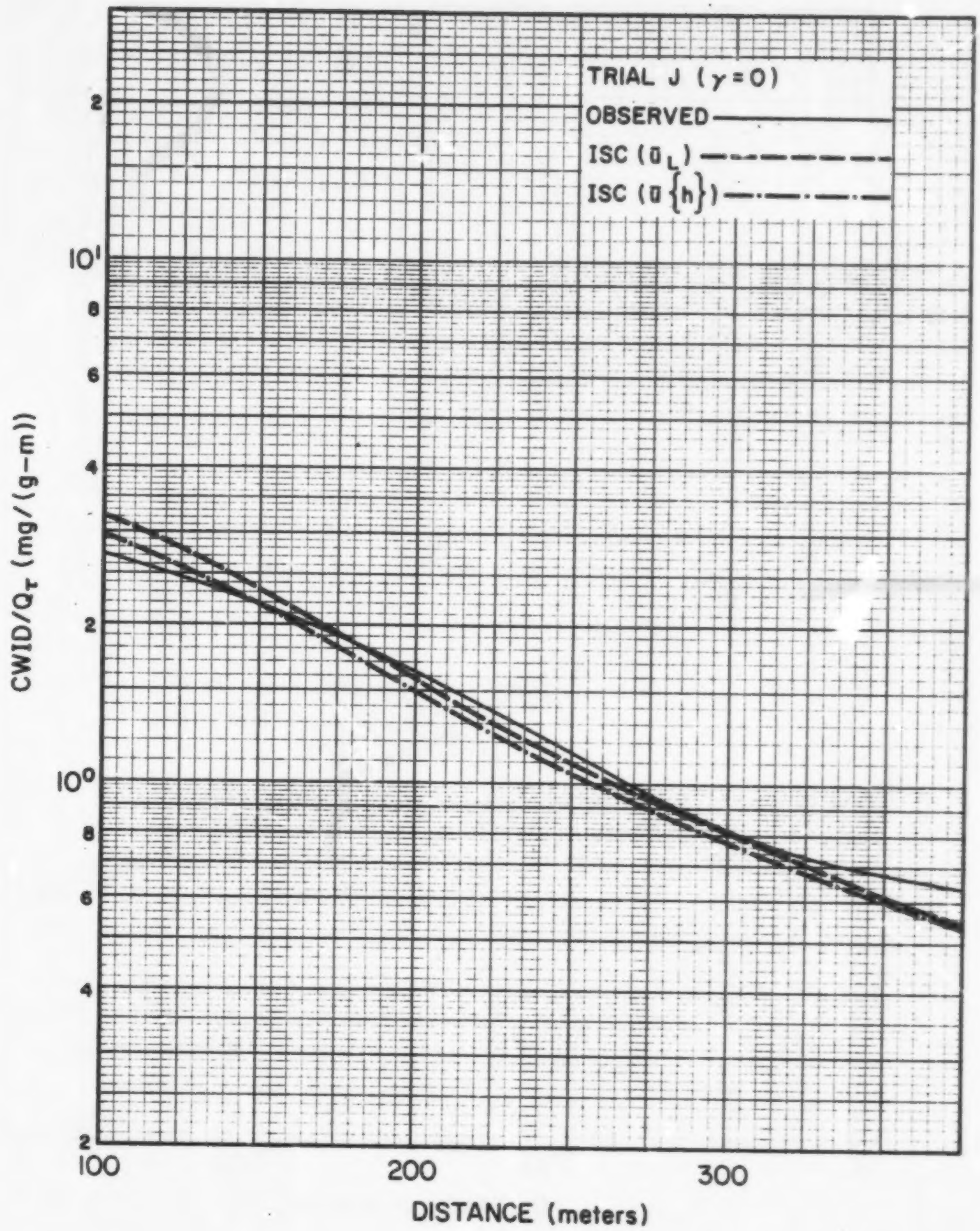

FIGURE A-16. Observed and calculated normalized crosswind integrated deposition versus distance for Walker Trial J with no reflection at the surface.

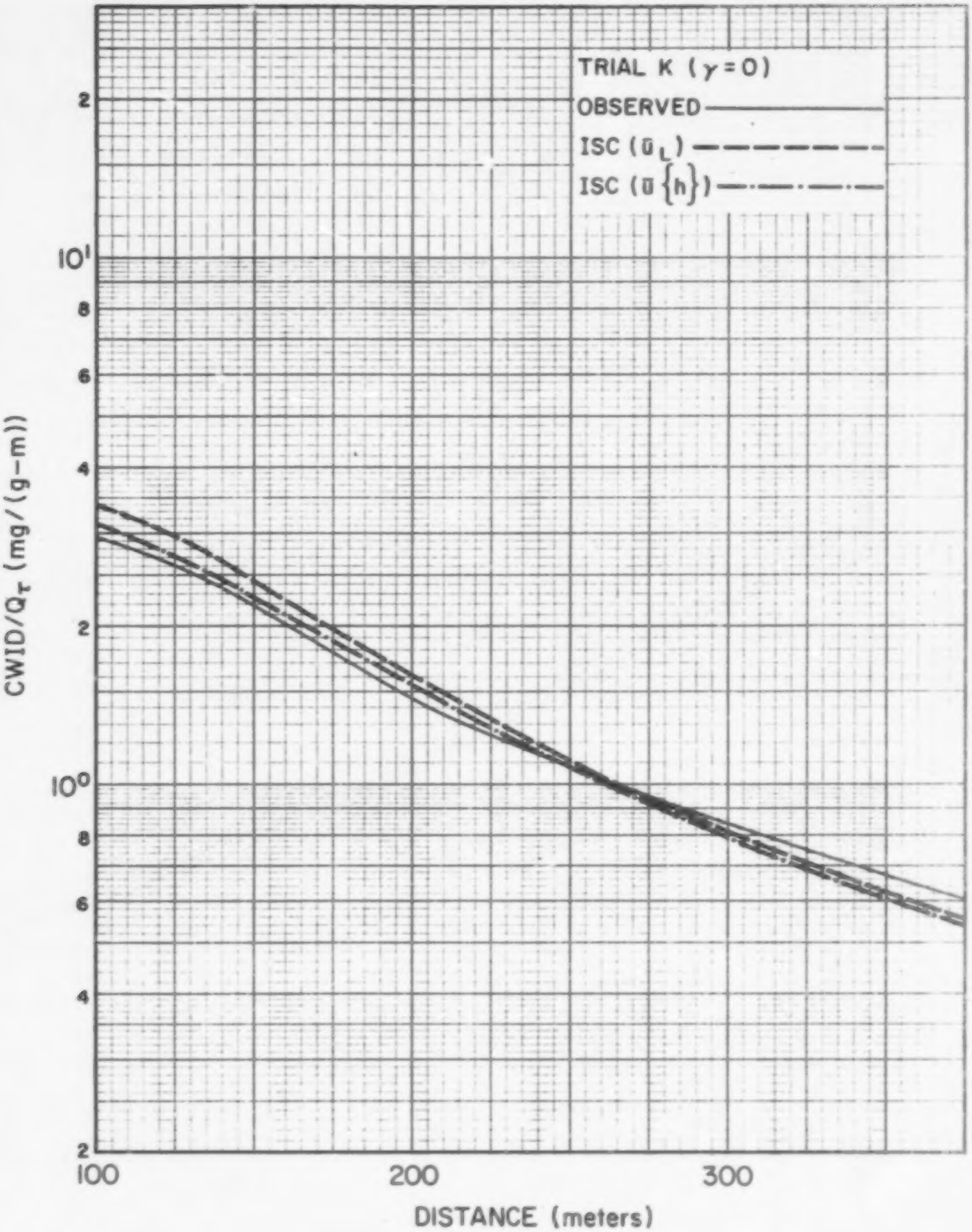

FIGURE A-17. Observed and calculated normalized crosswind integrated deposition versus distance for Walker Trial K with no reflection at the surface.

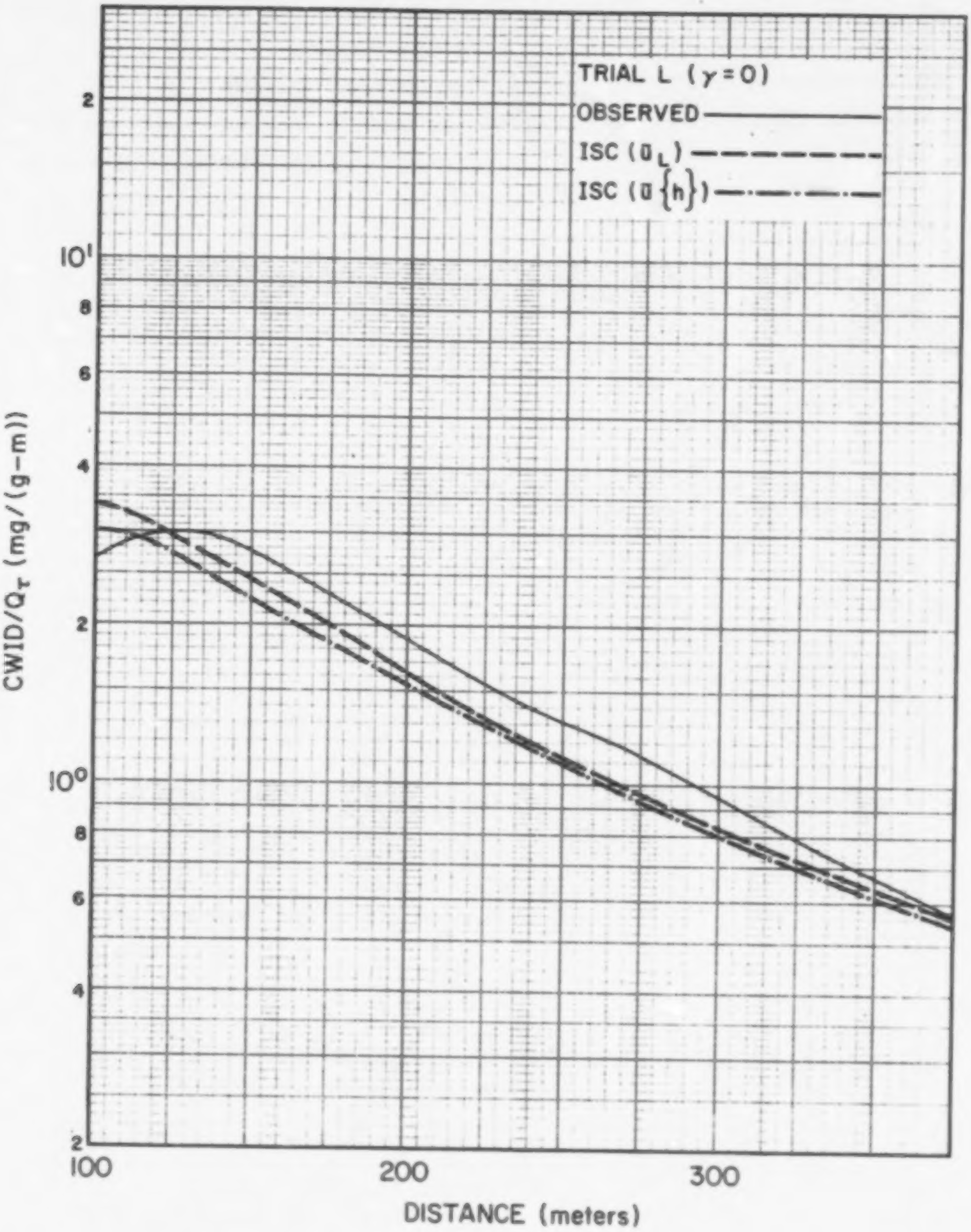

FIGURE A-18. Observed and calculated normalized crosswind integrated deposition versus distance for Walker Trial L with no reflection at the surface.

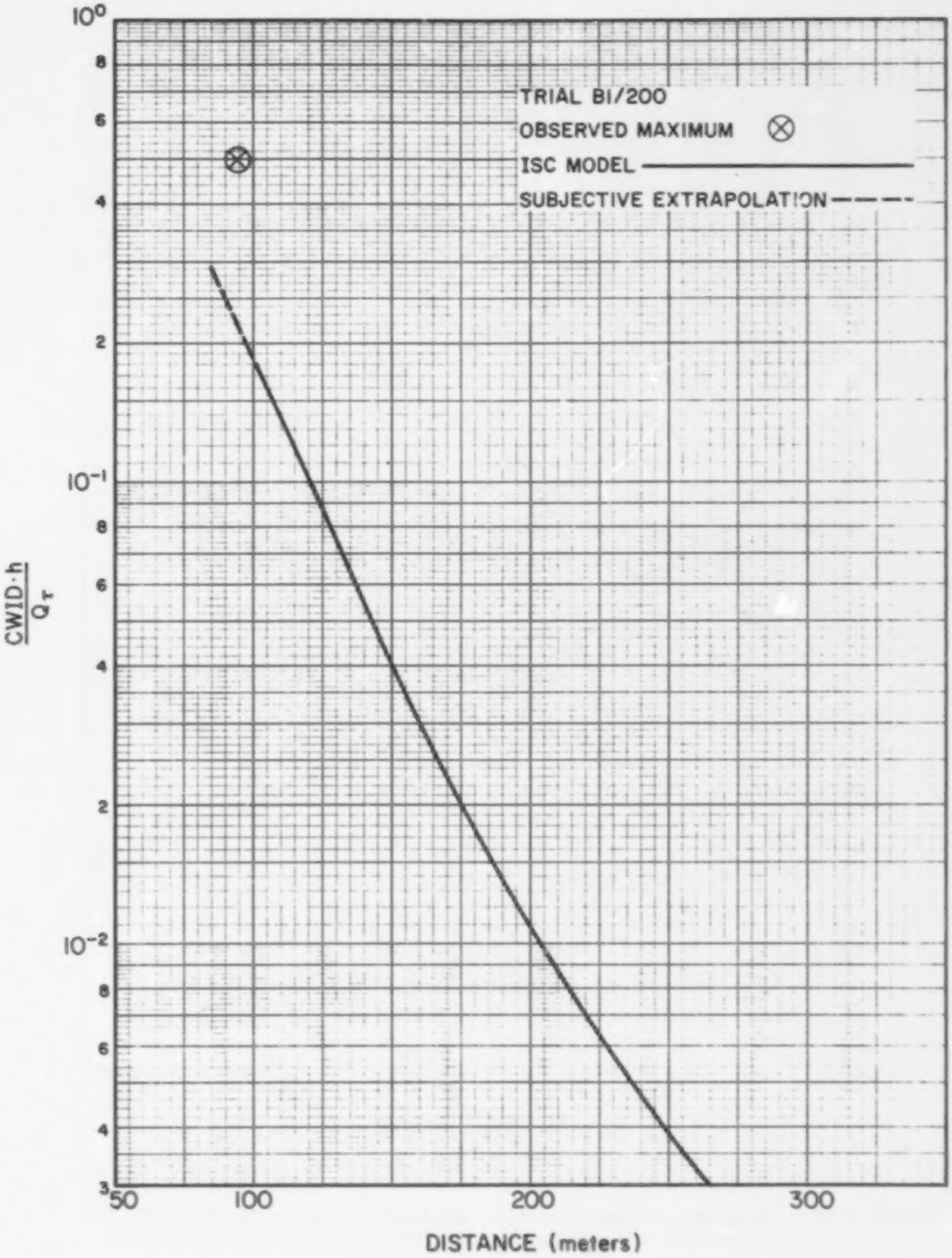

FIGURE A-19. Observed maximum and calculated profile of non-dimensional cross-wind integrated deposition for Stewart Trial B1/200.

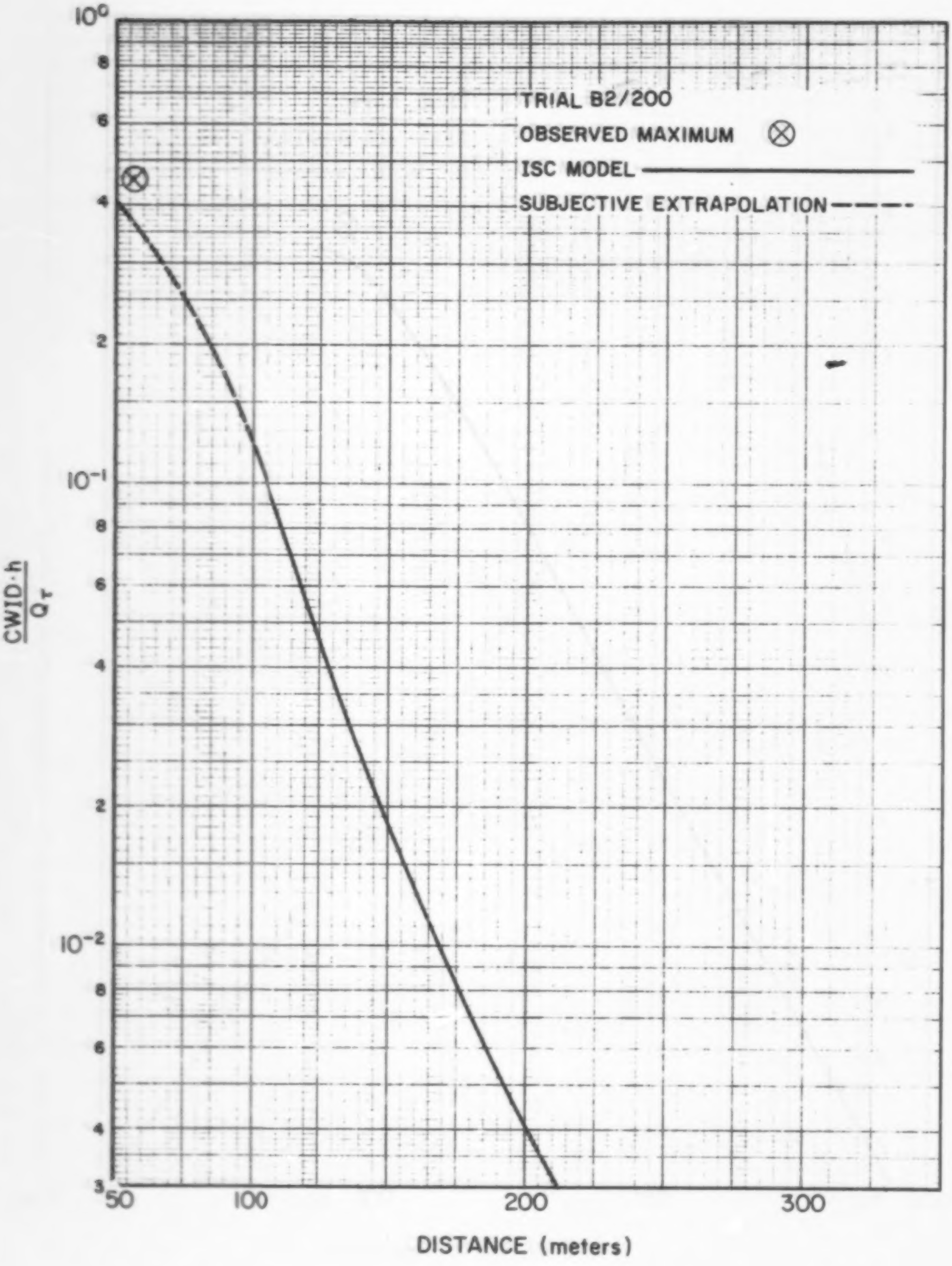

FIGURE A-20. Observed maximum and calculated profile of non-dimensional cross-wind integrated deposition for Stewart Trial B2/200.

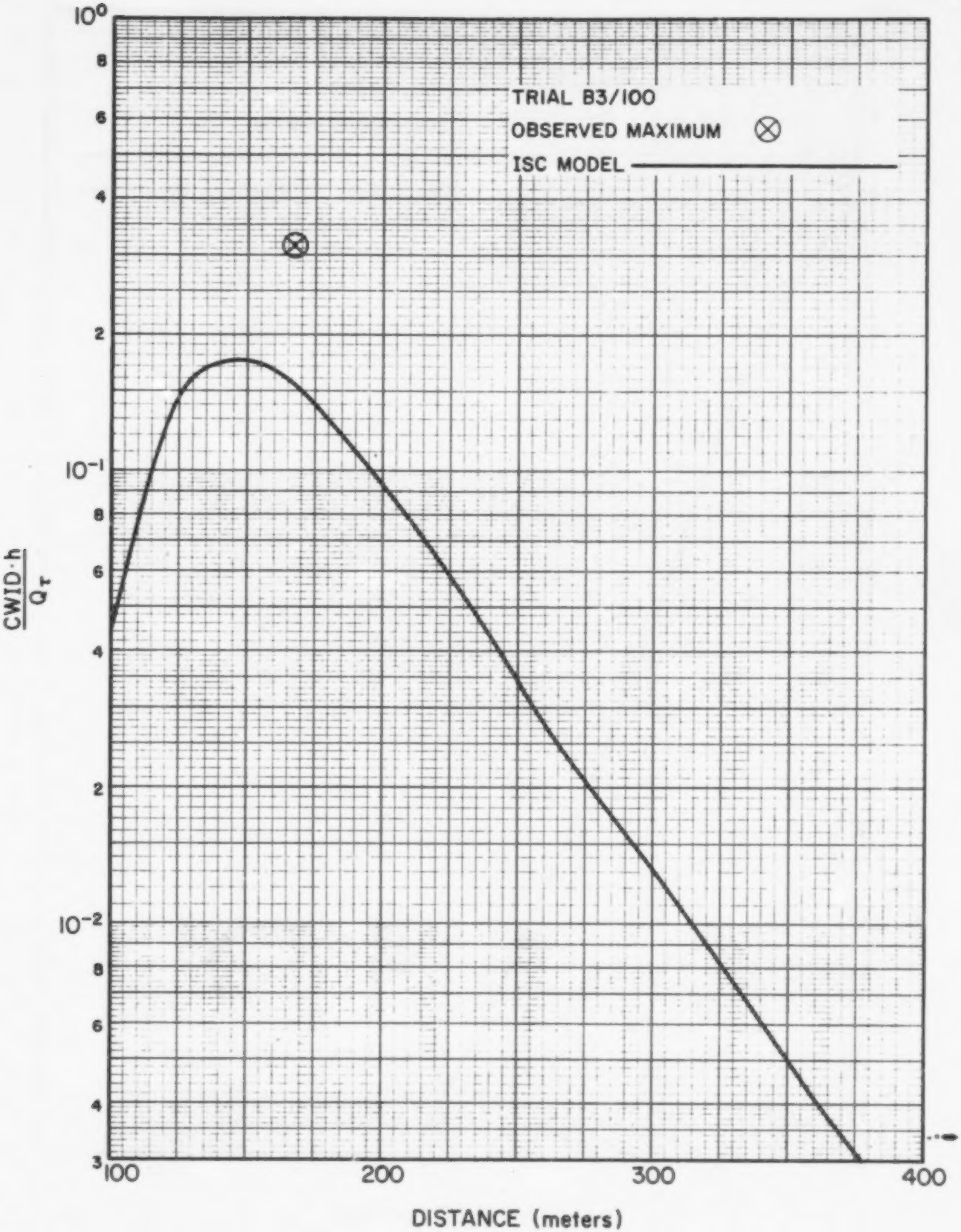

FIGURE A-21. Observed maximum and calculated profile of non-dimensional cross-wind integrated deposition for Stewart Trial B3/100.

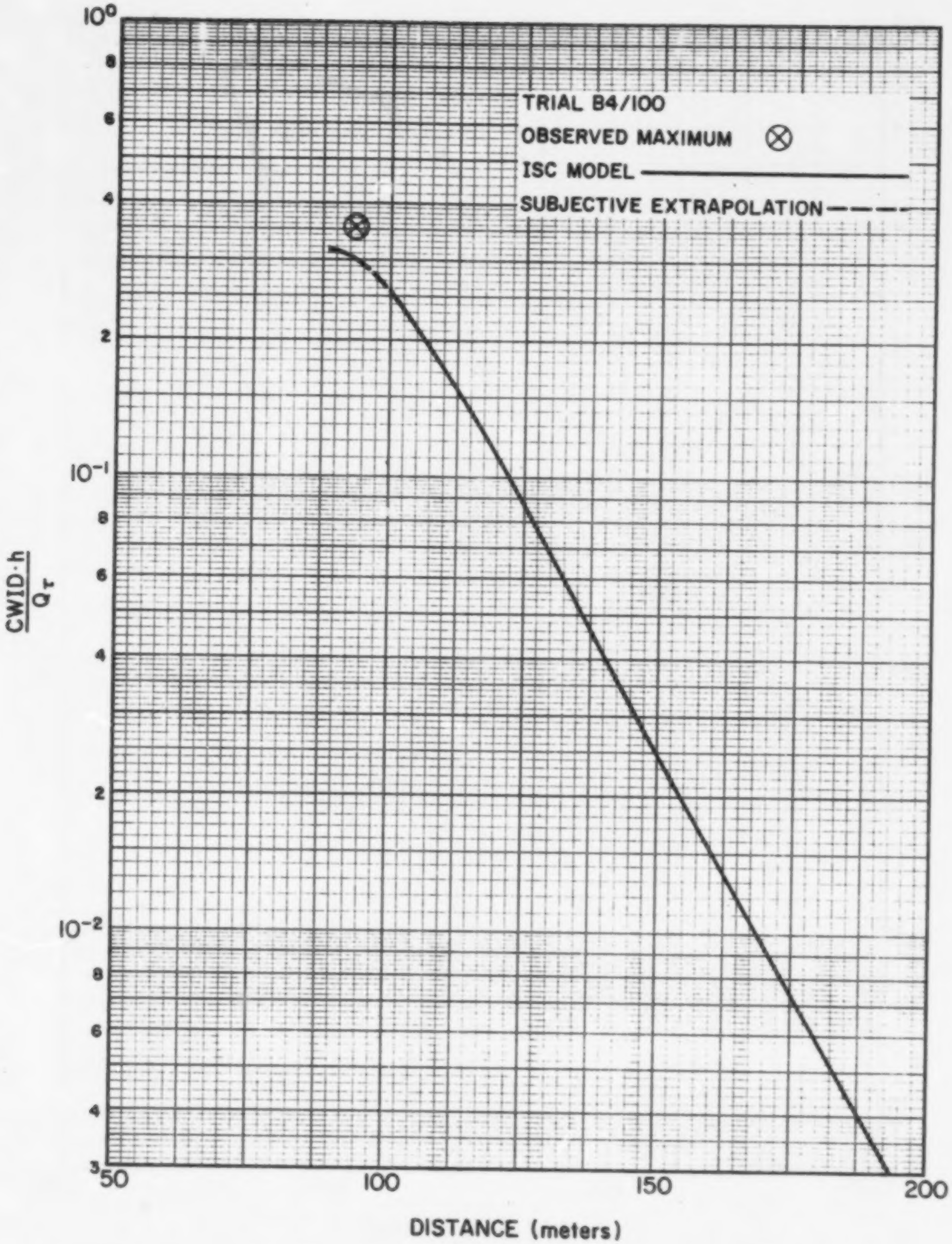

FIGURE A-22. Observed maximum and calculated profile of non-dimensional cross-wind integrated deposition for Stewart Trial B4/100.

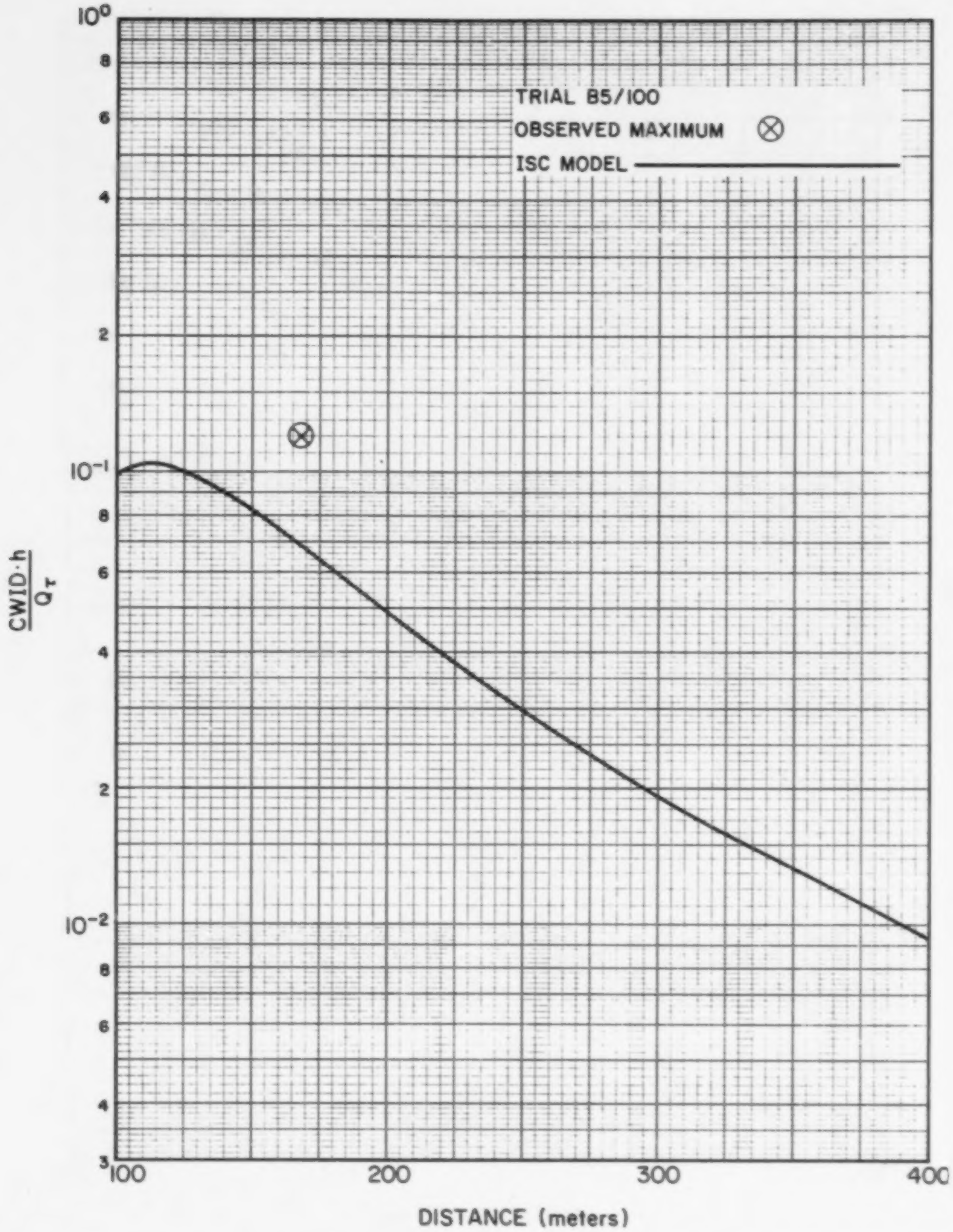

FIGURE A-23. Observed maximum and calculated profile of non-dimensional cross-wind integrated deposition for Stewart Trial B5/100.

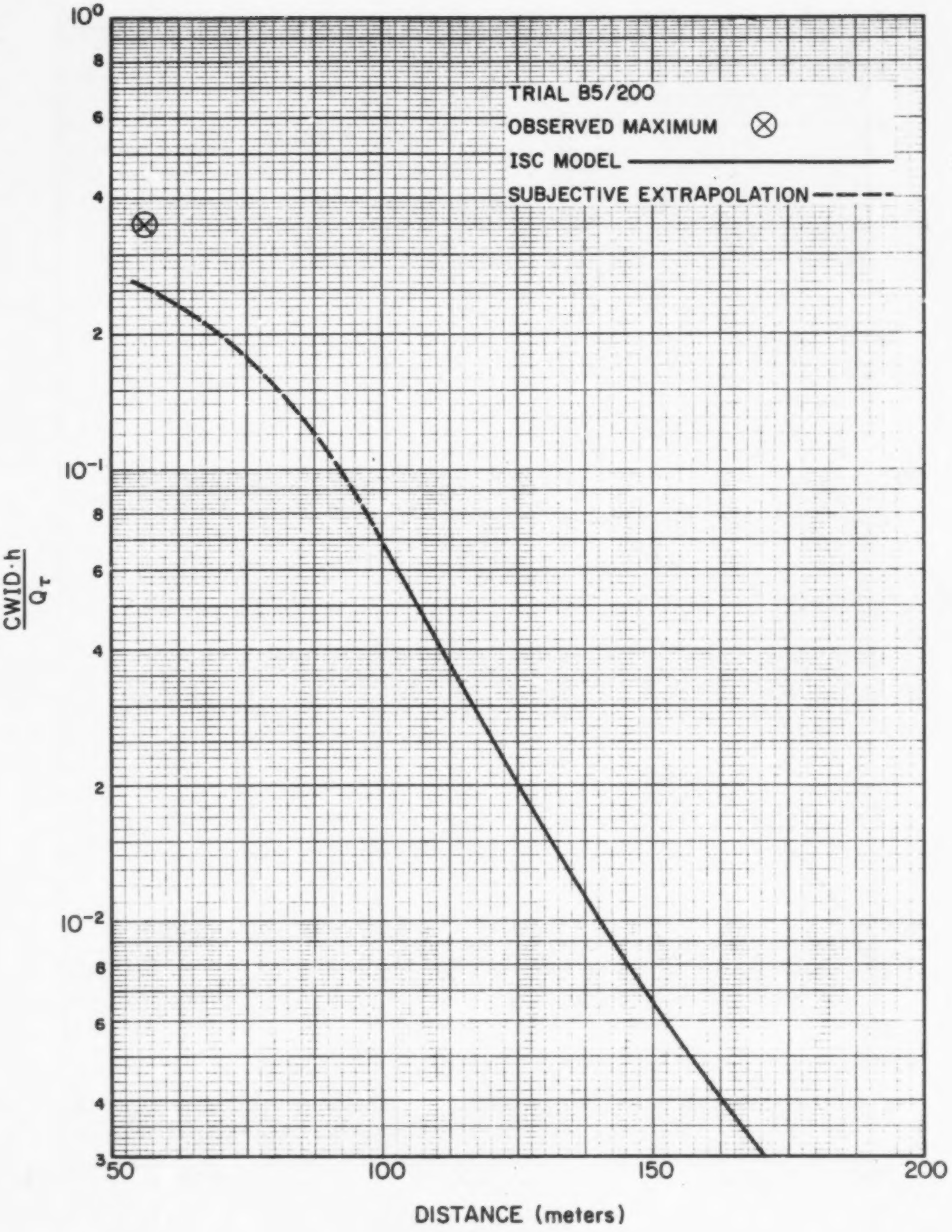

FIGURE A-24. Observed maximum and calculated profile of non-dimensional cross-wind integrated deposition for Stewart Trial B5/200.

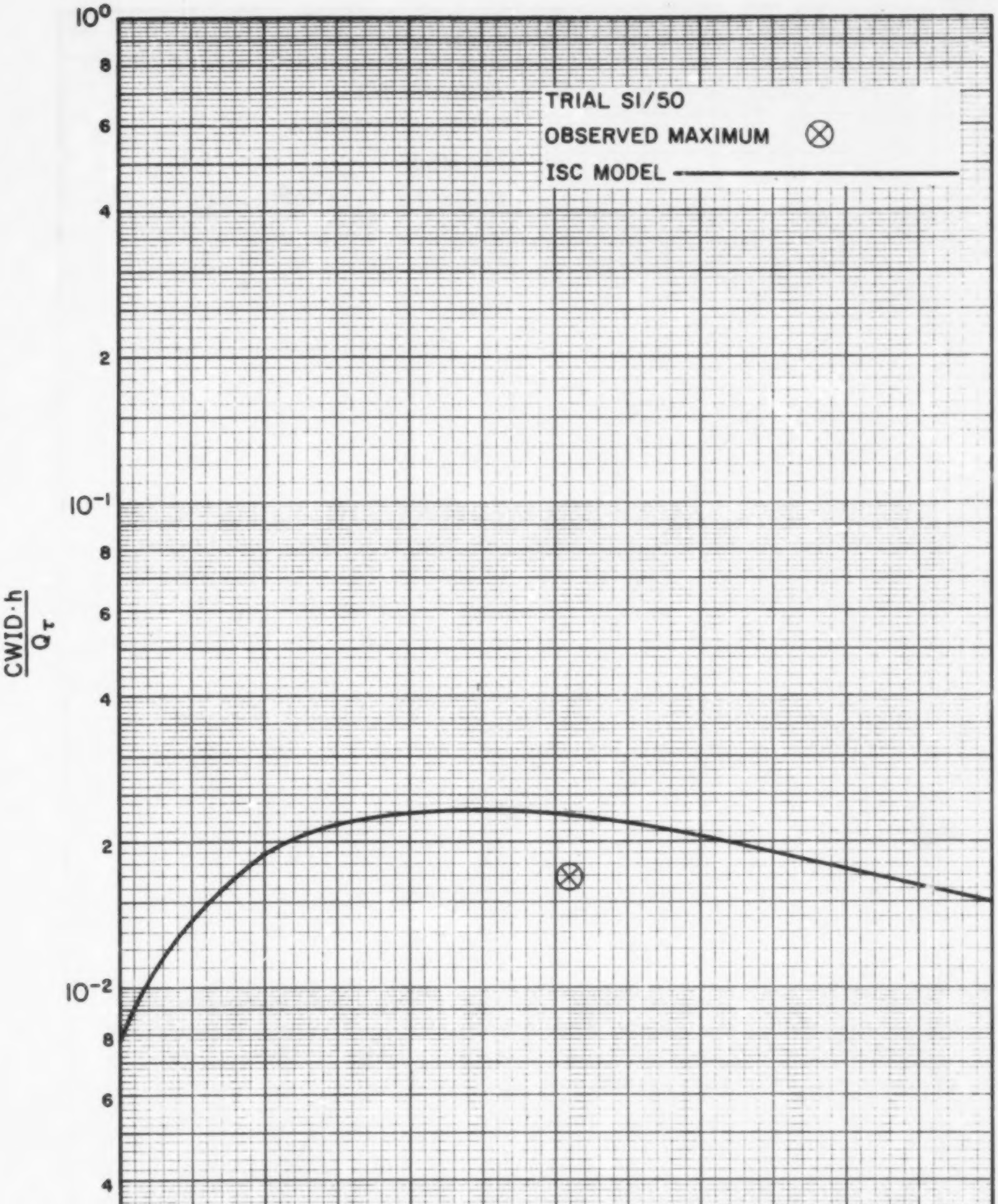

FIGURE A-25. Observed maximum and calculated profile of non-dimensional cross-wind integrated deposition for Stewart Trial S1/50.

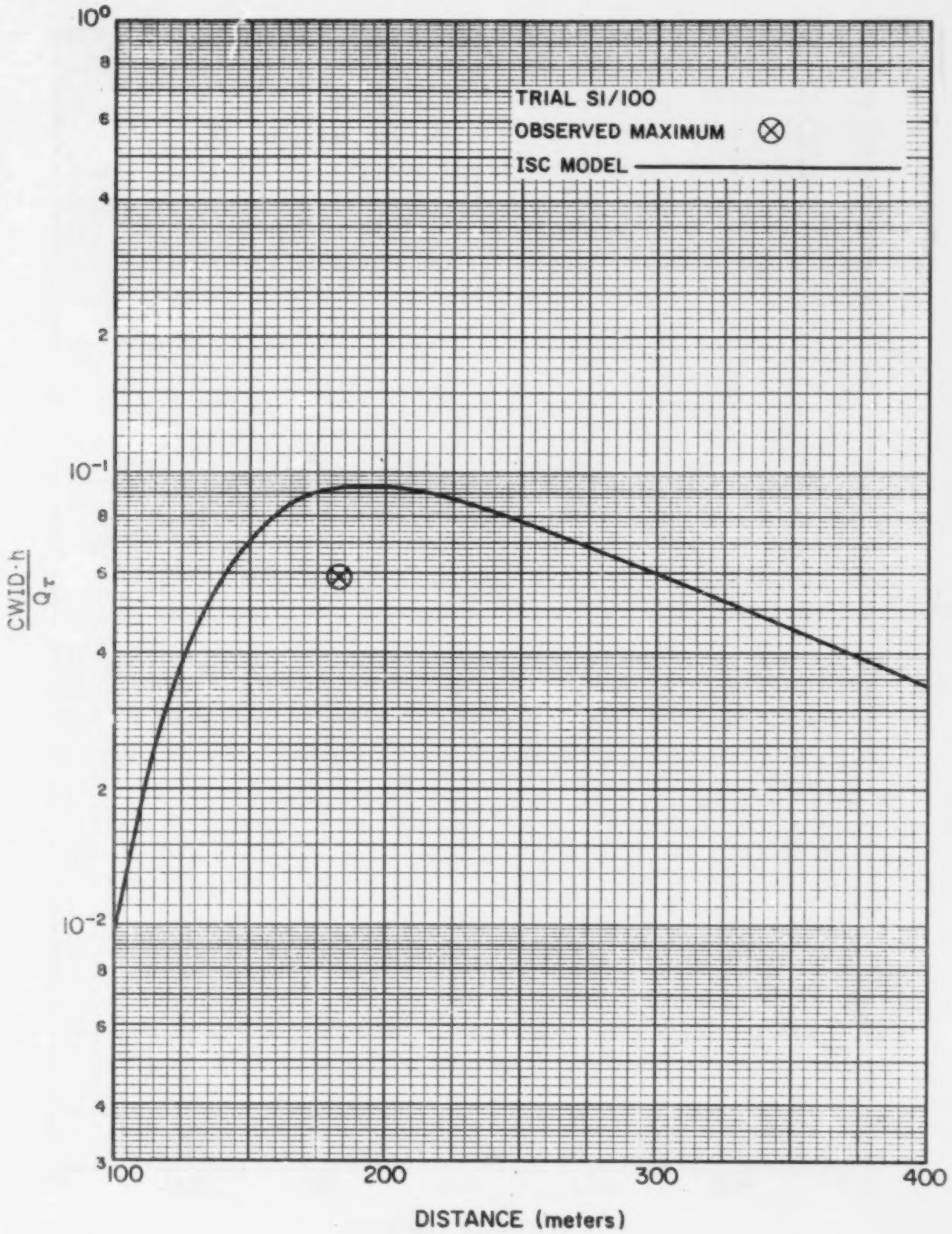

FIGURE A-26. Observed maximum and calculated profile of non-dimensional cross-wind integrated deposition for Stewart Trial S1/100.

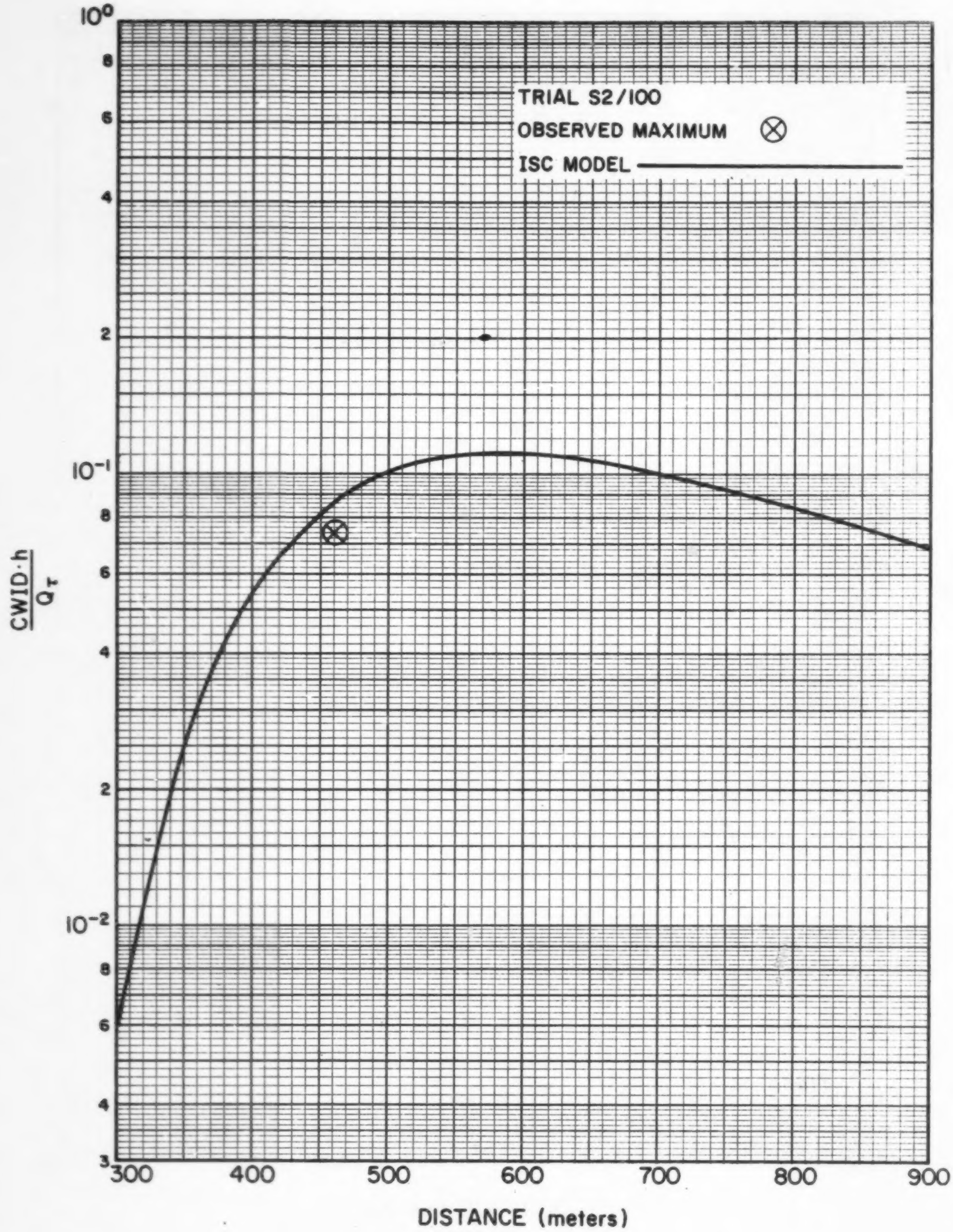

FIGURE A-27. Observed maximum and calculated profile of non-dimensional cross-wind integrated deposition for Stewart Trial S2/100.

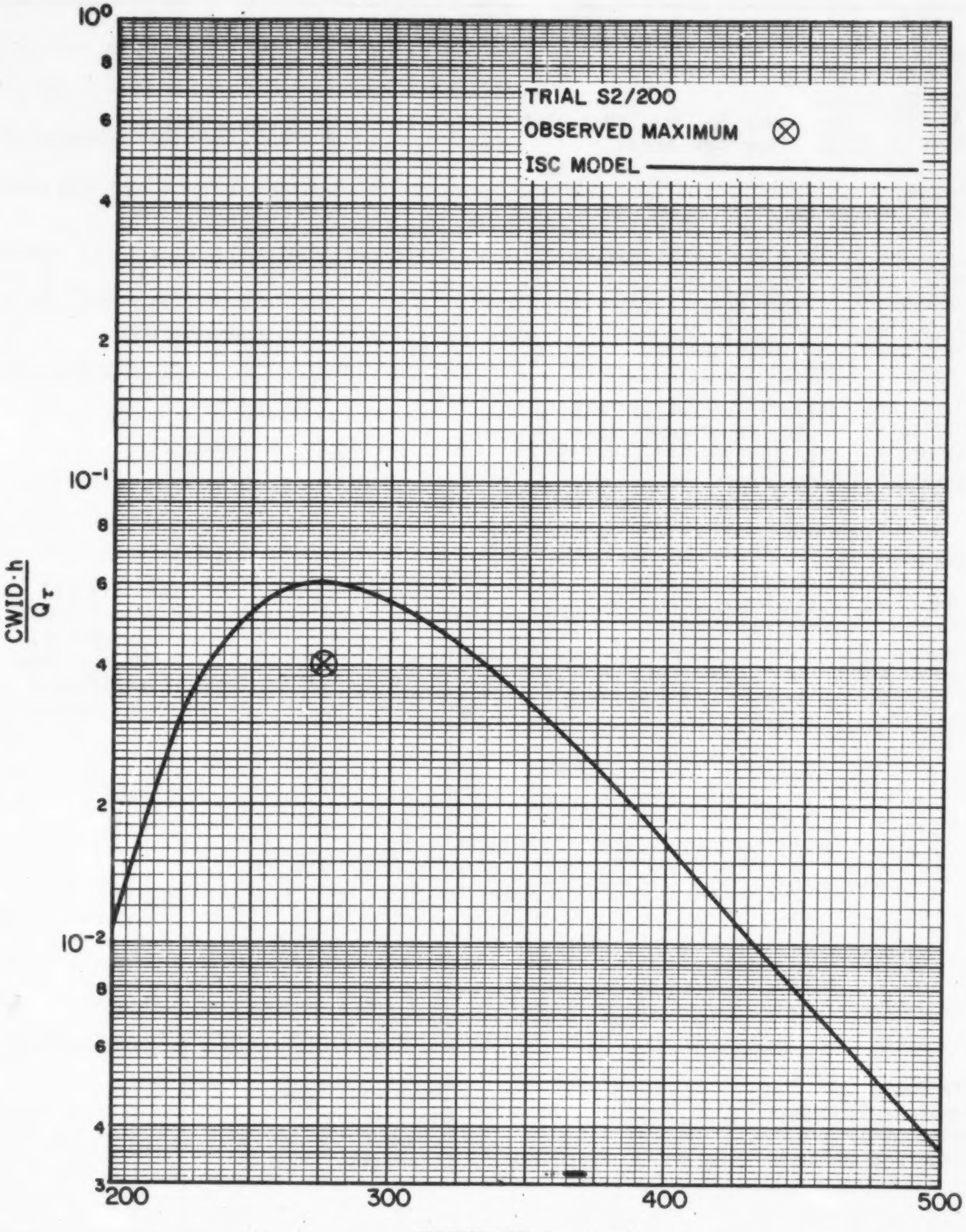

FIGURE A-28. Observed maximum and calculated profile of non-dimensional cross-wind integrated deposition for Stewart Trial S2/200.